Models and algorithms for the combinatorial optimization of WLAN-based indoor positioning system

You Zheng

▶ **To cite this version:**

You Zheng. Models and algorithms for the combinatorial optimization of WLAN-based indoor positioning system. Computers and Society [cs.CY]. Université de Technologie de Belfort-Montbeliard, 2012. English. NNT : 2012BELF0177 . tel-00827561

HAL Id: tel-00827561

https://theses.hal.science/tel-00827561

Submitted on 29 May 2013

HAL is a multi-disciplinary open access archive for the deposit and dissemination of scientific research documents, whether they are published or not. The documents may come from teaching and research institutions in France or abroad, or from public or private research centers.

L'archive ouverte pluridisciplinaire **HAL**, est destinée au dépôt et à la diffusion de documents scientifiques de niveau recherche, publiés ou non, émanant des établissements d'enseignement et de recherche français ou étrangers, des laboratoires publics ou privés.

SPIM

Thèse de Doctorat

école doctorale **sciences pour l'ingénieur et microtechniques**

UNIVERSITÉ DE TECHNOLOGIE BELFORT-MONTBÉLIARD

Models and Algorithms for the Combinatorial Optimization of WLAN-based Indoor Positioning System

ZHENG You

SPIM

Thèse de Doctorat

utbm université de technologie Belfort-Montbéliard

école doctorale **sciences pour l'ingénieur et microtechniques**

UNIVERSITÉ DE TECHNOLOGIE BELFORT-MONTBÉLIARD

Friday 20 of April 2012 at 14h15 – Amphitheatre I 102, Belfort, France

President	**Monsieur François SPIES** **Professeur des Universités** Université de Franche-Comté
Reviewer	**Monsieur Washington Yotto OCHIENG** **Professeur des Universités** Imperial College London (UK)
Reviewer	**Monsieur Adriano MOREIRA** **Professeur des Universités** Université de Minho (Portugal)
Examinator	**Monsieur Cyril LADERRIERE** **Docteur – Ingénieur Recherche** POLE STAR – Toulouse
Supervisor	**Monsieur Alexandre CAMINADA** **Professeur des Universités** Université de Technologie de Belfort-Montbéliard
Co-Supervisor	**Madame Oumaya BAALA** **Maître de Conférences** Université de Technologie de Belfort-Montbéliard

Abstract

Indoor Positioning Systems (IPS) using the existing WLAN have won growing interest in the last years, it can be a perfect supplement to provide location information of users in indoor environments where other positioning techniques such as GPS, are not much effective. The thesis manuscript proposes a new approach to define a WLAN-based indoor positioning system (WLAN-IPS) as a combinatorial optimization problem to guarantee the requested communication quality while optimizing the positioning error. This approach is characterised by several difficult issues we tackled in three steps.

At first, we designed a WLAN-IPS and implemented it as a test framework. Using this framework, we looked at the system performance under various experimental constraints. Through these experiments, we went as far as possible in analysing the relationships between the positioning error and the external environmental factors. These relationships were considered as evaluation indicators of the positioning error. Secondly, we proposed a model that defines all major parameters met in the WLAN-IPS from the literature. As the original purpose of the WLAN infrastructures is to provide radio communication access, we introduced an additional purpose which is to minimize the location error within IPS context. Two main indicators were defined in order to evaluate the network Quality of Service (QoS) and the positioning error for Location-Based Service (LBS). Thirdly, after defining the mathematical formulation of the optimisation problem and the key performance indicators, we proposed a mono-objective algorithm and a multi-objective algorithm which are based on Tabu Search metaheuristic to provide good solutions within a reasonable amount of time. The simulations demonstrate that these two algorithms are highly efficient for the indoor positioning optimization problem.

Keywords: WLAN-based indoor positioning system, combinatorial optimization problem, communication quality, positioning error, Tabu Search, Variable Neighborhood Search.

Résumé

La localisation des personnes et des objets à l'intérieur des bâtiments basée sur les réseaux WLAN connaît un intérêt croissant depuis quelques années ; ce système peut être un parfait complément pour fournir des informations de localisation statique ou dynamique dans des environnements où les techniques de positionnement telles que GPS ne sont pas efficaces. Le manuscrit de thèse propose une nouvelle approche pour définir un système WLAN de positionnement indoor (WLAN-IPS) comme un problème d'optimisation combinatoire afin de garantir à la fois une qualité de communication et une minimisation de l'erreur de positionnement via le réseau. Cette approche est caractérisée par plusieurs questions difficiles que nous abordons en trois étapes.

Dans un premier temps, nous avons conçu un réseau WLAN-IPS et mis en œuvre une plateforme de test. Nous avons examiné la performance du système sous diverses contraintes expérimentales et nous nous sommes penchés sur l'analyse des relations entre l'erreur de positionnement et les facteurs environnementaux externes. Ces relations ont permis de proposer des indicateurs pour évaluer l'erreur de positionnement. Ensuite nous avons proposé un modèle physique qui définit tous les paramètres majeurs rencontrés en WLAN-IPS à partir de la littérature. L'objectif initial des infrastructures WLAN étant de fournir un accès radio de qualité au réseau, nous avons introduit un objectif supplémentaire qui est de minimiser l'erreur de localisation dans le contexte IPS. Deux indicateurs principaux ont été définis afin d'évaluer la qualité de service (QoS) et l'erreur de localisation pour LBS (Location-Based Services). Enfin après avoir défini la formulation mathématique du problème d'optimisation et les indicateurs clés de performance, nous avons proposé un algorithme mono-objectif et un algorithme multicritère basés sur Tabu Search et Variable Neighborhood Search pour fournir des bonnes solutions en temps raisonnable. Les simulations montrent que ces deux algorithmes sont très efficaces pour le problème d'optimisation que nous avons posé.

Mots-clés: système de positionnement indoor basé sur WLAN, problème d'optimisation combinatoire, qualité de la communication, erreur de positionnement, Recherche Tabou (TS), Recherche à Voisinage Variable (VNS).

Contents

List of figures

List of tables

List of algorithms

Introduction

In the last decade, the area of Location-Based Services (LBS) has reached a large popularity that is still growing. Location-Based Services can actively push location-dependent information to mobile users according to their predefined profiles. Positioning systems which are used to provide Location-Based Services have been identified as an important component of emerging mobile applications for a long time. The Global Positioning System (GPS) is currently the system for location sensing in outdoor environments which is widely used. However, GPS does not perform properly in indoor environments because of multipath wave propagation problems and low signal reception inside buildings. Thus LBS for indoor applications is a new challenge and wins growing interest.

Nowadays, many Indoor Positioning Systems (IPS) are proposed to solve indoor positioning and navigation problem. Among them, WLAN-based indoor positioning system (Wireless Local Area Network) is one of the most popular since it has many advantages compared to other IPS. This kind of positioning system does not need any additional installation if a WLAN infrastructure already exists, then the implementation costs are low and the service can be offered under attractive conditions. Moreover, a lot of mobile devices have built-in support for WLANs. In WLAN-IPS, users are already connected to existing WLAN; thereby people can use the same infrastructure for positioning and communications.

A common approach for location determination in WLAN-IPS is based on a radio map of measurements of the received signal strengths coming from the surrounding Access Points (i.e. transceiver base stations for WLAN) and perceived by the terminal. Such an approach is called *fingerprinting technique*. Basically, the purpose of this manuscript is to propose a WLAN-IPS denoted CMTA-WPS which uses fingerprinting technique. CMTA-WPS computes a probabilistic location system and integrates the Centre of Mass (CM) and the Time Averaging (TA) techniques.

We must emphasize that the studies referenced in the literature mainly focus on two aspects for WLAN-IPS: one is the positioning and tracking algorithms which are used for estimating the location that associates the fingerprints with the location coordinates; the other is the reduction of the development cost of the measurement-based radio map. However, as almost all the researches look at the inherent factors to enhance the system performance, there is a lack of clear understanding of the impact of the systems performance from the external factors coming from the communication network itself such as the building architecture, the network design, the radio propagation characteristics, etc. It seems to be obvious that all these components impact highly on the confidence and quality of the location services. We have studied this impact in the work we present and for that purpose we have designed and implemented some tests on different cases to explore the system performance related to external environmental influences.

In addition, we ought not to neglect that the original purpose of these WLAN infrastructures is to provide the required connectivity, so that, both the positioning accuracy

and the communication quality become the targets of the network configuration design. In fact, according to our experiments, the positioning accuracy target and the communication quality target are antagonistic. For example, an increase of the density of Access Points (AP) can improve the system accuracy and precision, whereas the communication quality is degraded due to frequency interferences. Thus we attempt to answer the following question: is that possible to deploy a WLAN in order to guarantee the requested communication quality while having good properties for location services? This problem includes two aspects: WLAN planning for communication quality enhancement and positioning error reduction. Regarding the optimal wireless access, WLAN planning does not only consist in selecting a location for each transmitter and setting the parameters of all sites, but also acts on allocating one of the available frequencies to each selected AP. Regarding the indoor positioning system, once the received signal strength from all visible APs of the WLAN are measured and inputted, the location is estimated and outputted using a radio map and a machine learning technique.

These problems are really different but both services are based on the same network configuration and then the fundamental problem we emphasize is: *how to mathematically formulate and how to solve such difficult problem?* Theoretically we already know that the WLAN planning problem is NP-hard and the reference problem for frequency assignment which is the graph-colouring problem is NP-complete so the task is very hard. Concerning the location problem there is no theoretical complexity proof yet. To answer the above question, we propose in this work an innovative approach where WLAN planning for communication quality enhancement and positioning error reduction are modelled as combinatorial optimization problem and tackled together during the network configuration design process.

To describe our work this thesis manuscript includes four chapters. The first chapter provides the background information in the relevant areas of the existing indoor positioning techniques and technologies to determine the location. At first, the motivation and the application of the indoor positioning system are briefly introduced. Then, the principles of the positioning measurement techniques are described. Generally, these techniques are classified into two mutually exclusive groups: range-based or range-free. Range-based techniques are also called *geometry techniques*. Range-free techniques are subdivided into two categories: *scene techniques* and *proximity techniques*. Next, the existing indoor positioning systems are presented. Most systems are based on a single technology. Besides the use of GPS and optical devices, different types of wireless technologies and sensors are also employed for the indoor positioning. Some systems take mainly advantage of multiple techniques to improve the accuracy and to satisfy different positioning requirements. Furthermore, there are some systems whose application range is usually relatively narrow, such as the laser-based systems, the cellular-based systems, the magnetic positioning systems and the Bluetooth/FM based systems. Finally, on the basis of information on the performance of each system reported in the literature, we evaluated the indoor positioning systems using specific performance criteria. By analyzing this evaluation, we proposed some directions in which it may be worth paying attention in the future.

In the second chapter, we present our first contribution: the indoor positioning system CMTA-WPS as a research objective is described and explored. In the beginning of the

chapter, the principles of CMTA-WPS are introduced. As common WLAN-based fingerprinting positioning systems, CMTA-WPS works in two phases: the offline training phase and the online location determination phase. A description of how to build the radio map during the offline phase is given. Usually, there are two approaches to generate the radio map: site survey and propagation modelling. After comprehensively analyzing of the RF indoor propagation, the calculation methods and the improvements of the radio propagation model are discussed. For the online phase, the probabilistic location algorithm and some classic accuracy enhancement solutions including the centre of mass technique, the time averaging technique and positioning filters are presented. Next, two experiments are implemented to estimate the system performance and to study the relationship between the positioning environment and the positioning accuracy. For convenience of comparative analysis two series of experiments are done: the first series is based on simulation and the second series is based on real environment. Finally, two comparisons between our system and other WLAN-IPS from the literature are done. One is a comparison implemented in two different positioning environments with the distance error criteria. The other is a comprehensive performance comparison with new performance criteria.

As mentioned in the previous section, in order to satisfy the requested communication quality while reducing the location error, we define an effective approach where WLAN planning with both criteria is modelled as an optimization problem and tackled together during the WLAN deployment process. This is our main contributions to this research area. This approach includes two processes: the modelling process and the optimization process.

In the third chapter, the indoor WLAN-based positioning problem and the WLAN planning problem are expressed in a mathematical way. The access point location, the access point pattern, the antenna orientation, the emitted power and the antenna frequency channel are the decision variables. To describe the network behaviours with respect to communication and positioning, the whole model is decomposed into several sub-models, they are: *the AP model*, where a finite set of candidate sites and candidate APs are defined as well as the parameters setting of each AP type such as azimuth, emitted power and frequency channel; *the propagation model*, where the signal propagation for wireless channel estimation in the building is defined; *the requirement model*, where the traffic load requirement and the positioning accuracy requirement are defined; *the throughput model*, where the evaluation of the bit rates as well as the association rules between the clients and the AP are defined; *the positioning model*, where the evaluation of positioning error is defined. The communication quality and positioning accuracy goals can be evaluated thanks to one *Quality of Service* evaluation indicator and three positioning error evaluation indicators. Finally, the search space, the objectives and the set of constraints of our optimization problem are given based on the models definition and the evaluation indicators.

In the fourth chapter, two optimisation algorithms in the category of heuristics are developed to solve the combinatorial optimization problems which require reasonable amount of effort to get good solutions. We emphasize that it is not possible to prove the optimal solving of this problem because it is too complex, so all solutions can be only approximate solutions and not optimal. The WLAN-IPS optimization problem can be defined as a multi-objective optimization problem where communication quality and positioning accuracy

need to be concurrently optimized. The first heuristic belongs to the weighting method, which is a kind of Non-Pareto technique. In this heuristic, a global formulation based on a penalty function has been proposed in order to transform a multi-objective problem to a mono-objective problem. A hybrid Tabu Search and Variable Neighbourhood Search algorithm (TVNS), which combines both metaheuristics, is chosen to implement the mono-objective optimization problem. The second heuristic relies on the Pareto-based techniques and looks for a set of Pareto-optimal solutions. In Pareto optimisation, each solution represents a different trade-off between the objectives that are involved. A parallel version of TVNS algorithm is implemented to improve the quality of the current search front during the optimisation process. This algorithm integrates a multi-threaded parallelization strategy. Different results are presented and commented using all algorithms.

The last section remains all different works we did with the results and introduces the main perspectives for future studies.

Chapter 1 Overview of Indoor Positioning Systems

The indoor positioning system is able to provide a location-based service in indoor environment. The objective of this chapter is to give an overview of the indoor positioning system.

The chapter is organized as follows: after briefly introducing the motivation and the application of the indoor positioning system, the principle of the positioning measurement techniques are presented. Then the system architectures of the existing indoor positioning systems are stated one by one. Finally, we evaluated the major indoor positioning systems based on several indoor positioning system performance criteria and the information given by the literature. By analyzing this evaluation, we propose some directions which are worth to pay attention.

Contents

1.1 Introduction

Location aware service is a common requirement of many tasks performed by people in everyday life. Having this type of service, user can obtain information on both 'who' and 'where'. In order to provide location aware service, various positioning systems are developed, which try to locate and track objects and people in real time. Besides, technological and theoretical advances within the past decades have also caused a surge in the proliferation of the positioning systems.

Early positioning systems are mostly outdoor positioning system. These systems usually use two kinds of navigational systems. One, known as LORAN (Long Range Navigation) (wikipedia, 2010a) or Omega system (wikipedia, 2010b), uses low frequency radio transmitters in multiple stations and the time difference technique to aid ships in navigation. The second is the Global Navigation Satellite Systems (GNSS), the measurements of the cellular communication signals, the identification of nearby stations or even a vision-based technique to locate the user. However, these outdoor locating technologies are often inadequate in indoor environment. Most outdoor systems do not provide sufficient accuracy to discriminate between the individual rooms of a building. GNSS based systems can achieve sufficient accuracy, but are unreliable in indoor environment due to signal interference and attenuation caused by walls, floors, furniture, and other objects.

The motivation of the indoor positioning system is to provide a Location-based Service (LBS) in indoor environment. LBS are services that are offered or denied to users of electronic devices, based on the location of the user. The indoor LBS can be categorized by the provided service type (Giaglis *et al.*, 2002) as follows:

Emergency Services

The classic application for location-based services is summarized in this category. Individuals who are unaware of their exact location in a case of an emergency (injury, criminal attack, etc.) use their mobile device. In a case of life-threatening injuries a call for assistance is possible automatically revealing the exact users location and alarm emergency forces immediately using the positioning capability of the mobile device.

Navigation Services

Entering unfamiliar place the user can be guided within the current geographical location thanks to navigation application. These services allow to find special places depending on the users location with detailed maps or route descriptions transferred to the mobile device. For example, the conference attendant can be assisted in this navigation to find his destination room in the building.

Information Services

Providing information to a user depending on his/her position are placed in this category. Infotainment services notify about local events or location-specific multimedia content to interested users.

Discovery and Tracking Services

Services in this category help to find lost objects or persons and enable tracking them during their displacement. These services are useful in case of lost children and elderly people in malls or tracking product for the production line management.

In order to adapt positioning systems to the indoor environment, many new location technologies have been applied to indoor positioning. However, due to these limitations of the chosen technology, almost indoor positioning systems limit themselves to indoor applications only. Currently, research into indoor positioning systems has identified some possible technologies, but few of them have been produced to consumers. These technologies include Infrared Radiation (IR), Ultra-sound, Radio Frequency Identification Devices (RFID), Wireless Sensor Network (WSN), Wireless Local Area Network (WLAN), Bluetooth, Ultra-wide Bandwidth (UWB), Magnetic technology, Optical technology, etc. Each technology has its unique advantages in performing indoor location for indoor use, WLAN and UWB are among the most common. Equipped with one or several location technologies, indoor positioning systems use location techniques to locate objects and persons and offer absolute, relative and proximity location information. There are three main techniques for indoor position range estimations, Geometry, Scene and Proximity, that we will see in this chapter.

The remainder of this chapter is organized as follows: In Section 2 the principles of the different positioning measuring techniques are described the motivation for indoor positioning system is given. Subsequently, current indoor positioning technologies are then depicted in Section 3. Finally, in Section 4 conclusions are drawn.

1.2 The principle of existing indoor positioning techniques

Nowadays, many indoor positioning systems are proposed and implemented, and they transform the measurements into their corresponding coordinates by several indoor positioning techniques. Generally, the positioning techniques are classified into two mutually exclusive groups: range-based or range-free (He *et al.,* 2003). Range-based techniques try to strictly calculate distance values while range-free techniques try to strictly avoid calculating distance. In range-based localization techniques, the goal is to try to use the observed signal metric (whether time, signal strength, angle, or other) of the transmitter's signal to estimate what is the true distance between the receiver and each of the transmitters. Figure 1.1 shows the range-based localization in the ideal case.

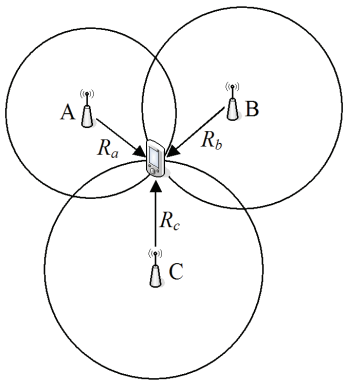

Figure 1.1 Range-based localization in the ideal case

However if it is possible the determined distance may not be a reliable estimate (shown in Figure 1.2), range-free localization techniques which try to infer something like a 'pattern' in the location space may be the better choices.

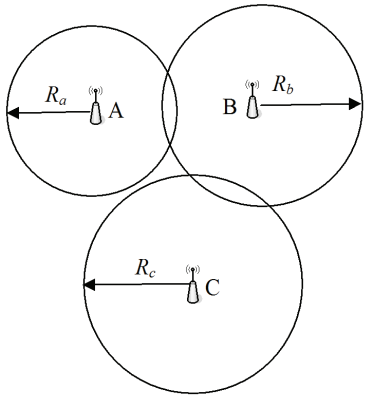

Figure 1.2 Range-based localization under the error conditions

Range-based techniques are also called Geometry techniques. Range-free techniques are subdivided into two categories: scene techniques and proximity techniques. Since these techniques are independent of each other, usually using more than one type of positioning techniques at the same time may provide better performance.

1.2.1 Geometry positioning techniques

Geometry uses the geometric properties of triangles to estimate the target location. It has two derivations: trilateration and triangulation. Trilateration estimates the position of an object by measuring its distances from multiple reference points. So, it is also called range measurement technique. Time of Arrival (TOA), Time Difference of Arrival (TDOA) and Received Signal Strengths (RSS) are the most universal methods of trilateration. In TOA or TDOA method, the distance is derived by multiplying the radio signal velocity and the travel time. In RSS method, the distance is calculated by computing the attenuation of the emitted signal strength. Roundtrip time of flight (RTOF) or Phase of Arrival (POA) methods are also used for range estimation in some systems. Triangulation locates an object by computing angles relative to multiple reference points. Angle of Arrival (AOA) is a typical method within this category, which estimates the location using the angles between the propagation direction of an incident wave and a reference orientation with the coordinates of the associated transmitters.

1.2.1.1 Trilateration

a) Time Of Arrival (TOA)

The TOA technique is based on measuring the difference in the arrival time, which is the signal propagation time from a radio transmitter to one or more signal receivers following a direct path. In order to enable 2-D positioning, TOA measurements must be made with respect to signals from at least three reference points. After synchronizing the transmitter and all the receivers, the difference in the propagation time can be determined by recording the receive time of the signal over each path.

The difference in the arrival time at each receiver is directly related to the difference in path length over which the signal travels (L.A.N., 1999). This is illustrated in Figure 1.3. If we assume that the transmission time from user to Base Station (BS) is Δt, then the distance between the user and the BS is $d = v \times \Delta t$.

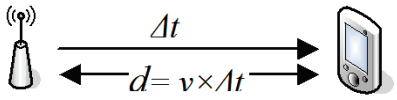

Figure 1.3 Positioning based on TOA technique

Since the radio signal propagates at the same velocity over each of these paths, an equation in terms of the difference in propagation times can be solved to determine the location of the transmitter, as stated in equation 1.1.

$$\sqrt{(x-x_i)^2+(y-y_i)^2+(z-z_i)^2} = v \times (t_i - t) \quad i = 1,\ldots,n \qquad \textbf{(1.1)}$$

Where v is the signal propagation speed, and (x,y,z) is the location of transmitter which transmits the signal at time t. The n receivers located at $(x_1,y_1,z_1),(x_2,y_2,z_2),\ldots,(x_n,y_n,z_n)$ receive the signal at time $t_1,t_2,\ldots,t_n$.

The principle of the above equation also can be vividly expressed by Figure 1.1. In this method the user should be located on the border of the circle where the base station is the center and the radius is R. When the signal is received by several base stations, the distance from the user to different stations can be determined, furthermore, the location of the target can be determined to be within the overlapping area of those circles. However, this is an ideal case, in which all the clocks are perfectly synchronized and there are no other influences.

If there are errors the result is shown in Figure 1.2. The difference from Figure 1.1 is readily apparent. For example, there might be no common areas between the circles. These errors could be due to multi-path, refraction, and noise. Additionally, since the velocity of light is very high and even a small time inaccuracy can lead to a large error. However, in some cases it is possible to compensate for these errors with the cost of increased system cost and complexity. As a result, in a real scenario, TOA usually is not used alone. To improve the positioning accuracy, some algorithms for TOA-based indoor location system such as Closest Neighbour (CN) and Residual Weighting (RWGH) are proposed in (Kanaan & Pahlavan, 2004). The CN algorithm estimates the location of the user as the location of the base station or reference point that is located closest to that user. The RWGH algorithm can be basically viewed as a form of weighted least-squares algorithm.

RTOF as a derivative of TOA is also implemented in positioning application. This method measures the return time-of-flight of the signal traveling between the transmitter to the receiver. In RTOF, relative clock synchronization replaces the absolute clock synchronization in TOA while the measurement mechanism of RTOF is the same as that of TOA. The difficulty of RTOF application is the measuring unit to know the exact delay/processing time caused by the responder. Figure 1.4 explains the measurement mechanism of RTOF.

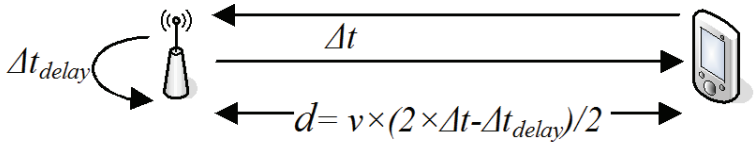

Figure 1.4 The measurement mechanism of RTOF

Some of the advantages of TOA are that it is rather straight forward to solve the set of equations to estimate the location of the device whose location is to be determined. The work is done by the receiver(s) (or by a third party who is given the received data), and the accuracy is roughly proportional to the resolution of the clock relative to the velocity of signal propagation. Note that the spatial resolution of TOA in conjunction with acoustic signals, such as ultrasonic pulses, is better than optical or radio TOA solutions, as the velocity of propagation is much slower.

However, drawbacks exist as well. One of the distinct limitations is spatial accuracy. If the time resolution is 1μs, this translates to an approximate 300 meters positioning resolution (optical or radio TOA solutions). This is assuming that the transmitter and receivers are well synchronized. There are also problems with multi-path propagation of the signal, thus requiring some way to determine the first arrival of a signal, in order to reject the later arrival of reflected copies of the signal. Unfortunately, indoors environment there are quite often a lot of reflections from a large variety of objects and the spatial resolution is not sufficient for many indoor applications. Thus, TOA is used more in the cellular location.

b) Time-Difference Of Arrival (TDOA)

TDOA is an extension based on TOA, which determines the position by measuring the time difference of signal arrival. This technique is used in a wide range of applications. Unlike TOA, TDOA only requires that all the transmitters are synchronized to a common clock. Since the transmitters are synchronized, the receiver can simply subtract the time-of-arrival from each of the transmitters and effectively eliminate the clock offset in the unsynchronized transmitter-receiver pair to determine the time difference. This significantly decreases the requirement for time synchronization. The measurement mechanism of TDOA is illustrated in Figure 1.5.

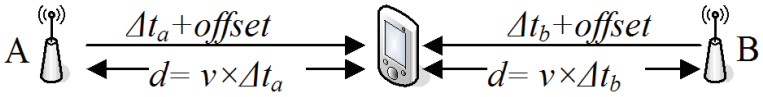

Figure 1.5 The measurement mechanism of TDOA

Receivers are located at known fixed positions, and the transmitter's position can then be determined by a hyperbolic function. The equation of the hyperbolic is given by:

$$D_{i,j} = \sqrt{(x_i - x)^2 + (y_i - y)^2 + (z_i - z)^2} - \sqrt{(x_j - x)^2 + (y_j - y)^2 + (z_j - z)^2} \qquad \textbf{(1.2)}$$

Where (x_i, y_i, z_i) and (x_j, y_j, z_j) represent the fixed receivers i and j, and (x,y,z) represent the coordinate of the transmitter. For computing the hyperbolic TDOA expression shown in equation 1.2

through nonlinear regression, a conventional method is to linearize the equations through the use of a Taylor-series expansion and create an iterative algorithm (Yamasaki *et al.,* 2005).

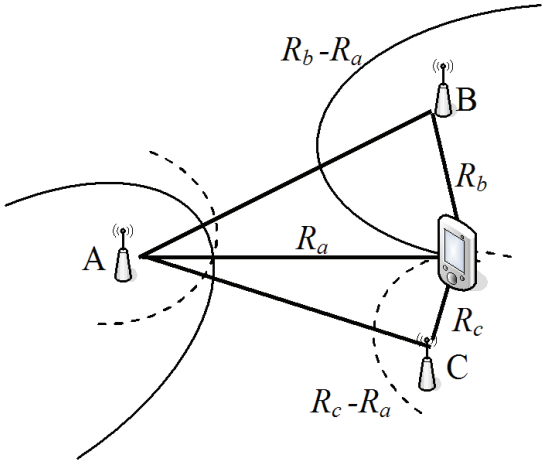

Figure 1.6 Positioning based on TDOA measurements

Figure 1.6 displays a 2-D target location based on TDOA measurements (a TDOA system requires a number of base stations that is one greater than the number of dimensions). The receiver lies on a trajectory which have a constant difference in distance to two fixed points (transmitter A and transmitter B or transmitter A and transmitter C). This curve is simply a hyperbola with the two transmitter locations as the foci. The estimated location of the receiver can be determined by the intersection of two hyperbolic curves (hyperbola R_b -R_a or hyperbola R_c -R_a).

However, in reality, the series of hyperbolic functions seldom intersect, due to various kinds of errors. Similar to TOA, a tiny error in the detected time leads to a large error in location.

c) Received Signal Strength (RSS)

RSS methods are based upon the measurement of the magnitude of an electric field at a certain point. If the transmitter power at the transmitter's antenna is known, then by measuring the received power it is possible to estimate the distance of the receiver from the transmitting antenna. Theoretical and empirical propagation models are used to translate the difference between the transmitted signal strength and the received signal strength into a range estimate, as shown in Figure 1.7.

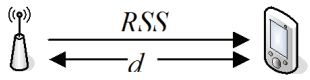

Figure 1.7 Positioning based on RSS

Due to severe multi-path fading and shadowing phenomena resent in the indoor environment, the general path-loss models do not always hold. The parameters employed in these models are site-specific. The accuracy of this method can be improved by utilizing the pre-measured RSS contours centered at the receiver (Yamasaki *et al.,* 2005) or multiple measurements at several base stations.

1.2.1.2 Triangulation

The triangulation is also called Angle of Arrival (AOA). It is widely used in wide area cellular networks. AOA determines the transmitter's location by the intersection of several pairs of angle direction lines. As shown in Figure 1.8, AOA methods may use at least two known reference points (A, B), and two measured angles θ_1,θ_2 to derive the 2-D location of the target P. Estimation of AOA, commonly referred to as direction finding, can be accomplished either with directional antennae or with an array of antennae.

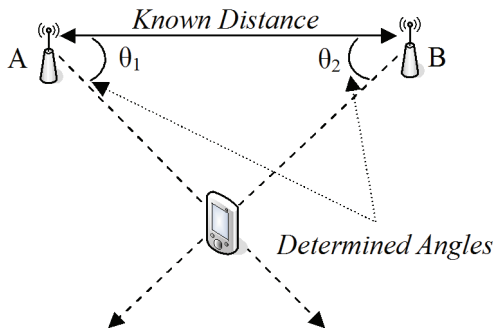

Figure 1.8 Mechanism of AOA

Although AOA can determine a position estimate with few measuring and doesn't need any time synchronization between measuring units, this ideal case requires a line-of-sight (LOS) transmission. Non-line-of-sight (NLOS) results in unpredictable errors, as shadowing, multi-path effect could contribute to the error. Further disadvantages of AOA technique are emphasized with relatively large and complex hardware requirements or location estimate degradation as the mobile target moves farther from the measuring units.

1.2.2 Proximity techniques

Proximity algorithms provide symbolic relative location information. Usually, it depends on a dense grid of antennas whose location is set in advance. When a mobile target is detected by a single antenna, it is identified and located within the neighbourhood of this single antenna. When more than one antenna detects the mobile target, it is considered to be located with the one that receives the strongest signal. This method is relatively simple to implement.

The systems using IR and RFID are often based on this method. The Cell Identification (Cell-ID) or Cell of Origin (COO) method also belongs to this technique.

1.2.3 Scene techniques

Scene analysis refers to the type of algorithms that first collect features (fingerprints) of a scene and then estimate the location of an object by matching online measurements with the closest a priori location fingerprints. In scene analysis the most common application is RSS-based finger printing technique.

Fingerprinting technique usually works in two phases: the offline training phase and the online location determination phase. During the offline phase, a site survey has to be executed in an environment to generate a so-called radio map. This radio map can be considered to be a collection of calibration points at different locations in the building, each with a list of RSS values for visible access points at that particular location. During the online phase, the calibration points are being used to calculate the most probable location of the user, whose actual location is unknown (Prasithsangaree *et al.,* 2002).

The main challenge to the techniques based on location fingerprinting is that the received signal strength could be affected by diffraction, reflection, and scattering in the propagation indoor environments.

The fingerprinting technique uses pattern classification techniques to estimate location. Some typical pattern classification techniques are described in detail in the following paragraphs.

1.2.3.1 k-Nearest-Neighbor (kNN)

The kNN algorithm is a method for classifying objects based on the closest distances and a majority weight of the k nearest neighbors. In the simplest case (k=1), the algorithm finds the single closest match. However, in practice, since there are errors in the positioning estimation, determining the single closest location fingerprint is not always available. A wise choice is to use the k nearest neighbour search, instead of the closest one, to get a closer estimate of the current location. Thus, in most indoor positioning system, the kNN estimates the user's location by computing the average of the k closest neighbours that have the smallest Euclidean distance with respect to the online RSS readings. In (Bahl & Padmanabhan, 2000), the author concluded that the location accuracy is improved as k increases. But in (Prasithsangaree *et al.,* 2002), the author proposed that there is a limit of k. In their experiment, the performance decreases when $k \geq 8$. Mathematically, the calculation of the generalized distance L is given by following equation:

$$L = \frac{1}{N}\left(\sum_{i=1}^{N}|s_i - f_i|^p\right)^{\frac{1}{p}} \qquad \textbf{(1.3)}$$

Where N is the number of access points, and s is the i^{th} element of the sample measurement vector, f is the i^{th} element of the fingerprint vector. p is the norm parameter. In the Euclidean distance, $p = 2$. There are various other distance metrics (one such being the Manhattan Distance), where $p \neq 2$ (Prasithsangaree *et al.,* 2002).

A famous positioning system RADAR proposed in (Bahl & Padmanabhan, 2000) uses this technique. Based on the basic kNN, WKNN (Li *et al.,* 2006) using an average weighted by the inverse of the RSS distances is also introduced to improve the accuracy.

kNN is simple to implement and provides reasonable accuracy; however, one drawback of standard kNN in indoor positioning is that the RSSs detected in the same location vary over time, which may cause measurements errors. Another drawback is that some information available in the historical fingerprints may be ignored since this algorithm solely depends on the value of signal strength.

1.2.3.2 Artificial Neural Networks (ANN)

Neural network methods assume that the RSS cannot be analyzed mathematically because they are too complex. These methods use non-linear discriminant functions for classification. In this method there is no generalized distance metric, rather it can be viewed as a black box information processing unit. During the off line stage, RSS and the corresponding location coordinates are processed respectively as the inputs and the targets for the training purpose. After the training step of neural networks, appropriate weights are obtained. Usually, a multi-layer Perceptron network with one hidden layer is used for ANN-based positioning system (Battiti *et al.,* 2002). The input vector of signal strengths is multiplied by the trained input weight matrix, and then added with input layer bias if bias is chosen. The result is transmitted to the transfer function of the hidden layer neuron. The output of this transfer function is multiplied by the trained hidden layer weight matrix, and then added to the hidden layer bias if it is chosen. The output of the system is the estimated location. The ANN is easy to be retrained in case of the information in the database is outdated or new data become available. ANN has been found to be better than kNN type implementations (Saha *et al.,* 2003), however the improvement is not very significant. Moreover, extensive training data would be needed to adequately train the neural network for accurate location.

1.2.3.3 Probabilistic methods

The probabilistic approach represents the location fingerprint as a conditional probability and uses Bayesian inference to estimate location (Madigan *et al.,* 2005). This approach requires knowledge of the underlying probability distribution that models the RSS values. A training set from real measurements or a radio propagation model with the radio parameters can be used to generate this distribution. After this training stage, when given a received signal vector, the probability of the mobile target in a location can be obtained by using Bayes' formula. Since our indoor positioning system is based on this kind of method, an explanation in more detail will be given in the later chapter.

With the additional information regarding the location distribution, some papers (Youssef & Agrawala, 2008), (Ling *et al.,* 2010) have been showed that this method yields higher accuracy compared to the kNN approaches. But this additional information also requires a large training set to accurately describe the RSS values at a given location.

1.3 The existing indoor positioning systems

There are many positioning systems based on one or more technologies to determine the location of objects and people. The different technologies have different accuracies, configurations, and reliabilities.

1.3.1 The GNSS based indoor positioning systems

Nowadays, there are many GNSS to be available, such as Global Positioning System (GPS), Galileo positioning system, Beidou navigation system and so on. GNSS receives signals from multiple satellites and employs a triangulation process to determine physical locations. GNSS is the

most popular system for outdoor navigation, yet for indoor navigation, some difficulties need to be overcome.

The accuracy of the GNSS is affected by high noise, echo-only or high multi-path signals and degraded geometry. In outdoor environment, the atmosphere for instance attenuates the GNSS signals by about 1 dB under normal circumstances. But in indoor environment, the attenuation of GNSS signal is 5-15 dB for residential houses, 20-30 dB for office buildings and >30 dB for underground car parks and tunnels. If large attenuation and non-homogeneities occur, the signals measured by the receivers might be echo-only signals that may contain large errors, depending on indoor geometry, as illustrated in Figure 1.9 (Lachapelle, 2004). Moreover one observation seen from the figure is that the angle of view into the sky by the GNSS receiver would decrease as the user moves further into the room. It means that the number of LoS satellites is decreasing when the user moves further into the room.

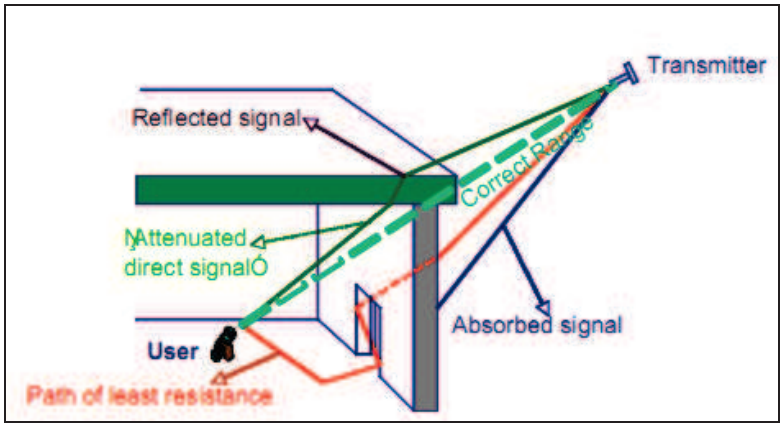

Figure 1.9 Possible GPS signal propagation paths into a building

To adapt GNSS to the indoor environment, the main approach is using Assisted GNSS (AGNSS) with High Sensitivity GNSS (HSGNSS) receiver (Mautz, 2009a). AGNSS method is providing the assist data to the user to short Time to First Fix (TTFF) by using a wireless network. This assist data increases information of the satellite such as ephemeris, almanac, differential corrections and other relevant information obtained from the GNSS satellites directly. Also, High Sensitivity GPS (HSGPS) receiver is used to track weak signals with a power level in the range of -188 dBW to -182 dBW (Anwar *et al.,* 2008). Other indoor GNSS approach could be established through the deployment of pseudolites. GNSS signal transmitters which enhance the signal availability replace the GNSS satellite constellation for indoor applications (Yun *et al.*, 2002). Although pseudolite GNSS can provide high indoor accuracy, the infrastructure is very expensive.

1.3.2 The optical based indoor positioning systems

With the rapid development of the Charge Coupled Device (CCD) sensors and microprocessor in the last few years, optical methods are now becoming an interesting alternative for positioning and navigation. There are two major applications scenarios. One is the high precision (mm or better) positioning system for the industrial applications, such as surface inspection or reverse engineering.

And the other is the normal accuracy (meter or better) positioning system for the civilian applications such as museum guide or pedestrians navigation.

In (Tilch & Mautz, 2010), the author classifies the systems into the following four categories:

Optical Tracking: Optical tracking means to observe a mobile object by a single or multiple static cameras in real-time in order to determine the object position.

View-based Navigation: The view-based approach relies on the view map generated by a sequence of views taken by a digital camera along a certain route in an initial phase. The system can estimate the positioning by matching the input image of surroundings and the stored images in the view map.

Use of coded targets: This strategy relies on some special marks to identify the locations. Compare with view-based strategy, the map generation process can be omitted, but some additional devices are used to deploy the unique identification of the targets by using a unique code for each target. A digital camera observes the unique codes of targets and gives the position determination of it.

Projection of laser spots or patterns: This class of optical indoor positioning systems consists of a digital camera and a laser-light emitting device. The aim of that approach is the determination of the camera position by observing projected laser-spots or grids.

1.3.3 The ultra sound based indoor positioning systems

Using ultra sound signal as a way of position measurement makes use of the biomimetic technology. In nature ultra sound signals are used by bats to navigate. It inspired people to design a similar navigating. After many years of development ultra sound transmit and receive devices are mature, but there are several disadvantages of this strategy because the ultra sound is sensitive to temperature variations and multi-path signals. In the ultra sound based positioning system, the beacon units as infrastructure are attached on the walls or ceilings at known positions. Each beacon unit broadcasts periodically ultrasonic pulses and simultaneously Radio Frequency (RF) messages with its unique identity number. The system uses TOA measuring method and triangulation location technique to locate the user (Mautz, 2009a).

Active Bats, Crickets and DOLPHIN are three existing typical ultra sound positioning systems. The Active Bat System is the pioneer work in the development of a broadband ultrasonic positioning system. It is designed by AT&T Cambridge and provides 3-D position and orientation information for user. The principle of operation is shown in Figure 1.10. In (Hazas & Hopper, 2006), it was shown that the 3D accuracy of a synchronous receiver is better than 5 cm in 95% of cases. Distributed Object Locating System for Physical space Inter networking" (DOLPHIN) is another ultrasonic positioning system explained in (Fukuju *et al.,* 2003) and (Minami *et al.,* 2004). DOLPHIN enables positioning of the objects with minimal manual configuration. System claims an accuracy of 2 cm to be reached in a room of 3mx3m size. The Cricket nodes are small ultrasonic devices developed by the MIT Laboratories (Priyantha *et al.,* 2000). A 3D positioning accuracy of 1-2 cm can be reached indoors within a maximum volume size of 10 m.

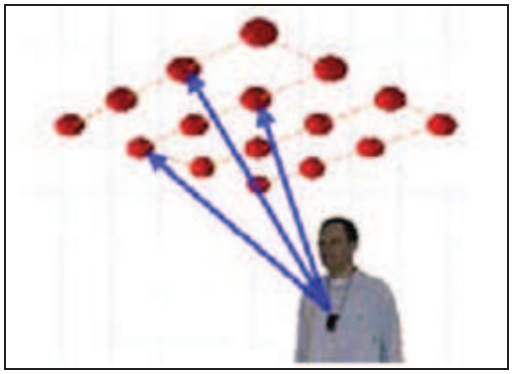

Figure 1.10 The principle of the Bat Ultrasonic Location System

1.3.4 The RFID based indoor positioning systems

An RFID system is composed by several components, including a number of RFID readers, RFID tags, and the communication between them. The RFID reader is able to read the data emitted from RFID tags. RFID readers and tags use a defined RF and protocol to transmit and receive data. There are two kinds of RFID tags: passive and active.

The passive RFID tag is a receiver. Thus these tags are small and inexpensive. But the coverage range of tags is short. With active RFID, the tags are transceivers, which actively transmit their identification and other information. Thus the cost of tags is higher. On the other hand, the coverage area of active tags is larger (Finkenzeller, 2003).

The existing majority of RFID positioning systems are based on three approaches. One of the commonly used approaches of RFID positioning is geometry-based (Time-based and Angle-based). This approach determines the tag positioning by incorporating the TOA, TDOA, RSS, AOA, etc. information of an RFID tag at multiple reader antenna positions. Due to the complexity of the indoor environment, such as the noisy, multi-path effect and NLOS properties, AOA, TOA and TDOA techniques cannot get a desirable accuracy in indoor context. Besides, AOA needs antenna array which has too high cost to fit for the indoor location, TOA and TDOA both require synchronization setting, it is infeasible for the inexpensive indoor hardware to provide fine-grain time synchronization. Also, the positioning algorithm needs a high cost to get a desirable accuracy as it needs a large number of references nodes. Thus this kind of approaches is not suitable for low cost indoor positioning systems.

Compared with the above approaches, fingerprinting approach is more robust and does not add additional sensor/actuator infrastructure. Thus both the famous RFID positioning systems SpotON (Hightower *et al.,* 2000) and LANDMARC (Ni *et al.,* 2004) are based on fingerprinting. In SpotON, the objects are located by homogenous sensor nodes by using an aggregation algorithm for 3D location sensing based on RSS analysis. LANDMARC uses conception of reference tag when decreasing the number of RFID reader but increasing accurate rate of tagged object. Reference tag is an active tag which is fixed in the known position. The kNN method is adopted to calculate the location of the RFID tags. Several variants of LANDMARC have been developed to improve the positioning accuracy or reduce the system complexity. In (Zhang *et al.,* 2008), the positioning error

can be reduced through removing the dissimilar reference tags. In (Bekkali *et al.,* 2007), Kalman filtering and probabilistic matching are used to reduce the effect of RSS fluctuation and noise.

Since a tag has a unique ID number and an RFID reader has a limited read range, proximity approach also fit for RFID. In this approach, the user carries an RFID reader. Tag IDs of read tags are transferred to the server. The server has the information of each tag coordinates. The server calculates the reader's position from the coordinates of detected tags. Figure 1.11 explains the outline of the system (Shiraishi *et al.,* 2008).

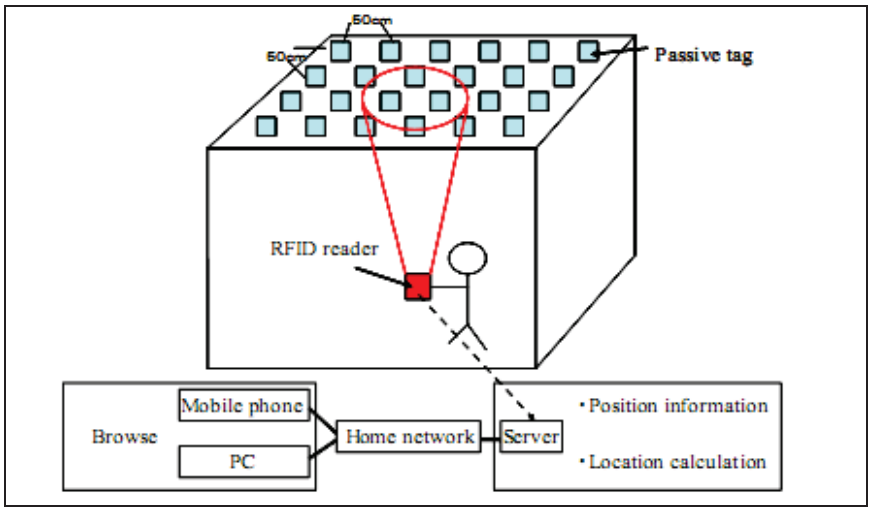

Figure 1.11 RFID-based system outline

RFID technologies have several advantages. The NLOS nature has significant advantage among all types of RFID systems. They can work at remarkable high speed. The other advantages are the promising transmission range and cost effectiveness. The RFID tag is light and small so that it can be taken by people to be tracked. However, this technique needs to be installed and maintained numerous infrastructure components in the working area.

1.3.5 The WSN based indoor positioning systems

Sensors are devices which convert a physical or environmental condition including sound, pressure, temperature, light, etc. into a proportional electrical signal. WSN, which is made by the convergence of sensor, micro-electro-mechanism system and networks technologies, is a novel technology about acquiring and processing information. Figure 1.12 shows the components in node of WSN (Culler *et al.,* 2004).

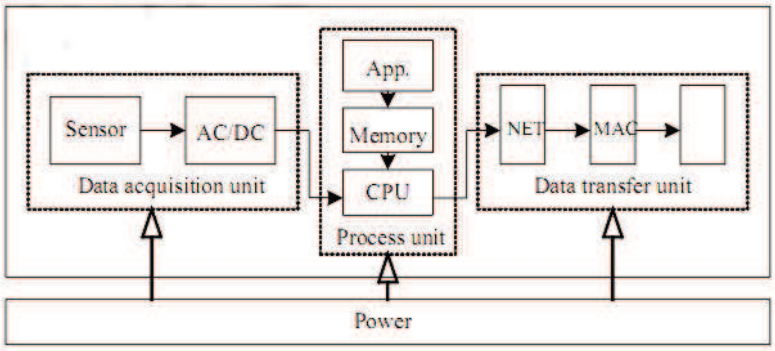

Figure 1.12 Components in node of WSN

From the measurements taken by the sensors fixed in predefined locations, a person or device can be located (Michel *et al.,* 2006). Currently, a universal WSN indoor positioning solution is applying the RSS method accompanying a ZigBee-based WSN (Sugano, 2006),(Chang *et al.,* 2009). ZigBee is a wireless communication based on the IEEE 802.15.4 standard (Alliance, 2010). It provides a low cost, low power and easy implementation wireless network. The ZigBee based sensors wireless network can be operated in the star topology or the peer-to-peer topology. The following process description outlines a common ZigBee based wireless network indoor positioning operation. Firstly, a target node sends the measure RSS requests to its neighboring fixed nodes. The neighboring fixed nodes measure the RSS and forward these data to positioning servers. The positioning server stores the target node coordinates determined through these collected RSS data and a triangulation location algorithm with a certain tracking filter. In addition, the target node also can actively participate in the localization process. Less accuracy, the limited battery power and lower computational ability are the main drawbacks.

1.3.6 The UWB based indoor positioning systems

UWB based indoor positioning systems have received an increasing interest over the last decade, since this technology can achieved in high accuracy resolution.

UWB technology offers various advantages compared with other positioning technologies used (Gezici *et al.,* 2005). Firstly, as is known to all, many positioning systems suffer from the multi-path distortion of radio signals in indoor environment. The UWB uses very short pulses with duration of less than few nanoseconds (Kelly *et al.,* 2002) make it possible to filter the reflected signals from the original signal. It can provide centimetre accurate positioning information. Secondly, other RF signals can not interfere with the UWB even at a very close range because UWB uses the different signal types and radio spectrum. Thirdly, the UWB is a NOLS technology with a range in free space of several dozens meters, which makes it practical to cover large indoor areas. The signal passes easily through walls, equipment and clothing only attenuated seriously by metallic and liquid materials. Moreover, UWB tags are low-power and cheap, which make the positioning system a cost-effective solution. All of properties indicate that UWB has the one of best cost-to-performance ratio of all available indoor location technologies.

As other RF indoor positioning system, trilateration, triangulation and fingerprinting have been applied to UWB. However, the nature of the UWB signal allows the time delay approach to provide

higher accuracy than other approaches since the accuracy of time delay positioning is inversely proportional to the effective bandwidth of the signals (Mahfouz *et al.,* 2008). Thus, most UWB positioning can be performed by using measuring TDOA in conjunction with AOA between a UWB tag and multiple sensors.

Now, many UWB based indoor positioning systems have been developed. The Ubisense system is a successful system among them (Steggles & Gschwind, 2005). It is a unidirectional UWB real-time positioning system with a conventional bidirectional time division multiple access (TDMA) control channel and takes advantages of both the TDOA and AOA techniques. The Ubisense components hardware is shown in Figure 1.13. The accuracy offered by Ubisense is about tens of centimetres.

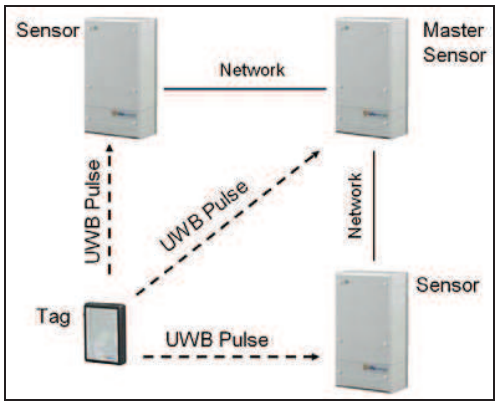

Figure 1.13 The Ubisense components hardware

1.3.7 The WLAN based indoor positioning systems

The WLAN, operating in the globally available 2.4 GHz ISM (Industrial, Scientific and Medical) band, is very popular during the last few years. IEEE 802.11 is currently the dominant WLAN standard. It provides the bit rate of 11, 54, or 108 Mbps within a range of 50-100m (Bing, 2002). Since the WLAN infrastructures are widely implemented in public areas, enterprise locations and homes and WLAN technology is also integrated in various wireless devices such as PDAs, laptops, mobile phones, etc, the WLAN based positioning systems which reuse these existing infrastructures and wireless devices become the most popular low cost indoor positioning solution. The positioning service also can be seen as a value-added service of WLAN.

There are various measurement techniques that can be used to determine the position of a mobile station. Among these methods, fingerprinting which is based on the WLAN RSS characteristic may be the best one as a result of the following reason. First of all, RSS is relatively simple and easy to get compared to other measurement information. Next, RSS is more robust in multi-path and NLOS conditions. Moreover, no cost needs for angle measurement and time synchronization by fingerprinting.

Through the research of many years, people have made some progress in WLAN-based indoor positioning technique and many WLAN-based indoor positioning systems are developed. For space limitations, we only discuss several typical systems here. RADAR (Bahl & Padmanabhan, 2000), as one of the pioneer in the WLAN-based indoor tracking field, was proposed by a Microsoft research

group. RADAR system relies on the radio map constructed by a radio propagation model or the empirical measurement of access point signal strength and multiple nearest neighbors in signal space (NNSS) location algorithm. Horus system is another star of indoor positioning system. It uses the probabilistic method and several modules to increase the location accuracy and reduce the computational requirements of the location determination algorithm (Youssef & Agrawala, 2008). The COMPASS system (King *et al.,* 2006) takes advantages of the earth's magnetic field to increase the location accuracy. A user's orientation is measured by a digital compass and considered in the location sensing process. Since digital compass is cheap and small, usually integrated into various hand devices, COMPASS can provide low cost and relative high accurate positioning services.

1.3.8 The hybrid indoor positioning systems

The above indoor positioning systems are only based on solo technology. However, these systems are difficult to improve the accuracy and to satisfy different positioning requirements. Thus some hybrid systems are proposed to resolve these two problems mentioned above.

The common solution for the first problem is to introduce the aid-hardware. With the recent technical improvements in the area of Micro Electrical Mechanical System (MEMS), various kinds of sensors such as motion sensors, direction sensors and optical sensors have received more and more research interest in the last few years. Combining the advantages of the sensors with a certain localization technique they can compensate each other in the hybrid system.

The COMPASS system by means of a WLAN in combination with a digital compass is a good example of hybrid system (King *et al.,* 2006). A major contribution of the COMPASS system makes directed fingerprinting really useful since the user can know own direction by digital compass.

A popular approach to hybrid system is introducing the Pedestrian Dead Reckoning (PDR) into RF localization System. PDR estimate the current position based on a previously determined position by evaluating acceleration and gyro data from an Inertial Measurement Unit (IMU). The IMU is mounted on the foot of a person and to perform so-called zero velocity up dates, namely, recalibrate the velocity estimation from the acceleration integration to zero whenever the foot comes to rest on the ground (Godha & Lachapelle, 2008). The PDR can help to navigate through areas with poor coverage or to compensate for variances in the position estimation that result from RSS fluctuations. While, there is a fundamental problem of PDR that long term accuracy is difficult to achieve without the use of additional calibration data. A RF localization approach can be used for long-term stability of PDR. In (Frank *et al.,* 2009) the authors combine wireless LAN fingerprinting localization with a foot mounted IMU and magnetometer and improve the localization accuracy by using Extended Kalman Filter (EKF) data fusion. Another approach is proposed in (Klingbeil & Wark, 2008) where the authors improve the localization accuracy in a WSN by fusing IMU data and experimentally demonstrate their setup.

A smart phone with built-in wifi module and camera is quite common, thus some hybrid systems using image processing and WiFi strength are proposed (Milan *et al.,* 2009), (Hattori *et al.,* 2009). Since the image information and the WiFi strength are independent of each other, the hybrid approach combining RF and image information was shown to provide a significant improvement over single-modality localization.

For the second problem, the multi-technologies fusion has been the new focus. Different wireless technologies have different coverage ranges and different accuracies. Normally, smaller coverage range of wireless technologies has better spatial resolution of it. For example, a hybrid system developed by France Telecom (Evennou, 2005) combines the advantages of WLAN and UWB technologies, where WLAN technology can provide positioning services covering large area and UWB can give highly accurate position estimated in some small required areas. The selective fusion location estimation (SELFLOC) (Youngjune *et al.,* 2004) infers the user location by selectively fusing both location information from multiple wireless technologies and multiple classical positioning techniques in a theoretically optimal manner. To service the information fusion better the view point of the multilayer approach are proposed in (Mestre *et al.,* 2010). Each technology belongs to a detail level based on its coverage area and the data collected from several technologies can be merged. At each phase a different technology is used, starting with the wider coverage range technology and ending in the lower range technology. Such hybrid system can not only provide different level of coverage but also may reduce the computational time of the positioning estimation correction and eliminate possible error sources. For example, someone wants to find his lost mobile phone. However, no solo location technique can solve the problem. If using multiple sources of information such as GSM, WiFi and WSN to do location estimation, everything will be easy. A certain building can be targeted by GSM. And then WiFi can know it in a part of a certain floor. Finally, the mobile phone is located with a precision of approximately 1 m by WSN.

1.3.9 Other indoor positioning systems

Compared with the indoor positioning systems outlined above, although the application range of following indoor positioning systems are usually relatively narrow, they still are worth us to pay close attention.

1.3.9.1 The laser based indoor positioning systems

These systems can provide very high precision (10μm-100μm) positioning system for the industrial applications, but the price is also very expensive. They are usually made up of portable instruments that combine angular and distance measurements using a laser interferometer or an absolute distometer to determine 3D coordinates. Leica Geosystems, Faro, ATT are the excellent representatives of laser tracker system manufacturer. Unlike a traditional laser tracker, iGPS is an innovative Laser based system developed by Nikon Metrology. It is based on internal time measurements related to spatial infrared lasers that intersect at multiple sensors in the local workspace (Depenthal & Schwendemann, 2009). According to the manufacturer, an accuracy of ±0.1 mm for 3D positions can be reached.

1.3.9.2 The cellular based indoor positioning systems

The cellular based system refers to a kind of systems which have used the mobile cellular network to estimate the location of mobile clients. The cellular-based system works only if the building is covered by several base stations. Normally, the cellular-based system use cell-ID approach or enhanced observed time difference (E-OTD) approach. The advantage of this technique is its ubiquitous distribution, easy implementation and the fact that all mobile cell phones support it. However, the accuracy of these approaches is generally low (in the range of 50m–200m). Such

accuracy is hard to accept in indoor positioning application. In order to meet indoor positioning requirement, GSM-based indoor localization system using wide signal-strength fingerprints is developed and presented in (Otsason *et al.,* 2005). The wide fingerprint includes the six strongest GSM cells and readings of up to 29 additional GSM channels, and weighted kNN technique is used to estimate the location. The results of experiments show that their indoor localization system can differentiate between floors and achieve median within-floor accuracy as low as 2.5 m. Although this accuracy is exciting, only few indoor environments can be suitable for this approach as they must be covered by more than six GSM station.

1.3.9.3 The magnetic based indoor positioning systems

Using magnetic signal is an old and classic way of position measuring and tracking. Compared with many existing positioning systems, the magnetic positioning systems utilizing artificial magnetic signals (alternating DC magnetic signal) do not suffer from NLoS problems where the signals are attenuated or even isolated by obstacles such as walls, furniture, body etc. Furthermore, the magnetic positioning systems can avoid negatively affected by multi-path, refractions and further wave propagation errors inside buildings. Thus the magnetic positioning systems are able to offer high accuracy. In a classic magnetic positioning system, reference stations consist of electrical coils are used that generate periodically static magnetic fields. For the position determination a mobile station is equipped with a magnetic field sensor. By measuring the field strength of at least three reference coils the 3D position can be determined using trilateration principle (Paperno *et al.,* 2001).

Besides the static positioning, the system is also intended for position estimation of persons and objects in kinematic applications. Motion Star is a well known commercial product in this application. Motion Star provides precise body motion tracking by measuring numerous magnetic sensors mounted on the different parts of a person (Ascension, 2010).

Although the magnetic positioning system has many advantages, its application fields are still narrow because of the limited coverage range and the expensive magnetic trackers. Thus many current researches focus on increasing the coverage range of each magnetic transmitter or using various magnetic infrastructures to cover enough area.

1.3.9.4 The Infra-Red based Indoor positioning systems

Infra-Red was a pioneer technology in the field of indoor positioning. Most of the Infrared Data Association (IrDA) wireless system is based on the LOS mode because the IR wave can not penetrate opaque materials. Active badges system is the first indoor location sensing system developed by AT&T Cambridge (Want *et al.,* 1992). The location of a person is determined from the unique IR signal emitted every ten seconds by a badge they are wearing. The signals are captured by sensors placed at various locations inside a building and relay information to a central location manager system. However, the major drawback of this system is the limited range of an IR network. Also, IR does not have any method for providing data networking services. To compensate the disadvantages of this system, several hybrid location systems use a combination of RF and IR signals. The EIRIS (ELPAS InfraRed Identification and Search System) uses an IRFID triple technology that combine IR, RF (UHF), and LF (RF low-frequency transponder) signals (Ito *et al.,* 2004). It combines the advantages of each technology, i.e., the room location of IR, the wide range of RF, and the tailored

range sensitivity of LF. However, there exists a trade-off between the accuracy and cost of detecting exact positions.

1.3.9.5 The Bluetooth/FM based indoor positioning systems

Bluetooth, the IEEE 802.15 standard, is a wireless communication method used by two devices over short distances (typically15–20m) and low bit rate (typically 1-2 Mbps). Bluetooth technology has been implanted in various types of devices such as mobile phone, laptop, desktop, PDA, etc. These devices equipped with Bluetooth technology can be reused in the positioning systems. In addition, Bluetooth chipsets are also low cost. Thus several Bluetooth-based positioning systems are proposed (Altini *et al.,* 2010), (Feldmann *et al.,* 2003). Most Bluetooth-based positioning systems use trilateration method (TDOA and RSS) to get the range information. However, Bluetooth-based positioning systems haven't attracted as much attention of researchers as other popular RF-based positioning systems (such as WLAN-based, UWB-based and WSN-based) since Bluetooth-based positioning doesn't present any particularly superior aspects to the opponents. Its coverage is smaller than WLAN-based. The accuracy is lower than UWB-based. The implementation cost is higher than WSN-based.

FM-based system is a minority positioning system and few researches have been done. To the best of our knowledge, Smart Personal Object Technology (SPOT) is the first FM-based positioning system which uses prototype hand watch with an embedded FM radio to localize using commercial FM broadcasting stations (Krumm *et al.,* 2003). The authors applied a Bayesian classifier to distinguish six areas, based on RSSI ranking of the local FM stations. But the system accuracy is very low. A more practical called FINDR (FM INDooR) is proposed in (Papliatseyeu *et al.,* 2009). The FINDR positioning system employs a set of short-range FM transmitters as wireless beacons and a programmable radio on the client device. FINDR is based on fingerprinting method and estimate the location using Gaussian processes regression and k-nearest neighbour (kNN) classification. The results of the system evaluation show a median accuracy of about 1.0 m and 5.0 m at 95% confidence level.

1.4 Conclusion

In this chapter, a state of the art indoor positioning system, including the measurement techniques and the system architectures, has been presented. However, an important question still remains unsolved: how to evaluate these indoor positioning systems? Scholars have made the deep research on this question and various kinds of indoor positioning system performance criteria are proposed in (Tsung-Nan & Po-Chiang, 2005), (Hui *et al.,* 2007), (Tesoriero *et al.,* 2010). Synthesizing these criteria, our performance benchmarking is composed of Performance, Cost, Complexity, Robustness, Power&Range and Limitation.

Performance

The accuracy and precision are two main performance parameters to evaluate an indoor positioning system. To evaluate the performance of the location system, the accuracy is one of the most important indicators. It shows how accurate the positioning system could achieve. Usually, the mean distance error is adopted as the performance metric, which is the average Euclidean distance

between the estimated location and the real location. The precision is defined as the success probability of position estimations with respect to predefined accuracy. It considers the distribution of distance errors. The Cumulative Probability Function (CDF) is used to describe the precision.

Cost

For a commercially available application, cost is an important factor. The cost is contains several parts: the cost of the infrastructure components, the cost of a positioning device for each user and the cost of system installation and maintenance.

Complexity

Complexity of a positioning system can be attributed to hardware, software, and operation factors. Hardware complexity indicates that the requested workload during the deployment and maintenance of indoor positioning system is large. Operation complexity means that the system isn't user friendly. These two kinds of complexities are not key factors to restrain the system performance since they can be reduced by pre-treatment. Thus we emphasize on software complexity, which is usually indicated by the system response time. Because of the limited CPU processing, each indoor positioning system has its maximum tracking speed. If a mobile target speed is faster than this limitation, the system can't offer the precise location estimation.

Robustness

A robust indoor positioning system should be able to keep on operation even in some abnormal situations. For example, some devices in the system are malfunctioned or the signals suffer from strong interference. Namely, the system robustness reflects the fault tolerance capability. The robustness is highly correlated with measuring techniques. In general, the technology with Scene technique has good robustness; the technology with proximity technique has medium robustness and the technology with geometry has poor robustness. In (Laoudias *et al.,* 2010), author investigates various kinds of positioning techniques in WLAN based indoor positioning system.

Power & Range

Power consumption and coverage range are also issues to be taken into account. High energy efficiency and large coverage range often bring low installation and maintenance cost.

Limitation

Due to the properties of positioning technology, each technology has its limitation. Studying these limitations can help people to better apply and improve these technologies. For example, some technologies such as UWB or Magnetic only cover a short range. For large areas, these systems are not scalable. Another example, most RF technologies can not avoid the interference from multi-path. Or for instance, Infrared technology is sensitive to sunlight and has to be in the LoS condition.

According to above discussion and referring to some relevant references (mautz, 2009b), (JANET, 2010), the summary and comparison of the current positioning systems in Table 1 are given to have a comprehensive understanding of the these systems. Three most representative and important evaluation criteria are used. One thing must be noted that, in fact, the information of each technology is merely concluded from several corresponding indoor positioning systems. Thus all these data indicate the average level of each technology.

Through above analysis, we can see that currently there is no perfect technology which can satisfy various requirements (performance, cost and responsiveness). A wise choice is applying

different technology to fulfill the different requirement. For example, for industrial applications, high accuracy is more important than cost and responsiveness, so laser tracker or a certain high precision optical technology looks like a really good choice. For conference scenario, the conference organizer needs location information to offer flexible services for the users, thus room level accuracy is enough. The key factors are cost and convenience. WLAN can meet these requirements. WLAN-based system can reuse the existing Wi-Fi infrastructure. Since almost hand devices have the built-in Wi-Fi function, users can be tracked only using client software. The WLAN-based system is easy to achieve room level accuracy and also easy to maintain over time. Another wise choice is fusing location information from multiple classical measuring techniques. For example, author in (Kwon *et al.,* 2004) developed a hybrid method that combines the benefits of the RF propagation loss model and fingerprinting technique. The contribution of this hybrid method is finding a trade off between accuracy and labor force cost. Later, a system, named OWLPS (Open WireLess Positioning System), implements several of the major mobile position computation algorithms and techniques: fingerprinting location, topology-based and viterbi-like algorithm, propagation models are proposed to further complete this hybrid method (Cypriani *et al.,* 2009). In another example, Ubisense uses a combination of Time-Difference Of Arrival (TDOA) and Angle Of Arrival (AOA) techniques to determine the location of a target (Steggles & Gschwind*,* 2005).

TABLE 1 THE SUMMARY AND COMPARISON OF THE CURRENT SYSTEMS

Technology	Accuracy	Cost	Responsiveness
A-GNSS	5m-50m	cheap	Within 1 minute for initial, following near real time
Optical	1mm/1m	expensive/ Cheap	near real time
Ultra Sound	1cm-10cm	cheap	near real time
RFID	50cm (passive) 2m (active)	cheap	seconds
WSN	10cm - 1m	medium	seconds
UWB	10cm-1m	expensive	near real time
WLAN	1m-10m	cheap	several seconds
Bluetooth	2m-15m	medium	several seconds
Infrared	5m-10m	cheap	near real time
GSM	50m-200m	cheap	near real time
Magnetic	1cm-10cm	expensive	near real time
Laser Tracker	10μm-100μm	expensive	near real time

Now improving the single technology based indoor positioning system is still a hot issue. However, after years of deep research, such positioning system has little space for improvement. Thus, in my view, the following directions may be worth to pay attention a fortiori in further.

1. Instead of using a single technology to estimate the locations of the targets, hybrid indoor positioning systems are needed. A few of the works have already been done supporting such idea. In previous section, the hybrid position systems are presented and divide into two categories.

One category is internetworking of the existing positioning technologies to own not only the large positioning range but also the high positioning accuracy. In this category, different technologies

can profit from each other thus the improvements are obvious. And the implementation is relatively easy to achieve. Thus hybrid indoor positioning systems belonged to this category will surely gain more and more attention.

The other category is integrating the sensor into current indoor positioning system. These sensors can be inertial, magnetic sensors, optical or other kinds. Some hybrid systems in view of sensors fusion are representative of this category. More details of this category are already given in the hybrid system section.

2. Integrating indoor and outdoor positioning system is another trend of indoor positioning systems (Ran *et al.,* 2004). This integration helps in tracking a mobile target indoor or outdoor using the same positioning system. Many works are done in this area.

3. Introducing new methodologies to the positioning system. Currently the commonly used methodology is machine learning. In this thesis, we will present a new procedure to model and optimize WLAN-based indoor positioning system to reduce the positioning error. The whole procedure can be divided into three steps.

- Firstly, we built a WLAN-based indoor positioning system as a test platform. In order to guarantee the representation of our system, two most common techniques, fingerprinting technique and probabilistic technique, are chosen. Based on a series of experimental comparison and analysis, we conclude that the positioning error will reduce if we increase the number of APs or change the placement of APs or change AP parameters (i.e. the emitted power or the azimuth). However, in practice, we should not neglect a fact that original purpose of these WLAN infrastructures is to provide the required communication connectivity. An increase of the density of AP can improve the system accuracy and precision, whereas the communication quality (due to frequency interferences) and the installation costs are increasing too. Thus, how to deploy a WLAN in order to guarantee the requested Quality of Service (QoS) while reducing the location error?
- To answer the above question, in the second step, we propose a new approach where WLAN planning and positioning error reduction are modelled as an optimization problem and tackled together during WLAN planning process. Based on our indoor positioning system, and learning from some mathematical models of WLAN planning, we establish the mathematical optimization model which includes the AP model, the RSS model, the QoS model, the positioning model and the radio wave propagation model. Moreover, two indicators are defined in order to evaluate the actual network QoS as well as the positioning error.
- After defining the model and the key performance indicators, in the final step, we propose to solve the problem with some metaheuristic algorithms. Since these objectives in the model are conflicting objectives, we firstly use an optimization method which is based on a penalty function to transform a multi-objective problem to a mono-objective problem to solve, and secondly we use a Pareto-optimality method which treats each objective in fair way respectively to tackle the optimization problem with all the compromising solutions in regards with the different objectives.

Chapter 2 A New Indoor Positioning System: CTMA-WPS

After summarizing and analyzing the current main existing positioning systems, our indoor positioning system called CMTA-WPS is described and explored in this chapter. CMTA-WPS uses location fingerprints and existing wireless local area network infrastructure. CMTA-WPS is based on probabilistic location determination system and integrates Centre of Mass technique and Time Averaging technique.

In the beginning of this chapter, we introduced the principle of CMTA-WPS. As a common WLAN positioning systems, CMTA-WPS works in two phases: the offline training phase and the online location determination phase. For offline phase, we focus on the method for radio map generation. For online phase, the probabilistic location algorithm and some accuracy enhancement solutions are presented. Then, two experiments are implemented to estimate the system and to study the relationship between the positioning environment and the positioning accuracy. Finally, two comparisons between our system and other typical WLAN based positioning systems are made. One is a comparison implemented in the two different positioning environments with the distance error criteria. The other is a comprehensive performance comparison with the new performance criteria.

The work in this chapter has been published in four conferences and presented in one workshop: 7th International Conference on Computer Systems and Applications 2009 (*ICCSA'09*), 8th International Conference on Networks (*ICN'09*), International Conference on Indoor Positioning and Indoor Navigation 2011 (*IPIN'11*), 10èmes Journées Doctorales en Informatique et Réseaux 2009 (*JDIR'09*), Journées CNRS Pôle Réseaux et Communications 2008 (*ResCom'08*).

Contents

2.1 Introduction

In chapter 1, the current main existing positioning systems are summarized and analyzed. The aim of these studies are to design an indoor positioning and tracking system that can provide accurate position estimate with relatively low computational complexity, so that it can be computed on mobile devices. The WLAN-Based Positioning System CMTA-WPS is such a system which is based on probabilistic location determination system and integrates Centre of Mass (CM) technique and Time Averaging (TA) technique.

As described in (Baala & Caminada, 2006a), (Baala & Caminada 2006b), CMTA-WPS is based on probability distribution of the signal calculated during the training phase. Unlike other systems collecting radio map from measurements, our radio map is generated by propagation model that takes as input the building topology and the WLAN network configuration. During the working phase, the mobile device detects a signal from each AP and uses the deployed position-determination model to calculate a real time position.

The structure of this chapter is organized as follows. First, the principle of CMTA-WPS is described, including offline phase and online phase. For offline phase, the two methods for radio map generation - site survey and propagation modelling - are discussed. For online phase, the probabilistic localization algorithm and some accuracy enhancement solutions are presented. Then, two experiments are implemented to test the performance of our system and to explore some kind of relationship between the setup of the positioning environment and the positioning accuracy. Finally, according to the conclusion from the above experiments we compare the performance of different positioning systems by the two different setups of the positioning environment. Moreover, based on the new performance criteria, a comprehensive performance comparison between our system and other typical WLAN based positioning systems is made.

2.2 Principle of CMTA-WPS

Our indoor positioning system CMTA-WPS is based on a WLAN-based indoor positioning system developed by the IBM China Research Laboratory (Xiang *et al.,* 2004) and integrates CM and TA strategies to improve the positioning accuracy. Generally, the mobile device makes use of the signal emitted from AP as the input for a positioning algorithm to infer a location. The model presented here reflects the correlation between the observed signal and position knowledge.

Let the set L denote the pre-selected positions (also called Marking Position i.e. MP) in a certain area and the set A denote the APs in the area. For each MP, m_i, the signal strength index s ($0 \le s \le 100$) (no unit on s) detected from AP j, follows a probability distribution $p_i^j(s)$, where:

$$\sum_{s=0}^{100} p_i^j(s) \qquad \textbf{(2.1)}$$

For any unknown location x, the authors assign a probability $P(m_i \mid O)$ to each MP m_i under observed signal O. Therefore, the position-determination problem is to find a MP m_i, at which the probability $P(m_i \mid O)$ is maximized. Mathematically, this probability can be represented as:

$$p(m_i/O)=\frac{P(O/m_i)P(m_i)}{P(O)} \tag{2.2}$$

Where $P(O|m_i)$ is the conditional probability of obtaining observation O at MP m_i; $P(O)$ is a normalized constant; and $P(m_i)$ is the prior probability of MP m_i being the correct position.

Since the model relies on pre-obtained knowledge, such as $p_i^j(s)$ and $P(m_i)$, the system works in two phases: the offline phase and the online phase.

2.2.1 Offline phase

In the so-called offline phase, signal strengths from multiple APs are recorded at predefined locations throughout the indoor space. The received signal strength vectors are saved together with the ground-truth locations where they are measured. Each entry (MP coordinates, RSS values and the corresponding identifiers of the received APs) is called *fingerprint* and is saved in a database called *radio map*. Since in the view of pattern classification these fingerprints in radio map are used to train the classifier, offline phase is also called training phase. Briefly, the objective of offline phase is to generate the radio map which serves positioning prediction on online phase. The radio map will be introduced more fully in next section.

2.2.1.1 Radio map

Radio map is the most important part in the indoor positioning system. The quality of radio map will directly determine the accuracy of positioning. Figure 2.1 illustrates the formation of radio map.

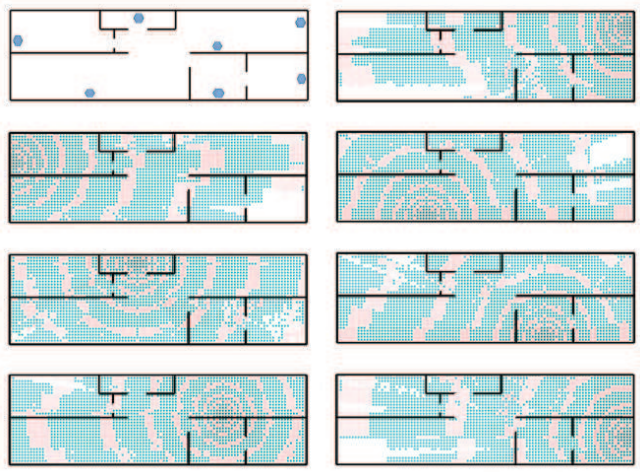

Figure 2.1 The formation of radio map

The top left graph in the figure shows the placement of APs and each point represents one AP. The following graphs describe the coverage of AP respectively. When these graphs fuse together, the radio map is formed. Namely, the radio map is the combination of all AP coverage information. In the actual operation, in order to be handled by a computer, a continue space is usually reduced to a

discrete space. Normally, an imaginary grid is placed on a scaled map of the experimental area and used to select different equidistant physical locations on the grid. Each grid node is called MP.

Currently, there are only few guidelines to choose the grid spacing. In (Baala & Caminada, 2006b), author varied the number of AP (1 to 5) and the number of MP (grid spacing values of 1m, 3m, 5m) in the experimented area to study how they affect system performance. A global positioning error indicator Global Error Ratio (GER) is used to evaluate these different scenarios. The result indicates that grid spacing should be chosen depending on the number of AP. In (King *et al.,* 2007), the author varied the grid spacing of the basic experiment from 0.5 meters stepwise by 0.5 meters until a spacing of 4.0 meters is reached. According to the analysis of this experiment result, the following conclusions are suggested: Although, a grid spacing of 0.5 meters leads to the best results, the amount of time required to collect the data for the training phase is hardly bearable if carried out by humans. So, to trade position error against time, a grid spacing between 1.0 and 2.5 meters is recommended by the author.

2.2.1.2 Site survey or propagation modeling

In the offline phase the major issue with practical implementation of RSS-based indoor positioning systems is how to create the radio map efficiently and accurately. Normally, there are two approaches to create the radio map: site survey (measurement based) and propagation modelling (model based).

In measurement based method, people walked to different locations in the building, and both the physical coordinates and the signal strength from each AP within range are measured and recorded at each location. In model based method, the signal strength at each location from all neighbouring APs are computed and recorded by a mathematical indoor RF signal propagation model. Obviously, measurement based generation method emphasizes the accuracy and reliability while model based generation method emphasizes the efficiency and effectiveness.

Choosing the radio map generation method is the first thing that we have to decide since it determines what the operation of the radio map shall be. For example, if an operator chooses measurement based generation method to create the radio map, selecting a grid spacing in this range should depend on the amount of time which he is willing to spend and the position accuracy which he is expecting. But if the operator chooses model based generation method to create the radio map, he faces no such problems.

Before comparing these two generation methods, it is firstly necessary to comprehensively analyze the RF indoor propagation. These analyses would help us to make informed decisions.

a) The radio wave propagation phenomena

There are five main phenomena in radio wave propagation: absorption, reflection, refraction, diffraction and scattering. The radio wave propagation can be considered as a combination of these five main phenomena (Rappaport, 1996).

Absorption

When a radio wave encounters and penetrates an obstacle, a portion of its energy is absorbed and converted into other energy. Inside a building, various obstacles attenuate the energy of the signal. These attenuations are generally greater than that associated with the atmosphere.

Reflection

Reflection is a feature of the radio waves. When a radio wave encounters an obstacle, all or part of the wave is reflected with a loss of power. There are two laws of reflection. First, the incident ray, the reflected ray and normal lie in the same plane at the point of incidence. Second, the angle of incidence equals the angle of reflection. Figure 2.2 illustrates this phenomenon.

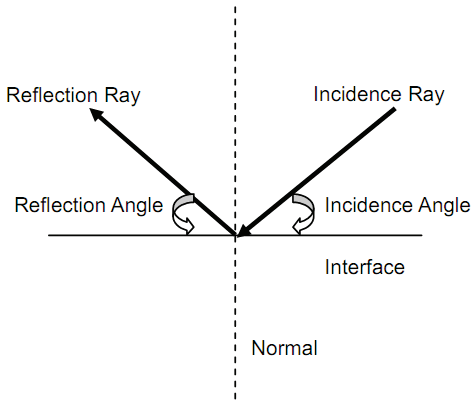

Figure 2.2 The reflection phenomenon

Refraction

Besides the reflection, the refraction phenomenon may happen when the radio wave enters a different environment. This is because the speed of the radio wave depends on the density of the medium where it spreads. Refraction changes the radio wave propagation trajectory as depicted in Figure 2.3.

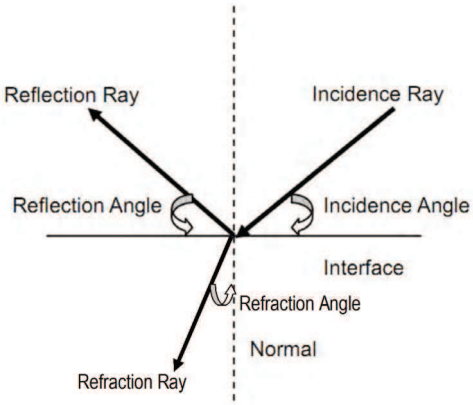

Figure 2.3 The refraction phenomenon

Snell's law is a formula used to describe the relationship between the angles of incidence and refraction which satisfies the following relationship:

$$\frac{\sin\theta_1}{\sin\theta_2} = \frac{n_2}{n_1} = \frac{v_1}{v_2} \qquad \textbf{(2.3)}$$

Where each θ is the angle measured from the normal, v is the velocity of radio wave in the respective medium and n is the refractive index of the respective medium. If the velocity of radio

wave is lower in the second medium ($v2<v1$), according to Snell's law the angle of refraction θ_2 is less than the angle of incidence θ_1. When the θ_1 reduces to zero, the refraction phenomenon is disappeared, only reflection phenomenon remains. This phenomenon is called Total Internal Reflection.

Diffraction

Diffraction refers to various phenomena which occur when a radio wave pass through the edges of the obstacle or a small opening. Figure 2.4 shows this phenomenon. The diffraction can be explained by Huygens' principle. If the size of the obstacle is smaller than the wavelength of the radio wave, the radio wave spreads around the edges of the obstacle and continues to propagate. If the obstructing object provides multiple, closely-spaced openings and the size of these openings are about the wavelength of the radio wave, the radio wave can produce of new Ring Waves which centre on these small openings and propagates in all directions.

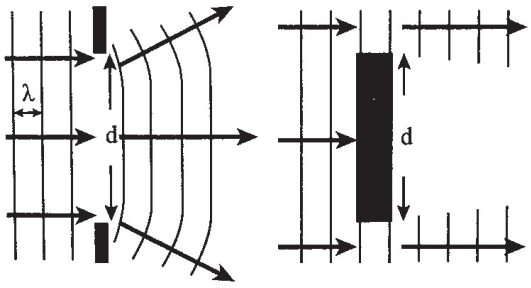

Figure 2.4 The diffraction phenomenon

Scattering

Scattering occurs when the medium through which the wave travels consists of objects with dimensions that are small compared to the wavelength, and where the number of obstacles per unit volume is large. Scattered waves are produced by rough surfaces, small objects, or by other irregularities in the channel.

b) The radio wave propagation effects

Various phenomena act on the radio propagation and produce different effects. There are four main effects in the radio propagation: Path Loss, Shadowing, Multi-path and Doppler (Seybold & NetLibrary, 2005).

Path Loss Effect

Path Loss Effect normally includes propagation losses caused by the natural expansion of the radio wave front in free space, absorption losses, when the signal passes through media not transparent to electromagnetic waves, diffraction losses when part of the radio wave front is obstructed by an opaque obstacle, and losses caused by other phenomena.

Shadowing Effect

Shadowing Effect is a phenomenon that occurs when a mobile moves behind an obstruction and experiences a significant reduction in signal power. Shadowing is dominated by the attenuation from blocking object and usually modeled as log-normal distribution.

Multi-path Effect

Multi-path Effect is the propagation phenomenon that results in radio signals reaching the receiving antenna by two or more paths. It is caused by reflection, diffraction and diffusion on the indoor scattering-rich obstacles. The effects of multipath include constructive and destructive interference, and phase shifting of the signal. This causes Rayleigh fading. The standard statistical model of this gives a distribution known as the Rayleigh distribution.

Doppler Effect

Doppler Effect occurs when transmitter and receiver have relative velocity. It can be described as the effect produced by a moving source of waves in which there is an apparent upward shift in frequency for observers towards whom the source is approaching and an apparent downward shift in frequency for observers from whom the source is receding.

All above are the abstract concepts of radio propagation theory and they can be used to explain the characteristics of radio propagation. However, since the indoor environment is much more complicated than the outdoor environment, it is very difficult to simulate indoor radio propagation by full analytical modelling or computer simulation. Thus, to get an insight into the RSS in the indoor environment, investigating the statistical properties of a single RSS set and the statistical properties of multiple RSS sets is an acceptable method. In fact the former researchers have made a few attempts and effort on one hand in such investigation. According to (Kaemarungsi & Krishnamurthy, 2004a), (Xiang *et al.,* 2004), we also did some experiments to analysis the RSS.

c) The statistical properties of a single RSS set

As we all know, the WLAN RSS appear in an irregular pattern due to the multi-path effect caused by reflection, diffraction and diffusion on the indoor scattering-rich obstacles. The phenomenon often degrades the performance of localization. In our investigation, two steps are implemented: one is trying to find a robust feature of WLAN RSS. The other is building and analyzing the RSS probability distribution from multiple APs at a static position. For the investigation, I implemented a stationary measurement experiment with three visible APs in one building of UTBM campus (building B in Figure 2.5). A 3-hour period of total 10,800 samples (the sample rate is one sample every second) was collected from each AP. The size of the building is about 120m x 40m and the material for external walls is beton and for internal walls is plaster.

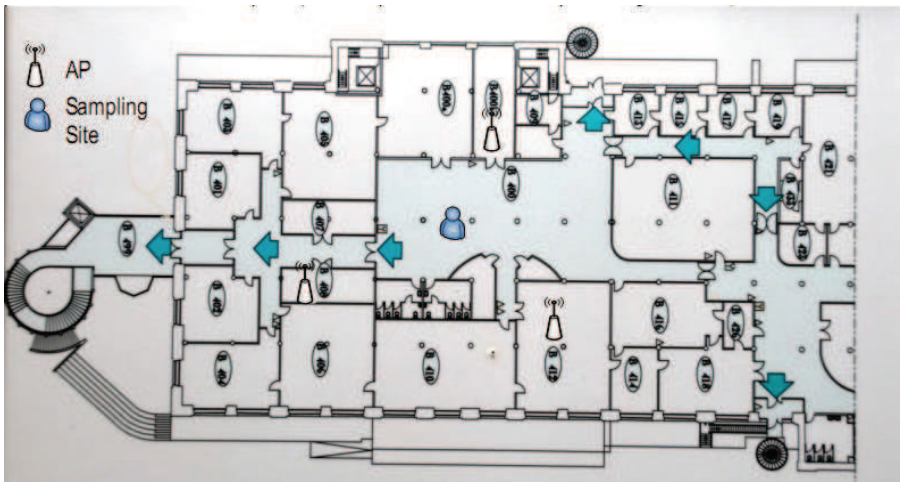

Figure 2.5 The setup of the measurement in one building of UTBM campus

To the best of our knowledge, only one solution called the average (median) filter can be found for finding a robust feature of RSS. In the average (median) filter treatment, RSS value is a linear combination of the signal intensity and an independent additive noise. In theory, the signal intensity should be a constant at a fixed location and the variation of RSS is only dominated by the additive noise. The decrease of variance of RSS results from the time average of RSS samples over a certain period of time since the additive noise is a zero mean process for all time. In our investigation, the test data is 1-hour period of total 3,600 samples from one AP. We average these samples on three different time windows 10 seconds, 1 minute and 5 minutes. According to the results, although the robustness of RSS feature is improving when the average time window is increasing, the RSS variation still exists. This is because the average in time domain does not eliminate the multi-path effect.

Since it is difficult to reduce or eliminate the RSS multi-path effect, the more feasible treatment method is to build the RSS probability distribution to store as many RSS features as possible. It was reported earlier that the RSS probability distribution is influenced by many factors, such as orientation effect, time effect, body effect, etc. In the second step, we only focus on two important effects: the orientation effect and the time effect.

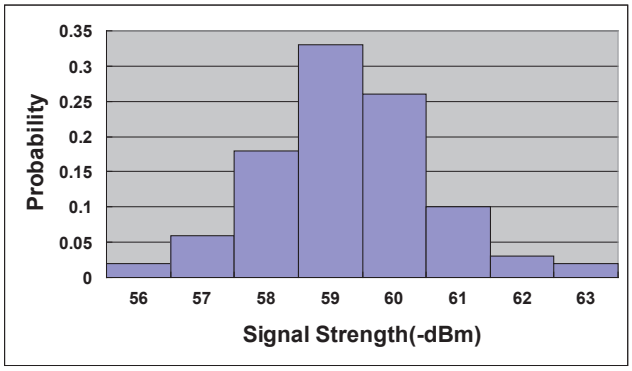

Figure 2.6 The short-term signal strength distribution

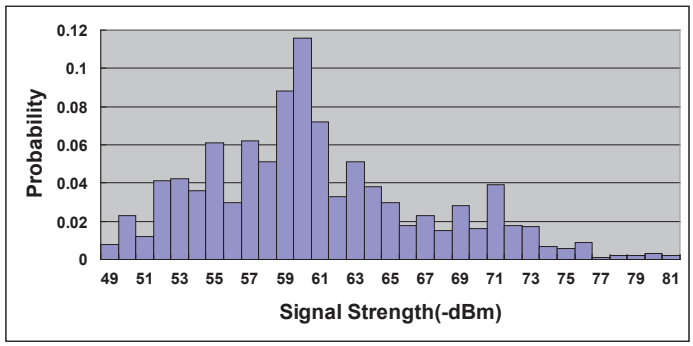

Figure 2.7 the long-term signal strength distribution

Considering the signal strength and signal variation, the samples from the second close AP are chosen. The short-term signal strength distribution is drawn by collecting 500 continues samples from above samples every second. The long-term signal strength distribution is built by collecting all 3-hour period of total samples. Figure 2.6 and Figure 2.7 show the short-term signal strength distribution and the long-term signal strength distribution from an AP at a fixed position respectively.

Some interesting observations can be concluded from these two figures:

These figures show that the measured signal strength at a fixed position varies over time. For the short-term signal strength distribution, all samples fall within the range of 56 to 63 -dBm. However, the variations of the long-term signal strength distribution can be as large as 33 dB. This phenomenon can be due to changes in the physical environment such as such as people presence, opening/closing of doors, changing humidity levels, and so on. The similar phenomenon has also been reported by many papers on WLAN signal propagation analysis (Xiang *et al.,* 2004), (Wang *et al.,* 2003).

In addition, the shape of the long-term signal strength distribution is very similar to the shape of the short-term signal strength distribution, which is nearly close to the normal distribution, except that there is a heavy "tail" in the long-term signal strength distribution. This is quite reasonable. The similarity indicates that some important distribution characteristics can be obtained in the short-term signal collection procedure. And since more samples are collected in the long-term analysis, a greater number of scarcely evident signal propagation characteristics are obtained in the collection procedure, which results in the heavy tail.

Besides the effect of dynamic environmental changes, the effect of the antenna receiver orientation on the signal strength is mentioned in many papers. Be aimed at this problem, we made relevant investigation. We collected a 10 minutes period of samples from one AP in four orientations which are reported in Figure 2.8.

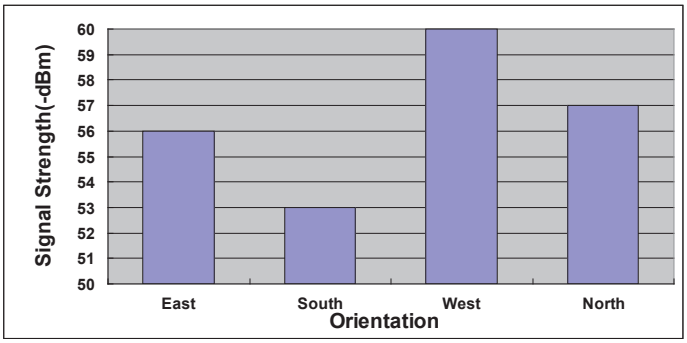

Figure 2.8 Effect of orientation on signal strength

The result indicates that there is a correlation between orientation and measured signal strength. There was a variation of about 1 to 7 dB among the different orientations. Some papers believe that the orientation information can be used to improve the positioning accuracy by treating different orientations of one location as different logical positions in a positioning system. COMPASS proposed in (King *et al.,* 2006) is a good example of signal orientations application. In the radio map of COMPASS, each reference point has fingerprinting with different orientations. COMPASS can provide the orientations of the users so that these directed fingerprinting becomes really useful. However, we are rather pessimistic about that. According to our research, such useful but weak signal strength characteristics can be easily masked by other interferes. For example, the standard deviations of signal strengths on different orientations in Figure 2.8 are 7.8, 8.2, 8.8 and 9.6 dB respectively. All of them are larger than the maximum variation of different orientations 7 dB. Moreover, we also did the experiments to compare the accuracy with oriented device and with

non-oriented device using a hybrid indoor positioning system (Lassabe *et al.,* 2010). There was nothing to suggest that the orientation information can be used to improve the positioning accuracy.

d) The statistical properties of multiple RSS sets

This investigation is to analyze the dependency of multiple RSSs from multiple APs. In WLAN communication, the interference on QoS occurs when there is another AP transmitting in the same frequency channel. However, are the RSS from multiple APs actually independent? Countering this problem, three sets of RSS sample from three APs are used to calculate correlation coefficient between each pair of RSS sets. A correlation coefficient indicates the extent to which two variables are related. It can range from -1.0 to +1.0. A positive correlation coefficient indicates a positive relationship and a negative coefficient indicates an inverse relationship when 0 means no correlation. The formula to compute a correlation coefficient $\rho_{X,Y}$ between two random variables X and Y with average values μ_X and μ_Y and standard deviations σ_X and σ_Y is defined as:

$$\rho_{X,Y} = corr(X,Y) = \frac{\mathrm{cov}(XY)}{\sigma_X \cdot \sigma_Y} = \frac{\frac{1}{n}\sum_{i=1}^{n}(x_i - \mu_X)(y_i - \mu_Y)}{\sigma_X \cdot \sigma_Y} \qquad \textbf{(2.4)}$$

For simplicity, we only consider 300 collected continue samples in five minutes from these three APs and calculate the correlation coefficients of each AP pair as shown in Table1.

TABLE1 THE CORRELATION COEFFICIENTS OF EACH AP PAIR

AP Pair	AP1, AP2	AP1, AP3	AP2, AP3
Correlation Coefficient	-0.0097	0.01	-0.069

The computational result shows that all the correlation coefficients between pair of APs fall in the intervals from -0.01 to 0.01. Therefore, we can conclude that the RSS from the APs are uncorrelated. This is due to Carrier Sense Multiple Access with Collision Avoidance (CSMA/CA) mechanism which is used in 802.11 based WLANs.

The above analysis of RSS samples showed that the variation of RSS is highly related to the time of day and the propagation environment. Thus a location measurement-based method is often used instead of the radio propagation model method, as it can give better estimates of the user locations for indoor environments. However, two problems in the fingerprinting system nowadays have been challenged on the way from laboratory to practical application.

Firstly, generating a measurement-based radio map is an exhaustive, time consuming and cumbersome effort. The RSSs from all APs on all MPs should be collected in a certain period of time. Then these fingerprint data should be arranged and classified. It could be argued that the RSS collection time sustains double-digit growth as the area increases, thus the problem is more serious when the area of concern, such as a shopping mall, is very large. Furthermore, in the fingerprinting systems the size of the data base is an important factor which influences the computation load during the online phase. A larger data base requires a higher power consumption and a longer data transmission time in a mobile-based system. Many research institutes did a lot of substantive work in an effort to remedy this problem. In (Lassabe et al., 2005) and (Kwon *et al.,* 2004), a hybrid method

that combines the strengths of the propagation model and fingerprinting methods is proposed. The idea is to achieve accuracy comparable with fingerprinting, but requiring a much smaller data collection effort. In (Roos *et al.,* 2002), author introduces a probabilistic technique to reduce the number of training points by dividing the environment into physical segments. In (Chen *et al.*, 2010), the author address the RSS-based localization problem in WLANs using the theory of compressive sensing (CS), which offers accurate recovery of sparse signals from a small number of measurements by solving an l1-minimization problem. The implementation has shown that the proposed system is able to estimate the location accurately by using only a small number of RSS measurements. In addition, such system does not require to collect a huge number of RSS time samples, and thus it consumes less memory and computation resources.

Secondly, as mentioned before, any major changes in the environment (the human activities, movement of large pieces of furniture or appliances, adding or removing walls) are dynamic, while a fingerprint is bound to the indoor environment description and infrastructure at the time the fingerprint was generated. Thus dynamic environmental changes means that signal strengths collected at one time may not accurately predict the signal strengths at other times. As a result, positioning accuracy decreases and the time and effort in building the radio map is essentially wasted. In other words, this process to generate a radio map is very sensitive to changes in the environment and possible sources of interference in the building. Since in this problem the radio map should be calibrated, this problem is also called calibration effort problem.

Nowadays how to reduce the calibration effort has always been one of the indoor positioning important tasks. In (Chen *et al.,* 2005), (Chen *et al.,* 2010), (Jie *et al.,* 2005), the sensor network to assist location system is utilized for adapting the radio dynamically. The unstable factors such as open/close doors and humidity are detected by the sensors and thus a collaborative positioning system is provided by such context-awareness radio map. While this approach does capture the signal strength changes, it is not well suited to ubiquitous positioning because only few buildings can be expected to accommodate the required, additional hardware. In (Hansen *et al.,* 2010), the author proposed the algorithmic strategies for dealing with this task. Instead of additional sensors, users upload fingerprints to an ever-evolving radio map with the aim of providing up-to-date signal strength information. Two distinct algorithms are considered for adapting to different signal strengths caused by dynamic changes in the environment. The first algorithm uses the notion of interval trees. Here, the fingerprints supplied by users are sorted according to the time of day they were measured and split into several subtrees that capture the characteristics at different time periods. The second algorithm does not explicitly consider the temporal aspect, but instead uses a divisive clustering technique with a single linkage criterion to group similar fingerprints together. In (Shih-Hau *et al.,* 2008), the author proposed a novel approach to extract the multipath resistant information from the temporal trajectory of the measured RSS in an indoor WLAN environment so that the multipath effect can be mitigated efficiently. Experimental results show that the mean of error is reduced by 42%, and the standard deviation of error is reduced by 29% on the average. Furthermore, the results show that the size of training samples can be greatly reduced in the proposed architecture. In (Sheng-Po & Yu-Chee 2008), the author proposed a scrambling method to exploit temporal diversity and spatial dependency of collected signal samples. Based on temporal diversity, its basic idea is to enlarge the comparison space by recombining observed samples in a short period of time. Through scrambling, samples with less interference are expected to appear. Then, spatial dependency will

exploit the moving trajectories of objects to select a better location estimation. In (Weber *et al.,* 2010), the research project is to solve calibration effort problem by appropriate RF engineering and optimized methods. The leaky feeder cables which are designed to provide homogeneous coverage throughout a building are applied for indoor localization.

Despite a large amount of works have been made on reducing the laborious site-survey and increasing the radio map robustness, the effectiveness is limited or some additional hardware costs are introduced. Thus model based generation method also became a current research hot spot. Propagation model can automatically generate the radio map, and also account for any changes in the environment. This would significantly reduce the effort and cost for indoor localization systems. There is only one weakness: accuracy. In fact, the applications of propagation model are not confined to the indoor positioning system, and other kinds of fields such as radio planning also need to use it. Thus various propagation models have been proposed and various propagation simulation software have been developed. With the development of science and technology, the accuracy of propagation models increase constantly.

Finally, we have a tendency to choose model based method to generate our radio map with the following three main reasons:

Firstly, we believe that the model based generation method is the future development trends. With the popularity of the indoor positioning service, large-scale radio map generating is unavoidable. Obviously, measurement based generation method is generally only useful on small-scale radio map generation. Consequently only the model based generation method would be suitable for large-scale radio map generation. Currently the wide application of the model based generation method in large-scale WLAN planning and design have proved this point.

Secondly, according to some reports and our experiments, in most situations, the errors of the model based generation method can be steadily controlled within several meters. In fact, this accuracy is within the demand for most indoor location-based services. Moreover, if using the high-level commercialized propagation simulation software or hybrid propagation model to generate the radio map, the error should be reduced further.

Thirdly, the purpose of our study is not limited to develop an indoor positioning system. Our study ultimate aim is to model the indoor positioning problem as an optimization problem so that introduces the indoor positioning improvement into WLAN planning. During the modelling, a series of large-scale radio maps with different AP parameters are necessary. Generating these radio maps by site-survey is unrealistic since it needs too much time and too many labours. Thus model-based method is our unique choice.

After determining the radio map generation method, the next problem is to find an appropriate propagation model. In the next section, the key of model-based generation method, the propagation model, will be presented in detail.

2.2.1.3 The indoor propagation model

To accurately determine an indoor location using wireless signals as references, an accurate indoor model of signal propagation is necessary. The indoor propagation channel differs considerably from the outdoor one. The distance between transmitter and receiver is short due to high attenuation caused by the internal walls and furniture and often also because of lower transmitter power. The

path loss and the time variation is more complicated. Although it is from earliest time that scholars have studied WLAN propagation model and various kinds of indoor propagation models have been proposed, the problem of finding the right balance between the computational load and accuracy remains an open issue. Currently, two kinds of propagation models are widely used for indoor environment: the empirical models and the deterministic models.

a) The empirical models

The empirical models are based on statistical information. Wide databases are firstly built from exhaustive measurement campaigns and then empiric evolving laws are extracted as functions of meaningful parameters such as distance, frequency, base station height, and others. Four types of empirical indoor models have been investigated in this section. These models allow predicting the average behaviour of waves in typical environments but surely not accurate predictions in each specific area.

Free Space Model

The free space model is a theoretical model. In free space, it is clear that the only one factor influencing RSS values is the distance between emitter and receiver, as this distance causes attenuation in RSS values. This attenuation is known as path loss, and it is modelled to be inversely proportional to the square of the distance between the emitter and the receiver. Received power P_R and distance d vary according to the relation:

$$P_R \propto \frac{1}{d^2} \tag{2.5}$$

And this relation can be determined by the Friis equation (Seybold, 2005):

$$\frac{P_R}{P_T} = G_R G_T \left(\frac{\lambda}{4\pi d} \right)^2 \tag{2.6}$$

Where: P_R and P_T are respectively the power available at the receiving antenna and the power supplied to the source antenna. G_R and G_T are respectively the receiver antenna gain and the transmitter antenna gain. λ is the carrier wavelength. d is the transmitter-receiver distance.

Usually, the quantity of propagation loss is typically represented in decibels and is defined as the logarithm of the quantity received power divided by transmitted power, as follows:

$$PL_{dB} = 10\log_{10}\left(\frac{P_R}{P_T}\right) = 10\log_{10} G_T + 10\log_{10} G_R - 20\log_{10} f - 20\log_{10} d + 20\log_{10}\frac{3*10^8}{4\pi} \tag{2.7}$$

In order to represent free space path loss as a function of a distance d from the transmitter, power at a reference distance d_0 from the transmitter is used as follows:

$$P_{dBm}(d) = P_{dBm}(d_0) - 20\log_{10}\left(\frac{d}{d_0}\right) \tag{2.8}$$

Usually d_0 is equal to 1 meter and then the above equation can be expressed by:

$$P_{dBm}(d) = P_0 - 20\log_{10}(d) \quad \textbf{(2.9)}$$

Where, P_0 is a reference loss value for the distance of 1 m.

Using this model, free space propagation loss can be determined when only the distance from the transmitter and the propagation loss at a reference distance from the transmitter are known.

However, this type of propagation model is only good in theory. Since in a real environment, received signal strengths are affected by walls, people, furniture, and other objects, as well as multipath phenomenon, it is often too difficult to implement in practice if a high degree of accuracy is required.

One-Slope Model (1SM)

This model is based on the free space model, but attempts to take into account the characteristics of indoor non-free space environments. It is the easiest way to compute the average signal level within a building without detailed knowledge of the building layout. The One Slope Model is very fast, because it depends only on the distance between transmitter and receiver. The only parameter which is considered is therefore the path loss exponent. The received power $P_{dBm}(d)$ which is d meters away from a specific AP is given by (Seybold, 2005):

$$P_{dBm}(d) = P_{dBm}(d_0) - 10n\log_{10}\left(\frac{d}{d_0}\right) \quad \textbf{(2.10)}$$

Where $P_{dBm}(d_0)$ is the signal power at a reference distance d_0 for the antenna far field. n is the path-loss exponent and is varied depending on the environment. The higher value exhibits more loss in indoor environment. Table 2 shows typical values used for various environments. Figure 2.9 presents this model.

TABLE 2 THE PATH-LOSS EXPONENT IN VARIOUS ENVIRONMENTS

Environment	Path-loss exponent
Free Space	2.0
In-Building line of sight	1.6-1.8
In-Building One-Floor non-Line of Sight	2.0-4.0
Obstructed In -Building	4.0-6.0

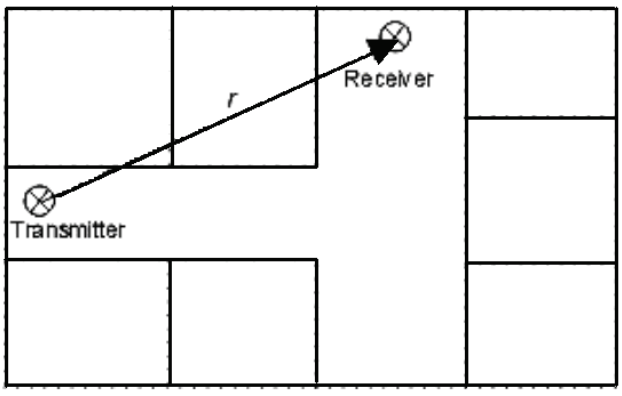

Figure 2.9 One Slope Model

This model can be improved by combining the simplified path-loss model with the effect of shadowing fading and multipath fading. The formulation for improved model is given by (Goldsmith, 2005):

$$P_{dBm}(d) = P_{dBm}(d_0) - 10n\log_{10}\left(\frac{d}{d_0}\right) - \eta_{dB} \quad \textbf{(2.11)}$$

Where η_{dB} is the fading factor which is valued by the statistics of the receive signal. Two fading mechanisms can be identified: long term fading (slow fading) and short term fading (fast fading). The long term fading arises when there are large reflected and diffracted objects along the transmission path. The long term fading can be caused by events such as shadowing. The indoor long term fading is often modelled using a log-normal distribution with a standard deviation. For the short term fading, the signals associated with each path are added vectorially at the receiver, thus giving rise to severe signal envelope fluctuations. The short term fading occurs in densely obstructive areas and are mainly due to scattering (multipath fading). The short term fading has been observed to nearly follow Rice and Rayleigh distributions.

Although this model is adaptable to various environments, its main limitation is that it treats buildings as if they are homogeneous structures. However, the topologies and materials of real buildings are irregular. To overcome this limitation, Multi-Wall Model is proposed.

Multi-Wall Model

Multi-wall model is a semi-empirical model that attempts to account with the heterogeneous make-up of buildings. This model gives the path loss as the free space loss added with wall losses and floor losses of the direct path between the transmitter and the receiver, represented by (Wang *et al.,* 2003):

$$\begin{aligned} P_{dBm}(d) &= L_{FS} - \sum_{i=1}^{p} WAF_i - \sum_{j=1}^{q} FAF_j \\ &= P_{dBm}(d_0) - 20\log_{10}\left(\frac{d}{d_0}\right) - \sum_{i=1}^{p} WAF_i - \sum_{j=1}^{q} FAF_j \end{aligned} \quad \textbf{(2.12)}$$

where L_{FS} is the free space loss for the distance d_0 between transmitter and receiver antennas. p is the number of walls intersected by the path, q is the number of penetrated floors by the path, WAF_i is the wall attenuation factors of i^{th} wall, and FAF_j is the floor attenuation factors of j^{th} floor. The attenuation factor for a floor or wall is a measure, in decibels, of the path loss incurred by a signal that passes through that surface. Figure 2.10 presents this model.

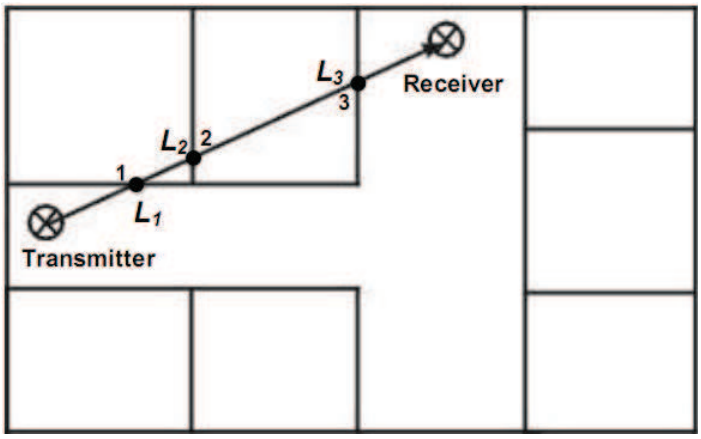

Figure 2.10 Multi-wall Model

This model is an improvement over the one slope model in that it distinguishes between indoor free space and solid objects. This model may perform well in certain circumstances. However, it suffers from limitations. This model assumes the RSS is distributed isotropically from the transmitter. It does not include propagation effects such as distance dependence of the path-loss exponent, angle dependence of the WAF, or reflection and diffraction. As a result, prediction accuracy can be poor in certain parts of a building and especially at large distances from the transmitter.

New Empirical Model

To improve the accuracy of the multi-wall model while retaining its simplicity, in (Kwok-Wai *et al.,* 1998), authors have proposed a model called New Empirical Model that takes into account angles of incidence on walls and floors, as well as a commonly observed break point phenomenon. In comparison with multi-wall model, this model has three main additions:

The first addition is to consider the angle dependence of attenuation factors. When electromagnetic radiation is incident on a wall or floor, most power are not normal to the wall or floor. Angle dependence of attenuation factors makes wall attenuation dependent on the angle of incidence and can capture this effect.

The second addition is to consider the break point phenomenon. At distances further away from the transmitter, however, the propagation loss increases significantly as the electromagnetic waves become obstructed by the ceilings or walls of the rooms in the building. The distance at which this transition in propagation loss occurs is referred to here as the break point.

By incorporating the angle dependence of attenuation factors and the break point effect into multi-wall model, an improved model with very little increase in computational effort is given by:

$$P_{dBm}(d) = P_{dBm}(d_0) - 10n_0 \log_{10}\left(\frac{d}{d_0}\right)U(d_{bp} - d) - 10\left[n_0 \log_{10}\left(\frac{d_{bp}}{d_0}\right) + n_1 \log_{10}\left(\frac{d}{d_{bp}}\right)\right]U(d - d_{bp}) - \sum_{i=1}^{p}\frac{WAF_i}{\cos\theta_i} - \sum_{j=1}^{q}\frac{FAF_j}{\cos\theta_j} \quad \textbf{(2.13)}$$

Where $U(.)$ is the unit step function: $U(d)=0$ if $d<0$, $U(d)=1$ if $d \geq 0$. There are two path-loss exponents n_0 and n_1. The first exponent models losses at distances d between the reference distance d_0 and the break point distance d_{bp}. The second exponent models losses at distances d greater than

the breakpoint distance d_{bp}. *p, q, WAF, FAF* are defined as in the multi-wall model. The angles θ_i and θ_j are angles of incidence between the propagation path and the surfaces it passes through.

The last addition is to consider the waveguide effect. In practice, propagation guided by corridors will sometimes provide an indirect path, which may be significantly greater than the propagation loss predicted from the straight-line path between the transmitter and receiver. One level of diffraction from corners is utilized to try and approximate or compensate the indirect path. The mainly drawback of this propagation model is that multiple-paths are not considered well and the path-loss remains a function of the transmitter-receiver distance.

b) The deterministic models

Most empirical propagation models in indoor scenarios are mainly based on the direct ray attenuation and some empirical parameters of the environment, thus some effects such as multi-path are difficult to be correctly reflected. Deterministic models are calculation methods which physically simulate the propagation of radio waves. Therefore the effect of the environment on the propagation parameters can be taken into account more accurately than in empirical models. Furthermore, with the deterministic model, it is possible to predict several propagation parameters. For example, the path loss, impulse response and angle-of-arrival can be predicted at the same time. Nowadays, several deterministic models have been proposed. Among them, Ray Tracing model is the most commonly used.

Ray Tracing model

The conventional ray tracing approach involves a number of rays launched at the transmit antenna in specified directions. For each ray its intersection with a wall is determined and the incident ray is divided into a wall penetrating ray and a reflected ray. Each of them is traced to its next intersection and so on. A ray is terminated when its amplitude falls below a specified threshold, or a chosen maximum number of reflections are reached. But this accuracy is obtained at the price of a high computational load. Indeed, this computational load is proportional to the number of launched rays and increases exponentially with the number of reflections each ray undergoes. Furthermore, as angular criteria are evaluated during the ray-optical prediction, the orientation of walls is extremely important. Small inaccuracies in the databases lead to totally different prediction results. The accuracy is also obtained at building databases with very high accuracy dimensions of building topology and very detailed description of the material properties. They are very difficult to obtain at reasonable costs and must be updated.

Currently, a large bulk of recent papers focused on trade-off between the accuracy and the computational complexity. In (Wlfle *et al.,* 2005), the Dominant Path Model is proposed, which try to meet these requirements: not depending on each micro detail, only focusing on the dominant paths and simple calibration. The Dominant Path Model can be subdivided into two steps: determination of the dominant paths (geometry) and prediction of the path loss along these paths. In (Suzuki & Mohan, 2002), (Aguado Agelet *et al.,* 2000), (Tetsuro & Teruya, 2002), their approach is based on the computation of a visibility graph aiming at reducing the time-consuming search of rays and walls intersections. The dominant path model is then obtained by removing all paths excepted the one providing the most power. In (Pechac & Klepal, 2001), the semi-deterministic model using a combination of deterministic ray-launching techniques and a stochastic approach to provide efficient predictions was proposed. In this approach, the main signal paths, i.e. direct path and most important

reflected and diffracted rays are calculated in a deterministic way while more complicated phenomena are taken into account by using empirical factors.

Finite Difference model

Finite Difference model simulates the electrodynamics based on the Maxwell's wave equations. ParFlow as one of such models is proposed in (Chopard *et al.,* 1997). This model can taken into account all propagation effects including reflection and diffraction naturally but the required spatial resolution is in turns theoretically very high. To reduce the computational load, the ParFlow theory is firstly transposed in the frequency domain leading to the Frequency Domain ParFlow (FDPF) approach as described in (Gorce *et al.,* 2003).

This Frequency Domain ParFlow model appears to suit well the indoor environment. Firstly, the computational load does not increase with the number of reflections. Secondly, any shape of obstacle can be easily handled. Thirdly, both accuracy and computational load can be accepted for practical application.

According to the previous introduction, it appears clearly that the empirical propagation models suffer from a lack of accuracy, while the deterministic propagation models need to balance accuracy with computational load requirements.

Our path loss predictions are intended to be used in indoor position system testing. For the testing purpose it is true that accuracy is the primary consideration. For the modelling purpose, the computational load is expected to be low.

It is obvious that ray-tracing models have the capability to predict accurately the indoor propagation if the number of reflections is very high and if diffraction is considered, but the computational efficiency of algorithms is the big problem. After taking various factors into account, choosing propagation model will follow a two-step approach. In the first step, a simple and appropriate empirical model is chosen to test the accuracy of our indoor positioning system. In the second step, if the accuracy of indoor positioning system is accepted, indoor positioning system modelling will continue to be implemented; otherwise an accuracy deterministic propagation model will be chosen and the Frequency Domain ParFlow model seems to be the better choice.

Finally, we decided to use multi-wall model which requires a low computational load and is easy to achieve. Indeed, the later test proved that this model is basically accurate and reliable. Thus choosing an accuracy deterministic propagation model will be our future works.

2.2.1.4 The improvement of the propagation model

The RSS obtained from propagation model is a single value, but the RSS in the real world is variable. Thus the propagation model should be improved to be adapted to the real environment and to reduce the positioning error. In this section, the improvement of the propagation model is discussed in three aspects.

a) Signal-distribution simulation

In indoor positioning system, the user most likely position is determined by combining the outputs of the propagation model and the measurements from the device Wi-Fi adapter. While differences between the simulation and actual measurements contribute unavoidable errors to this system, additional variability exists due to the inconsistent nature of Wi-Fi signal strengths.

Translating the signal value from propagation model to signal distribution is a good solution for this problem. Usually, the statistical properties of signal distribution are considered as a Gaussian probability density function whose PDF is of the form:

$$P(x) = \frac{1}{\sigma\sqrt{2\pi}} e^{-\frac{(x-\mu)^2}{2\sigma^2}} \quad \textbf{(2.14)}$$

In which μ is the average signal strength value at the location and σ is the standard deviation of the measured values. In this application, the coefficient term can be dropped due to the fact that a scalar multiplication of the entire distribution will have no effect on the location of the maximum or its value relative to other positions. The distribution becomes:

$$P(x) = e^{-\frac{(x-\mu)^2}{2\sigma^2}} \quad \textbf{(2.15)}$$

However, according to our previous RSS analysis, this distribution only simply reflects the short-term signal strength distribution, the statistical properties of the long-term signal strength distribution doesn't clearly reflect. A signal-distribution model proposed by IBM research solved this problem perfectly. They found that the shape of the long-term distribution is smoother than that of the short-term distribution. Moreover, the long-term distribution has a heavy tail because more weak samples are detected during the long-term data collection. Motivated by these analyses, they proposed a scheme to transform the short-term signal strength distribution into the long-term signal strength distribution. The scheme is composed of three steps (Xiang *et al.,* 2004):

Step 1: the short-term signal creation procedure

According to the author's idea, the short-term signal distribution is obtained by scanning the signal from each detectable AP at each reference point. However, we use the output of the propagation model instead of a series of RSS measurements. In fact our signal distribution can be seen as an extreme case of the short-term signal distribution, namely one sample short-term signal distribution.

Step 2: smoothing probability distribution shape

To smooth the shape of the former obtained signal distribution, a shaping filter is designed to obtain $p_i^j(s)$ the shaped probability distribution of the AP *j* at position *i*:

$$p_i'^j(s) = \frac{\sum_{k=1}^{K} e^{-\alpha\left(\left|s-o_j^k\right|\right)}}{\sum_{s=0}^{100}\sum_{k=1}^{K} e^{-\alpha\left(\left|s-o_j^k\right|\right)}} \quad \textbf{(2.16)}$$

Where s is the signal strength and K is the number of scanning operations. In our case, $k=1$. o_j^k represents the signal strength of the AP j in the k^{th} scanning operation. α is a control parameter. Usually, α is chosen as 2.

Step 3: adding heavy tail characteristics

The occasional weaker signal characteristic cannot be revealed by a short-term signal distribution. Therefore, a tailing filter is applied to the probability distribution trained from Step 2:

$$p_i^j(s) = \frac{p_i''^j(s)}{\sum_{s=0}^{100} p_i''^j(s)} \tag{2.17}$$

Where:

$$p_i''^j = \begin{cases} p_i'^j(s) & s < s_0 \\ p_i'^j(s) \times e^{\beta(s-s_0)} & s \geq s_0 \end{cases} \tag{2.18}$$

The signal strength threshold s_0 satisfies:

$$\sum_{s=0}^{s_0} p_i'^j(s) \leq \gamma \tag{2.19}$$

And:

$$\sum_{s=0}^{s_0+1} p_i'^j(s) > \gamma \tag{2.20}$$

Where α, β and γ are the control parameters and are obtained experimentally.

Through these three steps, the probability distribution shape $p_i^j(s)$ is as it is obtained with very large number of measurements. Figure 2.11 shows a real curve of these three steps from computation with our data.

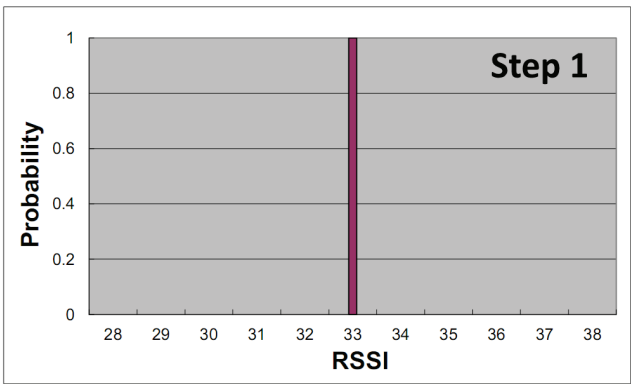

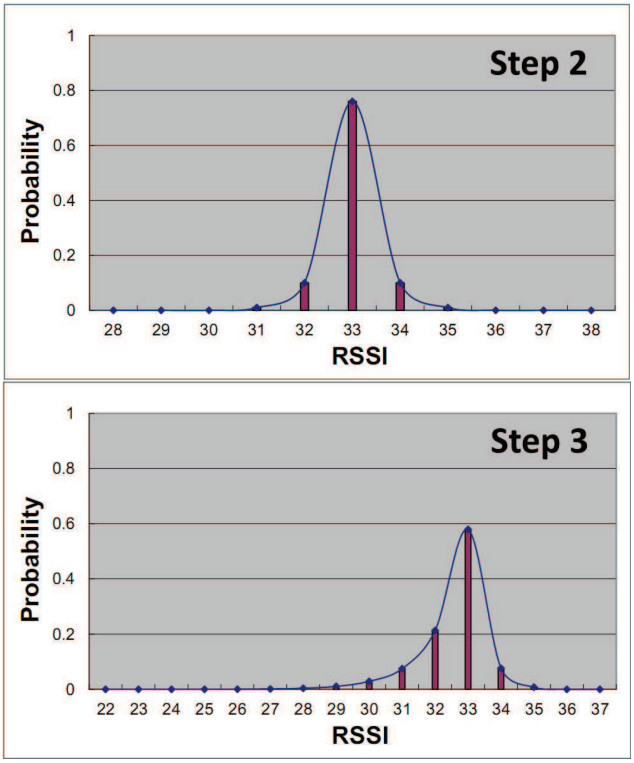

Figure 2.11 Real curve of three steps from data

b) Environment calibration

In indoor environments, we can observe a wide variation of RSS measurements and the trend persists at different time scales. These dynamics are caused by a number of environmental factors, and asymmetric non-Gaussian noise. It makes the indoor positioning system inaccurate. To overcome this problem wireless location systems need the calibration of the propagation model.

The calibration works in two phases: the offline phase and the online phase. The objective of offline calibration is to characterize the path loss and the noisy wireless channel affected by multipath and fading effects. In the offline calibration, the training RSSs are measured at some points in the area of interest and used to estimate the propagation model parameters. However, these parameters don't always remain consistent from the offline phase to the online phase in practice. Thus the online calibration is also needed to detect (and handle) the dynamic of the temporal propagation originated by unstable environmental conditions (such as humidity), space reorganization (e.g. furniture re-arranged or open-closed doors) and people's movement (temporal flow, human clusters around the mobile target, etc.). Generally a good online calibration should satisfy the following requirements:

Exploiting information without requiring human operators.

Adapting the system performance to real time environment.

No additional devices.

Currently, a series of research in indoor localization is devoted to propose solutions with such automatically real time online calibration. Through analysis and comparison of these methods, the

methods proposed in (Bernardos *et al.,* 2010), (Lim *et al.,* 2006) , (Moraes & Nunes, 2006), (Gwon & Jain, 2004) attract us. These methods have the similar idea:

The online calibration depends on APs which have well known position on the map and serve as anchors. These APs record the received signal strength (RSS) of beacon broadcasts from each other periodically and automatically. These captured real-time RSS data will train a propagation model by using a Least Mean Square (LMS) algorithm. Our general approach shares this basic idea, and applies it to our propagation model. The detailed process is as follows:

Denote $d_{i,j}$ as actual distance between anchors i and j, $p_{i,j}$ as the number of wall crossed by the direct path, we obtain *RSS'(i,j)* an estimation of the actual RSS:

$$P_{dBm}(d) = P_{dBm}(d_0) - 10n_{ij}\log_{10}\left(\frac{d_{ij}}{d_0}\right) - \sum_{i=1}^{p_{ij}} WAF_i + N(0,\sigma_{ij}) \qquad \textbf{(2.21)}$$

The additional parameter n_{ij} is the parameter of the channel model and *N(.)* is a zero-mean Gaussian random variable with standard deviation σ_{ij}. The signal power at a reference distance d_0 from the antenna $P_{dBm}(d_0)$ and the wall attenuation factor WAF should be estimated in a free space and only depend on physical properties of the devices hardware and wall respectively. Thus they are not affected by the environment and can be estimated a priori. During the online calibration phase we only estimate the additional parameters n_{ij} and σ_{ij}.

The least mean square error $\varepsilon_{i,j}$ is formulated as:

$$\varepsilon_{i,j} = \sqrt{(RSS - RSS')^2} \qquad \textbf{(2.22)}$$

$\varepsilon_{i,j}$ can be minimized by recursively adapting the constant parameters of the propagation model, n and σ.

In such online calibration the LMS algorithm accuracy is related to the number of APs and their geometrical distribution. Thus for properly utilizing the online calibration some restricted conditions should be introduced. For example, the online calibration is implemented only when the least mean square error $\varepsilon_{i,j}$ is larger than a certain value and the number of APs and their geometrical distribution are appropriate.

c) Device calibration

In indoor positioning system, the client devices are various, like mobile phones, laptops, personal digital assistants and MP3 players and different client devices have Wi-Fi modules and drivers. As Wi-Fi positioning relies on measured absolute RSS values, the characteristics of the different modules have to be considered. However, it tends to be ignored since many people think that such value difference is slight. In (Vaupel *et al.,* 2010), the measurement characteristics of different mobile Wi-Fi devices was studied in detail. In the research, the devices have been placed next to each other for several hours during night to exclude environmental changes. In Figure 2.12 the measured discrete RSS values of four mobile devices are depicted for one AP.

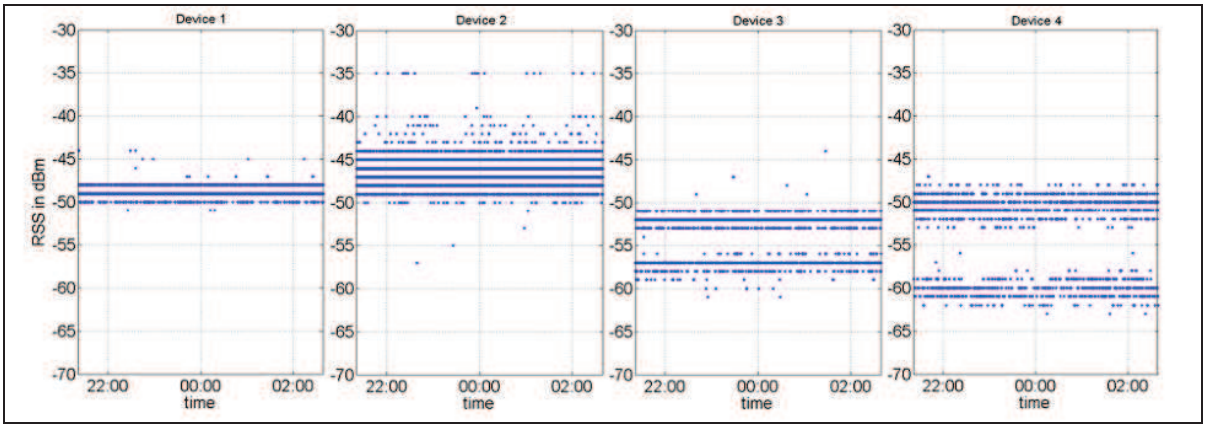

Figure 2.12 Stationary RSS measurements of one AP measured with different mobile devices

Clearly, the measured RSS values differ significantly. Thus, in order to achieve similar positioning results with different mobile devices, there is a need for classification of the hardware characteristics to enable calibration.

2.2.2 Online phase

During the online phase, the device, carried by a mobile user collects online RSS readings from detectable APs, which are then used together with the fingerprint database to estimate the device location. Unlike the visible divisions in the choice of radio map generation method in offline phase, the most RSS indoor positioning system choose a pattern classification approach to reflect the correlation between the observed signal and position knowledge. Among these approaches probabilistic approach is the most popular due to its strong anti-interference performance. We also use such probabilistic position determination model to calculate a position in real time. Depending on the type of calculations, it uses only pure signal probability distribution under stationary mode or also applies topology knowledge and some additional solutions to find a mobile device location under tracking mode.

2.2.2.1 Stationary mode

The stationary mode is the basic mode of indoor positioning system. In this model, the current estimate and the previous estimation are uncorrelated. In other words, the previous estimates cannot correct the current estimate. This situation generally occurs when the user is stationary. Thus in the stationary mode, the $P(m_i)$ which is the prior probability of position m_i being the correct position is set as a constant. The system returns the location of the most probable MP as a result.

2.2.2.2 Tracking mode

Contrary to the stationary mode, the indoor positioning system serves context-aware applications such as guide systems and tracking systems, in which the movement of a mobile device is subject to the area topology. In (Xiang *et al.,* 2004), the authors proposed a tracking-assistant positioning algorithm that relies upon topological knowledge to obtain the $P(m_i)$, which we also used.

Firstly, the authors define a tracking probability which is reversely proportional to the distance between the latest determined position and current position. The formula of the tracking probability $P(m_i / M_k^P, M_{k-1}^P, ..., M_1^P)$ for each marking position with the k prior determined positions M_k^P, $M_{k-1}^P, ..., M_1^P$ is as follows:

$$P(m_i) = P(m_i / M_k^P, M_{k-1}^P, \ldots, M_1^P) = \frac{1}{k \times D} \sum_{j=1}^{k} \left[e^{-(j-1)} \times dist^{-1}\left(m_i, M_j^P\right) \right] \quad \textbf{(2.23)}$$

Where $dist(m_i, M_j^P)$ represents the distance between position m_i and position M_j^P. D is a constant representing the maximum distance between positions.

A tracking probability represents the feasibility of the mobile device being moved to current position after a prior moving trace. Since the mobile device cannot move a long distance in a very short time, the tracking probability can be used as the prior probability of position m_i which is $P(m_i)$.

Then, considering the complexity of indoor environments, the authors use a weighted graph (vertex, edge), $G(V, E)$, to represent the position topology. MPs from set L are put into set V and one edge e is assigned to each position pair as $e(m_i\ m_j)$ if the physical distance between positions m_i and m_j is shorter than a threshold distance and if there is a direct way to connect two positions in physical space. Therefore, for any position pair m_i and m_j, we define the distance $dist(m_i\ ,\ m_j)$ as the length of the shortest path between two positions in graph $G(V, E)$. While calculating tracking probability, system checks the distances in graph and include them into processing.

Deploying the simple tracking probability may introduce a risk of imprecision for the system because of error propagation. The authors introduce a finite state machine to distinguish states of locations. The states are categorized into tracking states T and non-tracking states N. The states in T indicate that the positioning system should deploy the tracking probability in the determination process while the states in N mean that there is a risk associated with using tracking probability.

2.2.2.3 Enhanced parts

WPS uses a discrete-space estimation process that returns the radio map location that has the maximum probability given the RSS vector from different AP. A continuous-space estimation process takes as input the discrete-space estimated location and one of the radio map locations, and returns a more accurate estimate of user location in the continuous space. The output of the Centre of Mass (CM) technique can be used as an input to the TA technique to obtain a better estimate compared to using the discrete-space estimator.

a) Centre of Mass (CM)

The CM technique is a kind of weight-based averaging approach. The CM technique (Youssef & Agrawala, 2004) estimates the user location based on the list of candidate locations in the current estimation period. This technique is based on treating each location in the radio map as an object in the physical space whose weight is equal to the normalized probability assigned by a discrete-space estimation process. The normalization is used to ensure the sum of the probabilities of all locations equals one. The mathematical formula of CM is defined by:

$$x = \frac{\sum_{i=1}^{\min(N,\|\overline{X}\|)} p(i) * \overline{X}(i)}{\sum_{i=1}^{\min(N,\|\overline{X}\|)} p(i)} \quad \textbf{(2.24)}$$

Where N is the number of selected candidate locations $\overline{X}$ is the list of candidate locations. $p(i)$ is the positioning probability of candidate locations. $\overline{X}(i)$ is the i^{th} candidate locations in the list.

After investigating the distribution of estimated locations, in fact, the estimated locations have two kinds of situations disparately as shown in Figure 2.13: firstly, the estimated locations get together (as shown in Figure 2.13 (a)); secondly, the estimated locations are partitioned into several disjoint clusters (as shown in Figure 2.13 (b)). The reason is that the single space distance may be not proportional to the physical space distance.

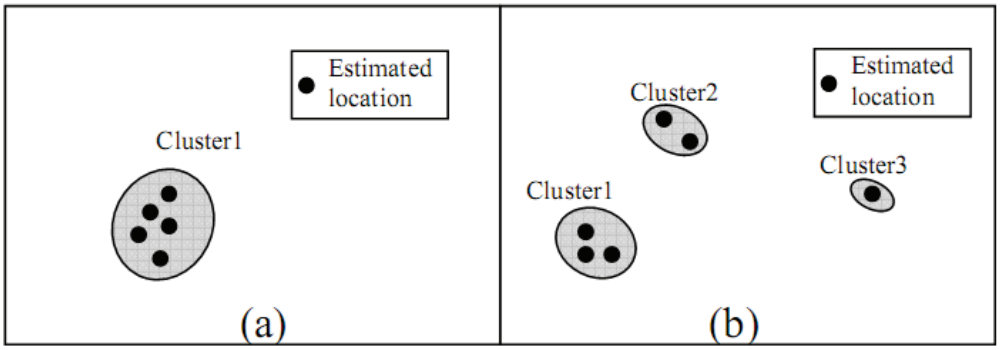

Figure 2.13 Two kinds of distribution of estimated locations

Obviously, CM technique has different behaviours in these two situations. Thus the ultimate step is to identify the category of the estimated locations, namely, to apply some clustering algorithm to partition all the estimated locations into several clusters. There are many clustering algorithms and Hierarchical Clustering (Johnson, 1967) is a basic and classic one. The Hierarchical Clustering process consists of three steps with considering each estimated location as a group initially.

At first, it combines the two "closest" groups into a single group.

Then, it recalculates the distance for each pair of groups. Here, the distance is the average of all the distance from any element of one cluster to any element of the other one.

Next, if the minimum distance is greater than the threshold, it stops. Otherwise, it repeats the first step.

In the first situation, the number of the selected candidate locations is an important factor affecting the performance of CM. Taking all the selected candidate locations to calculate the estimated result is not a good choice since not all of them do contribute. If we could select some of these candidate locations before calculation, a more accurate estimation could be found. To solve the

problem, we use the variation of input signal strength vector to decide the number of the selected candidate location. This variation can be inputted by user or use the default value from pervious tests. Only the candidate locations whose signal space distance of each visible AP is less than this variation can be accepted as selected candidate locations. In other words, we prefer the stable signals.

In the second situation, we take all the selected candidate locations to calculate the estimated result by CM in the stationary mode. However, in the tracking mode, one cluster is chosen as the delegate while the others are filtered out according to the previous estimated location, further estimated location and moving probability. If the above selecting rule still does not work, the cluster that has the maximum total cumulative probability will be selected.

b) Time Averaging technique (TA)

The TA technique is only used in tracking mode. The TA technique (Youssef & Agrawala, 2004) estimates the user location using the history of consecutive estimations. This technique uses a time-average window to smooth the resulting location estimation. This technique obtains the location estimation by averaging the last W location estimations obtained by a discrete-space estimator. The mathematical expression is as follows:

$$\bar{x}_t = \frac{1}{\min(W,t)} \times \sum_{t-\min(W,t)+1}^{t} x_i \qquad \textbf{(2.25)}$$

Where x_i is the i^{th} previous estimated location and W is the size of the averaging window.

c) Positioning filters

Positioning filters are applied in order to combine the new measurements with the past measurements and the motion model of mobile user. The pedestrian motion dynamics can be modelled by a general Bayesian tracking model and a filter is then derived to refine the position estimations. The tracking-assistant positioning algorithm proposed in (Xiang *et al.,* 2004) is a kind of positioning filter. Commonly there are two filters that are used to improve the accuracy of positioning systems (Guvenc *et al.,* 2003): Kalman Filter (KF) and Particle Filter (PF).

Kalman Filter has been studied and applied extensively in positioning applications. KF assumes linear measurement function, Gaussian initial distribution, and mutually independent Gaussian measurement and motion model noises that are independent of the initial state. Although the assumption of Gaussian RSS-position relationship is not often the case (Kaemarungsi & Krishnamurthy, 2004a), the application of the KF as the post-processing step is able to improve the accuracy of the positioning systems (Besada *et al.,* 2007), (Kushki *et al.,* 2006), (Ali-Loytty *et al.,* 2009). The parameters of the KF are needed to be found experimentally. (Jaegeol *et al.,* 2008) provides some guidelines on how to set the parameters for each update steps based on the map information.

The Particle Filter is a sequential Monte Carlo method that generates random samples, known as particles, according to a motion models and estimates their probability densities (Yueming & Hongyi, 2008), (Arulampalam *et al.,* 2002). Unlike the KF, the PF can be applied on non-Gaussian and non-linear models. In addition, map information can be used to further improve the performance of the particle filter by assigning zero weights to the invalid particles, such as those across the wall

(Wang *et al.,* 2007), (Chih-Hao *et al.*, 2008). Backtracking based on the map information is also proposed in (widyawan *et al.*, 2008).

PF usually produces a good estimate for the posterior distribution, but it requires a lot of computation compared to KF. This large computation workload cannot be handled by the mobile devices to give real-time updates to the user. Hence, the KF is chosen to post-process the estimates instead of the particle filter.

2.3 The framework of CMTA-WPS

In this section, we present the general framework of our indoor positioning system. Figure 2.14 describes the CMTA-WPS system design and the software framework. CMTA-WPS system is developed by C++. The system has multiple inputs and consists of two parts, coverage program and location program, which are respectively corresponding to offline phase and online phase.

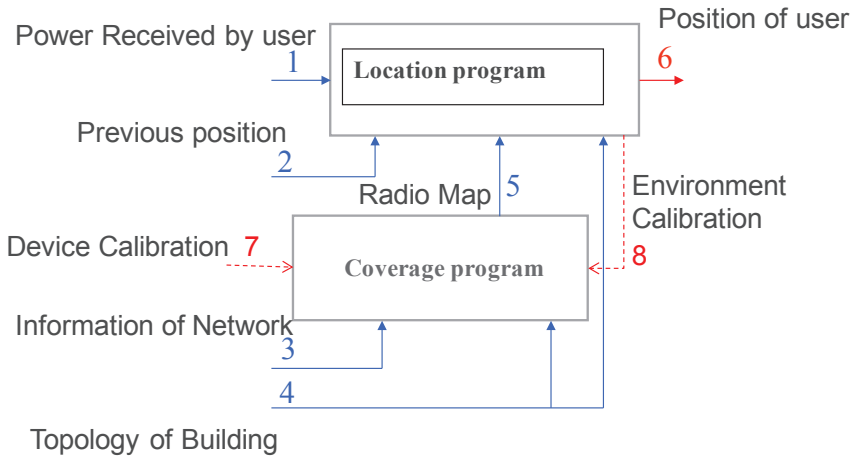

Figure 2.14 The general framework of CM-WPS

Coverage program: In this program, the RSS vector from each AP in every MP is calculated by the propagation model. The probability distributions of these signals are then calculated based on a shaping filter and a tailing filter. There are four inputs. The information of network and the topology of the building are required. The information of device calibration and environment calibration are optional. The network input describes the network and it contains information on the various APs used such as the positions and the parameters of APs. The topology of the building describes the topology information. All the walls and barriers are subdivided into individuals according to their types. Finally, whole topology information is composed by all the individual information which includes the type and position of individual. The two kinds of calibrations are started only when such needs are necessary and available. Except the environment calibration, the three other inputs are the pre-processing steps and should be ready in advance. All of them are costly in terms of time and resources.

Location program: This program returns the user location mainly based on the probabilistic techniques and various inputs which are the running mode of system. In stationary mode, two inputs are needed. One is the detected signal by user from each AP. The other is the radio map generated by

coverage program. In the tracking mode, in addition to above two inputs, positioning needs the user previous positions as input. If drastic environmental changes exist and the distribution and number of APs meet the requirements, the environment calibration will run automatically to update the radio map and to reduce the positioning error.

2.4 Experimental studies

There are many studies in the literature mainly focusing on indoor positioning system. However, there is a lack of clear understanding of how these systems may perform (in terms of accuracy and precision), how to design these systems (what is the impact of the building architecture and thus the radio propagation characteristics) and what impacts the design (what should be the spacing of the grid and where should APs be deployed). In order to answer the above questions, we have implemented and tested our CMTA-WPS to evaluate its performance. The objective is to explore first results related to accuracy and localization precision. We have implemented the experiments on two steps: the first step is based on simulations and the second step is based on real environment.

2.4.1 Test based on simulations

2.4.1.1 Experimental setup

The experiments took place at two artificial experimental environments with various AP configurations. The first building architecture is simple. It means that the building has few obstacles. In this case, it is better to focus on the AP number as well as their optimal placement. The second building is a typical example of offices architecture. It is more complex than the first one and has more different type of obstacles. By exploring this type of building we can study obstacles effect on MS localization.

a) Building 1: a simple environment

In the first stage of experimentation, we have measured the location error in a simple environment. To evaluate the positioning system CMTA-WPS, the objective is to understand how the variation in the AP number depending on the topology of the building influences the location error. The building layout is depicted by Figure 2.15. The deployment covers an experimental area of approximately 80m x 40m and uses 802.11g wireless LAN infrastructure to provide coverage.

For the analysis need, we selected 8 reference points (RPs) where several measurements have been made. The RPs are distributed on the whole area as shown in Figure 2.15.

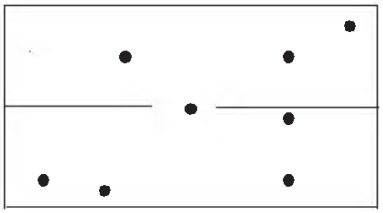

Figure 2.15 The building 1 layout and the reference points distrubution

Note that the few obstacles result in a complex environment for signal propagation. In other words, a WLAN composed of few AP number, for instance less than four AP cannot provide enough coverage for good location accuracy.

According to our previous work (Baala & Caminada, 2006a), we started from a 4-AP WLAN to guarantee well coverage. We tested the positioning system by varying the AP number and their locations. We did several series of measurements under different WLAN configurations inside the building. For shortness consideration, we will restrict the results description. Rather, we will only focus on six scenarios: four 4-AP WLAN configurations and two 5-AP WLAN configurations.

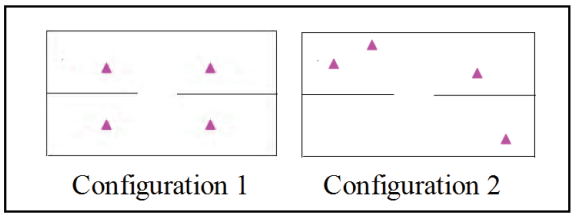

Figure 2.16 Building 1: configurations 1 and 2 for 4-AP WLAN

In the first case with 4-AP, the selected AP sites (placements) are different. As shown in Figure 2.16, AP in configuration 1 are placed symmetrically in the building, whereas they are scattered and unsymmetrical in configuration 2.

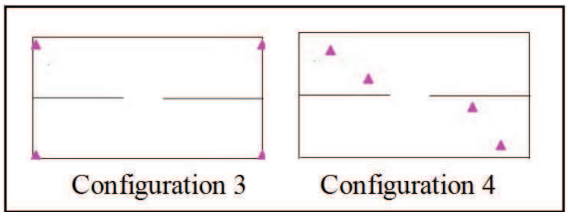

Figure 2.17 Building 1: configurations 3 and 4 for 4-AP WLAN

In the second case, we also select 4 APs. In configuration 3, AP are symmetrically placed in the building corners, whereas, in the configuration 4, they are scattered in a different way compared with configuration 2. Nevertheless, the average power of these RPs in symmetrical placement is lower than unsymmetrical placement.

In the third case, we have added another AP to configuration 1 and 2 (see Figure 2.16). In the configuration 5, the fifth AP was placed in the building centre resulting in a symmetrical configuration whereas in configuration 6, the fifth AP is placed in the left bottom corner as depicted by Figure 2.18.

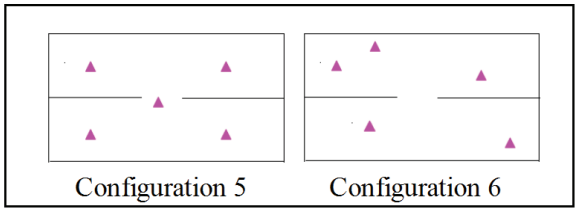

Figure 2.18 Building 1: configurations 5 and 6 for 5-AP WLAN

b) Building 2: a complex environment

In the second stage of experimentation, we have considered a more realistic building (see Figure 2.19) which is an office building having an experimental area of approximately 80m x 40m. It consists of seven rooms and a corridor. The deployment uses 802.11g wireless LAN infrastructure to provide coverage. It should be noted that both experiments are based on the same surfaces. Although, for this building there are more obstacles such as load-bearing walls, bulkheads and doors that may affect the wave propagation.

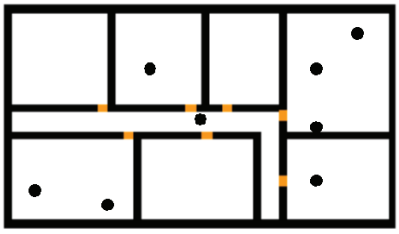

Figure 2.19 The building 2 layout and the reference points distribution

Despite the different number of obstacles, we used the same RPs in the building 2 as shown in Figure 2.19 since the two buildings cover the same surface.

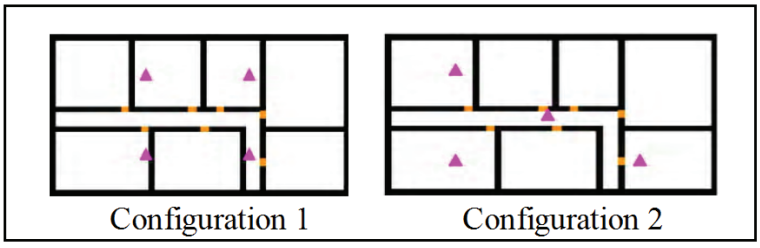

Figure 2.20 Building 2: configurations 1 and 2 for 4-AP WLAN

As in the first experimentation, we also varied the AP number and AP locations in order to evaluate the performance of our positioning system and the influence of AP location. We conducted several series of calculations under different WLAN configurations. Here again, we will restrict the results description and will only focus on six scenarios: four 4-AP WLAN configurations and two 5-AP WLAN configurations.

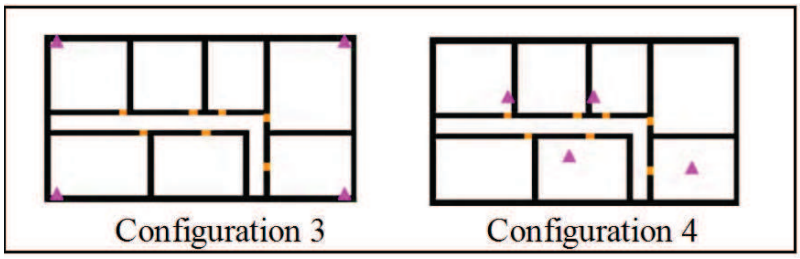

Figure 2.21 Building 2: configurations 3 and 4 for 4-AP WLAN

Note that, in these scenarios, AP placements of configuration 1, configuration 3 and configuration 5, in building 1, respectively in building 2, are symmetrical, and AP placements of

configuration 2, configuration 4, and configuration 6, in building 1, respectively in building 2, are asymmetrical.

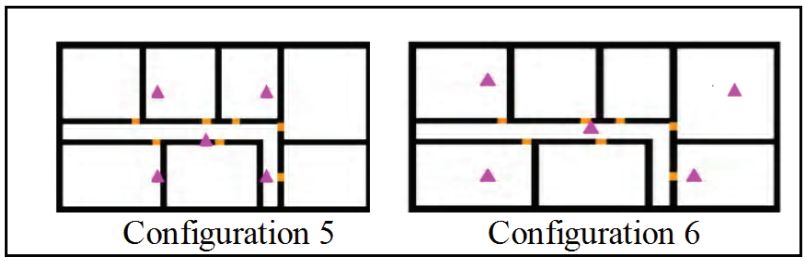

Figure 2.22 Building 2: configurations 5 and 6 for 5-AP WLAN

2.4.1.2 Results and analysis

We explored two situations for position determination: stationary mode and tracking mode. We run CMTA-WPS programme on both building 1 and 2 for each AP configuration. We have based the analysis on location error as a criterion to evaluate CMTA-WPS. The location error is defined as the average error of all the RPs. Note that these experiments are based on simulation, namely the input RSS of each RP is the RSS vector of this RP in the radio map. Thus all the environment perturbations are not taken into account in these experiments. Under such ideal conditions, the basic links among positioning error, AP placement, AP number and building topology can be reflected clearly.

The errors of the first experimentation inside building 1 are described in the chart of Figure 2.23. The left graphic describes the results relating to stationary mobile; the right graphic describes those of tracking. For each graphic, the bars numbered from 1 to 6 correspond to the 6 tested configurations.

As we started by building 1 where there are few obstacles, we aimed to better focus our research on the ideal AP placement and AP number. The experimentation shows that the location accuracy for tracking (maximum error of 1.4 meter) is better than for stationary mobile (maximum error of 3.2 meter). Indeed, tracking take advantage from prior knowledge of the building layout as well as previous positions of the mobile device.

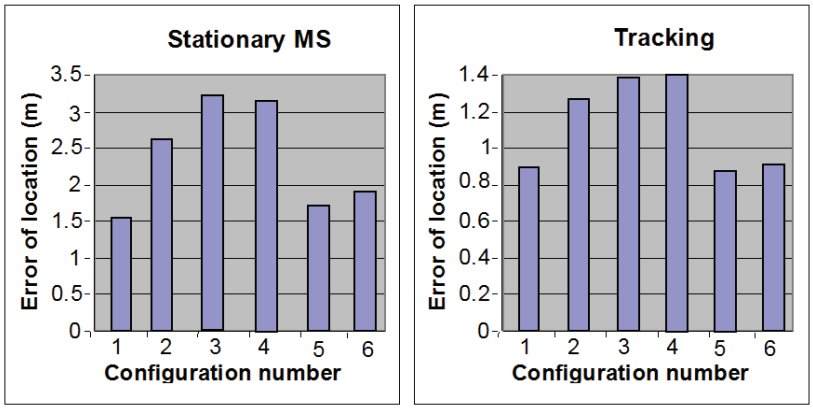

Figure 2.23 Location error inside building 1

A second observation is that the best results are obtained with 4-AP configuration 1 and 5-AP configuration 5 for stationary mobile or tracking particularly when the APs are placed symmetrically. So, adding a new AP does not always improve the accuracy (see configuration 6). It depends on the position of the added AP. We can also conclude that the placement of the added AP was not chosen judiciously and, as a matter of fact, the central position of the AP generates more perturbation than improvement. But with 5AP, we have global good results whatever the symmetry or not of the AP location (numbers 5 and 6). Moreover, symmetric configurations are not always better than asymmetric configurations. The symmetric configuration 3 is the worst one. In case 3, we can observe that the average signal power of the RPs is very low as shown in table 2.

The experimentation in building 2 reveals very different results as described in the chart of Figure 2.24. Since building 2 has many obstacles, the wave propagation is disturbed. It is more unlikely to have RP with the same maximum probability for a given RSS vector. Therefore, the positioning error in building 2 is much lower than in building 1 for all cases. Unlike the previous experimentation, the accuracy of the stationary MS is always better expected for configuration 3. Since tracking is based on prior knowledge, bad performance may come from errors accumulation at each previous position.

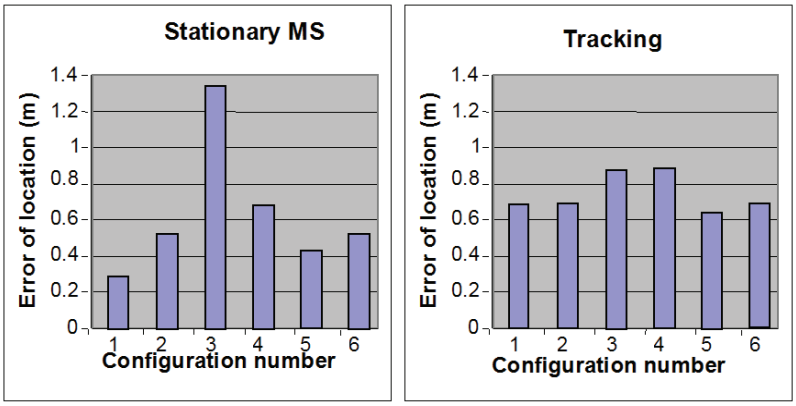

Figure 2.24 Location error inside building 2

More generally, the best results are obtained with a 4-AP WLAN and configuration 1 for stationary mobile and with a 5-AP WLAN and configuration 4 for tracking. In these configurations, the APs are placed symmetrically in the building. Here again, the configuration 3 in Figure 2.21 is still the worst performance in stationary MS and tracking although it is a symmetrical configuration. That is also due to the low average signal power.

We have also looked at the relationship between the average signal power of the RPs and the average location error.

Table 3 provides the average signal power in milliwatt of these RPs for different configurations in stationary MS mode in both buildings. High values of the average signal power reflect high RSS values. Since RSS values are very low in case of configuration 3 in both buildings (grey cells), the location error is very high, and oppositely RSS values are high in configuration 1 (grey cells) which is the best one. Also the average signal with 5-AP is better for configuration 5 and 6 and the location too.

TABLE 3 AVERAGE SIGNAL POWER

Configuration	Building 1 (*mw*)	Building 2 (*mw*)
1	26.43×10-6	27.71×10-6
2	1.45×10-6	20.34×10-6
3	0.64×10-6	0.53×10-6
4	1.15×10-6	6.79×10-6
5	20.34×10-6	21.36×10-6
6	18.69×10-6	20.96×10-6

By synthesizing Figure 2.23, Figure 2.24 and Table 3, we can get Figure 2.25. One blue point is the average signal power and the average location error of RPs in one configuration in stationary MS mode and the black line is the trend line. At all we have the 6 average signal power for the 6 configurations on the figures from the lowest to the highest average power.

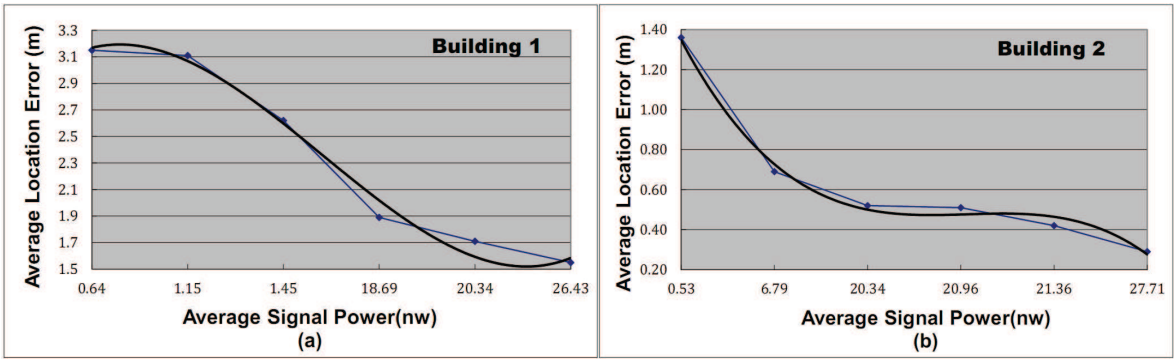

Figure 2.25 The average signal power and the average location error for all configurations

From these two figures, it is possible to reliably establish a relationship between the average signal power of the RPs and the average location error. The location error of stationary MS decreases while the average signal power increases. On the other hand, for tracking, the prior knowledge of previous positions is an important parameter which can influence the location error. This is why the relationship is not reliable in some experimentation.

Another indicator to assess this relationship is the RPs proximity of the deployed AP and the location error. Indeed the average signal power is higher when RPs are closer to APs. And the locations of these RPs are better.

From these tests, we can do some initial emphasis: firstly, only the value of the average received power for all AP is highly influencing the error location; secondly, the symmetric or asymmetric position of AP in the building is not always influencing the error location since it cannot guarantee to improve the average received power; thirdly, higher AP number has global good results since it can guarantee a global better average received power.

2.4.2 Test based on real environment

2.4.2.1 Experimental setup

We also implemented the test in real environment. The testbed for performance evaluation is located at the second floor of the university campus (building B), which covers an experimental area of approximately 120m x 40m with many classrooms and offices of different sizes. We uses 802.11g wireless LAN infrastructure to provide coverage. The topology of the test environment is described in Figure 2.26. It is very irregular so very complex in terms of wave propagation then very difficult for location purpose.

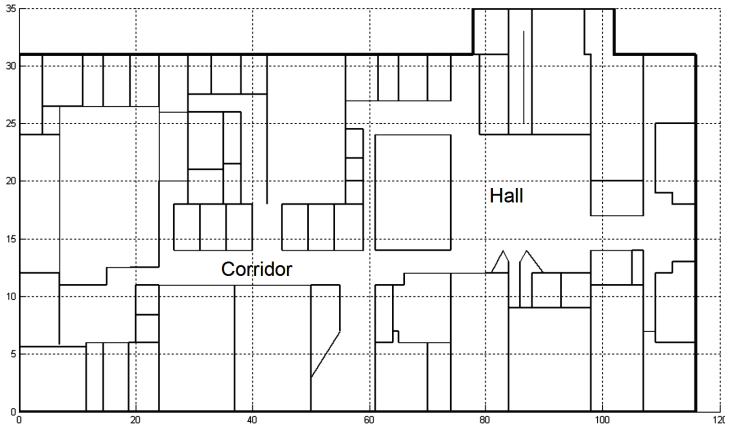

Figure 2.26 The topology of the test environment

From Figure 2.26, we can see that there are a long corridor in the left side of the floor and a large hall in the right side of the floor. It is well known that the performance of localization is often degraded due to the RSS severe variation resulted from multipath. Such a problem is inevitably encountered when the positioning system is deployed in a real indoor environment where the multipath effect is significant. As a matter of fact the behavior of the multipath is different with long corridor and large hall. So we categorized this floor into three scenarios to emphasize the topology effects: the whole floor, the left side floor with the corridor and the right side floor with the hall.

In research based on simulation, we conclude that good coverage of experimentation area together with symmetrical AP placement may promote location accuracy. The upper limit of AP number is also a constraint.

Considering the above conclusion, we extended the existing university network by manually deploying additional AP for a comprehensive coverage and non symmetric AP placement. For the analysis needs, we have selected several RPs uniformly distributed where 3 series of separated measurements have been made: 22 points in the whole floor with 5 AP, 19 points in the right side floor with 4AP and 10 points in the left side floor with 3 AP. The RP and AP are distributed on the whole floor as shown in Figure 2.27. Figure 2.28 describes the distribution of AP and RP on the right side floor. The distribution of AP and RP on the left side floor is described in Figure 2.29.

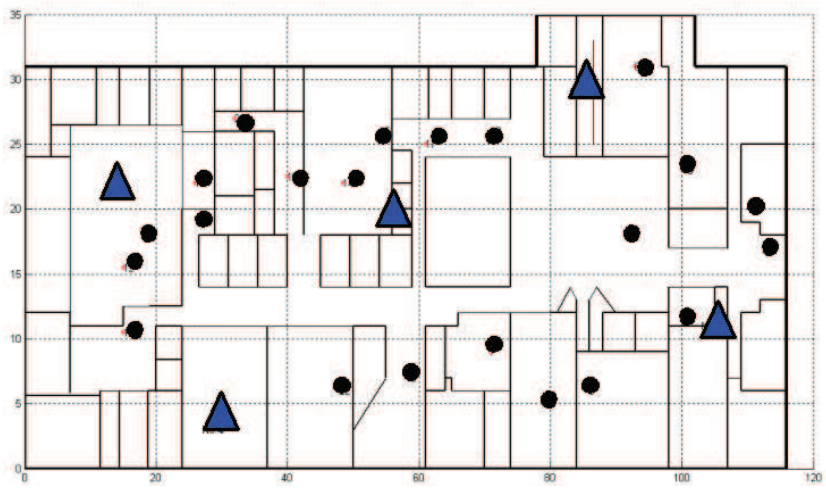

Figure 2.27 Scenario 1: AP and RP distribution on the entire floor

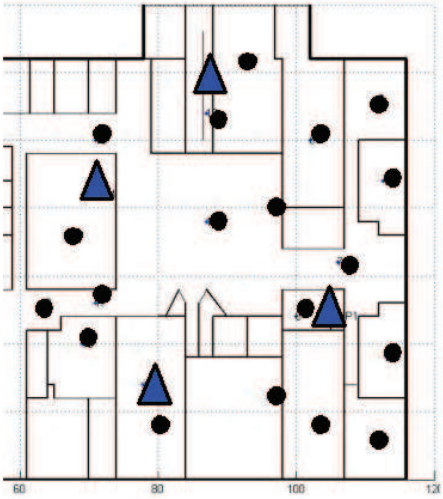

Figure 2.28 Scenario 2: AP and RP distribution on the right side floor

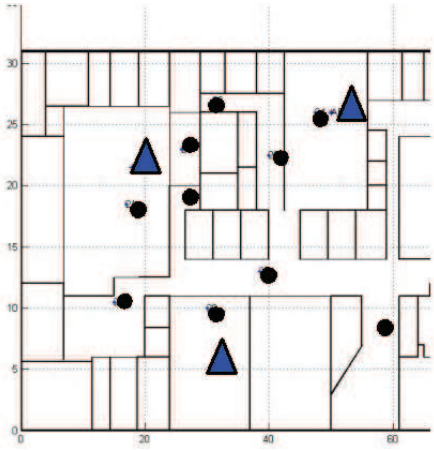

Figure 2.29 Scenario 3: AP and RP distribution on the left side floor

To carry out series of measurements, laptop computer with wireless card (Dlink DWL-G650, Receiver Sensitivity: -89dBm for 802.11g, -92dBm for 802.11b) and *Network Stumbler* (Milner, 2011) software were used as measuring equipment. We used passive scanning, in which the receiver

scans each of the available 802.11g channels periodically to discover the RSS values. There are many factors that can affect the WLAN based RSS measurements such as MS orientation, the time during the day (a lot of people or not), environment (tables, desks…), distance from transmitter, interference from other AP, and sensibility of the wireless card. We used a dedicated channel for our measurements to limit the effect of interference from other AP in the area. In order to address the MS orientation factor the measurements were done in multiple directions at the same location. After extracting the information associated with the desired AP we apply a five seconds averaging window to the collected data. All possible RSS are integer values expressed in -dBm. We did not care about other parameters (time, environment…) and did our measurements whatever particular conditions (different period during the day, people moving around …).

Here, we determine the distance between RP and the nearest wall using ultrasonic device. Since the position of the wall is known from floor architectural plans, it is easy to calculate the position of RP using Euclidian rule.

2.4.2.2 Results and analysis

a) Accuracy of location

To evaluate the performance of the location system, the accuracy is one of the most important indicators. To show how accurate the positioning system could be, we adopt the mean distance error as the performance metric, which is the average Euclidian distance between the estimated location (x', y') and the real location (x, y):

$$E(Error_{distance}) = E(\sqrt{(x'-x)^2 + (y'-y)^2}) \quad \textbf{(2.26)}$$

Figure 2.30 shows the average distance errors on the three scenarios with our CMTA-WPS system.

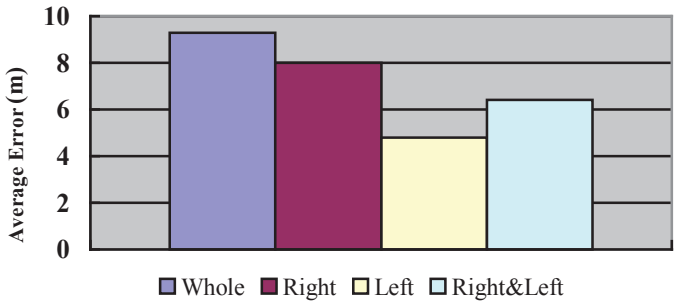

Figure 2.30 The average distance errors

From the result shown in Figure 2.30, left side scenario shows the best accuracy, about 4.8 meters, among the four. Right side scenario gets a middle distance error, about 8 meters. Whole floor scenario gets the worst accuracy. The results show 9.3 meters of distance error, which might be not acceptable in common indoor environments for most applications. This is due to low AP density (5 AP) as showed in a previous study about the simulation in a small building (Baala *et al.*, 2009). Moreover, we simulate the whole 7AP scenario by the combination of right side scenario and left

side scenario. Such combination can basically reflect the characteristics of the whole 7AP scenario because of two reasons. One reason is that only less than 30 percents of RPs have different signal vector between the combination scenario and the real whole 7AP scenario since the limitation of AP coverage. The other reason is that RPs having different signal vector have more visible APs in the real whole 7AP scenario than with 5 AP case. And then more visible APs usually can bring higher accuracy. According to the results of left side scenario, right scenario and combination scenario, we believe that increasing the AP number should decrease the location/distance error of whole floor scenario down to acceptable range.

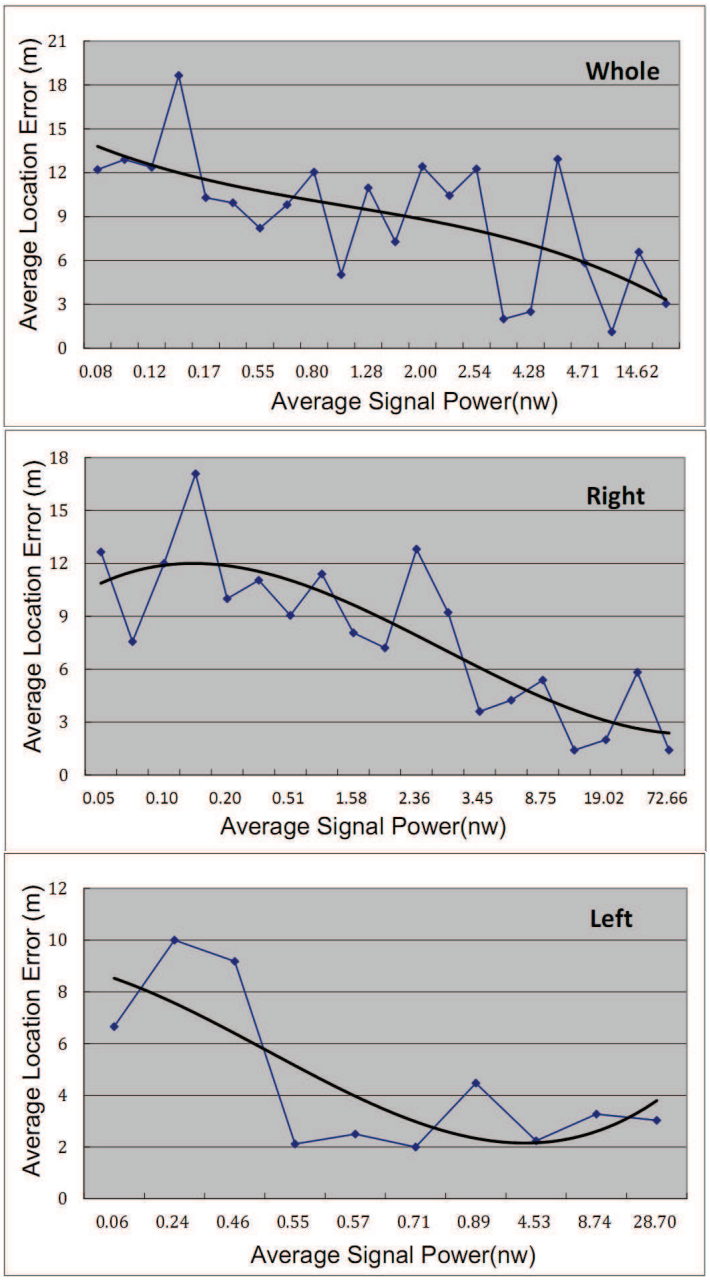

Figure 2.31 The signal power of RP and the average location error for three scenarios

In figure 2.31, we analyse again the correlation between average signal power and average location error. Here the three scenarios with the different areas are in three different figures. For each

figure one blue point is for one reference point and the number of reference points is different for each scenario and the black curve is the tendency. In simulation plotted in Figure 2.25 we conclude that the location error of stationary MS decreases while the average signal power increases. Here, in real environments we have the same observation for each area. We see again the correlation between the decrease of the average signal and the increase of the average location error.

b) Precision of location

Accuracy considers only the value of mean distance errors while precision considers the distribution of distance errors. When two positioning techniques are compared, the one with distribution of distance errors concentrated on smaller values would be preferred, since it is more likely that we could get smaller distance error by this positioning system. We analyze the Cumulative Distribution Function (CDF) of distance errors of different scenarios, as shown in Figure 2.32.

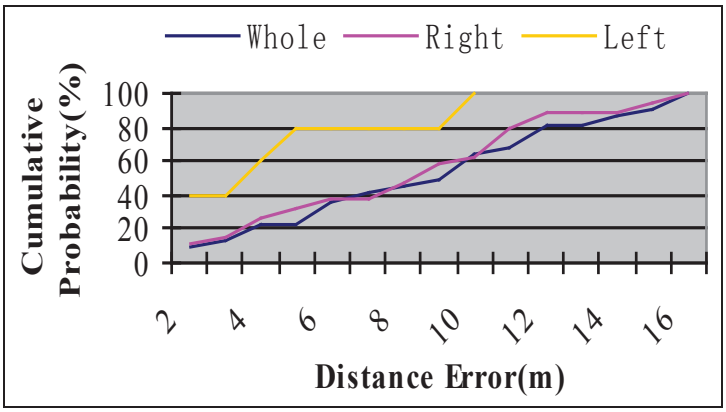

Figure 2.32 The Cumulative Distribution Function of distance errors

From the "precision" point of view, left side scenario still shows the best performance. In left side scenario, 80 percents of distance errors are within 5 meters. Right side scenario reports a value of 11 meters to reach the same cumulative probability. In the whole floor scenario, 80 percent of distance errors are within 2 to 12 meters. This analysis shows consistent result with the accuracy comparison but emphasizes the huge difference between left side and both other scenarios.

c) Impact of AP configuration on location

With former research based on the simulation in a small building (Baala et al., 2009), it is found that while increasing the average power of reference points, the accuracy of location is being improved. Considering this result, here we delete the weakest measured AP of each RP to increase the average power and check the effect on the average error for real building and measurements. Doing that we reduce the size of the signal analysis vectors but we improve the value of these signals, and it should confirm that it improve the quality of the location even with one less AP.

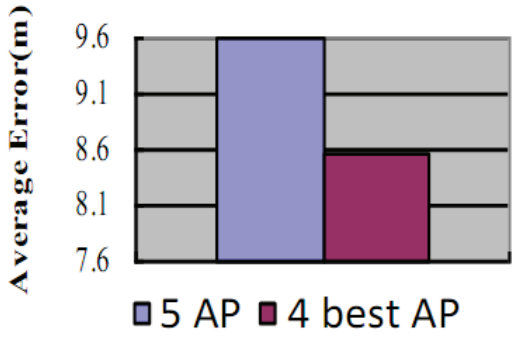

Figure 2.33 The average distance error on the whole building

Figure 2.33 on the whole building shows clearly that the location error of MS decreases while the average signal power increases. In fact, the positioning error caused by RSS variation is inversely proportional to RSS value. So deleting weakest AP is a good way to improve the accuracy if the number of AP for RP measurement is sufficient for location estimation and coverage. (Probably more than 3 might be a good rule in our experiment but it needs studies!). The worst RSS are correlated to location errors because in worst RSS case, we have more signal fluctuation. Low RSS are due to longer distance or higher obstacle between transmitter and receiver. Then the number of multi-path increases and the signal fluctuation are more important causing degradation in location accuracy.

Now we voluntary change the input signal vectors measured by the MS to do more tests on the impacts of AP number and AP configuration. Figure 2.34 shows the average distance errors relative to different AP configuration. It is done on the right side scenario.

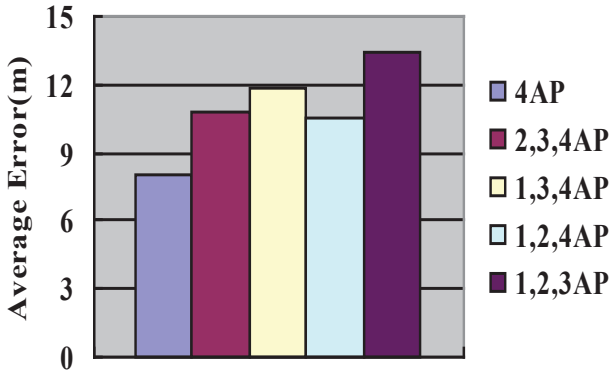

Figure 2.34 The average location error of different AP configurations.

Usually each AP has its own way to contribute to the system performance in different RP location. The error of one AP may be lowest in one location but highest in other location, this is why we have so much variation in all 3 AP cases. So we clearly emphasize the importance of AP placement in the building and not only the number of AP for location performance.

Due to the probabilistic location method, the system can correct the location by itself if the errors due to one or two RSS are much larger than others. Obviously, in the 4 AP case these benefits are larger than in 3 AP cases because the system has more information about RSS so averaging the location error of 4 AP is better for the position accuracy. The interpretation is that the largest signal error with the 4 AP case is better corrected by the system and then the location error of 4 AP is lower

than average location error of any 3AP case. From above analysis, we can conclude that in real environment increasing the AP number in order to reduce the location error might be a good rule but there is an upper limit of necessary signals to be considered. Now one open question is “where is this limit and how to compute it?” In the following chapters, we will try to answer this question.

2.4.3 Comparison to other systems

In addition to testing the system itself, it is also very necessary to compare our system with other WLAN-based fingerprinting systems. However, the system tests report that the accuracy of our system is influenced by the size of grid spacing and the number and positioning of AP. Therefore, we are also curious how much these factors affect the accuracy of other systems. In addition, we are also interested in effects on the size of building and on the radio map generation method.

2.4.3.1 Comparison of systems on same buildings

The main difficulty in comparison of location system is that in literature, there are many different buildings for each article. We know that building topology is influencing a lot the results but all these buildings are not available for comparison. Then we propose two cases, a comparison on the same building than other systems on a building which is available and a comparison with cases for which the buildings are not available but with new metrics which include building and network topology description.

In order to answer the performance questions, we perform the experiments with two different testbeds. The first testbed is the same setup as described in Figure 2.28 and Figure 2.29. The radio map is generated by our propagation model. 19 RPs in the right side floor and 10 RPs in the left side floor are used to evaluate the system respectively.

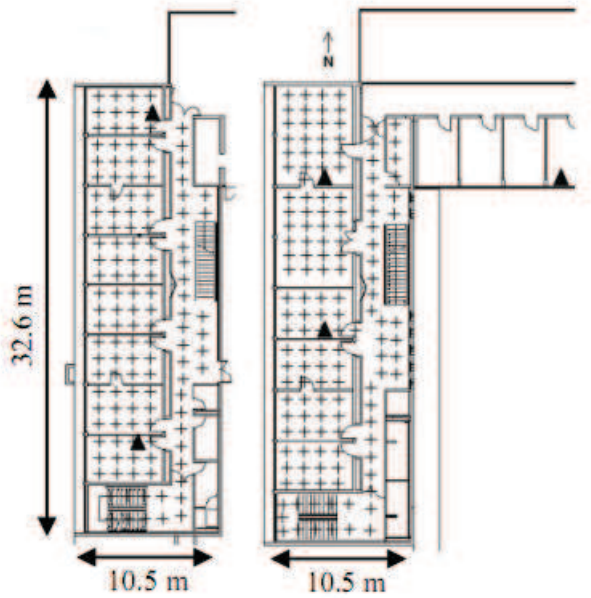

Figure 2.35 The second testbed at UFC building

The second testbed is another building; the first and second floors of the computer science laboratory of the Université de Franche-Comté (UFC). Figure 2.35 shows both floors. The building is very simple, a corridor and offices on left side. The building size is 32mx10m. Crosses are RPs stored in the radio map. There are 276 RPs available for testing. Another measurements set is used as test data and contains 86 points.

We compare the performance of our approach with the performance of other typical RSS-based positioning algorithms: RADAR from (Madigan *et al.,* 2005) and FRBHM from (Wlfle *et al.*, 2005). RADAR, which adopts the nearest neighbor(s) in signal-space technique, is usually considered as a reference algorithm to evaluate other positioning systems. FRBHM is based on a Friis formula with calibration (FBCM) and RADAR-like based hybrid model. This algorithm takes advantage of hybrid propagation model and radio map with closest in signal space search. Algorithms performances are defined by their positioning error with equation 2.2.1. The implementation of RADAR and FRBHM were done by Lassabe. The AP placement is the same for the three systems. Table 4 shows results on the first testbed with 1m grid spacing. Our model is in grey.

TABLE 4 AVERAGE ERROR (METERS) IN THE FIRST TESTBED AT UTBM BUILDING

Test Scenario	RADAR	FRBHM	CMTA-WPS
Radio map used	measurement	measurement and model	model
Right side floor	8.9	12.74	8.31
Left side floor	6.01	6.52	4.65

From this table, we observe that the test for the right side floor with 4 APs returns bad results. According to previous study, it might be bound to a topology more heterogeneous than the left side floor where we used 3 APs. We also observe that our positioning system always gets best accuracy, followed by RADAR and FRBHM. The reason is that the signal probability distributions are only used effectively in our positioning system, which also indirectly shows the effectiveness of the probability distribution filters. Since RADAR and FRBHM are based on the deterministic method, they cannot benefit from these signal probability distributions.

TABLE 5 AVERAGE ERROR (METERS) IN THE SECOND TESTBED AT UFC BUILDING

Number of AP	RADAR	FRBHM	CMTA-WPS
Radio map used	measurement	measurement and model	model
3	5.08	6.68	5.86
4	4.32	5.39	5.16
5	3.83	5.06	4.99

Table 5 shows results in the second testbed in the building of UFC. In this one we check the system with 3 different sizes of Wi-Fi network. The grid spacing is 1m. The table shows that for all the systems when the number of available AP decreases so does accuracy. This is also our original forecast and expectation. Another interesting result is that all the three systems are inaccurate in the first testbed with a low number of APs (3 or 4) compared to testbed size (approx. 3200 m^2), while the second testbed has 3 to 5 APs available for an approximate size of 350 m^2; then the AP density plays a huge role in performance in UFC building. However, RADAR always performing the best is confusing us. The radio map generation method may explain this gain. Indeed, the propagation model

method cannot be as precise as the measurement method to take into account a complex environment such as these testbeds, but it is good to see that the difference between RADAR and CTMA-WPS is not important while the cost to do the radio is very important it is at the advantage of the CTMA-WPS.

We also focus on the grid spacing and how it impacts the accuracy of the positioning system. Table 6 shows the variation of grid density for second testbed.

TABLE 6 AVERAGE ERROR (METERS) WITH GRID SPACING VARYING IN THE SECOND TESTBED AT UFC BUILDING

Grid spacing	RADAR	FRBHM	CMTA-WPS
Radio map used	measurement	measurement and model	model
1m	3.83	5.06	4.99
2m	3.65	5.13	5.44
3m	4.11	5.13	8.68
4m	4.49	5.24	6.14

The results seem a little strange since we assume when reducing grid density, accuracy decreases (oppositely to RADAR results where 2m in density is better than 1m in density). Indeed, our assumption is based on the presupposition that a positioning system always finds the closest reference point, and the theoretical average error is caused by grid spacing. But real-world positioning systems are usually not perfect and the estimated position is not closest to the user's real position. It brings another kind of error. There are some cases where these two kinds of error may cancel out. That may explain that the error is unstable when reducing grid density.

2.4.3.2 Comparison of systems on different buildings

In the above comparison, as most of the previous works we only concentrate on the accuracy, which means the average distance error, but it is inadequate and unfair if we need to compare the results on different buildings, because it clearly depends on the building size and AP density! 10 meters of error do not have the same meaning for $100m^2$ or $1000m^2$ building size with the same number of AP. It has been approved by our above comparison. Thus it is necessary to search new performance criteria for a comprehensive performance comparison on several buildings.

In the paper (Borenovic *et al.,* 2008), the authors proposed the new performance criteria that are more realistic. The authors introduced a first derived comparison parameter that should normalize positioning errors with respect to the size of the test areas where location techniques were implemented in. For that purpose, the ratio between the maximum positioning error for one particular test environment and the location median error on that environment is proposed. This ratio must be maximized for a good location. The maximum positioning error is only a function of the building size and is independent of any location system. The authors consider the test area as a two-dimensional rectangular environment. It is also assumed that the position of a user is a two-dimensional uniformly distributed random variable. It can easily be shown that the mean absolute difference of two uniformly distributed random variables on [0, 1] interval is equal to 1/3. Therefore, if we denote the dimensions of test environment as a and b, the maximum positioning error, $\varepsilon_{max}(a, b)$, is given as:

$$\varepsilon_{\max}(a,b) = \frac{1}{3}\sqrt{a^2 + b^2} \quad \textbf{(2.27)}$$

The authors of (Borenovic *et al.,* 2008) also proposed a second derived parameter to include the correlation between the total number of AP used by the location system, the size of the testbed area and the positioning accuracy. For that criterion the median position error, noted $\varepsilon_{50\%}$ is multiplied with the density of AP, noted ρ_{AP}, which the number of AP per square meter in the building. This criterion must be minimized. It is the major criterion for WPS comparison because it is the real performance of the system whatever the building and network sizes: the location precision is measured for the same density of signals and the same density of receiver points for all methods. And also it takes into account the cost of the network deployment for location services which is a fundamental criterion for location service exploitation.

These both criteria allow anyone to compare systems in different buildings. Table 7 shows all the comparisons result between our system and other major positioning systems of the literature. For that comparison, we directly took the results obtained by the different teams; we did not develop again the systems and run our own tests. So the comparison is based on the confidence we do on the publications. The symbols * is used for RF measurement approach and # is used for propagation model approach.

TABLE 7 COMPARISON OF SEVERAL POSITIONING SYSTEMS

Technique / Parameter	RADAR		Bayesian	Horus	Battiti et al. ANN	ETF-ANN (ANN-A)	Our System (Right)	Our System (Left)	Our System (Whole)
System number	1		2	3	4	5	6	7	8
Test bed size: a×b [m]×[m]	43×22		25×15	59×19	20×15	144×66	60×36	60×36	120×36
Covering area: S [m^2]	979		375	1121	300	8500	2160	2160	4320
Number of AP: N_{AP}	3		5	12	3	8	4	3	5
m^2 per AP: ρ^{-1}_{AP}	326		75	93	100	1062	540	720	864
Required APs number to cover *ETF-ANN* area size	26		113	91	85	8	8	8	10
RPs	70		132	110	56	433	2160	2160	4320
Rx orientation at each RP	4		4	1	1	1	1	1	1
No. of samples for avg.	20		20	300	100	1	1	1	1
Number of RP per m^2	0.22		0.35	0.4	0.19	0.05	1	1	1
Total No. of samples / m^2	60.1		28.2	120	18.7	0.05	1	1	1
Maximum error: ε_{max} [m]	16.3		9.72	35.8	8.33	52.8	23.3	23.3	41.8
Radio map * RF measurement # Propagation Model	*	#	*	*	*	*	#	#	#
Median error: $\varepsilon_{50\%}$ [m]	3	4.3	2	2	1.69	8.4	8.01	4.81	9.6
Criterion 1 to minimize: $\varepsilon_{50\%}/\varepsilon_{max}$	0.185	0.263	0.206	0.056	0.203	0.159	0.343	0.206	0.227
Criterion 2 to minimize: $\varepsilon_{50\%} \times \rho_{AP}$	9.2	13.2	26.7	21.5	16.9	7.91	14.8	6.68	11.1

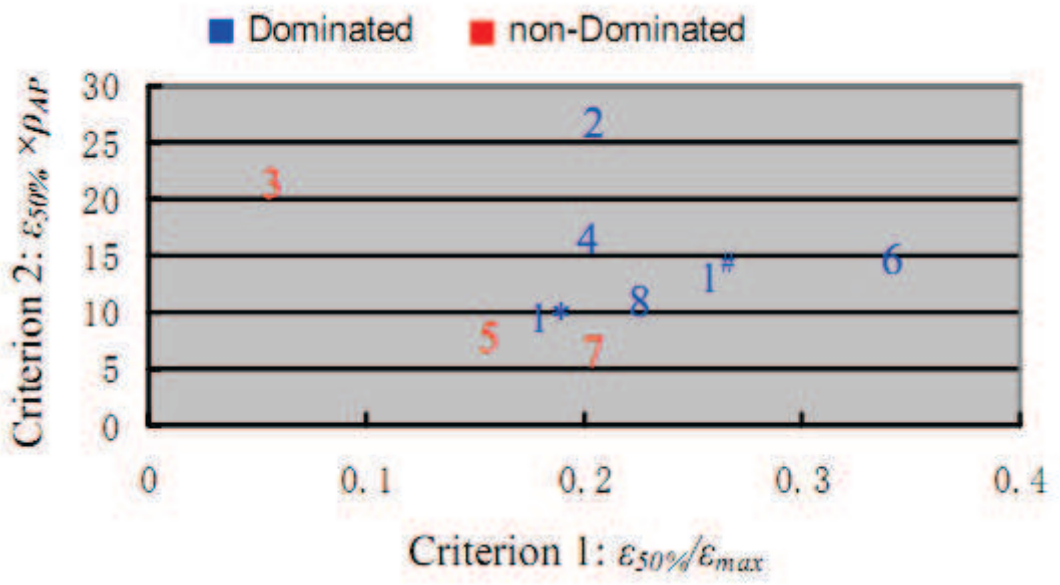

Figure 2.36 The performance of positioning systems based on Criterion 1 (includes building size) and Criterion 2 (includes network density) (each system is represented by its system number.)

From Table 7 and Figure 2.36, as common viewpoint, *Battiti et al.* with *ANN* technique shows the best performances exclusively regarding accuracy that is the median error whatever the building size (black cell in *Battiti*). On this criterion our system (9.6 on the whole building) and *ETF-ANN* (8.4) have the worse accuracy. This is because *Battiti et al.* building is also the smaller one (300m^2), then the maximum error is the smaller too! However, we clearly emphasise it is not possible to conclude on the real performance of WLAN Positioning System with that criterion.

Through above discussion, obviously, the location error is proportional to the building area. Now when using the ratio between the median error and maximum which includes the building size in performance evaluation (**criterion 1**), *Horus* technique gets the most favourable result (0.056), while the other systems are between 0.15 and 0.35. *Horus* is very efficient but we must emphasize that it uses 300 samples for averaging, and 120 samples per m^2, so it spends more time for on-line phase, and it uses much more AP than other systems (12 AP that is 3 to 4 time more than other test for a mean size building). The criterion 1 helps us to make a good judgment, but this is not the most relevant as it does not include the AP density so the benefits or the number of available signals.

Then let us introduce the AP density with the median error (**criterion 2**) to avoid the deviation due to AP number used for location. Criterion 2 means good positioning system should have two properties: low AP density and high location accuracy. How to find an appropriate balance between these two properties will be our further research. On this criterion the best performances are belong to our system in left side scenario and *ETF* is second. *CMTA-WPS* also performed well in other two scenarios. If the WLAN used for location is also used for communications, and probably we wish to, the criterion 2 is the more important because increasing the density of AP can improve the system accuracy and precision, but the frequency interference, then bad communication quality, and installation cost are increasing too, so there are big drawbacks!

Finally, the workload of offline measurement collection should be concerned as well. A more accurate radio map can provide a better localization performance. The other five systems use RF

measurement approach to generate the radio map. However, RF fingerprinting using on-site measurements is a time consuming process and a drawback for any process. To trade off between an accurate signal probability distribution and a heavy burden on the training procedure, it is ideal to replace this procedure with results obtained from suitable radio channel modelling techniques. Our positioning system uses the propagation model and some special filters to simulate the real measurement. And we believe this approach will be more efficient with some additional works dedicated to the improvement of the propagation model. However, we already prove that our model allows performing good location results for a lower cost.

2.5 Conclusion

In this chapter, we described our indoor positioning system CMTA-WPS. As its name indicates, this system is based on a WLAN-based indoor positioning system developed by the IBM China Research Laboratory combined with Centre of Mass technique and Time Average technique. In the offline phase section, two approaches for the radio map generation, measurement-based and model-based, were described and compared. Advantages and disadvantages of both approaches were discussed. As a result the radio map based on propagation modeling is recognized as a highly preferable approach to provide optimal and cost effective solutions. Then the overview of available propagation models and its usage was given. Deterministic propagation models provide the highest accuracy while empirical propagation models are relatively less time consuming. To be an elegant trade-off between accuracy and computation, a multi-wall propagation model is chosen.

In the online section, the basic operating mechanism of our indoor positioning system is described in detail. And some general positioning enhanced techniques such as Time Average, Centre of Mass and positioning filters are presented.

We have implemented the simulation and real test experiments. In the simulation experiment, we selected two buildings and conducted several experimentations using our WLAN-based indoor positioning system to give more insight on the impact of AP placement on location error. For the first building, we focused on the influence of the AP placement and the number of APs on location accuracy. The experimental performance shows that whatever the symmetric or asymmetric positions of AP distributed over the experimentation area, the average signal power is likely to be an important criterion for reducing location error. For the second building, we focused on the influence of the obstacles on the location error. The stationary MS and tracking performances are entirely different. Due to the positive effects of obstacles which make RSS vectors diverse, stationary MS are located more accurately. On the contrary, for tracking, location accuracy sometimes decreases. This is caused by the cumulated errors in the previous positions of the mobile device.

In the real test experiment, we studied the performance evaluation of our system. Commonly, inside one predefined building and with one predefined network the major performance criteria for indoor positioning systems are the accuracy and the precision in estimating a position. Our work is based on these two performance estimation criterions, a widely used error estimation method in many papers. We considered the test environment from three aspects: the entire floor, the right side floor and the left side floor of a 120×36 m^2 building (large area). Our system performs best in the left side of the floor and the average error is acceptable in normal indoor environments for most applications. This result indicates that the propagation model is not well adapted to the large open area architecture

as in the right side of the floor. Provided that in a previous study increasing the average power can reduce the position error, we delete the weakest AP to increase the average power. The result shows that the accuracy improves of 12%. By changing AP number and configuration, we confirm our former conclusion in a real environment.

To study the effects of positioning algorithms, radio map generation approaches and experimental area in reality, our system (probabilistic algorithm), RADAR (deterministic algorithm) and FRBHM (hybrid algorithm) were tested in two real environments. One environment is a large sized building and its radio map is built by an average accurate propagation model. Whereas the other environment is a medium sized building and its radio map is built by site survey. In the first environment, all the systems are responsive to the building topology changed. In the second environment, the positioning accuracy of all the systems is increasing when the number of AP is increasing. The performances of RADAR and our system are unstable when reducing grid density. On the opposite, the performance of FRBHM is quit stable. In both environments, all the systems show good performances to provide positioning support to context-aware applications. It means that a proper propagation model can meet positioning systems requirements in terms of accuracy. However, all the systems in second comparison have better good performances. This may confirm that the positioning accuracy is affected by the building size and the radio map generation.

We also focused on the comparison of CMTA-WPS to other major positioning systems of the literature by more practical criteria. The median error is a common criteria used in most papers. Battiti et al. with ANN technique has the best performances if one considers only the median error. Based on this criterion our system and ETF-ANN have the worse accuracy. However, note that all the indoor positioning systems we considered use different test environments and different networks. A new approach based on AP density and test area size seems to be a realistic and a fair way to quantify and evaluate the characteristics and performances. We used a criterion, denoted Criterion 1, which combines the size of the experimentation area and the median error and allows the comparison whatever the environments size. According to this criterion, Horus technique gets the most favourable result and our system performs averagely. It should be noted that Horus technique has the highest AP density. Next, we introduce the Criterion 2 that considers the AP density as an influence factor of error estimation, with this criterion our system is the best. Thus if we combine the Criterion 1 with the Criterion 2, our system achieves accuracy that is one of the best. Furthermore, it should be stressed out that our system is based on propagation model and some special filters to generate the radio map. It means the workload during the off-line phase is very low.

The above work opens up the path of our following work: **modelling indoor positioning problem**. After these experimentations based on different indicators (AP number, AP placement, obstacles number, average signal power, etc.) to estimate the location error, these indicators will be used to set the optimization parameters when modelling the indoor positioning problem.

Chapter 3 Modeling Indoor Positioning Problem

Most indoor positioning systems only focus on the network deployment for positioning but overlook that the original purpose of these WLAN infrastructures is to provide the required connectivity. In order to guarantee the requested Quality of Service (QoS) while reducing the location error, in this chapter we propose an effective approach where WLAN planning and positioning error reduction are modeled as an optimization problem and tackled together during the WLAN deployment process.

In modeling process, the indoor WLAN-based positioning is described in a mathematical way. The access point location, the access point pattern, the antenna orientation, the emitted power and the antenna frequency channel are set in the model. The AP model, the user requirement model, the throughput model and the positioning model have been defined according to the propagation model. QoS and positioning accuracy goals can be evaluated thanks to one QoS evaluation indicator and three positioning error indicators. Finally, the search space, the objectives and the set of constraints of our optimization problem are given based on the model and the indicators.

The work in this chapter has been published in 11ème Congrès de Recherche Opérationnelle et d'Aide à la Décision 2010 (*ROADEF'10*).

Contents

3.1 Introduction

The WLAN indoor positioning based on fingerprint technology has won growing interest in the last years. Recent studies in the literature mainly focus on improving the positioning and tracking algorithms which are used for estimating the location that associates the fingerprints with the location coordinates or reducing the cost of the measurement-based radio map development. Nevertheless, inspired by our previous experiments described in chapter 2, we can get positioning accuracy as target involved in the network configuration design. A network configuration refers to the deployment of a given number of APs with their assigned parameters (i.e. the allocated frequency, the emission power and the azimuth). Different configurations may correspond to different positioning accuracy. Furthermore, we ought not to neglect a fact that the original purpose of these WLAN infrastructures is to provide the required connectivity, so that, both the positioning accuracy and the communication quality should be considered in network configuration design. In fact, the positioning accuracy and the communication quality are two conflicting objectives. For example, an increase of the density of AP can improve the system accuracy and precision, whereas the communication quality (due to frequency interferences). These are major drawbacks!

Thus, we attempt to answer the following question: how to deploy a WLAN in order to guarantee the requested Quality of Service (QoS) while reducing the location error. Such a problem includes two aspects: WLAN planning and positioning error reduction. To provide users an optimal wireless access to their local network, WLAN planning does not only consists in selecting a location for each transmitter and setting the parameters of all sites, but also acts on allocating one of the available frequencies to each selected AP. Regarding the indoor positioning system, once RSS from all visible APs are measured and inputted, the location is estimated and outputted using the radio map and a machine learning technique. A more detailed description of this problem is shown in Figure 3.1.

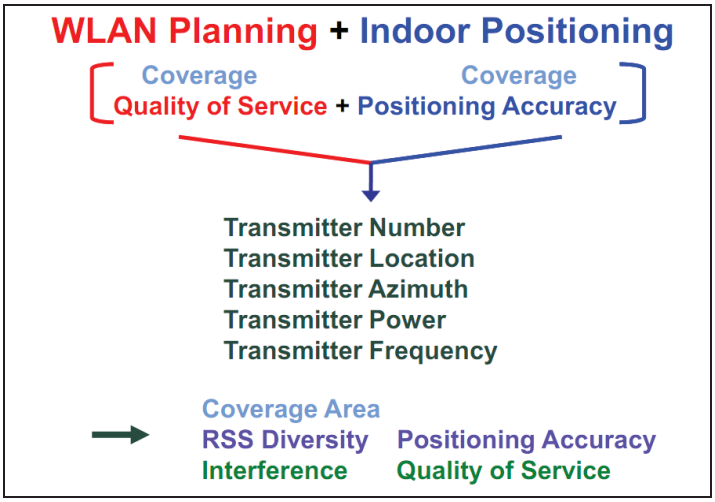

Figure 3.1 The relationship of each element of the problem

As shown here, in indoor WLAN-based positioning system, the basic requirement is to provide radio coverage on all assigned areas, which is a common requirement for communication and positioning. One complementary requirement concerns the positioning accuracy, which mainly relies

on the signal variation level and the distance between some points having the same RSS vector. Another complementary requirement concerns the efficiency and the throughput of the network, which mainly relies on the interfering signals level and the communicating signal level between cells. According to our studies, all these requirments are determined by the transmitter properties; for instance, transmitter number, transmitter location, transmitter azimuth, transmitter power, and transmitter frequency.

Such problem can be considered as an optimization problem. The generic process for mathematical optimization approaches involves three steps and is shown in Figure 3.2.

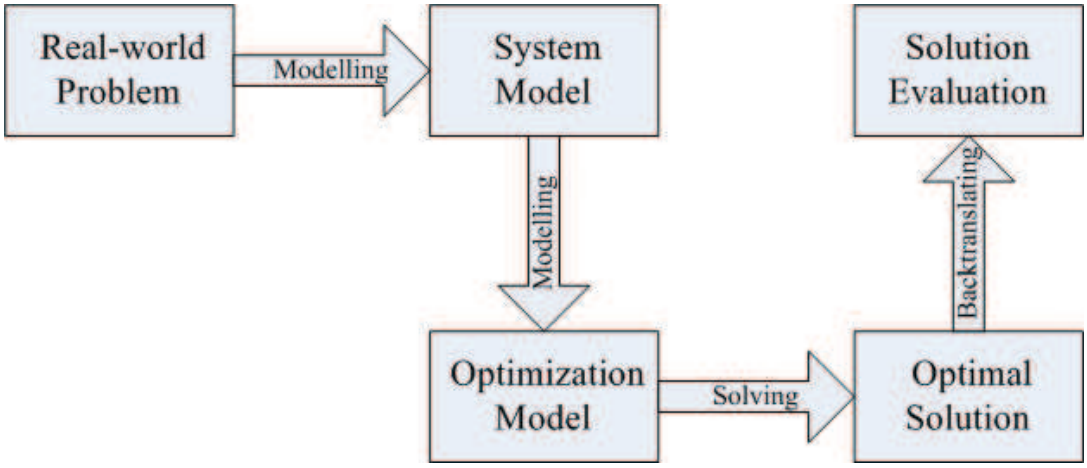

Figure 3.2 Solving a real-world problem with optimization method

The first step is a translation of the real world WLAN indoor positioning system into the system model. The system model is an outcome of a detailed system analysis using all engineering expertise available. The analysis develops a clear understanding of what is to be achieved, what are the important parameters, and what are the important quality indicators of a solution. Thus a major effort of this model is put into describing the system as accurately as possible. The positioning indoor models proposed in (Kaemarungsi & Krishnamurthy, 2004b) and (Hongpeng & Fei, 2007) belong to this kind of model (the system model).

Next, the optimization model is derived from the system model by further analysis of the system model and choosing the decision variable and fitness in the system model. The optimization model can be preferably solved using powerful advanced optimization algorithms. The optimization model states the optimization goal as well as the relevant constraints in mathematical terms. The optimization goal is either minimized or maximized depending on the context of the problem. The optimization model needs not reflect the full complexity of the system model. Important is that:

It is accessible to efficient computational solution.

A good solution to the optimization model can be transformed into a good solution to the system model.

The model proposed in this chapter belongs to such kind of model (the optimization model). Moreover, (Yubin *et al.*, 2010) and (Battiti *et al.,* 2003) also present the optimization model for indoor positioning system.

The final step is solving the optimization model by various kinds of optimization algorithms according to the complexity of the objective function and the constraints. Furthermore, the harvest is reaped by interpreting the mathematical solution in terms of the real world problem.

3.2 Optimization model

To represent the problem as an optimization model, the first step is finding the variables for the problem, whose values represent the elements of the problem that should be calculated as the input and the decision. The choice of variable definition plays a large role in how the optimization problem will ultimately be solved. Since WLAN design is widely studied for many decades, and some optimization models of WLAN planning are learnt from (Gondran *et al.,* 2007), (Jaffrès-Runser *et al.*, 2008), (Amaldi *et al.*, 2004) and (Bosio *et al.*, 2010). In WLAN indoor positioning system, we are interesting in the definition of problem variables and the description of network behaviours on communication and positioning. In addition, in order to facilitate the handling of problem, the whole model is decomposed into several sub-models, they are:

- **AP model**, where a finite set of candidate sites and candidate APs are predefined and the parameters setting of each AP type such as azimuth, emitted power and frequency channel is predefined;
- **Propagation model**, where the signal propagation for wireless channel in the building is predefined;
- **Requirement model**, where the traffic load requirement and the positioning accuracy requirement are predefined;
- **Throughput model**, where the evaluation of bit rates as well as the association rules between the clients and the AP are predefined;
- **Positioning model**, where the evaluation of positioning error is predefined.

The internal linkages among these models are represented in Figure 3.3 and then we are describing the models in the next sections.

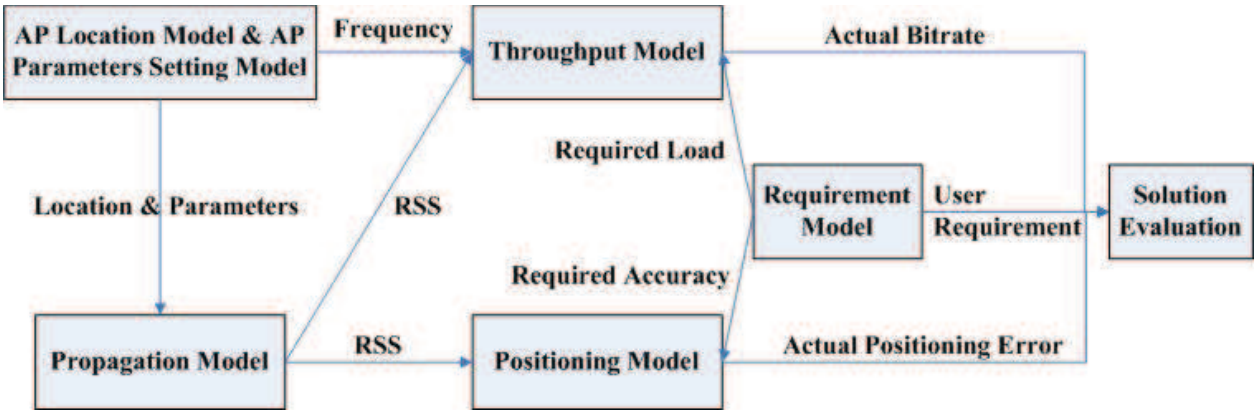

Figure 3.3 The internal linkages among the sub-models for optimization

3.2.1 AP model

3.2.1.1 AP location

a) Overview

In this model, a finite set of candidate sites is predefined. A site is a geographical location where an AP can be deployed. It is complex to construct the list of candidate sites. Usually, two factors should be taken into account for the distribution of the candidate sites: one is the distribution of the user's requirements; the other is the electromagnetic perturbation. Currently the methods include automatic methods, manual methods and hybrid methods. In addition, the list of candidate sites can also affect the quality of the results and the search time for optimization. In order to provide a best indoor positioning system better, we will use the list of candidate sites which is already validated in experiments. And the financial cost also should be considered.

b) Notation and definition

The following describes the variables for sites.

- The set of candidate AP locations is denoted by $S= \{1,..., n^S\}$.
- n^S is the total number of available candidate sites $n^S=|S|$.
- s is the s^{th} candidate site with $s \in \{1,..., n^S\}$.
- C_s^S is the installation cost of site s.

3.2.1.2 AP type

a) Overview

In this model, a finite set of candidate AP types is predefined. The AP types are distinguished by the types of manufacturer's equipments. There are mainly four differences among these AP types:

The cost of purchase and installation of AP.

The versions of the standards supported by AP. Currently, most APs belong to two types of the standards: the IEEE 802.11a which operates in 5 GHz band and IEEE 802.11b/g which operates in 2.4 GHz band.

The radiation pattern of the antenna of AP. The radiation pattern of an antenna is a plot of the relative field strength of the radio waves emitted by the antenna at different angles. It is typically represented by a three dimensional graph, or polar plots of the horizontal and vertical cross sections.

The list of the available emitted powers for AP.

b) Notation and definition

- The set of candidate AP types is denoted by $A= \{1,..., n^A\}$.
- n^A is the number of different types of AP, $n^A =|A|$.
- a indicates the a^{th} AP type, $a \in \{1,..., n^A\}$.

— C_a^A is the purchase and installation cost of AP type a. This cost is independent of the site installation cost C_s^S which is given in the AP location.

— r_a is the antenna radiation pattern of AP type a.

c) AP location and AP type

Combining AP location and AP type, we can derive a new variable w_s, which indicates the type of AP installed at site s. The value of w_s is defined as follows:

$w_s=a$, if the site s is chosen to install one AP of type a.

$w_s=0$, if the site s is unoccupied.

Namely, $w_s \in A \cup \{0\}$.

If we define a set S^O as the list of installed sites, then we can reach the inferences as follows:

$S^O=\{s \in S, w_s \in A\}=\{s \in S, w_s \neq 0\}$

n^O is the total number of all installed sites, $n^O=|S^O|$.

In practice we may encounter such a situation: a set of AP may be already installed before the optimization process as initial network. In this case, the aim of the planning is to expand this initial WLAN. Usually, these AP cannot be moved and their parameters cannot be modified.

Thus we can define a set S^I as a set of sites on which one AP is initially installed.

n^I is the total number of initially installed sites, $n^I=|S^I|$.

Clearly, $S^I \subset S^O \subset S$

Moreover, the user may require a maximum number of total AP, already installed AP and newly installed one, in its network in order to control the network budget. Then we define the maximum AP number n_{AP}^{max} as a problem parameter, and $n^O \leq n_{AP}^{max}$.

3.2.1.3 AP parameters setting

a) Overview

Once a type of AP is selected, it is necessary to determine the AP parameters setting; they are azimuth, emitted power and frequency channel.

Azimuth is an angular measurement in a spherical coordinate system. Here, it is defined as the angle between the North and the antenna radiation direction in the horizontal plane.

Emitted power is the power of the transmitter. The emitted power is usually in *dBm*, which is an abbreviation for the power ratio in decibels (*dB*) of the measured power referenced to one milliwatt (*mW*). Mathematically: emitted power [*dBm*] = 10×LOG10(emitted power [mW]/ 1*mW*)

The advantage of *dBm* is its capability to express both very large and very small values in a short form and to translate multiplication to addition. In many cases, planners would prefer to use comparatively high transmit power to increase the range of access points. However, the problem is

that RF interference with other nearby equipment would occur more often. The RF spectrum is limited, so we must control the amount of emitted power.

In radio communication systems, Equivalent Isotropically Radiated Power (EIRP) is used instead of the emitted power to evaluate the radiation power. EIRP represents the total effective transmit power of the radio, including gains that the antenna provides and losses from the antenna cable. EIRP can be calculated as follows:

EIRP[*dBm*]= emitted power [*dBm*] - cable losses [*dB*]+ antenna gain [*dB*]

In the EU, EIRP is limited to 20 *dBm* (100 *mW*) for 802.11b/g and to 23 *dBm* (200 *mW*) for 802.11a.

Frequency channel of AP has different standardization in the different place. In EU, frequency channel of AP is standardized by European Telecommunications Standards Institute (ETSI) in accordance with 802.11b/g or 802.11a.

In EU, 802.11b/g standards divide the 2.4 GHz spectrum into 13 channels. Two neighboring channels are separated by 5 MHz, as shown in Figure 3.4. Channels with at least 22 MHz separation are considered to be non-overlapping. Otherwise, they are called overlapping channels. The spectrum available to WLAN provides at most three non-overlapping channels (for example, channels 1, 6, and 11; see Figure 3.4). Since the 2.4 GHz spectrum is unlicensed, a WLAN may also be subject to the interference of external radiation sources (e.g., other WLANs, microwave ovens, DECT cordless telephones).

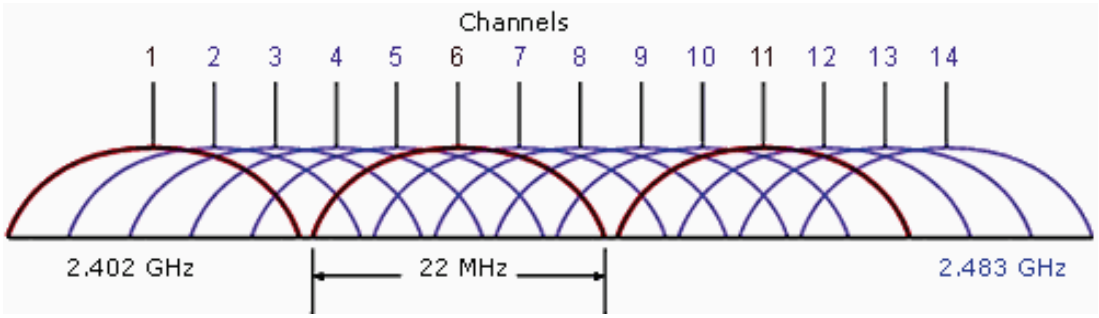

Figure 3.4 Channels specified by the I EEE 802.11b/g standards

Unlike 802.11b/g wireless networks, 802.11a wireless networks have 8 non-overlapping channels. In other words, it's going to be relatively easy to choose channels that are not in use by other nearby networks to avoid interference.

b) Notation and definition

For one AP of type a, the azimuth set is denoted by H_a. For different antenna types, we define:

- $H_a=\{0°\}$ for omni-directional antennas.
- $H_a=\{0°, 45°, 90°, 135°\}$ for bi-directional antennas.
- $H_a=\{0°, 45°, 90°, 135°, 180°, 225°, 270°, 315°\}$ for other directive antennas.
- n_a^H is the number of possible azimuth values for one type of antenna, $n_a^H=|H_a|$.

For one AP of type *a*, the emitted power set is denoted by P_a in accordance to manufacturers engineering rules. The emitted power is expressed in *dBm*.

— n_a^P is the number of possible emitted power values, $n_a^P = |P_a|$.

For one AP of type *a*, the frequency channel set is denoted by F_a. For different AP standards, we define:

— $F_a = \{1,...,13\}$ for 802.11b/g standards in EU.

— $F_a = \{1,...,8\}$ for 802.11a standard in EU.

— n_a^F is the number of possible frequency channel values, $n_a^F = |F_a|$.

For a site *s*, when the type of AP *a* is installed ($w_s = a$), we use h_s, p_s and f_s, to respectively denote the azimuth, the emitted power and frequency channel in use: $h_s \in H_a$, $p_s \in P_a$, $f_s \in F_a$.

To summarize the model explained in this section, one AP can be characterized by the following decision variables, (s, a, h_s, p_s, f_s). Thus the optimization process aims to find the best set of AP for the whole building according to some specified metric values.

3.2.2 Propagation model

3.2.2.1 Space discretization

a) Overview

As mentioned in the chapter 2, WLAN indoor positioning system works on a discrete space, thus it is necessary to divide the calculation area into a grid of pixels. The centre pixel in the grid is used to denote the whole pixels. We call this pixel centre a Marking Point (MP). In the three dimensions of space, the pixel step in horizontal plane is usually equal or higher than 1 m and the vertical pixel step is one per floor.

b) Notation and definition

With the given coordinate system *XYZ*, we define each grid as a unit:

— $I+1$ is the number of MPs along the *X* axis.

— $J+1$ is the number of MPs along the *Y* axis.

— $K+1$ is the number of MPs along the *Z* axis.

The set of MP in the calculation area is denoted by: $M = \{1,..., n^M\}$.

— n^M is the number of MP: $n^M = |M| = (I+1)\times(J+1)\times(K+1)$.

— m indicates the m^{th} MP, $m \in \{1,..., n^M\}$.

— X_m, Y_m, Z_m represents the X, Y, Z coordinates of MP m, respectively: $X_m \in [0, I]$, $Y_m \in [0, J]$, $Z_m \in [0, K]$.

Here, we define that the MPs are arranged in XYZ order in turn. In other word, let's suppose that $X_m=i$, $Y_m=j$, $Z_m=k$, *then:* $m=k\times J\times I+j\times I+i$.

— *dis(i,j)* represents the Euclidean distance between the MP *i* and the MP *j*.

$$dis(i,j)=\sqrt{(\mathrm{X}_i-X_j)^2+(\mathrm{Y}_i-Y_j)^2+(\mathrm{Z}_i-Z_j)^2} \quad \textbf{(3.1)}$$

X_s, Y_s, Z_s represents the X, Y, Z coordinates of the s^{th} candidate site, respectively: $X_s \in [0, I]$, $Y_s \in [0, J]$, $Z_s \in [0, K]$.

— *dis(s,m)* represents the Euclidean distance between the site *s* and the MP *m*.

$$dis(s,m)=\sqrt{(\mathrm{X}_\mathrm{s}-X_m)^2+(\mathrm{Y}_\mathrm{s}-Y_m)^2+(\mathrm{Z}_\mathrm{s}-Z_m)^2} \quad \textbf{(3.2)}$$

3.2.2.2 Received Signal Strength

a) Overview

To achieve a communication or positioning service, a user terminal needs to receive the radio transmission of an AP at an adequate level of power. The radio signal model defines the RSS expression and the different service demands related to the RSS level. For an AP with the given characteristics (s, a, h_s, p_s, f_s), a three-dimension coverage map is computed with a propagation model which has been described in detail in chapter 2. Since the propagation model considers a discrete space, the coverage map is defined as a set of mean RSSs associated with MPs. In the indoor positioning based on fingerprint technology, such coverage map is called the ***radio map***. Also, to achieve a high fidelity simulation, the concept of the signal distribution which was proposed in chapter 2 has been integrated in the model. For the coverage criterion, we define three kinds of RSS thresholds corresponding to different services.

b) Notation and definition

The mean RSS in MP *m* and coming from the site *s* is denoted by rss_{sm}, which is expressed in *dBm*. As we know, this value is a function of the AP decision variables. Thus, given the AP characteristic (s, a, h_s, p_s, f_s), for a MP *m*, we can get the expression as follows:

— $rss_{sm} = \chi(m, s, a, h_s, p_s, f_s)$ where, $\chi(.)$ is the indoor propagation model.

To be more precise, we combine rss_{sm} with the signal strength variation and get the random variable $\tilde{rss}_{sm}(p_{min} \le \tilde{rss}_{sm} \le p_{max})$, which represents the RRS in MP *m* detected from the site *s*. According to our signal distribution model, each value of $\tilde{rss}_{sm}$ follows a corresponding probability distribution. The probability density function (PDF) of this probability distribution is $p_{sm}(rss)$, where:

$$\sum_{rss=P_{\min}}^{p_{\max}} p_{sm}(rss)=1 \quad \textbf{(3.3)}$$

— p_{min} and p_{max} are the minimum and maximum limits of the random variable $\tilde{rss}_{sm}$. The maximum limit is decided by Wi-Fi standard and this value is equal to 20 *dBm* for 802.11b/g and to 23 *dBm* for 802.11a. The minimum limit is decided by the propagation model if there is no otherwise specified. According to our propagation model, the minimum limit p_{min} is equal to *-110 dBm*.

In fact, $\tilde{rss}_{sm}$ can be converted to rss_{sm} as follows:

$$dBm^{-1}(rss_{sm}) = \sum_{rss=P_{\min}}^{P_{max}} dBm^{-1}(rss) \times p_{sm}(rss) \quad \textbf{(3.4)}$$

Here, $dBm^{-1}(.)$ is the inverse transform of decibel.

Then, let the set $RSS_m = \{ rss_{sm} | \forall s \in S^O \}$ denote the RSS vector from all installed APs at MP *m*.

— n_m^{RSS} represents the size of RSS vector: $n_m^{RSS} = | RSS_m | = |S^O|$.

— rss_{sm}^{max} is the maximum received signal in the RSS vector RSS_m: $rss_{sm}^{max} = max(rss_{sm}), \forall s \in S^O$.

To classify different signal level for different services, three signal thresholds are predefined.

— rss^c is the communication threshold, which is the minimum signal power a client must receive for communication.

— Let the set S_m^C denote all visible APs at MP *m* for communication.

$$S_m^C = \left\{ s \middle| \forall s \in S^O, rss_{sm} \geq rss^c \right\} \quad \textbf{(3.5)}$$

— Let the set RSS_m^C denote the RSS vector from all visible APs at MP *m* for communication.

$$RSS_m^C = \left\{ rss_{sm} \middle| \forall s \in S_m^C \right\} \quad \textbf{(3.6)}$$

— n_m^C represents the number of RSS in RSS_m^C: $n_m^C = | S_m^C | = | RSS_m^C |$.

— rss^p is the positioning threshold, which is the minimum signal power a client must receive for positioning estimation demand.

— Let the set S_m^P denote all visible APs at MP *m* for positioning estimation demand.

$$S_m^P = \left\{ s \middle| \forall s \in S^O, rss_{sm} \geq rss^p \right\} \quad \textbf{(3.7)}$$

— Let the set RSS_m^P denote the RSS vector from all visible APs at MP *m* for positioning estimation demand.

$$RSS_m^P = \left\{ rss_{sm} \middle| \forall s \in S_m^P \right\} \quad \textbf{(3.8)}$$

— n_m^P represents the number of RSS in RSS_m^P: $n_m^P = |S_m^P| = |RSS_m^P|$.

— rss^i is the interference threshold, which is the minimum signal power from which a client can receive as an interferencing signal.

The relationship of between each RSS is as follows:

— Let the set S_m^I denote all visible APs at MP m as interference.

$$S_m^I = \left\{ s \middle| \forall s \in S^O, rss_{sm} \geq rss^i \right\} \quad \textbf{(3.9)}$$

— Let the set RSS_m^I denote the RSS vector from all visible APs at MP m as interference.

$$RSS_m^I = \left\{ rss_{sm} \middle| \forall s \in S_m^I \right\} \quad \textbf{(3.10)}$$

— n_m^I represents the number of RSS in RSS_m^I: $n_m^I = |S_m^I| = |RSS_m^I|$.

Since $rss^i < rss^p < rss^c$, we can conclude that: $S_m^I \subset S_m^P \subset S_m^C$.

3.2.3 User requirement model

3.2.3.1 Overview

In order to define the user demand, we use several zones, which are represented by polygons covering parts of the calculation area. Since our model works on a discrete space, to integrate these service zones into our model, these zones are represented by sets of MPs. We define two kinds of zones; they are the communication zone and the positioning zone.

Communication zone is characterized by a number of users or a desired bit rate by user for the service. We defined that one communication zone only corresponds to one kind of communication service. The MP inside communication zone, except those occupied by AP, is called Test Point (TP).

Unlike communication zone, *positioning zone* is only characterized by the positioning accuracy demand. The MP inside positioning zone, except those occupied by AP, is called Reference Point (RP).

Figure 3.5 shows the representations of the communication zone and the positioning zone.

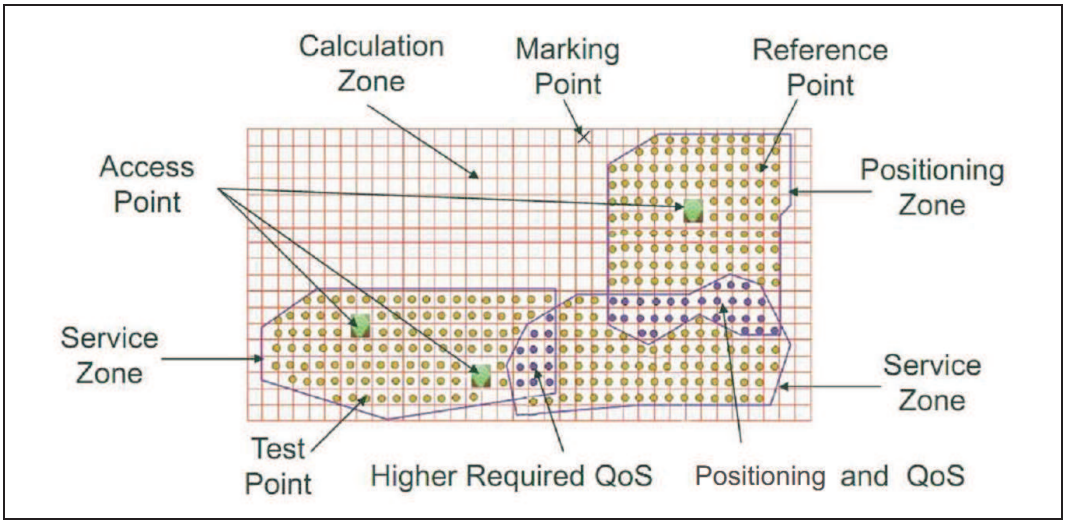

Figure 3.5 The representations of communication zone and positioning zone

Besides, both kinds of zone are characterized by an integer value varying from -1 to 1 to express the availability and importance of certain zone. This value is called *zone priority*. The value 1 means the service must be considered in this zone. The value 0 characterizes a zone of no importance so that we do not care the satisfaction of the service in such zone. The negative value -1 characterizes a zone, where the service is forbidden. In other words, such zone must not be covered by the APs.

These zones can also overlap each other. In the overlapping area, if there is no confliction in their requirements and in their zone priorities, all the requirements and zone priorities in the overlapping areas are taken into account. For example, when a communication zone with positive zone priority and a positioning zone with positive zone priority are overlapping, both desired bit rate and positioning accuracy are considered. If there is confliction in their requirements and their zone priorities are not negative, the higher requirement and positive zone priority are taken into account. For instance, when two communication zones with positive zone priority are overlapping, the higher desired bit rate is considered. If one of overlapping zones has negative zone priority, only the negative zone priority is considered.

3.2.3.2 Notation and definition

- The set of communication zones is denoted by $C= \{1,..., n^C\}$.
- n^C is the total number of communication zones: $n^C=|C|$.
- c is the c^{th} communication zone with $c \in \{1,..., n^C\}$.
- In c^{th} communication zone, the set of TPs is denoted by $T_c= \{1,..., n_c^T\}$.
- n_c^T is the total number of TPs in this communication zone c: $n_c^T =|T_c|$.
- t is the t^{th} TP with $t \in \{1,\ldots, n_c^T\}$.
- X_t, Y_t, Z_t represents the X, Y, Z coordinates of TP t, respectively: If $t=m$, $X_t= X_m$, $X_t =Y_m$, $Z_t =Z_m$.
- u_c is the total number of users in the communication zone c.
- b_c^u is the bit rate in kbps desired by each user for the communication zone c.

— p_c is the zone priority value allocated to the communication zone *c,* and each TP in this communication zone has the same zone priority: $p_c \in\{-1,0,1\}$.

A communication zone is characterized by above four variables: T_c, u_c, b_c^u and p_c. With these variables, we can get the following deductions:

— Let b_c represent the total desired bit rate in kbps inside the communication zone *c*: $b_c = b_c^u \times u_c$.

Supposing users are evenly distributed in the communication zone, let u_c^T represents the number of users per TP for the communication zone c: $u_c^T = u_c / n_c^T$.

— And let b_c^T represents the bit rate in kbps desired by user per TP for the communication zone *c*: $b_c^T = b_c / n_c^T = u_c^T \times b_c^u$.

— And let rss_{st} represent the mean RSS in TP *t* and coming from the site *s*. If *t=m*, $rss_{st}=rss_{sm}$.

— And let the set $RSS_t=\{rss_{st} | \forall s \in S^O\}$ denote the RSS vector from all installed AP at TP *t*. If *t=m*, $RSS_t=RSS_m$.

— The set of positioning zones is denoted by $P= \{1,..., n^P\}$.

— n^P is the total number of positioning zones: $n^P=|P|$.

— *p* is the p^{th} positioning zone with $p \in\{1,..., n^P\}$.

— In p^{th} positioning zone, the set of RPs is denoted by $R_p= \{1,..., n_p^R\}$.

— n_p^R is the total number of RPs in this positioning zone *p*: $n_p^R =|R_p|$.

— *r* is the r^{th} RP with $r \in\{1,..., n_p^R\}$.

— X_r, Y_r, Z_r represents the X, Y, Z coordinates of RP *r*, respectively: If *r=m*, $X_r= X_m$, $X_r = Y_m$, $Z_r = Z_m$.

— a_p is the positioning accuracy in meter desired by the user for this positioning zone *p.* Let denote a_p^R as the positioning accuracy in meter desired by user per RP, obviously, $a_p^R = a_p$.

— p_p is the zone priority value allocated to this positioning zone *p,* and each RP in this positioning zone has the same zone priority: $p_p \in\{-1,0,1\}$.

— And let rss_{sr} represent the mean RSS in RP *r* and coming from the site *s*, if *p=m*, $rss_{sr}=rss_{sm}$.

— And let the set $RSS_r=\{ rss_{sr} | \forall s \in S^O \}$ denote the RSS vector from all installed AP at RP *r*. If *r=m*, $RSS_r=RSS_m$.

When several zones are overlapping at one MP *m* (*m=t=p*), let C_t represents the set of communication zones covering the TP *t*: $C_t=\{c | \forall c \in C,\ t \in T_c\}$, and let P_r represents the set of positioning zones covering the RP *r*: $P_r=\{p | \forall p \in P,\ r \in R_p\}$.

— We denote b_t as the bit rate in kbps desired by user in the TP *t:*

$$b_t = \begin{cases} \max\limits_{c \in C_t} b_c^T & if \ \forall c \in C_t, \ p_c \geq 0 \\ 0 & if \ \forall c \in C_t, \ \exists p_c = -1 \\ 0 & if \ \forall p \in P_r, \ \exists p_p = -1 \end{cases} \quad \textbf{(3.11)}$$

— We denote a_r as the positioning accuracy desired by user in the RP *r:*

$$a_r = \begin{cases} \max\limits_{p \in P_r} a_p & if \ \forall p \in P_r, \ p_p \geq 0 \\ 0 & if \ \forall c \in C_t, \ \exists p_c = -1 \\ 0 & if \ \forall p \in P_r, \ \exists p_p = -1 \end{cases} \quad \textbf{(3.12)}$$

3.2.4 Throughput model

3.2.4.1 SINR

a) Overview

In this model, the key task is to obtain the real bit rate offered to the users in a given TP. As the propagation model has already given a very accurate description of the channel characteristics such as distance and multi-path, instead of trying to model the protocol Carrier Sense Multiple Access with Collision Avoidance (CSMA/CA) explicitly, a wise way to model the thourghput is to use the *SINR* (Signal to Interference plus Noise Ratio). Such evaluation method is also applied in the frequency assignment in cellular networks. The mathematical formula of SINR at a TP is:

$$SINR = \frac{P_{served}}{\sum P_{interference} + N} \quad \textbf{(3.13)}$$

Where P_{served} is the RSS from the served AP at this TP, $P_{interference}$ are channel interferences at this TP, and N is the surrounding environment noise.

From above formulation, no doubt, two issues had to be resolved firstly. One is how to define the served AP. The other is how to calculate the channel interferences.

For the first issue, the association policy which links each TP to the served AP is not fixed by the IEEE 802.11 standard and the manufacturers are free to implement their own policies. Currently, the most commonly used policy, the so-called *best server policy*, is that the MS is always served by the station from which it receives the highest signal power. Our model adopts this policy. For the second issue, we model interference and medium contention indirectly by considering the amount of overlap between APs operating on the same channel or adjacent channels. To do so, we treat channel interference in a similar way as being proposed in (Gondran *et al.*, 2008a) and define a parameter $\gamma(.)$ which is the protection factor corresponding to the attenuation coefficient between channels. Let Δf represents the channel distance between the carrier signal and the interfering signal. So that, $\gamma(.)$ may be considered as a function of Δf. $\gamma(.)$ decreases when Δf increases: if $\Delta f = 0$, $\gamma(\Delta f) = 1$ and if $\Delta f \geq 5$,

$\gamma(\Delta f)$=0. All intermediate values depend on the receiver equipment features. Table 1 shows the value of protection factor for standard 802.11b/g which comes from (Gondran, 2008).

TABLE 1 THE VALUE OF PROTECTION FACTOR FOR STANDARD 802.11B/G

Channel Distance	Protection Factor ($0 \le \gamma(.) \le 1$)	Protection Factor in dB ($-\infty \le \gamma(.) \le 0$)
0	1	0
1	0.7272	-1.38
2	0.2714	-5.66
3	0.0375	-14.26
4	0.0054	-22.68
5-12	0	$-\infty$

For a given client, there are two types of interfering signals: those coming from the AP not associated to the given client, they are downlink signals; and those coming from all other clients, they are uplink signals. Usually in literature and also in practice, only the downlink signals coming from AP are taken into account to quantify interferences because uplink signals are too numerous for simulation. In our approach as well, the uplink signal are not used for interference computation.

According to above discussion, the mathematical formula of SINR at a TP can be expressed more precisely:

$$SINR = \frac{P_{best\,RSS}}{\sum P_{other\,RSS} \times \gamma(\Delta f) + N} \qquad \textbf{(3.14)}$$

Where $P_{best\,RSS}$ is the highest RSS at this TP. $P_{other\,RSS}$ are other RSSs perceived at this TP with smaller values than the best RSS.

In this formula 3.14, $P_{best\,RSS}$ and $P_{other\,RSS}$ are expressed in milliwatt. However, in our model, all the powers are in decibel scale. Thus we prefer to use the SINR calculation in decibel:

$$SINR_{[dB]} = P_{best\,RSS[dBm]} - (\Sigma\, P_{other\,RSS[mW]} \times \gamma(\Delta f) + N_{[mW]})_{[dB]}$$

Notice that all the mentioned RSS values in the expression for SINR calculation are deterministic. However, in practice this is not always so simple. The previous signal propagation analysis indicates that WLAN signals vary significantly over time since the propagation of signals in an indoor environment is heavily affected by multi-path effects, dead spots, noise, and interference. Thus, the users at one TP could not always be served by the same AP. This makes the above SINR computation inaccuracy, because the serving AP choice strongly influences the above SINR computation.

Based on the signal propagation analysis, we have modeled the RSS distribution to simulate the real environment. Here, we prefer to take advantage of this RSS distribution.

Let ρ_{st} denote the probability for a given user in a TP t to be served by the AP in site s. The average SINR ζ_{st} at TP t can be computed when the serving AP is installed in the site s. In fact, unlike in cellular network, in WLAN the user will keep on connecting with the AP associated in the

first time unless the RSS of this AP is lower than the communication threshold. Thus, in order to facilitate understanding, ρ_{st} may be considered as the percentage of the users served by the AP in the site s at TP t, and ζ_{st} is the average SINR at TP t provided by AP in the site s.

Then the dynamic SINR on t $SINR_t$ can be structured by two sets. One is a set of the average SINR for each possible serving AP ζ_t: $\zeta_t=\{\zeta_{st}|\forall s \in S^O\}$. The other is a set of their associated probability ρ_t: $\rho_t=\{\rho_{st}|\forall s \in S^O\}$, where S^O has been defined in previous section as the list of AP installed sites.

Next, the expressions for ρ_{st} and ζ_{st} are derived respectively. As defined in the previous section, for a TP t, the probability ρ_{st} for a user in this TP to be served by the AP in site s can be written as:

$$\rho_{st} = P\left(\tilde{rss}_{st} > \tilde{rss}_{ht} \middle| \forall h \in S^O, h \neq s\right) \tag{3.15}$$

$$= \sum_{x=P_{\min}}^{P_{\max}} P\left(x > \tilde{rss}_{ht} \middle| \forall h \in S^O, h \neq s\right) p_{st}(x) \tag{3.16}$$

$$= \sum_{x=P_{\min}}^{P_{\max}} \left(\prod_{\substack{\forall h \in S^O \\ h \neq s}} \sum_{u=P_{\min}}^{x} p_{ht}(u) \right) p_{st}(x) \tag{3.17}$$

Before calculating ζ_{st}, we introduce the random variable $\tilde{rss}_{ht}$, which represent the RSS on t from AP in site h when AP in site s is the serving AP. Then the corresponding interference power on t when s is serving is defined as I_{st}:

$$I_{st} = \sum_{h \neq s, \forall h \in S^O} \tilde{rss}_{ht} \times \gamma\left(\Delta f_{h,s}\right) \tag{3.18}$$

Thus according to equation (3.13) the SINR on t for each possible serving AP s, ζ_{st} is given by:

$$\zeta_{st}[mW] = E\left[\frac{\tilde{rss}_{st}}{I_{st} + N}\right] \tag{3.19}$$

$$= \sum_{x=P_{\min}}^{P_{\max}} dBm^{-1}(x) \cdot E\left[\frac{1}{I_{st} + N} \middle| \tilde{rss}_{st} = x\right] P\left(\tilde{rss}_{st} = x \middle| \tilde{rss}_{st} > \tilde{rss}_{ht}, \forall h \in S^O, h \neq s\right) \tag{3.20}$$

$$= \sum_{x=P_{\min}}^{P_{\max}} dBm^{-1}(x) \cdot E\left[\frac{1}{I_{st} + N} \middle| \tilde{rss}_{st} = x\right] \frac{P\left(\tilde{rss}_{st} > \tilde{rss}_{ht}, \forall h \in S^O, h \neq s \middle| \tilde{rss}_{st} = x\right) P\left(\tilde{rss}_{st} = x\right)}{P(\tilde{rss}_{st} > \tilde{rss}_{ht}, \forall h \in S^O, h \neq s)} \tag{3.21}$$

$$= \sum_{x=P_{\min}}^{P_{\max}} dBm^{-1}(x) \cdot E\left[\frac{1}{I_{st}+N}\middle| rss_{st}^{\sim} = x\right] \frac{\left(\prod_{\substack{\forall h \in S^O \\ h \neq s}} \sum_{u=P_{\min}}^{x} p_{ht}(u)\right) p_{st}(x)}{\rho_{st}} \quad \textbf{(3.22)}$$

$$= \sum_{x=P_{\min}}^{P_{\max}} dBm^{-1}(x) \cdot \sum_{y=P_{\min}}^{P_{\max}} \frac{1}{dBm^{-1}(y)+N} p\left(y \middle| rss_{st}^{\sim} = x\right) \frac{\left(\prod_{\substack{\forall h \in S^O \\ h \neq s}} \sum_{u=P_{\min}}^{x} p_{ht}(u)\right) p_{st}(x)}{\rho_{st}} \quad \textbf{(3.23)}$$

According to the probability theory, the Probability Density Function of total interference $p_{st}^{I} = p(y/ rss_{st}^{\sim} = x)$ arises from the $(|S^O|-1)$-fold convolutions of each interference PDF $p_{ht}^{rss} = p(y/rss_{st}^{\sim}=x)$:

$$p_{st}^{I} = p_{1t}^{rss} \cdot \gamma(\Delta f_{1,s}) * p_{2t}^{rss} \cdot \gamma(\Delta f_{2,s}) * \ldots * p_{(|S^O|-1)t}^{rss} \cdot \gamma(\Delta f_{(|S^O|-1),s}) \quad \textbf{(3.24)}$$

$$= \underset{\substack{h \neq s \\ t<x}}{*} \left(p\left(rss_{ht}^{\sim} = t \middle| rss_{ht}^{\sim} < x\right) \cdot \gamma(\Delta f_{h,s}) \right) \quad \textbf{(3.25)}$$

$$= \underset{\substack{h \neq s \\ t<x}}{*} \left(\frac{p_{ht}(t)}{\sum_{t=P_{\min}}^{x} p_{ht}(t)} \cdot \gamma(\Delta f_{h,s}) \right) \quad \textbf{(3.26)}$$

It is now theoretically possible to compute the ζ_{st} using this formula. However, the computation over the whole set of AP can be difficult to be performed in a large network when we calculate the expectation of total interferences and noise. Thus we have to make the computation of ζ_{st} much simpler. We have an idea inspired by the approximate method proposed in (Jugl & Boche, 2000).

Under the condition that σ is reasonably low and use the delta method (Davison, 2003), the expectation of total interference and noise $E[rss_{st}^{\sim}/(I_{st}+N)]$ can be approximated as $E[rss_{st}^{\sim}]/E[I_{st}+N]$. Then, $E[I_{st}+N]$ can be approximately computed as the sum of two terms, one considering the contribution of the interference, and one taking into account the influence of noise. More precisely, $E[I_{st}+N] \approx E[I_{st}]+E[N]$. Moreover, we assume that N is a random Gaussian noise with mean μ_N and variance σ_N, so $E[I_{st}+N] \approx E[I_{st}]+\mu_N$. Mathematically, the approximation is given by:

$$E\left[\frac{rss_{st}^{\sim}}{I_{st}+N}\right] \approx \frac{E[rss_{st}^{\sim}]}{E[I_{st}+N]} \quad \textbf{(3.27)}$$

$$\approx \frac{E[\widetilde{rss_{st}}]}{E[I_{st}]+E[N]} \tag{3.28}$$

$$= \frac{E[\widetilde{rss_{st}}]}{E[\sum_{h\neq s}(\widetilde{rss_{ht}} \times \gamma(\Delta f_{h,s}))]+\mu_N} \tag{3.29}$$

$$= \frac{E[\widetilde{rss_{st}}]}{\sum_{h\neq s} E[\widetilde{rss_{ht}}] \times \gamma(\Delta f_{h,s})+\mu_N} \tag{3.30}$$

$$= \frac{E[\widetilde{rss_{st}}]}{\sum_{h\neq s} E[\widetilde{rss_{ht}} \Big| \widetilde{rss_{ht}} < \widetilde{rss_{st}}, \forall h \neq s, h \in S^O] \times \gamma(\Delta f_{h,s})+\mu_N} \tag{3.31}$$

Although we did a series of mathematical approximation, the calculation seems still complex. Thus this may require further simplification of the computation. According to previous RSS statistics analysis and our RSS distribution model, the variation of RRS is less than 8 dB in almost all cases. It means that the probability $P(\widetilde{rss_{st}}<\widetilde{rss_{ht}})$ is very small (less than 5%) if $|rss_{st} - rss_{ht}|>8$. In other words, $\widetilde{rss_{ht}}$ can be approximately regarded as an interference RSS under such condition. For these reasons, the following approximations are given:

For a TP t, we only consider the AP in site s where $rss_{st} \geq rss^i$ the interference threshold. It means that among the RSS vector we only consider the available RSS.

As well, only the AP in site s with $rss_{st} \geq rss^c$ can be the serving AP candidate, and the other APs are always considered as interference APs.

If the difference between the highest average RSS and the second highest average RSS in the vector RSS_t is larger than 8dB, the AP with highest average RSS is always considered as the serving AP. In other words, the serving AP choice does not influence the SINR computation. Thus we will use the equation 3.14 to calculate the SINR.

If there are some average RSSs in the vector RSS_t and if the difference between the highest average RSS and any one of these average RSSs is no more than 8dB, we have to consider the serving AP choice.

In our RSS distribution model, the range of variation is up to 18dB. However, the RSS usually varies near the average RSS. For example, 91.8% variation has been within the range between average *RSS-3dB* to average *RSS+5dB*. The high precision RSS distribution model is good for positioning. For radio planning, however, such high precision RSS distribution model is not only worthless but also increase the computation. Thus a wise method is an appropriate precision model. Here, our RSS distribution model is proportionally translated into a less precision model which varies from *average RSS-3dB* to *average RSS+5dB*.

b) Notation and definition

— The set of RSS vector which are from RSS_t and greater than interference threshold is denoted by RSS_t^I: $RSS_t^I = \{ RSS_m^I | t=m \}$.

— The set of sites where the RSS in RSS_t^I vector come from is denoted by S_t^I: $S_t^I = \{ S_m^I | t=m \}$.

— n_t^I is the number of RSS in RSS_t^I: $n_t^I = \{ n_m^I | t=m \}$.

— The set of RSS vector which are from RSS_t and greater than communication threshold is denoted by RSS_t^C: $RSS_t^C = \{ RSS_m^C | t=m \}$.

— The set of sites where the above RSS vector come from is denoted by S_t^C: $S_t^C = \{ S_m^C | t=m \}$.

— n_t^C is the number of RSS in RSS_t^C: $n_t^C = \{ n_m^C | t=m \}$.

— Let the set RSS_t^S denote the RSS vector from these possible serving APs in RSS_t.

$$RSS_t^S = \left\{ rss_{ht} \left| \underset{h \in S_t^C}{Min} \left| rss_{st}^{\max} - rss_{ht} \right| \le 8 \right. \right\} \quad \textbf{(3.32)}$$

— The set of sites where these possible serving APs are installed is denoted by:

$$S_t^S = \left\{ h \left| \underset{h \in S_t^C}{Min} \left| rss_{st}^{\max} - rss_{ht} \right| \le 8 \right. \right\} \quad \textbf{(3.33)}$$

— n_t^S is the total number of possible serving APs in TP t: $n_t^S = |S_t^S|$.

— Let rss_{st}^b denote the best average RSS in RSS_t and from AP in site s. If $n_t^S = 1$, then $rss_{st}^b = rss_{st}^{max}$.

Then, we can define the SINR in TP t as the communication quality computation in this point.

— For a given AP configuration and a best RSS rss_{st}^b in this TP, the SINR at the TP t for the serving AP located on site s is:

$$SINR_t = \frac{rss_{st}^b}{\sum_{p \in S_t^I, p \neq s} rss_{pt} \times \gamma\left(\Delta f_{p,s}\right) + \mu_N} \quad \textbf{(3.34)}$$

As in previous definition, $\Delta f_{p,s}$ represent the channel distance between the serving signal from AP at site s and the interfering signal from AP at site p. $\gamma(.)$ is the signal attenuation between channels as a function of Δf. The attenuation depends on several features such as WLAN standard and equipment. N is a random Gaussian noise with mean *100 -dBm* and variance *5 dB* in our experiments.

If $n_t^S > 1$, it means that there must be some APs which have a chance to be the serving AP. It is necessary to think about the effect of the serving AP choice in the SINR computation, so the dynamic

SINR is the logical choice. According to previous analysis and approximation on the dynamic SINR, the formation of the dynamic SINR at the TP *t* is such that:

$$SINR_t = \left\{ \left(\rho_{st}, \zeta_{st} \right) \middle| s \in S_t^S \right\} \tag{3.35}$$

— ρ_{st} is the probability that AP in site *s* becomes the serving station, and it can be determined by the following derived formula:

$$\rho_{st} = P\left(\tilde{rss_{st}} > \tilde{rss_{ht}} \middle| \forall h \in S_t^S, h \neq s \right) \tag{3.36}$$

$$= \sum_{x=rss_{st}^{low}}^{rss_{st}^{up}} \left(\prod_{h \in S_t^S, h \neq s} \sum_{u=x}^{rss_{st}^{up}} p_{ht}(u) \right) p_{st}(x) \tag{3.37}$$

Where rss_{st}^{low} is the lower bound of rss_{st}: $rss_{st}^{low} = rss_{st}-5$. rss_{st}^{up} is the upper bound of rss_{st}: $rss_{st}^{up} = rss_{st}+3$.

— ξ_{st} is the average SINR when AP in site *s* becomes the serving station, and it can be determined by the following derived formula:

$$\zeta_{st} = E\left[\frac{\tilde{rss_{st}}}{I_{st} + N} \right] \tag{3.38}$$

$$\approx \frac{E[\tilde{rss_{st}}]}{E[I_{st}] + E[N]} \tag{3.39}$$

$$= \frac{E[\tilde{rss_{st}}]}{E[\sum_{\substack{h \neq s \\ h \in S_t^S}} \tilde{rss_{ht}} \times \gamma(\Delta f_{h,s})] + E[\sum_{\substack{k \neq s \\ k \in S_t^I \\ k \notin S_t^S}} \tilde{rss_{kt}} \times \gamma(\Delta f_{k,s})] + E[N]} \tag{3.40}$$

The expectation of noise:

$$E[N] = \mu_N \tag{3.41}$$

The expectation of RSS from serving AP:

$$E[\tilde{rss_{st}}] = \sum_{x=rss_{st}^{low}}^{rss_{st}^{up}} dBm^{-1}(x) \cdot P\left(\tilde{rss_{st}} = x \middle| \tilde{rss_{st}} > \tilde{rss_{ht}}, \forall h \in S_t^S, h \neq s \right) \tag{3.42}$$

$$= \sum_{x=rss_{st}^{low}}^{rss_{st}^{up}} dBm^{-1}(x) \cdot \frac{\left(\prod_{h \in S_t^S, h \neq s} \sum_{u=x}^{rss_{st}^{up}} p_{ht}(u) \right) p_{st}(x)}{\rho_{st}} \tag{3.43}$$

The expectation of interference from APs which are impossible to be serving AP:

$$E[\sum_{\substack{k \neq s \\ k \in S_t^I \\ k \notin S_t^S}} \widetilde{rss_{kt}} \times \gamma(\Delta f_{k,s})] = \sum_{\substack{k \neq s \\ k \in S_t^I \\ k \notin S_t^S}} E[\widetilde{rss_{kt}}] \times \gamma(\Delta f_{k,s}) \tag{3.44}$$

$$= \sum_{\substack{k \neq s \\ k \in S_t^I \\ k \notin S_t^S}} rss_{kt} \times \gamma(\Delta f_{k,s}) \tag{3.45}$$

The expectation of interference from APs which are possible to be serving AP:

$$E[\sum_{\substack{h \neq s \\ h \in S_t^S}} \widetilde{rss_{ht}} \times \gamma(\Delta f_{h,s})] = \sum_{x=rss_{st}^{low}}^{rss_{st}^{up}} \left(\sum_{\substack{h \in S_t^S \\ h \neq s}} E[\widetilde{rss_{ht}} \,|\, \widetilde{rss_{ht}} < x, \forall h \in S_t^S, h \neq s] \times \gamma(\Delta f_{h,s}) \right) \tag{3.46}$$

$$= \sum_{x=rss_{st}^{low}}^{rss_{st}^{up}} p_{st}(x) \left(\sum_{h \in S_t^S, h \neq s} \left(\left(\sum_{v=x}^{rss_{st}^{up}} dBm^{-1}(\mathrm{v}) \times p_{ht}(v) \right) \times \left(\prod_{r \in S_t^S, r \neq s, r \neq h} \sum_{u=x}^{rss_{st}^{up}} p_{rt}(u) \right) \times \gamma(\Delta f_{h,s}) \right) \right) \tag{3.47}$$

Through a number of simplifying steps, now the average SINR has a complex expression rather than a heavy computation. Actually, in our later test, the number of possible APs $|S_t^S|$ is usually less than 2 and no more than 3. Besides, Σp_t can also be reused in calculation. In fact, when $n_t^S = 1$, the calculation of average SINR ξ_{st} is the same as calculation of $SINR_t$, and the corresponding probability ρ_{st} is also equal to 1. In other words, ξ_{st} when $n_t^S = 1$ is a particular case of ξ_{st} calculation.

Thus we can combine these two kinds of SINR into one. That is,

$$SINR_t = \left\{ (\rho_{st}, \zeta_{st}) \,|\, s \in S_t^S \right\} \quad \text{if } n_t^s > 0$$

— ρ_t is the set of probability of each possible serving AP for the TP t: $\rho_t = \{\rho_{st} | \forall s \in S_t^S\}$. ζ_t is a set of the average SINR for each possible serving AP for the TP t: $\{\zeta_{st} | \forall s \in S_t^S\}$.

If $n_t^S = 0$, there is no serving AP and no SINR at TP t.

— $SINR^c$ is the minimal SINR threshold to communicate at the minimum nominal rate. This threshold is decided by a given standard. So let $SINR^{cb}$ denote the threshold for 802.11b, $SINR^{cg}$ denote the threshold for 802.11g and $SINR^{ca}$ denote the threshold for 802.11a. Thus if the SINR at TP t provided by the AP in site s is lower than this threshold, we consider there is no association between the AP in the site s and the users at TP t.

Moreover, since we take into account the RSS variation, when the *RSS* from serving AP is very low, the connection between user and serving AP is unstable.

— Let the set $RSS_t^{unstable}$ denote the RSS vector of these unstable possible serving APs in RSS_t^C.

$$RSS_t^{unstable} = \left\{ rss_{st} \left| \underset{s \in S_t^S}{Min} \left| rss_{st} - rss^c \right| \le 5dB \right. \right\} \quad \textbf{(3.48)}$$

The set of sites where these unstable possible serving APs are installed is denoted by:

$$S_t^{unstable} = \left\{ s \left| \underset{s \in S_t^S}{Min} \left| rss_{st} - rss^c \right| \le 5dB \right. \right\} \quad \textbf{(3.49)}$$

— $n_t^{unstable}$ is the total number of unstable possible serving APs in TP *t*: $n_t^{unstable} = |S_t^{unstable}|$.

When $n_t^{unstable} \ge 0$, this means there will be the probability of disconnection between user and serving AP.

— Let $\rho_{st}^{unstable}$ denote this probability when serving AP at site *s*; it can be calculated as follows: $\rho_{st}^{unstable} = P(rss_{st} < rss^c)$.

— u_{st} is a decision variable which indicates whether the TP *t* is associated to the AP in site *s*.

$$\forall t \in T_C, \forall s \in S_t^S, u_{st} = \begin{cases} 1 & \text{if } \zeta_{st} \ge SINR^C \text{ and } s \notin S_t^{unstable} \\ P\left(rss_{st} > rss^c\right) & \text{if } \zeta_{st} \ge SINR^C \text{ and } s \in S_t^{unstable} \\ 0 & \text{if } \zeta_{st} < SINR^C \end{cases} \quad \textbf{(3.50)}$$

— Let u_t denote the network coverage: $u_t = \Sigma \rho_{st} \times u_{st}, \ \forall s \in S_t^S$.

So, if $u_t = 1$, the network covers the TP *t*. If $u_t = 0$, the network does not cover the TP *t*. If $0 < u_t < 1$, the network coverage in the TP *t* may be unstable. In fact, the unstable coverage situation can be classed as two cases: the network provides good coverage or the network provides poor coverage. Thus we redefine the network coverage situation for coverage criterion. If $0.6 \le u_t \le 1$, the network covers the TP *t*. If $0 \le u_t < 0.6$, the network does not cover the TP *t*.

— T_{S1}^C is the set of TPs which are in the c^{th} communication zone and are served steadily by the AP located on site *s*: $T_{S1}^C = \{t \in T_c \mid u_{st} = 1\}$.

— T_{S0}^C is the set of TPs which are in the c^{th} communication zone and are not served steadily by the AP located on site *s*: $T_{S0}^C = \{t \in T_c \mid 0 < u_{st} < 1\}$.

— T_S^C is the set of TPs which are in the c^{th} communication zone and are served by the AP located on site *s*: $T_S^C = T_{S1}^C \cup T_{S0}^C$.

— u_c^s is the total number of users in the c^{th} communication zone served by the AP located on site *s*: $u_c^s = \{\Sigma u_c^T \times \rho_{st} \times u_{st} \mid \forall \ t \in T_S^C\}$.

— T_0^C is the set of TPs which are in the c^{th} communication zone and are not served by any AP: $T_0^C = \{t \in T_c \mid \Sigma u_{st} = 0,\ s \in S_t^S\}$.

— u_c^0 is the total number of users in the c^{th} communication zone and not served by any AP: $u_c^0 = \{\Sigma u_c^T : t \in T_0^C\}$.

3.2.4.2 Throughput

a) Overview

After determinig the SINR at TP *t*, the next step is the calculation of the actual throughput in WLAN. Throughput is defined as the ratio of the expected delivered data payload to the expected transmission time. It is the percentage of undistorted packets the user sees after overheads. Overheads consume part of the nominal bit rate including:

1. Air time lost due to collisions between APs and users trying to transmit simultaneously.
2. Idle guard times, built into the protocol.
3. Air time lost due to beacon frames.
4. Protocol overheads (e.g. synchronization, address, acknowledgement and control).
5. Switching to ensure compatibility.

Moreover, throughput is affected by several factors. The resulting impact on throughput efficiency depends on the traffic mix. We highlight below the main problems affecting WLAN throughput:

— **Nominal bit rate downshifts with distance:** as the distance increases, the radio signal gets weaker and more distorted. As the signal degrades further, a *downshift* to a lower bit rate occurs. Downshifting allows the radio link to use simpler modulation scheme that makes it easier for the equipment to distinguish between digital zeroes and ones. The equipment downshifts progressively to lower and lower bit rates, as needed, as shown in Table 2.

TABLE 2 STANDARD NOMINAL BIT RATES

Standard	Bit Rates (Mb/s)
802.11a	54, 48, 36, 24, 18, 12, 6
802.11b	11, 5.5, 2, 1
802.11g	54, 48, 36, 24, 18, 12, 6

— **Contention between multiple-active users:** the throughput decreases if there are multiple simultaneously-active users transmitting data on the WLAN radio channel. The reason for this decrease is that with multiple active users trying to send at the same time, some of their packets collide. In a collision, the colliding parties wait a defined *backoff* time before retransmitting. This results in lost airtime which affects the system's throughput.

— **Interference of radio frequency:** the unlicensed nature of radio-based WLANs means that devices that transmit energy in the same frequency spectrum can potentially cause interference to a WLAN system. The interference is a usual problem and may be due to man-made noise or

WLAN itself. Compared to the man-made noise interference in 802.11a, the man-made noise interference in 802.11b/g is a more serious issue since many industrial, medical equipment and household appliances, for example, microwave ovens, Bluetooth devices… are operating at 2.4 GHz ISM band. When too many ISM devices operate in a small area, it results in interference as well as declines in performance. Especially, interference not only causes higher frame error rate, but also higher re-transmission rate. Nowadays, most WLAN manufacturers have already noticed this and designed their products to account for this interference. Thus the chief consideration of interference is the WLAN itself which is a growing headache as WLAN popularity grows. It mostly arises from other APs on the same and/or adjacent radio channels, and can be mutual and harmful.

— **Interoperability of wireless devices:** wireless LAN systems from different vendors may not be interoperable for different reasons. Firstly, different technologies will not interoperate; for instance, a system based on spread spectrum frequency hopping technology will not communicate with another system based on spread spectrum direct sequence technology. Secondly, networks using direct frequency bands will not interoperate even if they employ the same technology. Thirdly, systems from different vendors may not interoperate even if they both employ the same technology.

Referring to (Gondran, 2008), the throughput is calculated in two steps. The first step is using estimates of the SINR on a link to calculate thresholds for each bit rate, which define the range of SINRs providing the appropriate bit rate. This conversion is related primarily to a SINR-based bit rate adaptation scheme. Though currently there are many SINR-based bit rate adaptation schemes (Pavon & Sunghyun, 2003), (Chun-cheng *et al.,* 2007) , (Jiansong *et al.*, 2008), most of them are only evaluated only using research testbeds or simulation and are highly sophisticated. In order to make modeling more convenient and reliable, instead of calculating these thresholds based on a certain SINR-based bit rate adaptation scheme, receiver sensitivity are used to decide the threshold for each bit rate.

TABLE 3 RELATIONSHIP OF SINR THRESHOLD AND DATA RATE FOR THE STANDARD 802.11A/B/G

IEEE Standard	Coding	Modulating Type	Nominal Bitrate (Mbit/s)	Adapter (802.11b/g)		Adapter (802.11a)	
				Sensitivity Threshold (dBm)	SINR (dB)	Sensitivity Threshold (dBm)	SINR (dB)
802.11b	DSSS (11bits)	BPSK	1	-94	6	×	×
802.11b	DSSS (11bits)	QPSK	2	-93	7	×	×
802.11b	CCK (4bits)	QPSK	5.5	-92	8	×	×
802.11b	CCK (8bits)	QPSK	11	-90	10	×	×
802.11g/a	OFDM (1/2)	BPSK	6	-86	14	-85	16
802.11g/a	OFDM (3/4)	BPSK	9	-86	14	-84	17
802.11g/a	OFDM (1/2)	QPSK	12	-86	14	-82	19
802.11g/a	OFDM (3/4)	QPSK	18	-86	14	-80	21
802.11g/a	OFDM (1/2)	16-QAM	24	-84	16	-77	24
802.11g/a	OFDM (3/4)	16-QAM	36	-80	20	-73	28
802.11g/a	OFDM (2/3)	64-QAM	48	-75	25	-69	32
802.11g/a	OFDM (3/4)	64-QAM	54	-71	29	-68	33

Receiver sensitivity as an important parameter of Wi-Fi equipment indicates how a faint RF signal can be successfully received by the receiver. The lower the power level that the receiver can successfully process, the better the receiver sensitivity is. The receiver sensitivity is generally specified for noise-only condition, thus the minimum SNR (Signal to Noise Ratio) is determined by receiver sensitivity and noise. In Wi-Fi equipment, receiver sensitivity is generally stated as a function of network speed. Manufacturers will usually specify their receiver sensitivity at one or more of the 11 Mbps, 5.5 Mbps, 2 Mbps or 1 Mbps data rates. It also can be considered as the relationship between SNR threshold and nominal bit rate. When SINR is nearly regarded as SNR, the relationship between SINR threshold and nominal bit rate can be obtained. The Table 3 illustrates the relationship between receiver sensitivity (the SINR threshold) and data rate according to specification of WLAN adapter for the standard 802.11a/b/g (data come from Cisco Aironet 802.11a/b/g Wireless CardBus Adapter Data Sheet. The noise is equal to -101 dBm for standard 802.11a and -100 dBm for standard 802.11b/g.).

Since we have succeeded in converting SINR into the corresponding nominal bit rate in the first step, we can calculate the throughput according to the nominal bit rate, the different parameters of the MAC layer and the protocol CSMA/CA, the number of users communicating with the AP at different nominal bit rate allowed by the standard, etc... Firstly, we need a thorough study of the MAC layer and the protocol CSMA/CA.

The IEEE 802.11 standard defines both the physical and MAC layers. Although the IEEE 802.11a, 802.11b and 802.11g adopt different physical layer technologies, they share a common MAC. The 802.11 MAC supports two basic medium access protocols: distributed coordination function (DCF) and point coordination function (PCF). Since PCF is centralized and can only be used in the network of infrastructure mode, it has not drawn much attention from either the research community or industry. Thus we only focus on the DCF, which is a default medium access control mechanism of the IEEE 802.11, known as CSMA/CA. DCF is implemented within wireless stations and APs. Thus, DCF supports both ad-hoc mode and infrastructure mode.

The IEEE 802.11 defines two types of carrier-sense mechanism: physical carrier-sense and virtual carrier-sense (Standard, 1999). Physical carrier-sense is provided by PHY. Virtual carrier-sense mechanism is handled by MAC. Either one of carrier-sense indicates that the medium is busy. The medium should be busy, otherwise, it can be considered as idle.

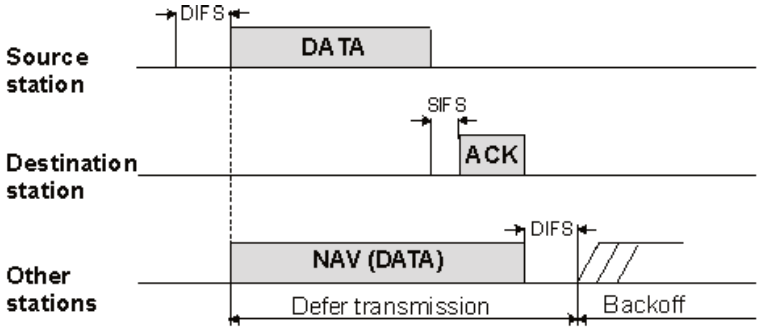

Figure 3.6 The timing diagram of basic CSMA/CA

Once a wireless station is associated with an Access Point (AP), it can start sending and receiving data to other wireless stations. If multiple stations attempt to transmit data at the same time

on the same channel, CSMA/CA is needed to coordinate the transmissions and prevent collision. According to the automatic medium sharing, before a station starts transmission, it senses the channel to determine if it is idle or not. Figure 3.6 illustrates the data frame exchange sequence. If the channel is idle for at least a Distributed Inter-Frame Space (DIFS) interval, the frame is transmitted. Otherwise, a backoff time slot is chosen randomly in the interval [0, CW*slot). The contention window (CW) is incremented exponentially with an increasing number of attempts to retransmit the frame. Upon receipt of a correct packet, the destination station waits a Short Inter-Frame Space (SIFS) interval and transmits a positive acknowledgment frame (ACK) back to the source station, indicating transmission success. During the backoff period, the backoff timer is decremented in terms of slot time as long as the channel is determined to be idle. When the backoff timer reaches zero, the data frame is sent out. If collision occurs, a new back-off time slot is chosen and the backoff procedure starts over until some time limit is exceeded. After successful transmission, the CW is reset to minimum CW. The virtual carrier-sense uses Network Allocation Vector (NAV) to reserve the medium for a fixed time period. The function of the NAV is a timer to indicate the amount of time that the medium will be reserved. If the NAV is not 0, it indicates the medium is busy. On the other hand, when the NAV is 0, the medium is available. The advantage of the NAV is to prevent interruption from other wireless stations during a sequence of frame transmission. The carrier-sense mechanism uses NAV state, transmitter status and physical carrier-sense to determine the status of the medium.

The DCF access mechanism can be extended by the transmission of special short frames Request To Send (RTS) and Clear To Send (CTS) frames prior to the transmission of actual data frame. A successful exchange of RTS and CTS frames permits to reserve the channel for the time duration needed to transfer the data frame. The RTS/CTS mechanism provides better network performance if hidden stations are present in the network.

The rules for transmission of an RTS frame are the same as those for the data frame under DCF access, i.e. the transmitter sends an RTS frame after the channel has been idle for a time interval exceeding DIFS. After receiving an RTS frame the receiver responds with a CTS frame, after the SIFS time. The CTS frame acknowledges the successful reception of RTS frame. After the successful exchange of RTS/CTS frames the data frame is sent by the transmitter, after waiting for a time interval of SIFS. In case of CTS frame is not received within the defined time interval, the RTS is retransmitted following the backoff procedure specified for DCF. The channel access method using RTS/CTS frames is presented in Figure 3.7.

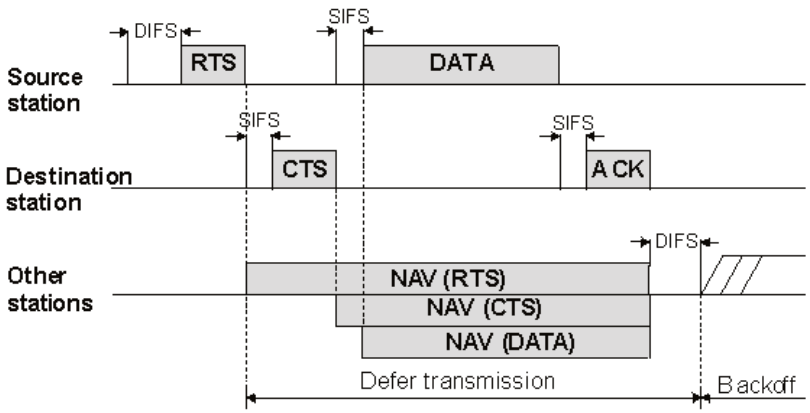

Figure 3.7 The timing diagram of CSMA/CA with RTS/CTS

Here, the data delivered by the source station is called MAC Service Data Unit (MSDU). It has arbitrary lengths (up to 2312 bytes) to the MAC layer. Large MSDU handed down from the Logical Link sublayer (LLC) to the MAC may require fragmentation to increase transmission reliability. To determine whether to perform fragmentation, MSDU is compared to the Fragmentation Threshold. Fragmentation Threshold is determined by the rules of the particular PHY in use. If the MSDU size exceeds the value of Fragmentation Threshold, then the MSDU is fragmented into multiple MPDU, which includes a MAC header and a trailing CRC. An illustration of fragmentation is shown in Figure 3.8.

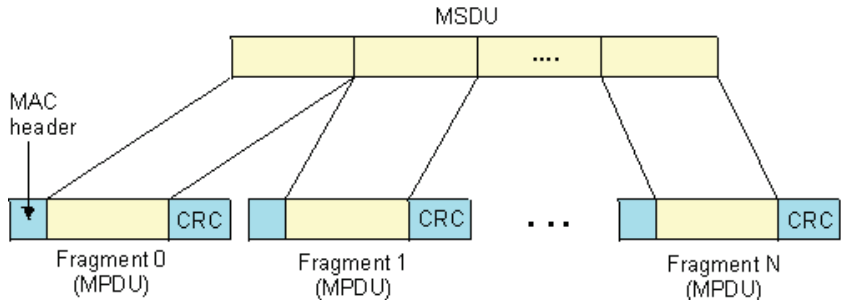

Figure 3.8 DATA fragmentation

The above analysis is only based on successful data transmission. In fact, in the real environments, there is no *constant throughput* in a WLAN. The instant saturation throughput has a too large variance to be significant, even in optimal conditions. Moreover, if once an error occurs, a packet has to be retransmitted by the attempting station. Since errors may be caused by many possible situations, it leads to a very complex throughput calculation. For simplicity, some common assumptions have been made:

1. For the AP, only downlink traffic is considered.

2. No management frames like beacon, probe request/response and dissociation/reassociation frames have been taken into account. The condition is ideal thus; there is no retransmission of packet loss, interference or collision. The buffers of the sender and the receiver could not result in overflow or underflow since there are sufficient frames to be transferred continuously. The medium access method is Distributed Coordination Function (DCF). Fragmentation is not used in MAC layer and the propagation delay is not considered. There is no RTS/CTS frame since the hidden nodes problem is not considered.

3. The Theoretical Saturation Throughput (TST) in the MAC layer is chosen as Figure 3.8 to characterize the throughput since this indicator is immune to the effects of environmental noise. TST is achieved when the AP always has a frame ready to be transmitted, and it reaches the maximum for optimal transmission conditions and appropriate offered traffic. In other words, TST corresponds to calculating the maximum capacity that the AP must supply to meet demand. Normally, TST only indicates the saturation throughput between the serving AP and a given user. If more than one user is served by this AP, it is preferable to consider the Average Theoretical Saturation Throughput (ATST) as an indicator. For the convenient calculation of the ATST, we assume that the channel access is shared equitably among the clients. In other words, the AP sends the same number of frames to all its customers.

Based on above-mentioned assumptions, we have a CSMA/CA transmission cycle shown in Figure 3.9. And the detail of each packets are illustrated in Figure 3.10

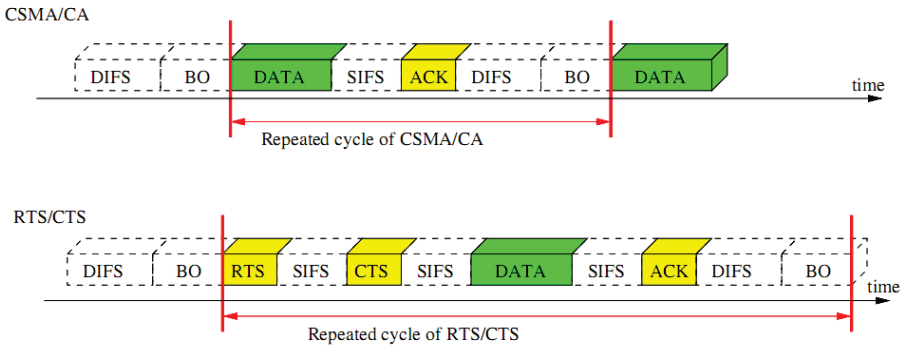

Figure 3.9 A transmission cycle

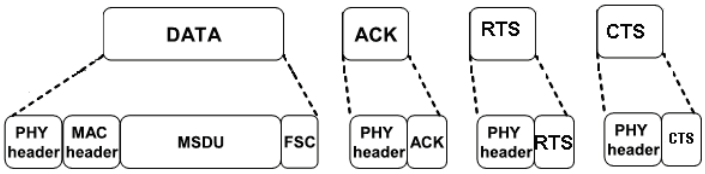

Figure 3.10 The detail of each frame

In above figures, BO is the back-off slot, which is selected randomly following a uniform distribution from 0 to CW*slot with the expected value of CW*slot /2. MSDU is the MAC Service Data Unit which is considered as transmission payload. FSC is a frame check sequence which is referred to as the end of the frame. FSC allows stations to check the integrity of received frames. In order to calculate the TST, we firstly convert all of the overheads at each sublayer into a common unit - time. Thus the total delay per MSDU can be calculated as a summation of all the delay components as below:

For CSMA/CA cycle without RTS/CTS:

The total Delay per MSDU = DIFS Duration + BO Duration + Data Duration + SIFS Duration + ACK Duration.

For CSMA/CA cycle with RTS/CTS:

The total Delay per MSDU = RTS Duration + CTS Duration + DIFS Duration + BO Duration + 3*SIFS Duration + Data Duration + ACK Duration.

At physical layer, the modulation and other timing related parameters are responsible for the physical layer overhead. The time spent to transmit a data frame can be computed as follows:

For 802.11b or 802.11b/g mixed mode:

Data Duration = (PHY Overhead Duration + MAC Overhead Length + FSC Length + MSDU Length) / Nominal Bit rate.

For 802.11g or 802.11a mode:

Data Duration = PHY Overhead Duration + Transmission Time for a symbol × ceil (MAC Overhead Length + FSC Length + MSDU Length) / Number of Data bits per OFDM Symbol.

Where the function ceil(.) returns the smallest integer greater than or equal to the value to map a real number to the largest previous following integer.

The duration of each delay component was determined from the standards. All delay components vary with the spread spectrum technology but not with the data rate. The transmission time of an MPDU depends on its size and data rate. The CW size does not increase exponentially since there are no collisions. Thus, CW is always equal to the minimum CW size (CW_{min}), which varies with different spread spectrum technologies.

In (Jun *et al.,* 2003), the author proposed that the total delay per MSDU can be simplified to a function of the MSDU size in bytes:

The total Delay per MSDU = a ×MSDU size + b

Where *a* and *b* are the scenario parameters and each pairs of *a* and *b* corresponds to the standard with a certain MAC schemes and spread spectrum technology.

From the above definition of throughput, it is now possible to express the throughput as a function of the MSDU size in bytes:

TST = Payload/Delay = 8 × MSDU size / (a ×MSDU size + b) Mbps

Table 4 shows values of *a* and *b* for every possibly scenarios:

TABLE 4 VALUES OF *A* AND *B* FOR DIFFERENT STANDARD MODE WITH DIFFERENT MAC SCHEMES AND SPREAD SPECTRUM TECHNOLOGIES

IEEE Standard	Coding	Nominal Bit Rate	CSMA/CA		RTS/CTS	
			a	b	a	b
802.11b	DSSS	1 Mbps	8.000000	1138.00	8.000000	1814.00
802.11b	DSSS	2 Mbps	4.00000	1002.00	4.00000	1678.00
802.11b	HR-DSSS	5.5 Mbps	1.45455	915.45	1.45455	1591.45
802.11b	HR-DSSS	11 Mbps	0.72727	890.73	0.72727	1566.73
802.11a	OFDM	6 Mbps	1.33333	230.17	1.33333	358.17
802.11a or g	OFDM	9 Mbps	0.8889	218.62	0.8889	346.62
802.11a or g	OFDM	12 Mbps	0.66667	194.00	0.66667	294.00
802.11a or g	OFDM	18 Mbps	0.44444	189.79	0.44444	289.79
802.11a or g	OFDM	24 Mbps	0.33333	117.67	0.33333	265.67
802.11a or g	OFDM	36 Mbps	0.22222	113.59	0.22222	261.59
802.11a or g	OFDM	48 Mbps	0.16667	167.00	0.16667	247.00
802.11a or g	OFDM	54 Mbps	0.14815	167.00	0.14815	247.00
802.11b/g mixed	OFDM HR-DSSS	6 Mbps	1.33333	538.00	1.33333	873
802.11b/g mixed	OFDM HR-DSSS	9 Mbps	0.8889	514.55	0.8889	849.55

802.11b/g mixed	OFDM HR-DSSS	12 Mbps	0.66667	501.15	0.66667	836.15
802.11b/g mixed	OFDM HR-DSSS	18 Mbps	0.44444	488.77	0.44444	823.77
802.11b/g mixed	OFDM HR-DSSS	24 Mbps	0.33333	483.25	0.33333	818.25
802.11b/g mixed	OFDM HR-DSSS	36 Mbps	0.22222	478.88	0.22222	813.88
802.11b/g mixed	OFDM HR-DSSS	48 Mbps	0.16667	476.91	0.16667	811.91
802.11b/g mixed	OFDM HR-DSSS	54 Mbps	0.14815	474.44	0.14815	809.44

Based on above table, it is easy to get the TST value with a given MSDU. Recall from third assumption, the channel accession is shared equitably among the clients. Thus we can define an accession cycle which is from the AP sending a frame to the first user up to sending a frame to the last user. The ATST of this cycle is also the ATST of whole time. Thus the ASTA can be calculated as follows:

ASTS in a cycle = Total MSDU in a cycle / Total Delay in a cycle

Total MSDU in a cycle = Number of User× MSDU Size

Total Delay in a cycle = ΣNumber of User per TP × Total Delay per MSDU per TP, for all covered TPs.

Here we consider the ASTS as the indicator of real downlink bit rate, and then the real downlink bit rate provided by the network at the TP *t* is equal to ASTS divided by the number of covered TPs.

b) Notation and definition

— D^N is the set of downlink nominal bit rate supported by the standard. So let D^{Nb} denote for 802.11b, D^{Ng} denote for 802.11g and D^{Na} denote for 802.11a.

— n^N is the total number of available downlink nominal bit rates: $n^N=|D^N|$.

— d_k^N is the k^{th} nominal bit rate in set D^N.

— d_t^N is the nominal bit rate in TP *t*. $d_t^N \in D^N \cup \{0\}$. Its value is determined by the $SINR_t$, according to the Table 3.

— L_t^{MSDU} is the size of the MSUD of the user in TP *t*. The size of MSDU is up to 2312 bytes and it is determined by some QoS management schemes. If not specified differently, we use the average MSDU which is equal to 1156 bytes.

— *a* and *b* are the MAC parameters which are used to calculate the total delay per MSDU according to the Table 4.

— TD_t^S is the total delay per MSDU at TP *t* by the serving AP in site *s*. $TD_t^S = a \times L_t^{MSDU} + b$.

— $ATST_s$ is the Average Theoretical Saturation Throughput in Mbps for all the users served by the AP in site *s*. The calculation is as follows:

$$\mathrm{ATST}_s = \frac{\sum_{t \in T_S^C} u_c^T \times \rho_{st} \times u_{st} \times L_t^{MSDU}}{\sum_{t \in T_S^C} u_c^T \times \rho_{st} \times u_{st} \times TD_t^S} \quad \textbf{(3.51)}$$

— d_t is the real downlink bit rate (in kbps) provided by the network at the TP t:

$$d_t = \sum_{s \in S_t^s} \frac{ATST_s}{u_c^s} \times \rho_{st} \quad \textbf{(3.52)}$$

— Δ_t is the deviation between the downlink bit rate required at the TP t called b_c^u and the bit rate provided by the network: $\Delta_t = d_t - b_c^u$.

Now we can judge whether the downlink bit rate required at the TP t is satisfied by Δ_t:

If $\Delta_t \geq 0$, the request at TP t is satisfied. If $\Delta_t < 0$, the request at TP t is not satisfied.

3.2.5 Positioning model

In the positioning model, the key is defining a way to evaluate the positioning error. Recent indoor positioning system research has mainly focused on algorithms that compute the best match. Although, most research only provided experimental results, they neglected an in-depth analysis of the impact of different factors for position errors. At a first glance, it is nearly impossible to find an appropriate way to pre-estimate the positioning error. As mentioned before, deriving the functional relationship between the position of the mobile terminal and the raw RSSI measurements is a hard task, both because of the difficulty in obtaining detailed knowledge about the building and because of the complexity of radio propagation indoor, characterized as site-specific, severe multipath, and with low probability for a line of sight propagation path between transmitter and receiver. These are also the main reasons for the difficulty in positioning error estimation. However, viewing from a statistical perspective, the positioning error can be divided into two components: systematic error and random error.

3.2.5.1 Systematic error

The systematic errors are biases in measurement which lead to the situation where the mean of many separate measurements differs significantly from the actual value of the measured attribute. There are many sources of systematic error, such as the calibration of measurement instruments or an estimate based on a mathematical model or physical law. Systematic error can be difficult to identify and correct. Given a particular experimental procedure and setup, it does not matter how many times you repeat and average your measurements; the error remains unchanged. No statistical analysis of the data set will eliminate a systematic error, or even alert you to its presence. The systematic errors caused by measurement instruments depend on the characteristics of measurement instruments, which is unsuitable for our model. Thus we only focus on the systematic errors due to the drawback of the system which can be located and minimized with careful analysis of the system procedure.

a) Aliasing

After studying the principle of positioning based on fingerprint technique, we noticed that there is only one drawback of fingerprint technique. Sometimes this drawback is referred to as *aliasing*. Aliasing means, that there are several distinct locations having the same visible APs and receiving the same signal strength value from each visible AP. Namely, the RSS vectors of these distinct locations are the same. This phenomenon is due to variations in the signal strength caused by obstacles so that locations are not necessarily at the same distance to the AP.

As is known to all, fingerprint technique relies on the best mach between the input RSS vector and the RSS vectors stored in the radio map. So when there are several RPs having the same RSS vector as a certain input RSS vector, fingerprint technique is not able to indicate which RP is the correct position. Thus if aliasing appears at some RPs, positioning based on fingerprint technique will become invalid in these RPs. In other words, aliasing is a source of positioning error.

Notice that aliasing error considers only the average RSS which is a constant value. For the aliasing error in our model, the average RSS consideration and the average RSS with the signal variation consideration are identical since the similarity of these RSS vector with the same average RSS is maximal. It will also be explained in the random error section.

To evaluate the aliasing error, we proposed an indicator called *Refined Specific Error Ratio (RSER)*. Let $RSER_r$ denote RSER at RP r. The expression of $RSER_r$ is as follows:

$$RSER_r = \frac{1}{(n(n-1))} \sum_{i=1}^{n} \sum_{\substack{j=1 \\ j \neq i}}^{n} dist(i,j) \quad \textbf{knowing that if } \boldsymbol{n = 1 \text{ then } RSER_r = 0} \tag{3.53}$$

Where,

i, j: the sequence number of RPs having the same RSS vector at the position r.

n: the number of RPs having the same RSS vector at the position r.

dist (i, j): the Euclidean distance between the RP i and the RP j.

The above equation indicates that RSER computes an arithmetic mean of the distances among a set of MPs having the same RSS vector. Namely, RSER is essentially a statistical aliasing error on a RP.

Moreover, as a global view of RSER, the *Refined Global Error Ratio (RGER)* was defined as the average of all RSER relating to each RP of the experimentation area:

$$RGER = \frac{1}{n} \sum_{r=1}^{n} RSER_r \tag{3.54}$$

Where,

n is the number of RPs in the experimentation area.

Recall in chapter 2, we have done some tests based on simulation. According to the study of these tests, it is possible to reliably establish a relationship between the average signal power of the

RPs and the average location error. In fact, different average signal powers of the RPs correspond to different AP configurations and the average positioning errors in simulation are reflected by aliasing errors. Thus the above relationship can be converted to the relationship between AP configuration and the aliasing error. Since we have an aliasing error indicator, now we can deeply explore these APs configurations in the previous tests based on simulation.

Here, in order to display the results of the simulation directly and conveniently, we normalized RSER and RGER based on statistical studies to provide the percentage of error ratios. The definition of $RSER_r^{Normalized}$ and $RGER^{Normalized}$ are proposed as follows:

$$RSER_r^{Normalized} = \left[\frac{e^{\frac{RSER}{2}}}{e^{\frac{RSER}{2}} + 1} \times \left(\frac{2 \times RSER}{2 \times RSER + 1} \right)^5 \right] \times 100 \quad \textbf{(3.55)}$$

$$RGER^{Normalized} = \frac{1}{n} \sum_{r=1}^{n} RSER_r^{Normalized} \quad \textbf{(3.56)}$$

Note that the parameters in 3.55 such as the power exponent are adjusted according to the statistical analysis of the RSER distribution from all the simulations so that the RSER values can be evenly distributed between 0 and 1.

From the above formulation, we determine the relationship between the local error μ and RSER as follows:

When RSER = 0 meter $RSER_r^{Normalized} = 0\%$;

When RSER = 1 meter $RSER_r^{Normalized} \approx 8\%$;

When RSER = 5 meters $RSER_r^{Normalized} \approx 58\%$;

When RSER > 11 meters $RSER_r^{Normalized} > 80\%$.

TABLE 5 RSER CELL COLOURS CORRESPONDENCE

$RSER_r^{Normalized}$	Cell Colour
0 % ~ 10 %	
10 % ~ 20 %	
20 % ~ 30 %	
30 % ~ 40 %	
40 % ~ 50 %	
50 % ~ 60 %	
60 % ~ 100 %	

Figure 3.11 and Figure 3.12 show the results obtained from the experimentations. The cell colour relates the normalized RSER value. The colour values are summarized in the Table 5. The

green cell colour corresponds to a location error of about one meter. The red cell colour is relative to a location error of more than five meters. All the other colours stand for a location error between one and five meters.

We notice that performing the normalized RGER values, according to WLAN configurations we checked, is a way to choose the best configuration relative to building architecture; for instance, selecting the configuration having the minimal normalized RGER seems to be the more convenient. The colours mapping of the normalized RSER values reflects the error ratio at each RP. Note that, to determine location error, RSER and RGER do not take into account the prior knowledge of previous positions. Thus both indicators reflect only the performance estimation of stationary MS in the global experimentation area.

Area Topology	$RSER_r^{Normalized}$	$RGER^{Normalized}$
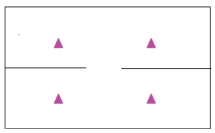	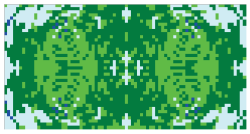	12.87%
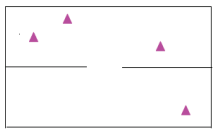	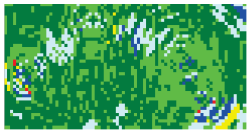	13.33%
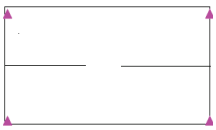	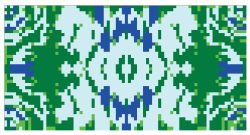	20.89%
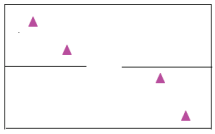	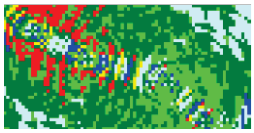	20.56%
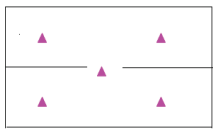		9.70%
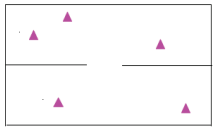		11.86%

Figure 3.11 Indicators variation in symmetric open-space building 1 for different WLAN configuratiion

Figure 3.11 shows the results obtained from the experimentations in the first building. Two major observations emerge.

Firstly, in the previous section in chapter 2, we concluded that adding a new AP does not always improve the accuracy. But studying the normalized RGER, we can adjust the conclusion as follows: adding a new AP does not always improve the accuracy in some area parts but improves it globally. For example, the normalized RGER value is 12.87% in the 1st configuration whereas it equals 9.70% in the 5th configuration. Looking at the normalized RSER colours mapping of these two configurations, we observe centred symmetrical green parts which are more extended in the 5th configuration compared to configuration 1.

Secondly, both conditions of symmetrical configuration and high average signal power give better results in the global experimentation area which is symmetric. Here, the normalized RGER of the 1st configuration is lowest in all the 4-AP configurations since it is symmetrical. For the same reasons, the normalized RGER of the 5th configuration is lower than the one of the 6th configuration.

Area Topology	$RSER_r^{Normalized}$	$RGER^{Normalized}$
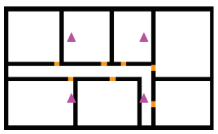		6.36%
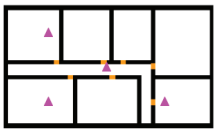	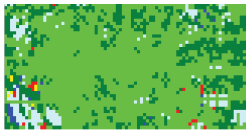	6.76%
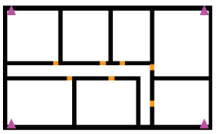	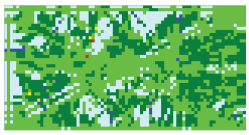	10.84%
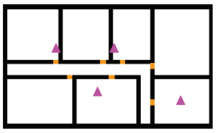	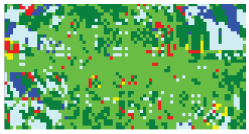	13.31%
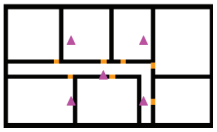	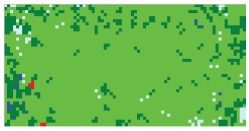	3.67%
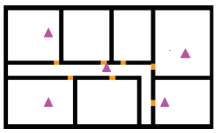	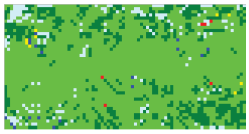	5.68%

Figure 3.12 Indicators variation in asymmetric building 2 for different WLAN

Besides the two observations mentioned above, Figure 3.12 also reveals that the global accuracy of the asymmetric closed-space (the second building) is better than symmetric open-space (the first building) with the same AP configuration. Indeed, in a closed-space environment, the probability to have RP with the same signal vector is lower and it reduces by 2 or 3 the RGER value.

The above explorations may also be summarized as increasing the number of APs or change the placement of APs can reduce RPs which contain aliasing.

b) Geometric dilution of precision

If location is computed using range-based techniques, the final location measurement uncertainty derived from the propagation and timing models will be magnified by a *Dilution Of Precision* (DOP) factor (Zirari *et al.*, 2009a):

$$variance(\delta x)=DOP\times\sigma^2_{user} \quad (3.57)$$

Where

δx is the user positioning error; σ^2_{user} is the user equivalent range error, that is the variance of the error in the pseudo-range measurements.

DOP is a standard, unit-less quantity, summarizing the quality of aggregate geometric measurements. The most general form of DOP is Geometric DOP (GDOP). Figure 3.13(a) and Figure 3.13(b) illustrate low and high GDOP situations using a hypothetical 2D location system based on distance measurements to 2 base stations respectively (Langley, 1999).

In this hypothetical 2D distance-measurement location system, in (a) low dilution of precision occurs because the measurement points have good separation from each other relative to the object being located conceptually, and the area of uncertainty in the intersection is small.

In this hypothetical 2D distance-measurement location system, in (b) high dilution of precision occurs because the measurement points have poor separation from each other relative to the object being ranged. The distance measurement error is the same as in Figure 3.13(a), but the location uncertainty will be larger.

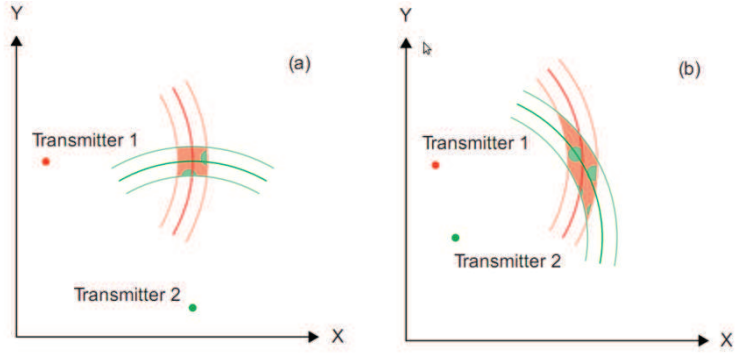

Figure 3.13 Low GDOP (a) and high GDOP (b) situations based on distance to 2 base stations

The term GDOP becomes the most popular criterion used to estimate the position accuracy with respect to the Global Navigation Satellites System (GNSS) such as GPS or Galileo. In fact, GDOP

has not been a metric to be exclusively applied to GNSS but has evolved to be adapted to other positioning systems such as the GSM or Wi-Fi.

In (Zirari *et al.*, 2009b), the authors propose to model the GDOP for WLAN. This model can be calculated as below:

For a certain RP, S_{AP} is a set of visible AP and $S_{AP}=\{AP_1, AP_2 \dots AP_n\}$. The number of visible APs n is one of the decisive elements on the accuracy of a positioning system as they avoid multipath problems. The needed number of visible access points to improve accuracy depends on the dimension of the positioning system. At least three APs for a two dimension positioning system and at least four APs for a three dimension one. If the number of AP is not sufficient, the value of the precision of dilution coefficient is set automatically as infinite. The optimal value is equal to one.

The radius between the visible AP_i and the user u is defined by $d_{i,u}$:

$$d_{i,u} = \sqrt{(x_i - x_u)^2 + (y_i - y_u)^2 + (z_i - z_u)^2} \tag{3.58}$$

Where x_i, y_i, w_i are the AP_i coordinates; x_u, y_u, z_u are the user unknown coordinates.

Equation 3.59 are linearised by using Taylor's expression at first order around the approximate user position (x'_u, y'_u, z'_u) and neglecting the higher order terms. Defining $d'_{i,u}$ as $d_{i,u}$ at (x'_u, y'_u, z'_u), we can write:

$$\Delta d_{i,u} = d_{i,u} - d'_{i,u} = a_{i,x}\Delta x_u + a_{i,y}\Delta y_u + a_{i,z}\Delta z_u \tag{3.59}$$

Where:

$$a_{i,\xi} = \frac{\xi_i - \xi'_u}{d'_{i,u}},\ \xi \in \{x, y, z\} \tag{3.60}$$

$$\Delta\eta_u = \eta_u - \eta'_u,\ \eta \in \{x, y, z\} \tag{3.61}$$

$$d'_{i,u} = \sqrt{(x_i - x'_u)^2 + (y_i - y'_u)^2 + (z_i - z'_u)^2} \tag{3.62}$$

For n visible AP, we obtain:

$$\begin{cases} \Delta d_{1,u} = a_{1,x}\Delta x_u + a_{1,y}\Delta y_u + a_{1,z}\Delta z_u \\ \Delta d_{2,u} = a_{2,x}\Delta x_u + a_{2,y}\Delta y_u + a_{2,z}\Delta z_u \\ \vdots \\ \Delta d_{n,u} = a_{n,x}\Delta x_u + a_{n,y}\Delta y_u + a_{n,z}\Delta z_u \end{cases} \tag{3.63}$$

We can write the above system in a compact matrix formulation as:

$$\begin{bmatrix} \Delta d_{1,u} \\ \Delta d_{2,u} \\ \vdots \\ \Delta d_{n,u} \end{bmatrix} \approx \begin{bmatrix} a_{1,x} & a_{1,y} & a_{1,z} \\ a_{2,x} & a_{2,y} & a_{2,z} \\ & \vdots & \\ a_{n,x} & a_{n,y} & a_{n,z} \end{bmatrix} \begin{bmatrix} \Delta x_u \\ \Delta y_u \\ \Delta z_u \end{bmatrix} \quad \textbf{(3.64)}$$

Or globally:

$$\Delta d \approx HX \quad \textbf{(3.65)}$$

Where

$$\Delta d = \begin{bmatrix} \Delta d_{1,u} \\ \Delta d_{2,u} \\ \vdots \\ \Delta d_{n,u} \end{bmatrix}, \quad H = \begin{bmatrix} a_{1,x} & a_{1,y} & a_{1,z} \\ a_{2,x} & a_{2,y} & a_{2,z} \\ & \vdots & \\ a_{n,x} & a_{n,y} & a_{n,z} \end{bmatrix} \textbf{ and } \quad X = \begin{bmatrix} \Delta x_u \\ \Delta y_u \\ \Delta z_u \end{bmatrix} \quad \textbf{(3.66)}$$

The Wi-Fi GDOP follows the equation below:

$$GDOP = \sqrt{Tr[(H^T H)^{-1}]} \quad \textbf{(3.67)}$$

Where H^T is the transpose of matrix H. $(H^TH)^{-1}$ is the inverse of matrix H^TH. $Tr[(H^TH)^{-1}]$ is the trace of matrix $(H^TH)^{-1}$.

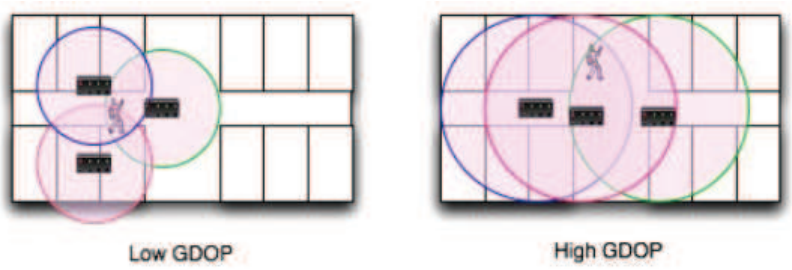

Figure 3.14 The AP geometry impacts on the Wi-Fi positioning system accuracy

Figure 3.14 shows the AP geometry impacts on the Wi-Fi positioning system accuracy. Clearly, the overlapping area is directly proportional to GDOP. The experimentations which were done in (Zirari *et al.*, 2009b) proves that the Wi-Fi GDOP is really influenced by the number and the signal strength of APs and is also a good indicator of the positioning accuracy.

Table 6 shows the rating for different GDOP values (Dutt *et al.*, 2007).

TABLE 6 THE RATING FOR DIFFERENT GDOP VALUES

GDOP Value	1	1-2	2-5	5-10	10-20	>20
Rating	Ideal	Excellent	Good	Moderate	Fair	Poor

From above table, we can see that the GDOP value equals one is the highest possible confidence level to be used for applications demanding the highest possible precision at all times. And then as the confidence level comes down, GDOP value decreases. When the GDOP value is between 2 and 5, it means positional measurements might be used to make reliable in-route navigation suggestions to the user. If the GDOP value is more than 20, the positioning estimation will be useless.

c) Neglectable error

Due to the characteristic of the wireless network cards, the estimated locations in most indoor positioning system are based on the signal strength data in a discrete and limited range. However, in real-world condition, signal strength distribution is continuously distributed in all the real numbers range, without lower or upper bounds. Thus two kinds of errors introduced in (Battiti *et al.*, 2003) are worth considering. One is due to the signal strength discretization, the other is due to signal strength below sensitivity.

About the first reason, the signal strength value returned by a wireless network card is integer. Assume that signal strength value is in dBm and rounded to the nearest integer. In other words, if the actual lies in the interval [s − 0.5dBm, s + 0.5 dBm), the returned signal strength value is equal to s. In this case, the maximum difference between the actual signal and integer signal is no more than 1 dBm. We can convert this maximum difference to the maximum discretization error according to the signal strength density function. The results indicate that the discretization error is very marginal and need not be taken into account.

About the second reason, the missed signal strengths are always below the noise level. It means that these signals are submerged sometimes by numerous background noises, so that we cannot obtain the useful information in order to minimize the localization error. This signal strength is very low and not usefull for location thus we will neglect such error.

In summary, these two kinds of errors are not considered when modelling the positioning error.

d) Notation and definition

There we summarize the notation we will use in the next sections from this part about systematic error.

— $R_r^{aliasing}$ is the set of all RPs having the same RSS vector than RP r, aliasing appears at these RPs:

$$R_r^{aliasing} = \left\{ i \middle| \forall i \in R_p, p \in P;\ \ RSS_i = RSS_r \right\} \quad \textbf{(3.68)}$$

As defined herein, R_p is the set of RPs in p^{th} positioning zone and P is the set of positioning zones.

— $n_r^{aliasing}$ is the number of all RPs having the same RSS vector than RP r: $n_r^{aliasing} = | R_r^{aliasing} |$.

— $RSER_r$ is the aliasing positioning error in RP r.

$$RSER_r = \begin{cases} 0 & if\ n_r^{aliasing} = 1 \\ \dfrac{1}{n_r^{aliasing}(n_r^{aliasing}-1)} \displaystyle\sum_{i \in R_r^{aliasing}} \sum_{\substack{j \in R_r^{aliasing} \\ j \neq i}} dist(i,j) & if\ n_r^{aliasing} \geq 2 \end{cases} \quad \textbf{(3.69)}$$

— $GDOP_r$ is the GDOP in RP r.

When $|n_r^P| \geq 3$, where n_r^P is the number of RSS at RP r, the H_r matrix is calculated as:

$$H_r = \begin{bmatrix} a_{1,x} & a_{1,y} & a_{1,z} \\ a_{2,x} & a_{2,y} & a_{2,z} \\ \vdots & & \\ a_{|n_r^P|,x} & a_{|n_r^P|,y} & a_{|n_r^P|,z} \end{bmatrix} \quad \textbf{(3.70)}$$

$$H_r = \left[\frac{X_s - X_r}{dist(s,r)}, \ \frac{Y_s - Y_r}{dist(s,r)}, \ \frac{Z_s - Z_r}{dist(s,r)}, \right], \ \forall s \in S_r^P \quad \textbf{(3.71)}$$

Where, S_r^P is a set of all visible APs at RP r for positioning estimation.

— After having H_r matrix, the GDOP in RP r can be calculated by following expression:

$$GDOP_r = \begin{cases} \sqrt{Tr[(H_r{}^T H_r)^{-1}]}, & \forall \mathrm{r} \in \mathrm{P}, \ \left|\mathrm{n_r^P}\right| \geq 3 \\ +\infty & \forall \mathrm{r} \in \mathrm{P}, \ \left|\mathrm{n_r^P}\right| < 3 \end{cases} \quad \textbf{(3.72)}$$

3.2.5.2 Random error

a) Overview

In measurement we often encounter such a situation: the measurable values are inconsistent during some repeated measures althought a constant attribute or quantity of measures are taken. Random errors are errors that lead to such instability. Random error is caused by unpredictable fluctuations in the readings of a measurement apparatus, or in the experimenter's interpretation of the instrumental reading; these fluctuations may be in part due to interference of the environment with the measurement process. In the indoor positioning system, there are many factors that can affect random error, such as AP orientation, time of day (a lot of people or not), environment (tables, desks…), distance from transmitter, interferences from other AP, interference from other systems (Bluetooth, microwave-owen…), sensibility of the wireless card... The error caused by these key factors is uncertain and time-varying, so that it is difficult to pre-estimate and eliminate it.

In statistics, the random error is considered as the error caused by observing a sample instead of the whole population. The random error can be found by subtracting the value of the whole population statistic from the value of the sample statistic. Thus, in contrast to systematic error, random error is usually estimated and minimized through statistical analysis of repeated

measurements. However, in positioning system, it is almost impossible to use statistical method to reduce the random error because for instance users do not stay for long periods in the same place and they cannot collect enough samples to match the whole population statistic. Moreover, the positioning error is sensitive to the RSS variation. Therefore, rather than minimizing or eliminating the random error, estimating the error is more practical.

Before estimating the random error, we overlook some unimportant factors that may affect random error and we assume that the signal strength variation is the only one reason that causes the random positioning error. Thus we will estimate the random positioning error through the analysis of the probabilistic estimation of signal strength variation and the relationship between the random positioning error and signal strength variation. According to our studies, the random positioning error mainly depends on the building structure. Inside structurally limited areas the signals received from one AP tends to be within a certain range, despite inevitable small scale fading effects. For instance, the signal strength measurements collected in one single office room often cover only a quite limited range of generally possible values. In such a case all fingerprints collected in this office are quite similar and they are hardly picked as the efficient fingerprints for the high accuracy positioning. In other words, these RPs in this office are indistinguishable. These phenomena can be used to explain why the large error is usual found in open space buildings as shown in our previous tests.

In conclusion, the random error of one RP can be evaluated by all the RPs in the indistinguishable area of this RP. Thus a random error indicator based on the matching scheme of probabilistic system and RSS distribution model is proposed; this indicator at RP r is expressed as follows:

$$\bar{e}_r = E(r) = \sum_{r' \in R_p} dist(r', r)\, p(r'|r) \tag{3.73}$$

Where $dist(r, r')$ is the Euclidean distance between the RP r and the RP r'. $p(r'|r)$ is the conditional probability of obtaining estimated position r' when the user's position is r.

Clearly,

$$\sum_{r' \in R_p} p(r'|r) = 1 \tag{3.74}$$

In fact, this probability is a criterion to estimate the similarity between two fingerprints. Set R_p denote all the RPs in the p^{th} positioning zones since the positioning systems do not return estimation outside the positioning zones. In fact, this indicator is essentially an average positioning error. Thus we tend to call this indictor as *average positioning error*.

In the next step, the key problem is how to calculate the conditional probability $p(r'|r)$. Indeed, since the indoor positioning system is based on fingerprinting, the estimated position basically depends on the input RSS vector measured in the RP and the radio map. Thus $p(r'|r)$ is determined by O_r which is denoted as the *obtaining observation* at RP r and $RSS_{r'}$ which is denoted as the *fingerprinting* at RP r'. However, the outcome is handled in different ways by different algorithms. For example, the k-nearest-neighbors technique returns the average of k nearest neighbors in signal space. Bayesian technique returns the sum of each possible location with its probability. Through analysis of many practical algorithms, we find that two common rules are obeyed by these practical

algorithms: the RSS vector of outcome is "near" the input RSS vector in the signal space (to simplify the $p(r'|r)$ calculation, "near" is approximated by "nearest" in the following discussion); and the small variations in input RSS vector must cause small variations in the algorithm outcome.

Based on above two rules, $p(r'|r)$ can be considered as:

$$\begin{aligned} p(r'|r) &= \sum_{O_r=O_r^{\min}}^{O_r^{\max}} p(O_r|r \cap r'|O_r) \\ &= \sum_{O_r=O_r^{\min}}^{O_r^{\max}} p(O_r|r) \times p(r'|O_r) \end{aligned} \quad \textbf{(3.75)}$$

O_r is a m-tuple RSS vector: $O_r = (o_{r1}, \ldots, o_{rk}, \ldots, o_{rm})$. Here o_{rk} represents the signal strength detected from k^{th} AP in RSS vector O_r, and m is number of APs. O_r^{Var} is an interval $[O_r^{min}, O_r^{max}]$ where the variation of O_r is located. $O_r^{min} = (o_{r1}^{min} \ldots, o_{rm}^{min})$ and $O_r^{max} = (o_{r1}^{max} \ldots, o_{rm}^{max})$. $[o_r^{min}, o_r^{max}]$ is the variation of RSS at RP r from its serving k^{th} AP and its size is $|o_{rk}^{min} - o_{rk}^{max}|$. Thus it is evident that $|O_r^{Var}|$, the number of all the possible O_r, is equal to $\Pi_{k=1}^{k=m} |o_{rk}^{min} - o_{rk}^{max}|$.

Note that in this model we use the RRS in fingerprinting combined with our RSS distribution model to simulate the obtaining observation at RP. In our signal propagation studies, it was found that the standard deviation of the RSS is large when the MS is located near an AP and receives a strong RSS. These locations usually have a direct line-of-sight of the received signal between the AP and the MS. On the contrary, the standard deviation is small when the MS is located far from the AP with weak RSS. Such locations often have non line-of-sight of the received signal between the AP and the MS. In other words, large standard deviations are found inside large and open space buildings, while small standard deviations are found inside small and closed spaces. Notice that our model described in chapter 2 only considers the signal strength variation over time. However, unlike throughput estimation, positioning accuracy is greatly influenced by the signal strength variation. Thus it is necessary to introduce the distance between RP and its serving AP as a parameter to compensate the above signal strength distribution.

Herein through a large number of experimental results analysis we proposed is a signal variation repair parameter σ_{rk}^{RSS} which represents the RSS variation of detecting signal strength from k^{th} AP at RP r. This parameter can predict the possible RSS variation in the positioning area. The mathematical expression is as follows:

$$\sigma_{rk}^{RSS} = round(\sigma^I + \sigma^M) = round(\sigma^I + K \times log(d)) \quad \textbf{(3.76)}$$

Where d is the distance between AP and receiver, σ^I is the signal variation from environment interference. σ^M is the signal variation caused by multi-path effect. Multi-path effect has a great impact on signal variation. Since the variation comes from a large number of reflected radio waves, and the signal strength of these reflected radio waves are decreasing with the increase of the propagation distance, such variation is inversely proportional to the distance between AP and receiver. Thus σ^M can be calculated as $K \times log(d)$ simply and proximately. K is an adjustable parameter for different scenarios (empirical value).

To use the formula 3.76, we need to have enough data for determining the two parameters σ^J and K at first. These data are the signal variation over the distance between AP and receiver at different orientations. Since known σ^J and K, the formula 3.76 becomes a mathematical formula that expresses the relationship between the distance between AP and receiver and the signal strength variation.

In the next step, to adapt the distribution model to the signal strength variation over distance, we do the following modifications to this model:

Firstly, the RSS variation probability density is simply modelled as a Gaussian distribution where the average is rss_{rk} and the standard deviation is σ_{rk}^{RSS}.

Then a two-steps scheme described in Chapter 2 to transform the short-term signal strength distribution into the long-term signal strength distribution is applied to make the RSS distribution model more accuracy than Gaussian model.

Finnaly, we get the modified probability density p'_{rk} and we prefer to use this RSS distribution model to calculate the average error.

In formula 3.75, $p(O_r \mid r)$ is the conditional probability that observed signal vector at RP r is equal to $RSS_{r'}$. Generally, $p(O_r \mid r)$ can be represented as:

$$p(O_r|r) = \prod_{k=1}^{m} p(o_{rk}|r) = \prod_{k=1}^{m} p'_{rk}(o_{rk}) \qquad \textbf{(3.77)}$$

$p'_{rk}(o_{rk})$ is the probability when detecting signal strength from k^{th} AP at RP r are equal to o_{rk}.

In formula 3.75, $p(r' \mid O_r)$ is defined as the probability when input RSS vector is O_r and the outcome from indoor positioning system is r'. Mathematically, $p(r' \mid O_r)$ can be represented as:

$$p(r'|O_r) = p\left(Sdis(RSS_{r'}, O_r) = \min_{r'' \in R_p} Sdis(RSS_{r''}, O_r) \right) \qquad \textbf{(3.78)}$$

$Sdis(RSS_{r'}, O_r)$ is the distance between $RSS_{r'}$ and O_r in the signal space. According to fingerprinting technique and the "nearest" rule, if $Sdis(RSS_{r'}, O_r)$ is minimum among all or a certain range location fingerprinting in radio map, $p(r' \mid O_r)=1$; else $p(r' \mid O_r)=0$.

Finally, the probability $p(r' \mid r)$ can be calculated as:

$$p(r'|r) = \sum_{O_r = O_r^{\min}}^{O_r^{\max}} \prod_{k=1}^{m} p'_{rk}(o_{rk}) \times p\left(Sdis(RSS_{r'}, O_r) = \min_{r'' \in R_p} Sdis(RSS_{r''}, O_r) \right) \qquad \textbf{(3.79)}$$

The above expression has an excessive computational cost. On the one hand, the interval $[O_r^{min}, O_r^{max}]$ contains $\Pi_{k=1}^{k=m} |o_{rk}^{min} - o_{rk}^{max}|$ elements which is a large quantity even with a small signal variation and a small AP number. On the other hand, to calculate $p(r' \mid O_r)$, we have to search all the RPs. Thus it is necessary to reduce computational complexity of the $p(r' \mid r)$ calculation.

Two hypotheses on the $p(r' \mid r)$ calculation can help to handle this problem:

Firstly, assume that all the RSS vectors located in the interval $[O_r^{min}, O_r^{max}]$ are uniformly replaced by the output RSS vectors which come from radio map and are located in the interval $[O_r^{min}, O_r^{max}]$. In fact, in any fingerprinting based positioning algorithm, any input RSS vector will be assigned to a RSS "near" vector from radio map. In other words, for an input vector O_r, it can be replaced by $RSS_{r'}$ when $p(r' \mid O_r)=1$. Since we assume that the probability of replacement for each RSS vector from radio map is equivalent, $Sdis(RSS_{r'}, O_r)$ has the same probability to be the global minima for each possible RP.

Secondly, assume that the $p(O_r \mid r)$ is replaced by $p(RSS_{r'} \mid r)$ when $p(r' \mid O_r)=1$. In fact, since we only consider the "nearest" RSS vector as the outcome, thus $Sdis(RSS_{r'}, O_r)$ is small when $p(r' \mid O_r)=1$. In this case, the difference between $p(O_r \mid r)$ and $p(RSS_{r'} \mid r)$ is also very small.

The above assumptions provide a reasonable approximation. Let R'_p denote the RPs whose RSS vector are located in the interval $[O_r^{min}, O_r^{max}]$. Clearly, $R'_r \subset R_p$. $n_{R'r}^{RSS}$ is the number of RSS vector of R'_r, and the number of possible observed RSS in the interval $[O_r^{min}, O_r^{max}]$ is $\Pi_{k=1}^{k=m} |o_{rk}^{min} - o_{rk}^{max}|$. Thus based on the first assumption, we have the following approximation:

$$\sum_{O_r=O_r^{\min}}^{O_r^{\max}} p(r' \mid O_r) \approx \frac{\prod_{k=1}^{k=m} \left| o_{rk}^{max} - o_{rk}^{min} \right|}{n_{R'_r}^{RSS}} \tag{3.80}$$

Based on the second assumption, if $p(r' \mid O_r)=1$, of $p(O_r \mid r)$ is given by:

$$p(O_r \mid r) \approx p(RSS_{r'} \mid r) = \prod_{k=1}^{m} p'(rss_{kr'} \mid r) = \prod_{k=1}^{m} p'_{rk}(rss_{kr'}) \tag{3.81}$$

Combining equation 3.80 and equation 3.81, by normalizing the probability, we can get the following estimate for $p(r' \mid r)$:

$$p(r' \mid r) = \frac{\prod_{k=1}^{m} p'_{rk}(rss_{kr'})}{\sum_{r'' \in R'_r} \prod_{k=1}^{m} p'_{rk}(rss_{kr''})} \tag{3.82}$$

Substituting equation 3.82 into equation 3.73, the expression of the average positioning error indicator at a RP r can be rewritten as:

$$\bar{e}_r = \frac{\sum_{r' \in R'_r} dist(r', r) \prod_{k=1}^{m} p'_{rk}(rss_{kr'})}{\sum_{r'' \in R'_r} \prod_{k=1}^{m} p'_{rk}(rss_{kr''})} \tag{3.83}$$

b) Notation and definition

- Let O_r denote the observed RSS vector at RP r.
- n_r^O is the number of RSS in the O_r: $n_r^O = |O_r| = n_r^P$.
- o_{rk} represents the signal strength detected from the k^{th} AP in RSS vector O_r: $O_r = (o_{r1}, \ldots, o_{rk}, \ldots, o_{rn_r^o})$.
- Let σ_{rk}^{RSS} denote the possible RSS variation from the k^{th} AP at RP r. σ_r^I is the signal variation from environment noise interference at RP r. σ_{rk}^M is the signal variation caused by multipath effect from the k^{th} AP at RP r. Then; $\sigma_{rk}^{RSS} = \text{round}(\sigma_r^I + \sigma_{rk}^M) = \text{round}(\sigma_r^I + K \times log(dis(k,r)))$, where, σ_r^I and K can be obtained from measurements.
- o_r^{Var} is the interval of the o_{rk} variation $[o_{rk}^{min} - o_{rk}^{max}]$, and $|o_r^{Var}|$ is the variation size of the o_{rk}.
- O_r^{Var} is the interval of the O_r variation $[O_r^{min}, O_r^{max}]$. $O_r^{min} = (o_{r1}^{min} \ldots, o_{rm}^{min})$ and $O_r^{max} = (o_{r1}^{max} \ldots, o_{rm}^{max})$. The number of all the possible O_r, $|O_r^{Var}|$ is: $\Pi_{k=1}^{k=m} |o_{rk}^{min} - o_{rk}^{max}|$.
- p'_{rk} is the probability density function of the RRS distribution in RP r and as detected from the k^{th} AP with the varying signal strength variation.
- Let R'_r denote the RPs whose RSS vector is located in the interval $[O_r^{min}, O_r^{max}]$. $R'_r = \{r: RSS_r \in [O_r^{min}, O_r^{max}]\}$
- APE_r is the Average Positioning Error indicator at RP r.

$$APE_r = \frac{\sum_{r' \in R'_r} dist(r', r) \prod_{k=1}^{m} p'_{rk}(rss_{kr'})}{\sum_{r'' \in R'_r} \prod_{k=1}^{m} p'_{rk}(rss_{kr''})} \quad \textbf{(3.84)}$$

To avoid any high positioning error existing in positioning zones, a minimum global average positioning error APE^{min} is given by the user or by default as a constraint.

3.2.5.3 Relationship between the three positioning errors

a) Overview

So far, we have three kinds of positioning error. Two are belong to the system error, which are aliasing error and GDOP. One is concerned with random positioning error, which is the average error.

Recall that, in indoor positioning system, unlike the random error which is difficult to be minimized, aliasing error and GDOP are directly relatived with AP configurations, thus we can minimise these two errors by modeling them as an optimization problem. For the random error, the only thing we can do is to estimate it.

In fact, the information of aliasing error is closely related with the average positioning error, thus in our positioning model, we can use the average positioning error to estimate both the aliasing error and the positioning random errors. GDOP is a good candidate to specify the most adequate APs

distribution and generally speaking lower GDOP will bring lower average positioning error. But that does not mean that GDOP can be replaced by the average positioning error, since GDOP is one of the factors affecting the average positioning error. In fact, GDOP itself only represents a trend of the average positioning error; it is roughly interpreted as the ratio of the position error to the signal strength variation range. And GDOP combined with the signal strength variation of all the visible AP determines the average positioning error.

To sum up, the average positioning error and the GDOP will be chosen as the primary and the secondary positioning error indicator in our model. That means when comparing the positioning accuracy of two network configurations we should consider the average positioning error at first and if the average positioning errors of two network configurations are the same or similar then we will use GDOP. The aliasing error can be applied to improve the solution search in optimization since there are inherent connections between aliasing error and average positioning error.

b) Notation and definition

— Δ_r is the deviation between the positioning accuracy required at RP r in the positioning zone p and the positioning accuracy estimated at RP r in the positioning zone p:

$\Delta_r = APE_r - a_p$.

Where a_p is the positioning accuracy in meter desired by the user for this positioning zone p and APE_r is the average positioning error indicator at RP r.

Now we can judge whether the positioning accuracy required at RP r is satisfied by Δ_r:

— If $\Delta_r \geq 0$, the positioning accuracy required at RP r is unsatisfied. If $\Delta_r < 0$, the positioning accuracy required at RP r is satisfied.

3.3 Optimization problem

After the optimization model being introduced in the previous sections, now we define this optimisation problem to solve. This optimisation problem is generally addressed by the following steps.

We select sites from a list of candidate sites where we can install one AP. Once the AP sites are set, it is necessary to determine which AP is suitable to be placed on sites from a list of different types of AP. Then each AP must choose its radio parameters among a finite list of azimuth and a finite list of emitted power. It is also necessary to assign a frequency channel to each AP. All these choices correspond to decision variables of the problem.

For indoor positioning optimisation problem, there are two main objectives. One main objective is to minimise the user's unsatisfied demands on QoS; the other main objective is to minimise the user's unsatisfied demands on positioning accuracy. Additionally, the network installation and maintenance cost can be considered as an economy-oriented objective. According to the optimization problem, we also define some constraints to satisfy on the problem.

3.3.1 Variables

In the previous optimization model, there are many notations and definitions. To better understand the problem, we will recall these notations and definitions. All the notations and definitions are classified into three major categories. They are input variables (Table 7), decision variables (Table 8) and intermediate variables (Table 9).

TABLE 7 THE LIST OF THE INPUT VARIABLES

S	The set of candidate AP locations.
n^S	The total number of available candidate sites $n^S=\|S\|$.
s	The *sth* candidate site with $s \in \{1,..., n^S\}$.
C^S_s	The installation cost of site s.
n^{max}_{AP}	The maximum number of available AP.
A	The set of candidate AP types.
n^A	The number of different types of AP $n^A=\|A\|$.
a	The *ath* AP type, $a \in \{1,..., n^A\}$.
C^A_a	The purchase and installation cost of AP type a.
r_a	The antenna radiation pattern of AP type a.
S^I	The set of sites on which one AP is installed initially.
n^I_S	The number of the set of sites on which one AP is installed initially.
H_a	The azimuth set For one AP of type a.
n^H_a	The number of possible azimuth values: $n^H_a=\|H_a\|$.
P_a	The emitted power set For one AP of type a.
n^P_a	The number of possible emitted power values: $n^P_a=\|P_a\|$.
F_a	The frequency channel set For one AP of type a.
n^F_a	The number of possible frequency channel values: $n^F_a=\|F_a\|$.
M	The set of MP in the calculation area.
n^M	The number of MP: $n^M=\|M\|$.
m	The *mth* MP, $a \in \{1,..., n^M\}$.
p_{sm}	The PDF of the RRS distribution in MP m and as detected from site s.
p_{min}	The minimum limits of all the RSS.
p_{max}	The maximum limits of all the RSS.
rss^c	The minimum signal power a client must receive for communication.
rss^p	The minimum signal power a client must receive for positioning estimation demand.
rss^i	The minimum signal power a client can receive as interference.
C	The set of communication zones.
n^C	The total number of communication zones: $n^C=\|C\|$.
c	The *cth* communication zone with $c \in \{1,..., n^C\}$.

T_c	The set of TPs In *cth* communication zone.
n_c^T	The total number of TPs in this communication zone *c*: $n_c^T = \| T_c \|$.
t	The *tth* TP with $t \in \{1, ..., n_c^T\}$.
u_c	The total number of users in this communication zone *c*.
b_c^u	The bit rate in kbps desired by user for this communication zone *c*.
p_c	The zone priority value allocated to this communication zone *c*.
C_t	The set of communication zones covering the TP *t*.
b_t	The bit rate in kbps desired by user in the TP *t*.
P	The set of positioning zones.
n^P	The total number of positioning zones: $n^P = \|P\|$.
p	The *pth* positioning zone with $p \in \{1, ..., n^P\}$.
R_p	The set of RPs In *pth* positioning zone.
n_p^R	The total number of RPs in this positioning zone *p*: $n_p^R = \| R_p \|$.
r	The *rth* RP with $r \in \{1, ..., n_p^R\}$.
a_p	The positioning accuracy in meter desired by user for this positioning zone *p*.
p_p	The zone priority value allocated to this positioning zone *p*.
P_r	The set of positioning zones covering the RP *r*.
a_r	The positioning accuracy desired by user in the RP *r*.
$\gamma(.)$	The signal attenuation between channels.
μ_N	The mean of the random Gaussian noise.
$SINR^c$	The minimal SINR threshold to communicate at the minimum nominal rate.
D^N	The set of downlink nominal bit rate supported by the standard.
n^N	The total number of available downlink nominal bit rates $n^N = \|D^N\|$.
d_k^N	The *kth* nominal bit rate in set D^N.
L_t^{MSDU}	The size of the MSUD of the user in TP *t*.
a , b	The MAC parameters which are used to calculate the total delay per MSDU.
σ_r^I	The signal variation from environment interference at RP *r*
K	The parameter for calculating the signal variation caused by multi-path effect from AP in site *s* at RP *r*.

TABLE 8 THE LIST OF THE DECISION VARIABLES

w_s	The type of AP installed at site *s:* $w_s \in A \cup \{0\}$.
h_s	The azimuth of AP installed at site *s:* $h_s \in H_a$.
p_s	The emitted power of AP installed at site *s:* $p_s \in P_a$.
f_s	The frequency channel of AP installed at site *s:* $f_s \in F_a$.

TABLE 9 THE LIST OF THE INTERMEDIATE VARIABLES

S^O	The list of installed sites.
n_S^O	The number of all the installed sites.
$dis(i,j)$	The Euclidean distance between the MP i and the MP j.
$dis(s,m)$	The Euclidean distance between the site s and the MP m.
rss_{sm}	The mean RSS in MP m and coming from the site s: $rss_{sm} = \chi(m, s, a, h_s, p_s, f_s)$. Specially, rss_{st} if $m = t$; rss_{sr} if $m = r$.
$\tilde{rss}_{sm}$	The RRS in MP m and as detected from site s: $p_{min} \le \tilde{rss}_{sm} \le p_{max}$.
RSS_m	The RSS vector detected from all installed APs at MP m. Specially, RSS_t if $m = t$; RSS_r if $m = r$.
n_m^{RSS}	The number of RSS vector: $n_m^{RSS} = \lvert RSS_m \rvert = \lvert S^O \rvert$. Specially, n_t^{RSS} if $m = t$; n_r^{RSS} if $m = r$.
rss_{sm}^{max}	The maximum received signal in the RSS vector RSS_m. Specially, rss_{st}^{RSS} if $m = t$.
S_m^C	All visible APs at MP m for communication. S_t^C if $m = t$.
RSS_m^C	The RSS vector of S_m^C at MP m for communication. Specially, RSS_t^C if $m = t$.
n_m^C	The number of RSS in RSS_m^C: $n_m^C = \lvert S_m^C \rvert = \lvert RSS_m^C \rvert$. Specially, n_t^C if $m = t$.
S_m^P	All visible APs at MP m for positioning estimation. Specially, S_r^P if $m = r$.
RSS_m^P	The RSS vector of S_m^P at MP m for positioning estimation. Specially, RSS_r^P if $m = r$.
n_m^P	The number of RSS in RSS_m^P: $n_m^P = \lvert S_m^P \rvert = \lvert RSS_m^P \rvert$. Specially, n_r^P if $m = r$.
S_m^I	All visible APs at MP m as interference. Specially, S_t^I if $m = t$; S_r^I if $m = r$.
RSS_m^I	The RSS vector of S_m^I at MP m as interference. Specially, RSS_t^I if $m = t$; RSS_r^I if $m = r$.
n_m^I	The number of RSS in RSS_m^I: $n_m^I = \lvert S_m^I \rvert = \lvert RSS_m^I \rvert$. Specially, n_t^I if $m = t$; n_r^I if $m = r$.
$S_t^{unstable}$	The set of sites where these unstable possible serving APs are installed.
$RSS_t^{unstable}$	The RSS vector of these unstable possible serving APs in RSS_t^C.
$n_t^{unstable}$	The total number of unstable possible serving APs in TP t: $n_t^U = \lvert S_t^U \rvert$.
S_t^S	The set of sites where these possible serving APs are installed for TP t.
$\rho_{st}^{unstable}$	The probability of disconnection between user and serving AP when serving AP at site s: $\rho_{st}^U = \rho_{st} \times P(rss_{st} < rss^c)$.
RSS_t^S	The RSS vector from these possible serving APs in RSS_t.
n_t^S	The total number of possible serving APs in TP t: $n_t^S = \lvert S_t^S \rvert$.
rss_{st}^b	The best average RSS in RSS_t and from AP in site s.
$SINR_t$	The average SINR at TP t.
ξ_{st}	The average SINR when AP in site s becomes the serving station.
ρ_{st}	The probability that AP in site s becomes the serving station
u_{st}	An indicator of whether the TP t associate to the AP in site s.
ρ_t	A set of probability of each possible serving AP for the TP t: $\rho_t = \{\rho_{st}: s \in S_t^S\}$.
ζ_t	A set of the average SINR for each possible serving AP for the TP t: $\{\zeta_{st}: s \in S^O\}$.
T_{S1}^c	The set of TPs which are in the cth communication zone and served steadily by the AP

	located on site *s*.
T_{S0}^{c}	The set of TPs which are in the *cth* communication zone and not served steadily by the AP located on site *s*.
T_{S}^{c}	The set of TPs which are in the *cth* communication zone and served by the AP located on site *s*.
u_c^s	The total number of users in the *cth* communication zone and served by the AP located on site *s*.
T_0^c	The set of TPs which are in the *cth* communication zone and not served by any AP.
u_c^0	The total number of users in the *cth* communication zone and not served by any AP.
d_t^N	The nominal bit rate in TP t.
TD_t^S	The total delay per MSDU at TP *t* by the serving AP in site s.
$ATST_s$	The Average Theoretical Saturation Throughput in Mbps for all the users served by the AP in site s.
d_t	The real downlink bit rate (in kbps) provided by the network at the TP t.
Δ_t	The deviation between the downlink bitrate required at the TP *t* and the bit rate provided by the network.
$R_r^{aliasing}$	The set of all RPs having the same RSS vector with RP *r*.
$n_r^{aliasing}$	The number of all RPs having the same RSS vector with RP *r:* $n_r^A = \| R_r^A \|$.
$RSER_r$	The aliasing positioning error in RP *r*.
$GDOP_r$	The GDOP in RP *r*.
O_r	The observed RSS vector at RP *r*.
n_r^O	The number of the RSS in the O_r: $n_r^O = \|O_r\| = n_r^P$.
o_{rk}	The signal strength detected from *kth* AP in RSS vector O_r: $O_r = (o_{r1}, \ldots, o_{rk}, \ldots, o_{rn_r^O})$.
σ_{kr}^{RSS}	The possible RSS variation from kth AP at RP *r*.
o_r^{Var}	The interval of the o_{rk} variation $[o_{rk}^{min} - o_{rk}^{max}]$, and its size is $\|o_{rk}^{min} - o_{rk}^{max}\|$.
o_r^{Var}	The interval of the O_r variation $[O_r^{min}, O_r^{max}]$, and its size is $\|O_r^{min}, O_r^{max}\|$. $O_r^{min} = (o_{r1}^{min} \ldots, o_{rm}^{min})$ and $O_r^{max} = (o_{r1}^{max} \ldots, o_{rm}^{max})$.
p'_{rk}	The PDF of the RRS distribution in RP *r* and as detected from *kth* AP with the varying signal strength variation σ_{kr}^{RSS}.
R_r'	The RPs for which RSS vector locate in the interval $[O_r^{min}, O_r^{max}]$.
APE_r	The Average Positioning Error indicator at a RP *r*.
APE^{min}	The global minimum average positioning error.
Δ_r	The deviation between the positioning accuracy required at RP *r* in the positioning zone *p* and the positioning accuracy estimated at RP *r* in the positioning zone *p*.

3.3.2 Combinatorial expression of the search space

Clearly, this problem is a combinatorial optimization problem, which is minimizing the objective function on a set of feasible solutions under a given set of constraints. A solution to such problem is an assignment of one value to all the variables in their finite domains. Thus, in contrast to the description of a problem, which is usually short, the search space is exponential in the problem dimension. In the following section, we analyze the combination of allowed values in detail.

Using all the parameters defined in model, we can calculate the number of possible configurations for each site:

$$n^C = 1 + n^F \times \left(\sum_{a \in A} n_a^H \times n_a^P \right) \quad \textbf{(3.85)}$$

Knowing that n $(n=n_S^O - n_S^I)$ new APs are deployed at $n^S - n_S^I$ available sites, the combination of such deployment is as follows:

$$C_{n^S - n_S^I}^{n} \times \left(\sum_{a \in A} n_a^H \times n_a^P \times n^F \right)^n \quad \textbf{(3.86)}$$

Since n varies from 0 to the maximum AP number n_{AP}^{max}, the total combination is as follows:

$$\sum_{n=0}^{n_{AP}^{\max}} C_{n^S - n_S^I}^{n} \times \left(\sum_{a \in A} n_a^H \times n_a^P \times n^F \right)^n \quad \textbf{(3.87)}$$

We set an example to emphasize the large size of the combination. In this example, let suppose there are 500 available sites and the maximum AP number is 50. The list of the parameters is given:

- n_a^F=13: we consider the standard 802.11 b/g.
- n_S^I =0: no AP is installed initially.
- n^A =3: 3 types of AP: omni-directional antenna (n_a^H=1), bi-directional antenna (n_a^H=4), directive antenna (n_a^H=8).
- n_a^P=4: there are 4 levels of possible emitted power.
- n^S=500: there are 500 available sites.
- n_{AP}^{max} =50: the maximum AP number is 50.

So based on the above parameters, the total number of combination is:

$$\begin{aligned} &\sum_{n=0}^{n=50} C_{500}^{n} \times \left(13 \times \left(8+4+1\right) \times 4\right)^{n} \\ &= \sum_{n=0}^{n=50} C_{500}^{n} \times 624^{n} \\ &\approx 10^{270} \end{aligned} \quad \textbf{(3.88)}$$

We can see in this example that it is impossible to systematically evaluate the objective function for every feasible solution within a lifetime. There are some combinatorial optimization problems which are denoted by *P-problem* that can be solved by some algorithms in a time polynomial to the size of the problem. Unfortunately, our problem is proved being *NP-Hard*; problems for which the time required to solve them is an exponential function of their input size. It is thus necessary to find search strategies to prune the search space and to reach a solution in a reasonable time.

3.3.3 Objectives of the problem

As previously discussed, there are three objectives in the indoor positioning problem we have defined. They are positioning accuracy, QoS and economical cost. In the following section, we will describe them one by one.

3.3.3.1 Positioning accuracy objective

For each network configuration, to estimate the positioning accuracy, we check that all RPs satisfy the following criterion which is a coverage criterion to get a signal on all RP of the positioning area:

$$\textbf{To satisfy:} \quad \forall r \in R_p, p \in P; \quad \Delta_r \geq 0 \quad \textbf{(3.89)}$$

In fact, since this criterion is too restrictive to be satisfied for many network configurations, we consider it as an objective and try to minimize it. We defined the expression of the positioning accuracy objective λ_P as follows:

$$\textbf{To minimize:} \quad \lambda_P = \sum_{r \in R_p, p \in P} \max(0; -\Delta_r) \quad \textbf{(3.90)}$$

Besides the positioning accuracy, we also care the distribution of the positioning error and the GDOP of each RP in all the positioning zones. For two configurations having the similar positioning accuracy, we think that the homogeneous positioning accuracy and small GDOP are more important for user. Thus we give a definition to extend the positioning accuracy objective when there are two configurations having the similar positioning accuracy.

Let λ_P^1 denote the positioning accuracy for configuration 1 and λ_P^2 denote the positioning accuracy for configuration 2. Suppose $\lambda_P^1 < \lambda_P^2$. When $\lambda_P^1 / \lambda_P^2 \geq \eta$ (η is a value which reflects the similarity of the positioning accuracy between two configurations. In our case, this value is equal to *0.9),* we have the following definitions:

— Δ_r^i is Δ_r in configuration i. $i \in \{1,2\}$.

— $n^i_{\Delta r}$ is the number of RP where $\Delta^i_r<0$.

— $\sigma^i_{\Delta r}$ is the standard deviation of Δ^i_r. That is:

$$\textbf{To minimize: } \sigma^i_{\Delta r} = \sqrt{\frac{\sum_{r\in R_p, p\in P, \Delta^i_r<0} (\Delta^i_{\Delta r} - \lambda^i_P / n^i_{\Delta r})^2}{n^i_{\Delta r}}} \quad \textbf{(3.91)}$$

$GDOP^i_r$ is $GDOP_r$ in configuration i where $i \in \{1,2\}$.

τ^i_{DGOP} is the parameter for the total $GDOP^i_r$ in configuration i. That is:

$$\textbf{To minimize: } \tau^i_{GDOP} = \sum_{\substack{r\in R_p \\ p\in P}} 1 \Big/ GDOP^i_r \quad \textbf{(3.92)}$$

$\Phi_{1,2}$ is the evaluation criterion to compare two configurations:

$$\textbf{Selection criterion: } \Phi_{1,2} = \alpha \times \frac{\sigma^1_{\Delta r}}{\sigma^1_{\Delta r} + \sigma^2_{\Delta r}} + \beta \times \frac{\tau^1_{GDOP}}{\tau^1_{GDOP} + \tau^2_{GDOP}} \quad \textbf{(3.93)}$$

Here, the weights α and β are the default values which can be modified by the user. And we define $\alpha+\beta=1$, thus the range of $\Phi_{1,2}$ falls in the interval [0,1]. In our case, since we are more concerned about the uniformity of the distrubtion of the positioning accuracy, so we assign 0.7 to α and 0.3 to β. If $\Phi_{1,2} \geq 0.5$, we define that the configuration 1 is better than the configuration 2. Else, we define the configuration 2 is better than the configuration 1.

3.3.3.2 QoS objective

For each network configuration, we also calculate the QoS at all TPs and check their satisfaction according to the following criterion:

$$\textbf{To satisfy: } \forall t \in T_c, c \in C; \quad \Delta_t \geq 0 \quad \textbf{(3.94)}$$

As for the positioning accuracy criterion, we consider the QoS criterion as the QoS objective λ_C which is defined as follows:

$$\textbf{To minimize: } \lambda_C = \sum_{t\in T_c, c\in C} \max(0; -u^T_c \times \Delta_t) \quad \textbf{(3.95)}$$

For two configurations having a similar QoS, we prefer the configuration with homogeneous QoS. Thus we give the following definition:

Let λ^1_C denote the QoS for the configuration 1 and λ^2_C denote the QoS for the configuration 2. Suppose $\lambda^1_C<\lambda^2_C$. When $\lambda^1_C/\lambda^2_C \geq \zeta$ (ζ is a value which reflects the similarity of QoS between two configurations. In our case, this value is equal to *0.9),* we have the following definition:

— Δ_t^i is Δ_t in configuration i. $i \in \{1,2\}$.

— $n_{\Delta t}^i$ is the number of TP where $\Delta_t^i < 0$.

— $\sigma_{\Delta t}^i$ is the standard deviation of Δ_t^i. That is:

$$\textbf{To minimize: } \sigma_{\Delta t}^i = \sqrt{\frac{\sum_{t \in T_c, c \in C, \Delta_t^i < 0} (\Delta_{\Delta t}^i - \lambda_C^i / n_{\Delta t}^i)^2}{n_{\Delta t}^i}} \quad \textbf{(3.96)}$$

If $\sigma_{\Delta t}^1 \geq \sigma_{\Delta t}^2$, we define that the configuration 1 is better than the configuration 2. Else, we define the configuration 2 is better than the configuration 1.

3.3.3.3 Economical cost objective

For each network configuration, we also consider the cost of the network construction which contains the site installation cost, the purchase of AP and the installation costs of AP. Mathematically, the economical cost objective is expressed as follows:

$$\textbf{To minimize: } \sum_{\substack{S \in S^O \\ S \notin S^I}} \left(C_S^S + C_{w_s}^A \right) \quad \textbf{(3.97)}$$

If possible, the network maintenance can be added as a new cost.

3.3.4 Constraints of the problem

In addition to constraints (3.89) and (3.94), in the indoor positioning problem we have a set of variables, each with domain of possible values, and a set of constraints involving some of the variables. A constraint is a relation between some variables limiting the set of values that the variables can assume. A constraint can involve any number of variables. The solution to our problem must satisfy the following constraints:

Constraint 1: All MPs covered by the network must meet a minimum guaranteed QoS and a minimum positioning accuracy required by the user.

For the minimum guaranteed QoS, it can be explained as that SINR at all the TPs in communication zones is higher than the minimum required SINR to allow communication. Thus we have:

$$\textbf{To satisfy: } \forall t \in T_c, c \in C; \quad SINR_t \geq SINR^c \quad \textbf{(3.98)}$$

For the minimum positioning accuracy, it can be explained as that the APE at all the TPs in positioning zones is higher than a default global minimum average positioning error. Thus we have:

$$\textbf{To satisfy: } \forall r \in R_p, p \in P; \quad APE_r \geq APE^{\min} \quad \textbf{(3.99)}$$

Considering the priority value of each zone, the mathematical expression of the Constraint 1 can be written as follows:

$$\forall t \in T_c, \mathrm{p_c} > 0, c \in C; \quad \sum u_{st} = 1$$
$$\forall r \in R_p, \mathrm{p_p} > 0, p \in P; \quad APE_r \geq APE^{\min} \tag{3.100}$$

Constraint 2: The maximum number of newly installed AP does not exceed a given number fixed by the user.

This constraint can be expressed as: $n_S^O \leq n_{AP}^{max}$.

Constraint 3: All the decision variables of the problem such as AP type, emitted power, azimuth and frequency should be included in their domain of definition.

This constraint can be expressed as: $\mathrm{w_s} \in \mathrm{A} \cup \{0\}$, $h_s \in H_a$, $p_s \in P_a$, $f_s \in F_a$.

Constraint 4: In each RP, the number of visible AP must not be less than three.

This constraint can be expressed as: $n_r^P \geq 3$.

In fact, although three AP is the theoretical bottom line of an accuracy positioning estimation for two-dimensional space (in our model, the Z is a constant value for MPs in the same floor, thus our model can be considered working in a two-dimensional space.), this constraint is a little too strict for a user group with small density since small user density satisfying this constraint will cause the waste of the communication resources. Thus for a small network, this constraint can be relaxed to two or one APs.

3.4 Conclusion

In this chapter, we present the optimization model for the WLAN indoor positioning based on fingerprinting technique. Although some papers have proposed the indoor positioning optimization model, so far as we know, our optimization model is the most complete for the WLAN indoor positioning based on fingerprinting technique. In comparison with other indoor positioning optimization models, our model not only considers the signal coverage requirement, but also considers the frequency interference among the APs. Besides, in our model the signal variation is fully taken into account during QoS estimation and the positioning error estimation. Our model is also the first to integrate DGOP and the homogeneous positioning accuracy into positioning estimation.

In our model, there are five decision variables which construct the search space with its finite domains. They are the site, the type of AP, the azimuth, the emitted power and the frequency channel. The SINR is used as a QoS indicator to estimate the throughput at each TP. Such estimation includes two steps. In the first step, we convert the SINR into the corresponding nominal bit rate according to the receive sensitivity of the Wi-Fi equipment. Then we can calculate the throughput according to the nominal bit rate, the different parameters of the MAC layer and the protocol CSMA/CA, the number of users communicating with the AP at different nominal bit rate allowed by the standard, etc... There are three positioning error indicators in our model. They are the RSER which is use to estimate the aliasing positioning error, the GDOP which is use to estimate the geometric dilution of precision and the APE which is use to estimate the averagepositioning error.

After completing the optimization model, we have described the optimization problem. Since our optimization problem is a combinatorial optimization problem, we define it as a triple (S, O, Ω), where S is a given search space, O is the objectives, which should be either maximized or minimized, and Ω is the set of constraints that have to be fulfilled to obtain feasible solutions.

Previous stuies have proved our optimization problem is a NP-Hard problem, for which the time required to solve them is an exponential function of their input size. So, for these difficult problems, one settles for approximate or nearoptimal solutions. Literature abounds with various methods known as heuristics for obtaining approximate solutions. Genetic Algorithms, Simulated Annealing and Local Search are some of them. In the next charpter, we will focuse on this part.

Chapter 4 Heuristics for problem solving

After analyzing the computing complexity of the WLAN-based indoor positioning optimization problem in the previous chapter, we cannot tackle them by exhaustive search, either to find an optimal solution or even to find a very good quality solution. For solving such combinatorial optimization problems, we resort to heuristic methods, which require reasonable amount of effort to get a good but non optimal solution.

In this chapter, we present two heuristics to provide a solution where WLAN planning and positioning error reduction are dealt simultaneously as an optimization problem. The first heuristic belongs to the weighting method, which is a kind of Non-Pareto technique. In this heuristic, a global formulation of the problem based on a penalty function has been proposed in order to transform a multi-objective problem to a mono-objective problem. Then a hybrid Tabu Search and Variable Neighborhood Search algorithm is implemented to obtain a good solution. The other heuristic relies on the Pareto-based techniques. In this way, each solution represents a different trade-off between the objectives that are involved. A parallel version of the hybrid algorithm is chosen to search a set of Pareto-optimal solutions.

The work in this chapter has been published in four conferences: International Conference on Indoor Positioning and Indoor Navigation 2010 (*IPIN'10*), International Conference on Wireless Days 2010 (*WD'10*), International Conference on Signal Processing and Communication Systems 2010 (*ICSPCS'10*), 12ème Congrès de Recherche Opérationnelle et d'Aide à la Décision 2011 (*ROADEF'11*).

Contents

4.1 Introduction

In the previous chapter, we have analyzed the combination of the decision variables, and the result indicates that the size of search space is increasing very fast with the inputs dimension so that we cannot find the optimal solution by evaluating all the candidate solution in the search space. Thus, algorithms need to be designed for solving this combinatorial optimization problem with a reasonable amount of effort to get a good eventually near-optimal solution. Due to the practical importance of combinatorial optimization (CO) problems, many algorithms have been already developed to tackle them.

These algorithms may be classified as either exact algorithms or approximate algorithms. Exact algorithms are guaranteed to find for every finite size instance of a CO problem an optimal solution in bounded time. They are most often used if a clear relation between the characteristics of the possible solutions and their utility for a given problem exists. If the relation between a solution candidate and its fitness are not so obvious or too complicated, or if the dimensionality of the search space is very high, it becomes harder to solve a problem deterministically. Trying it would possible result in exhaustive enumeration of the search space, which is not feasible even for relatively small problems. Such problems in such situation are usually belong to a NP-hard problem and are solved by approximate algorithms. In approximate algorithms we sacrifice the guarantee of finding optimal solutions for the sake of getting good solutions in a significantly reduced amount of time. This means that the results are traded in guaranteed correctness of the solution for a shorter runtime. Since our problem is NP-hard, and no polynomial time algorithm exists, we have to choose the approximate algorithms to solve it in acceptable time.

In optimization, heuristics are used to help in deciding which one of a set of possible solutions must be examined next (Pearl, 1985). In Wikipedia's definition (Wikipedia, 2011a), a **heuristic** *is a technique designed to solve a problem that ignores whether the solution can be proven to be correct, but which usually produces a good solution or solves a simpler problem that contains or intersects with the solution of the more complex problem. Heuristics are intended to gain computational performance or conceptual simplicity, potentially at the cost of accuracy or precision*.

However, in the last 30 years, a new kind of approximate algorithm combining basic heuristic methods in higher level frameworks are proposed. These methods are nowadays commonly called metaheuristics (Talbi, 2009). In Wikipedia's definition (Wikipedia, 2011b), *A* ***metaheuristic*** *is a heuristic method for solving a very general class of computational problems by combining user given black-box procedures — usually heuristics themselves — in a hopefully efficient way.*

For problems like ours, metaheuristics are often more effective than heuristics to find good solutions. For example, Hill-climbing algorithm is effective, but it has a significant drawback called pre-mature convergence. Since it is greedy, it always finds the nearest local optima independently of its global quality. The metaheuristics can overcome this disadvantage, a lot of results have proved it, so we decide to use metaheuristics to solve our problem.

According to the definition of metaheuristic, we may say that metaheuristics are high level strategies for exploring search spaces by using different heuristic methods. In (Blum & Roli, 2003), the author gives the essence of metaheuristic: it is a dynamic balance between diversification and intensification procedures. The term diversification generally refers to the exploration of the search

space to quickly identify regions in the search space with potentially high quality solutions, whereas the term intensification refers to the exploitation of the accumulated search experience to avoid wasting too much time in regions of the search space which are either already explored or which do not provide high quality solutions.

In fact, the search strategies of different metaheuristics are highly dependent on the philosophy of the metaheuristic itself. The search strategies can be further divided into *population-based strategies* and *trajectory strategies*. Population-based strategies manipulate a collection of solutions rather than a single solution at each stage. As they deal with a population of solutions, population-based algorithms provide a natural, intrinsic way for the exploration of the search space. Yet, the final performance depends strongly on the way the population is manipulated. The most studied population-based methods in combinatorial optimization are Evolutionary Computation (EC) and Ant Colony Optimization (ACO) (Talbi, 2009). In EC algorithms, a population of individuals is modified by recombination and mutation operators, and in ACO a colony of artificial ants is used to construct solutions guided by the pheromone trails and heuristic information. Trajectory metaheuristics, on the contrary, work on a single solution at any time. Such metaheuristics can be seen as intelligent extensions of local search algorithms (Talbi, 2009). The goal of this kind of metaheuristic is to escape from local minima in order to proceed in the exploration of the search space and to move on to find other hopefully better local minima. Tabu Search, Iterated Local Search, Variable Neighborhood Search, GRASP and Simulated Annealing are the most popular trajectory metaheuristics.

We have already said that the optimization algorithm is about trying to find the best possible solutions and the objective function is used to evaluate the solution quality. In the case of optimizing a single objective, an optimum is either its maximum or minimum, depending on what we are looking for. However, in our model there are several objectives conflicting in nature. It means that several incommensurability and competing objectives are required to be optimized simultaneously. This is known as Multi-objectives Optimization (MO) problem, which can be formally defined as:

$$\min_{x}\left[\mu_1(x), \mu_1(x), \ldots, \mu_1(x)\right] \qquad \text{s.t. } g(x) \le 0, h(x) = 0, x_1 \le x \le x_u \qquad \textbf{(4.1)}$$

Where, μ_i is the *i-th* objective function, *g* and *h* are the inequality and equality constraints, respectively, and *x* is the vector of optimization or decision variables. The solution to the above problem is a set of *Pareto points*. Thus, instead of being a unique solution to the problem, the solution to a MO problem is a possibly infinite set of Pareto points.

A design point in objective space μ^* is termed Pareto optimal if there does not exist another feasible design objective vector μ such that $\mu_i \le \mu^*$ for all $i \in \{1,2,\ldots,n\}$, and $\mu_j < \mu^*$ for at least one index of $j, j \in \{1,2,\ldots,n\}$.

Currently, there are two commonly approaches to solve MO problem. One is called Non-Pareto technique which is an intuitive approach to solving the MO problem. The basic idea is to reduce the multiple objectives to a single objective or several ranking objectives by trading off conflicting objectives. In this case, approaches do not incorporate directly the concept of Pareto optimum and are incapable to produce certain portions of the Pareto front, but such approaches are efficient and easy to implement and the objective function can be optimized using existing mono-objective optimization

algorithms. The quality of the indoor positioning system relies on the optimization of several objectives, then with this approach the optimal solution is the result of a fixed trade-off between them. These approaches have some limitations when they handle the MO problems. The main methods are as follows (gatech, 2011):

—The first one is called weighting method. In this method, each objective is assigned a weight representing its importance. We generate a composite objective function, usually from a weighted sum of the objectives. The solution obtained will depend on the values of the weights specified, the main drawback of this method is that the objective trade-off is fixed and so the solutions in the search space are fixed too.

—The second one is called ranking method. In this method, we rank the goals in priority levels, often referred to as a pre-emptive formulation. In this case, the lexicographic minimum (or maximum) can be obtained in n successive steps: firstly, by minimizing (or maximizing) the first lexicographic objective f1 to produce a solution s1, then, add a constraint to avoid deteriorating of f1 and solve the problem with objective function f2 using s1 as a starting point to produce a solution s2, etc. The solution to a given step is a good solution for the next step.

—The third one is called epsilon-constraint method. In this method, we pick one criterion as the most preferred or primary and transform the remaining criteria into constraints bounded by some allowable levels. Hence, a single objective minimization is carried out for the most relevant criterion subject to additional constraints on the other criteria. Note that the levels can be altered to generate the entire Pareto optimal set.

Among above three methods, the ranking method requires a pre-defined ordering of objectives and its solution performance will be affected by it. Thus the ranking method is appropriate to handle only few objectives since it might be too strict to rank correctly. The epsilon-constraint method has broader applicability, but it also has potentially high computational cost because of the constraint satisfaction requirement. Compared with the ranking method and the constraint method, weighting method is not only feasible but also easy to implement. Thus weighting method is most widely in use. We also prefer to choose this method as we do not know in advance the criteria ranking and the feasibility of the problem instance in case of constraints definition.

The other kind of approaches for MO optimization problem relies on the Pareto-based techniques and looks for a set of Pareto-optimal solutions, each solution representing a different trade-off between the objectives that are involved. Thus, instead of being a unique solution to the problem like in the first kind of approaches, the solution given by second kind of approaches is a possibly infinite set of Pareto points. We will use this approach also to compare solutions in location and quality of service criteria.

This section is organized as follows. In section 2, we develop the weighting method to construct the MO problem by a single aggregate objective function, and then a mono-objective algorithm is presented to solve the problem. In section 3, we consider these conflicting objectives in a fair way and try to find the Pareto optimal set with a Pareto-based algorithm.

4.2 Non-Pareto optimization

4.2.1 Objective function

In weighting method, the first step is to aggregate all the criteria into a single one. In our problem, there are three criteria, which are positioning accuracy, QoS and economical cost. And we already said that these three criteria are conflicting when changing the decision variables. To achieve these conflicting criteria simultaneously, our optimization problem, which is to determine a feasible AP network configuration satisfying all constraints, will be formulated as a unique objective which is to minimize the following fitness function:

$$\sum_{\text{Site}} C_{\text{Site}} + \sum_{TP} \beta \times \Delta_{tp} + \sum_{RP} \gamma \times \text{E}_{rp} \qquad \textbf{(4.2)}$$

Where, C_{Site} is the cost of the network construction which contains the sites installation cost, the purchase of AP and the installation costs of AP. β is the penalty coefficient assigned to the Test Point. Δ_{tp} is the deviation between the required bit rate and the real bit rate, this is the Quality of Service criteria defined on all Test Points. γ is the penalty coefficient assigned to the Reference Point. E_{rp} is the magnitude of positioning error in all Reference Point. We remain that the Test Point set is a subset of the Reference Point set; it means that the requirement for QoS is not always defined in the coverage zone. In this function, the first term is the network installation cost; the second term is the cost of unsatisfied demands on QoS and the third term is the cost of unsatisfied demands on positioning. All components are transformed in the same unit that is Euros. So, the indoor positioning challenge is completely shift into an economical challenge. Of cause, the above objective function must be optimized under the constraints which were proposed in chapter 3.

Referring to the WLAN planning optimization, there are several powerful metaheuristics, e.g. tabu search, simulated annealing, genetic algorithms…, which can be applied to this difficult planning problem. Both tabu search and simulated annealing use the concept of neighborhood search. Many papers show that it is very easy to obtain a good solution by these trajectory metaheuristics (Vanhatupa *et al.*, 2007), (Jaffres-Runser & Gorce, 2008), (Jasmine *et al.*, 2008), (Unbehaun & Kamenetsky, 2003). Genetic algorithms are efficient too but are more complex to tune and are often hugely time consuming.

The trajectory metaheuristics are based on the basic local search algorithm and integrate explicit strategies to avoid local minima. Local search algorithms start from one or several initial solutions and iteratively try to replace the current solution by a better solution in an appropriately defined neighbourhood of the current solution. The algorithm may decide to apply degradation rules to escape from local minimum and try to find a best one. The algorithm stops after a given run time, or after exploring all the neighbors or if one global optimum is found (we need to know the optimal fitness in advance). The neighbourhood and the local minimum are formally defined as follows:

A neighbourhood structure is a function $N:S \rightarrow S^p$ that assigns to every $s \in S$ a set of neighbours of size p which depends on N and $N(s) \subseteq S$. $N(s)$ is called the neighbourhood of s (Blum and Roli 2003).

Having the definition of a neighbourhood structure, we can define the concept of a local minimum.

A local minimum with respect to a neighbourhood structure N is a solution s such that $\forall s' \in N(s): f(s) \leq f(s')$. We call s a strict local minimum if $f(s) < f(s'), \forall s' \in N(s)$ (Blum and Roli 2003).

To solve our combinatorial optimization problem, a hybrid Tabu Variable Neighbourhood Search (TVNS) algorithm, enhanced with some strategies, is implemented. We choose this category of method because we have a good experience on resource allocation problem in radio network context and this method gave good results in a previous problem on QoS optimization for WLAN planning (Gondran *et al.*, 2008b).

4.2.2 The hybrid Tabu Variable Neighbourhood Search Algorithm

4.2.2.1 Initialization

In trajectory metaheuristic, the algorithm starts from an initial solution and describes a trajectory in the state space. The initial solution is very important for the solution quality. The construction of initial solution should be fast and a good starting point for local search. Usually, the construction of initial solution is done with two methods: one method is to generate a random solution in search space, which is frequently adopted for unreal problems; the second method is to construct the initial solution with a specific heuristic dedicated to the problem to solve, which is quite common for real problems. In our problem, providing radio coverage on all assigned areas is a common requirement for communication and positioning. Thus the most intuitive way to find a good starting solution for QoS objective and positioning objective is to use an algorithm that considers a coverage constraint to build the initial solution. Moreover, since the frequency allocation is out of consideration on the coverage criterion, thus we can tackle the frequency allocation separately during the optimization phase.

The initial solution problem can be represented as a coverage planning problem which is to minimize the number of radio Access Points (AP) that are able to cover all Marking Points (MP) used for the radio map and then frequency planning which is to minimize the interference by allocating the best frequency for each AP. The coverage planning problem amounts to a well-known combinatorial optimization problem, namely the minimum cardinality set covering problem (Amaldi et al., 2005). Because the coverage planning problem is NP-hard, we devise effective heuristic based on Greedy Randomized Adaptive Search Procedure (GRASP) to provide good solutions within a reasonable amount of time (Feo & Resende, 1995). GRASP is a simple metaheuristic that combines two phases, solution construction and solution improvement, at each iteration. The construction phase builds a good solution in regards to the constraints on radio coverage (i.e. we try to maximize the satisfaction of the coverage constraints given in Equation (3.89), whose neighbourhood is investigated until a local minimum is found during the improvement phase. The best solution found is returned upon termination of the search process. A more detailed description of greedy search procedure by pseudo-code is shown below:

Notation:

- $\boldsymbol{C}$: all the possible configurations. The configuration is one type of AP installed in a given site with a given azimuth and a given power.
- $\boldsymbol{C_s}$: the set of the selected configurations in current greedy search. Initially, $C_s:=\Phi$ or $C_s:=$ {already installed AP configurations} if a network already exists.
- $\boldsymbol{C_c}$: the set of the configurations whose coverage is totally overlapped by the coverage of selected configurations C_s as illustrated in Figure 4.1.

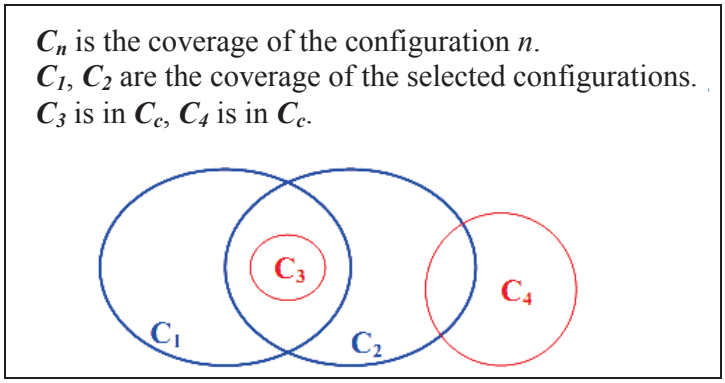

Figure 4.1 Definition of the set C_c

- $\boldsymbol{c}$: one configuration in the candidate list. This list is called Restricted Candidate List (RCL), which is composed of the configurations which are candidate for installation in the current network. These configurations are those with MP not covered by the current solution and that can be newly covered by one of these as illustrated in Figure 4.2.

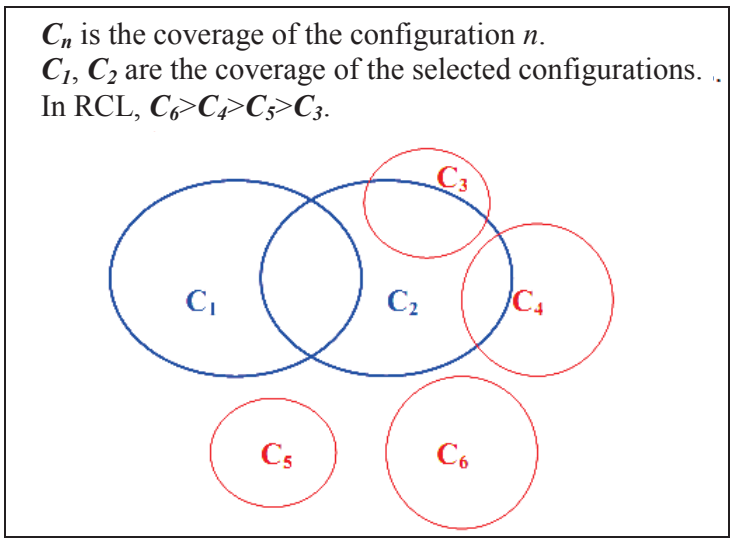

Figure 4.2 Ordering of coverage in RCL

- $\boldsymbol{n_c}$: the number of MPs covered by the configuration c and not already covered by C_s or C_c, which represents the additional coverage of the configuration c.
- $\boldsymbol{m_{MP}}$: the total number of MPs which are in the positive priority zones.
- $\boldsymbol{m}$: the number of MPs which are not covered.
- $\boldsymbol{n_{max}}$: the maximum number of AP to install.

ALGORITHM 1: Greedy random (GRASP) for coverage algorithm

1. Initialize C_s and $C_c = \Phi$
2. Calculate the residual coverage n_c for all the candidate configuration $c \in C \backslash \{C_s \cup C_c\}$
3. Update C_c
4. **While** $m \neq 0$ **and** $|C_s| \leq n_{max}$ **do**
5. $c_{min} \leftarrow \min\{ n_c \mid c \in C \backslash \{C_s \cup C_c\}\}$
6. $c_{max} \leftarrow \max\{ n_c \mid c \in C \backslash \{C_s \cup C_c\}\}$
7. $RCL \leftarrow \{c \in C \backslash \{C_s \cup C_c\} \mid n_c \leq c_{min} + \alpha \times (c_{max} - c_{min})\}$ with α in [0,1]
8. Select randomly one element c from RCL
9. $C_s \leftarrow C_s \cup \{c\}$
10. Calculate the residual coverage n_c for all the candidate configuration $c \in C \backslash \{C_s \cup C_c\}$
11. Update C_c by excluding all c without residual coverage
12. **Endwhile**
13. **Return** C_s

Where the C_c updating function can be sketched as follows:

1. **For** all $c \in C \backslash \{C_s \cup C_c\}$
2. **If** $n_c = 0$
3. $C_c \leftarrow C_c \cup \{c\}$
4. **Endif**
5. **Endfor**

In ALGORITHM 1, the factor α used to define the restricted candidate list determines the strength of the heuristic bias. The case α=0 corresponds to a pure greedy algorithm, while α=1 is equivalent to a random construction. Therefore, α is a critical parameter which influences the sampling of the search space. The most important schemes to define α are presented in (Feo & Resende, 1995). We use the simplest scheme — the constant α scheme.

At the end of the greedy random coverage, we start to consider the frequency allocation. It will allow us to compute the QoS of the initial solution as we need the frequency plan for SINR computation and client to AP assignment. Instead of randomly assigning one frequency channel to each selected AP, we choose the Iterated Local Search (ILS) method, which is the most general scheme among the explorative strategies. It starts from an initial solution until it finds a local optimum; then it perturbs the solution and it restarts local search. It is simple but powerful and very good to meet the requirements as initial algorithm — fast and better than random. In our ILS, a simple multi-start algorithm is chosen to perturb the solution. The pseudo-code of frequency allocation process for initial frequency plan is given as:

Notation:

- From the greedy random coverage output C_s we define now that $C_s = \{(c_1, f_1), \ldots, (c_n, f_n)\}$. c_i represents the i^{th} selected configuration in C_s and f_i is its allocated frequency. n is the number of the selected configurations in C_s.
- $\boldsymbol{Q(C_s)}$: the evaluation function of QoS objective when the selected configuration is C_s. It is evaluating the throughput described in Equation (3.95).
- $\boldsymbol{n_{multi\text{-}start}}$: the number of restarts.
- F is the set of available frequency.

ALGORITHM 2: Iterative Local Search (ILS) for frequency assignment algorithm

1. Initialize C_s, the frequencies are assigned randomly
2. $C_s^* \leftarrow C_s$
3. $k \leftarrow 1$
4. **While** $k \leq n_{multi\text{-}start}$ **do**
5. $C_s' \leftarrow \Phi$
6. **While** $C_s' \neq C_s$ **do**
7. $C_s' = C_s$
8. **For** $i = 1 \ldots n$ **do**
9. **For** all $f \in F \backslash \{f_i\}$ **do**
10. $C_s'' \leftarrow C_s \backslash \{(c_i, f_i)\} \cup \{(c_i, f)\}$
11. **If** $Q(C_s'') < Q(C_s)$
12. $C_s \leftarrow C_s''$
13. **Endif**
14. **Endfor**
15. **Endfor**
16. **Endwhile**
17. **If** $Q(C_s) < Q(C_s^*)$
18. $C_s^* \leftarrow C_s$
19. **Endif**
20. Initialize C_s
21. $k \leftarrow k + 1$
22. **Endwhile**
23. **Return** C_s

The C_s initialization is randomly assigning one frequency channel to each selected configuration, which can be sketched as follows:

1. For $i = 1...n$ **do**

2. f_i = random_select(F)

3. **Endif**

4. $C_s \leftarrow \{(c_1, f_1),\ldots, (c_n, f_n)\}$

For the initial solution, two simple algorithms GRASP and ILS are applied successively for AP installation while optimizing coverage then frequency assignment while optimizing QoS. As it is well-known in the litterature, in comparison of these two simple algorithms more sophisticated algorithms like simulated annealing or Tabu search can bring better solution. Some exact algorithms such as column generation may even give the best solution for coverage optimization; of course, the search time is also longer with the solution improving. In fact, for the initial solution, the minor is the AP number, the better is the solution. However, the requirement of the coverage criterion is lower than the requirement of QoS criterion. It means that the AP number for QoS criterion should be more than the AP number for coverage criterion. Thus we believe that these two algorithms are pertinent because getting good solutions, not the best one, on the coverage objective is sufficient for the next step. To find out the answer, we did a test. We replace GRASP with simulated annealing for generating the initial solution. The results show that the initial solution returned by SA is better than by GRASP, but this better initial solution does not bring a better global optimization solution at the end of the full process. In other words, GRASP and ILS are definitely possible to be competent for initial solution generation. In the following experiment part, the initial solution will be produced by using GRASP and ILS algorithm.

4.2.2.2 Metaheuristic: Tabu Variable Neighbourhood Search

In this section, we will discuss the global optimization algorithm for our optimization problem. A heuristic which is a global optimization algorithm has converged if it cannot reach new solution anymore or it is stuck in a local optimum, i.e. if it keeps on producing solution from a small subset of the problem space. There is no guarantee on optimality anyway unless the exploration is complete. Metaheuristc global optimization algorithms will usually converge at some point in time. However, in most real world applications, the fitness function has multiple maxima or minima. It means the optimization process converges to a local optimum and it is no longer able to explore other parts of the search space than the area currently being examined. It also means this algorithm needs more diversification to prevent convergence to bad local optima and increase the probability of finding a better one, may be the global optimum.

In fact, since we cannot know the characteristics of solution space, it is not possible to find a perfect global optimization algorithm. Most often, experience, rules of thumb, and empirical results based on models obtained from related research areas are the only available guides.

In conclusion, the diversification and the empirical information are two specific considerations for choosing an appropriate algorithm among so many different algorithms. Based on the above specific considerations, we combine Variable Neighbourhood Search with Tabu Search and choose

to implement a hybrid Tabu Variable Neighbourhood Search (TVNS) algorithm, enhanced with some heuristic strategies.

For diversification the essence of the trajectory metaheuristic is to add the diversification into the local search to improve the solution quality. Tabu Search uses a short term memory to escape from the local minima while Variable Neighbourhood Search applies a strategy based on dynamically changing neighbourhood structures to avoid the local minima. Since these two heuristics are completely different mechanisms of diversification, when mixing these two heuristics, the effect of diversification would not overlap each other and should not be reduced. So we will have more diversification.

For empirical information, TS and VNS are well implemented by our research team for radio planning optimization (Gondran, 2008), (DIB, 2010) and the results indicate that these two metaheuristics can be competent with such difficult planning problem. In fact, unlike the unreal problems from mathematics, our problem is engineering oriented and the solution space of such model has a specific structure we can exploit with the fitness and with introducing heuristics. Sometimes, the application of the specific information derived from model is more powerful than the self-improvement of algorithm. Before the representation of TVNS, the background of VNS and TS is introduced.

a) Variable Neighborhood Search algorithm

Variable Neighborhood Search (VNS) is a metaheuristic proposed in (Hansen & Mladenovic, 1999), (Hansen & Mladenovic, 2001), which explicitly applies a strategy based on dynamically changing neighbourhood structures to descent to local minima and escape from the valleys which contain them. VNS heavily relies upon the following observations (Hansen *et al.*, 2008):

- **Fact 1:** A local minimum with respect to one neighbourhood structure is not necessarily a local minimum for another neighbourhood structure.
- **Fact 2:** A global minimum is a local minimum with respect to all possible neighbourhood structures.
- **Fact 3:** For many problems local minima with respect to one or several neighbourhoods are relatively close to each other.

At the initialization step of VNS, a set of neighbourhood structures has to be defined. Usually, a sequential order of these neighbourhood structures in VNS is pre-defined according to the principle that one neighbourhood is included in the other, for example ordering by the Hamming distance. However, the neighbourhoods in our problem do not have such order dependencies.

After generating the initial solution and initializing the neighbourhood index, the algorithm iterates until a stopping condition is met. The basic VNS is described with the following pseudo-code in Figure 4.3 knowing that for initialization a finite set of pre-selected neighborhood structures is defined $\{N_1 , N_2 , \ldots, N_{kmax}\}$ and an initial feasible solution x is generated.

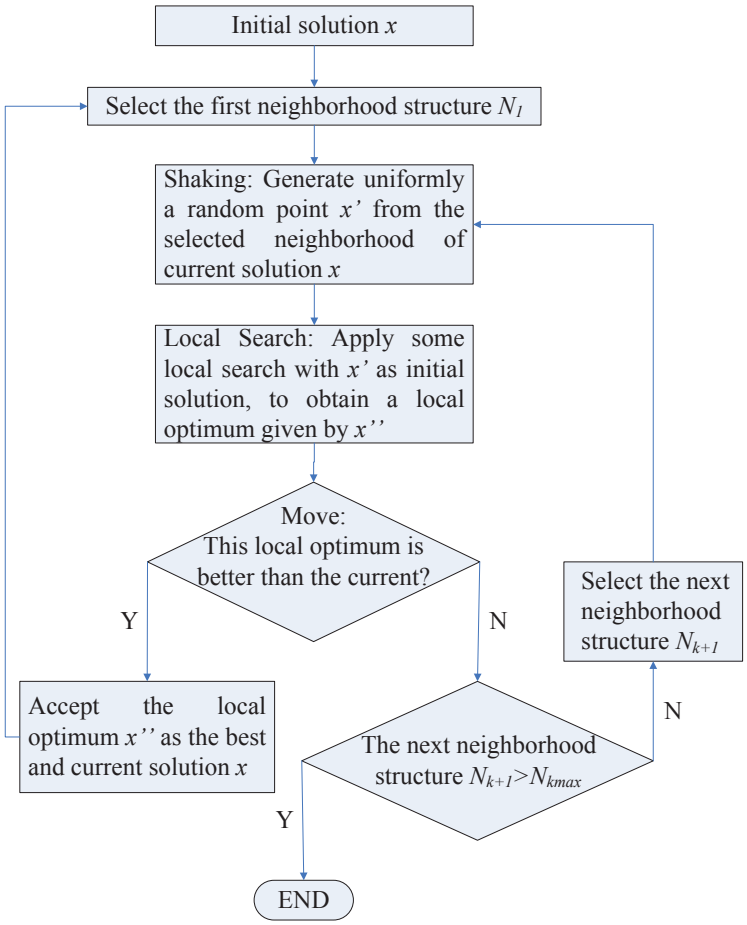

Figure 4.3 Basic Variable Neighborhood Search algorithm

We can observe that VNS main cycle is composed of three phases: shaking, local search and move. In the shaking phase, a solution x' in the k^{th} neighbourhood of the current solution x is randomly selected. The objective of the shaking phase is to perturb the solution so as to provide a good starting point for the local search. However, the trade-off between intensification and diversification of the search in VNS should be considered in a shaking procedure. It means that a good starting point should not be too far from the current solution to avoid the degeneration into a simple random multi-start. A good algorithm for balancing intensification and diversification in VNS is the so-called Large Neighbourhood Search (Pisinger & Ropke, 2010), where some randomly chosen attributes of the solutions are destroyed, and then the solution is re-built by some constructive heuristic enlarging the move from the current solution. In our optimization, we use this LNS algorithm to do the shaking procedure.

Then, in the local search phase, a local search method is performed. While the basic local search method such as first improvement heuristic or best improvement heuristic is clearly useful for approximate solution of many combinatorial and global optimization problems, it remains difficult or long to solve very large instances. To improve the basic VNS, one method is to extend it with for example, General VNS (GVNS), by replacing the basic local search step by Variable Neighbourhood Descent (VND) (Hansen *et al.*, 2008). Another method is to hybrid VNS and another metaheuristics. For example, TS is used instead of local search within the basic VNS. In our optimization, we choose to use Tabu Search for this step as it is a very good local search procedure.

At the end of the local search phase, the new solution x'' is compared with x and, if it is better, it

replaces x and the algorithm starts again with $k=1$. Otherwise, k is incremented and a new shaking phase starts using the k^{th} neighbourhood. This phase is the move phase. In this phase, the process of changing neighbourhoods in case of no improvements corresponds to a diversification of the search. However, different neighbourhood structures have different descent effect and a steep descent will bring premature convergence. Thus a sensible idea is selecting the neighbourhoods with a specified probability. Such probabilities can be constant and come from the experiences and the empirical rules or can be dynamic and are generated by using machine learning strategy. Furthermore, the objective functions are usually unsteady or fluctuating, it makes more complicated for the optimization process to find the right directions to proceed to. In this case, a single-minded pursuit of best improvement may result in local optima. An efficient method is to introduce the degradation to accept some inferior solution and then to avoid falling into local optima.

b) Tabu Search algorithm

Tabu Search (TS) is a popular metaheuristics for CO problems, which is developed by Glover (Glover, 1986) in the mid 1980s (Glover & Taillard, 1993). The basic TS algorithm applies a Hill Climbing (HC) algorithm enhanced with a tabu list which stores the elements recently evaluated. By preventing the algorithm from visiting them again, a better exploration of the problem space can be enforced. At each iteration the best solution comes from the solutions that are in the neighbourhood of the current solution and do not belong to the tabu list. If all the solutions in the neighbourhood of the current solution are forbidden by the tabu list, the algorithm might terminate or a specific selection strategy such as selecting randomly or selecting the last solution in the tabu list starts to run. Then this solution is added to the tabu list and one of the solutions that were already in the tabu list is removed in a FIFO order. The algorithm stops when a termination condition is met. The basic Tabu Search is described with the following pseudo-code where $N(x)$ is the neighborhood of the solution x and $f(x)$ is the fitness of the solution x.

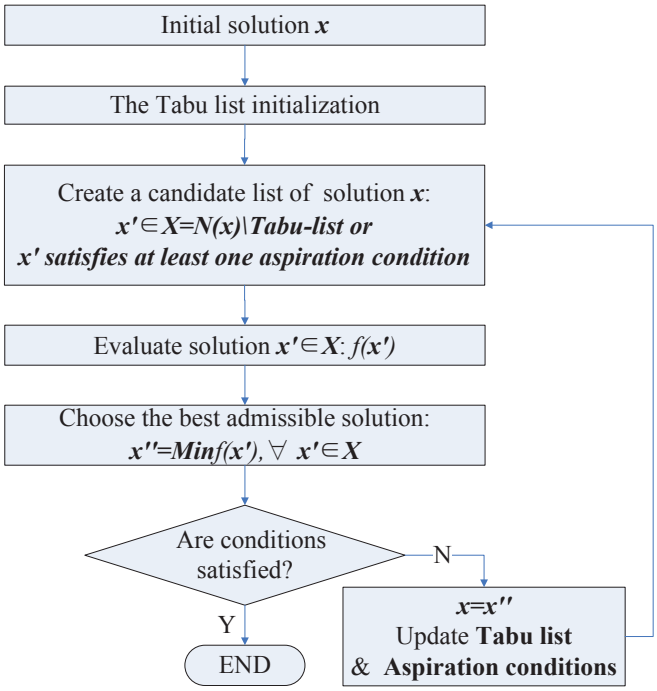

Figure 4.4 Basic Tabu Search algorithm

From the above description of basic Tabu Search algorithm, the core of Tabu Search is

embedded in its short-term memory process. In fact, this process includes three main strategies. One strategy is the forbidden strategy which controls what enters in the tabu list. Another one is the freeing strategy which controls what and when exits the tabu list. At last there is the short-term strategy which manages interplay between the forbidden strategy and the freeing strategy to select trial solutions.

A tabu list is composed of two parts: one is the content of the tabu list and the other is the length of the tabu list, which is also called tabu tenure. In the above description of basic Tabu Search algorithm, Tabu list contains the solution, but managing a list of solutions is highly inefficient and is not practical. Because normally the size of the problem space is very large, so if we want a tabu list actually to work, the tabu tenure should be also large. Therefore, instead of the implementation of the solutions themselves, the tabu list can store the solution attributes. Attributes are usually components of solutions, moves, or differences between two solutions. Since a solution attribute often corresponds to more than one solution, such tabu list is much more efficient. But at the same time some information are also lost. To overcome this problem, aspiration criteria are usually used to free a forbidden solution. The most commonly used aspiration criterion selects solutions which are better than the current best one. The length of the tabu list is used to control the memory of the search process. Generally, small tabu tenure makes the search concentrate on small areas of the search space. On the opposite, large tabu tenure forces the search process to explore larger regions since it forbids a higher number of solutions or solution attributes. In order to better adapt the problem, some dynamic tabu tenure strategies are presented (Taillard, 1991), (Battiti & Tecchiolli, 1994), (Battiti & Protasi, 1996), (Devarenne *et al.*, 2006). In these strategies, the tabu tenure can be varied adaptively during the search to make algorithm more robust. A simple but efficient dynamic tabu tenure strategy is that the tabu tenure is increased if solutions or solution attributes repeat frequently and if there are no improvements for a long time search.

Moreover, in (Glover & Laguna, 1998), the author thought that the history of the search is also very useful, thus he proposed a kind of long term memory which is based on four principles: recency, frequency, quality and influence of moves. Such long term memory is particularly effective in a MO environment. In our approach, we are going to use short-term memory and long term memory in the TS.

c) Hybridation of Tabu Search and Variable Neighborhood Search algorithms

For TVNS algorithm, there are two ways of making hybrids of VNS and TS: use TS within VNS or use VNS within TS. The recent literature mentions that performances are better when including TS within VNS. A tabu list is constructed for each level in different neighborhoods (Kovaevi-Vuji, 1999) or a TS is used as local search part inside VNS (Wang & Tang, 2008). In the second way of hybridization, we only mention a nested VND within a TS framework that is proposed in (Brimberg *et al.*, 2000).

d) Neighborhood construction

As previously mentioned, neighbourhood structure definition is a core of these trajectory strategies since they work on one or several neighbourhood structures imposed on the solutions of the search space. Neighbourhood structures should be effective and easy to be implemented. Fortunately, there are many existing examples of radio planning optimization which are a good guidance of

neighborhood construction. Referring to these examples, we have the following definitions.

Firstly, in our model, a solution is composed of the decision variables of the problem, which are the AP placement, the AP type, the AP transmission power, the AP direction of emission and the AP frequency. We can define the neighborhood structure for each decision variable. However, it makes the search space too scattered and leads the VNS to be ineffective. To balance the size of search space and the efficiency of the neighborhood structure, we can convert to merge some decision variables into one decision variable. We define a decision variable by combining the AP type, the AP transmission power and the AP direction of emission. We call it AP configuration which is one type of AP with assigned pattern, power and azimuth. Then we have three decision variables, AP site, AP configuration and AP frequency. Physically the search will be either on location selection or in antenna selection or in frequency channel selection which are three different understanding of WLAN planning problems. Therefore, based on these decision variables, we define the following six neighborhood structures in the solution space:

Notation:

- For a solution $e=\{(c_1, s_1, f_1), \ldots, (c_n, s_n, f_n)\}$, where c_i is the i^{th} AP configuration at site s_i, and f_i is the assigned frequency for this AP.
- $E(e)$ is the fitness function of solution e.
- C is the set of the candidate AP configuration. S is the set of the candidate site. S^O is the installed site. F is the set of the available frequency.

Neighborhood structures:

Delete Move (N_{DM}): a selected AP is deselected from the solution. For a solution e, mathematically:

$$e' \in N_{DM}(e) \;\; if \; \exists (c_i, s_i, f_i) \in e, e' = e \setminus \{(c_i, s_i, f_i)\} \tag{4.3}$$

Addition Move (N_{AM}): a new AP configuration for an unoccupied site is added in the solution. For a solution e, mathematically:

$$e' \in N_{AM}(e), \;\; if \; \exists (c_i', s_i', f_i') \in C \times S \times F \setminus S^O, \; e' = e \cup \{(c_i', s_i', f_i')\} \tag{4.4}$$

Swap Move (N_{SM}): a selected AP configuration is deselected, and a deselected AP configuration is selected for an unoccupied site. In fact, this operator can be seen as the combination of *Delete Move* operator and *Addition Move* operator. For a solution e, mathematically:

$$\begin{aligned} &e' \in N_{SM}(e), \\ &if \; \exists (c_i, s_i, f_i) \in e \; and \; (c_i', s_i', f_i') \in C \times S \times F \setminus S^O, e' = e \setminus \{(c_i, s_i, f_i)\} \cup \{(c_i', s_i', f_i')\} \end{aligned} \tag{4.5}$$

Frequency Allocation (N_{FA}): reallocates a frequency for all AP in the solution. For a solution e, mathematically:

$$e' = \{(c'_i, s'_i, f'_i) \in N_{FA}(e), \ \ if \ \forall 1 \le i \le n, s'_i = s_i \ and \ c'_i = c_i \ and \ f'_i \in F \setminus \{f_i\} \quad \textbf{(4.6)}$$

However, since the search space of frequency allocation is wide and the basins of attraction of good local optima are small in a simple random frequency allocation algorithm, such neighborhood structure is almost useless for the solution improvement. To design neighborhood structure for an effective search, we try to reallocate a good frequency in the solution. Here, the ILS multi-start algorithm is always used to change the frequency; it is the same algorithm used in initialization, it is applied to assign the best new frequency from a solution *e*.

Configuration Allocation (N_{CA}): reallocates a configuration for a selected site in the solution. For a solution *e*, mathematically:

$$e' = \{(c'_i, s'_i, f'_i) \in N_{CA}(e), \ \ if \ \forall 1 \le i \le n, s'_i = s_i \ and \ f'_i = f_i \ and \ c'_i \in C \setminus \{c_i\} \quad \textbf{(4.7)}$$

Obviously, the neighborhood structure N_{CA} is a refinement of the neighborhood structure N_{SM}. The change of configuration is done randomly.

Configuration Allocation (N_{CFA}): reallocates configuration and frequency for all sites in the solution without limit on the number of reallocation. For a solution *e*, mathematically:

$$e' = \{(c'_i, s'_i, f'_i) \in N_{CFA}(e), \ \ if \ \forall 1 \le i \le n, s'_i = s_i \ and \ f'_i \in F \setminus \{f_i\} \ and \ c'_i \in C \setminus \{c_i\} \quad \textbf{(4.8)}$$

In this structure, in order to obtain a good neighbor, we apply a descent procedure to refine solutions in the neighborhood $N_{CA}(e)$ and in the neighborhood $N_{FA}(e)$. Here it is deterministic. Thus for a solution *e*, the neighborhood structure N_{CFA} is described with the following pseudo-code.

ALGORITHM 3: The neighborhood structure N_{CFA}

1. $e'' \leftarrow \Phi$;
2. **While** $e'' \neq e$ **do**
3. $e'' = e(c_i, s_i, f_i)$
4. **For** $i = 1...n$ **do**
5. **For** all $c \in C \setminus \{c_i\}$ **do**
6. **For** all $f \in F \setminus \{f_i\}$ **do**
7. $e' \leftarrow e \setminus \{(c_i, f_i)\} \cup \{(c, f)\}$
8. **If** E(e') < E(e)
9. $e \leftarrow e'$
10. **Endif**
11. **Endfor**

12. **Endfor**

13. **Endfor**

14. **Endwhile**

15. **Return** *e*"

Seen from the above pseudo-code that the neighborhood structure N_{CFA} would be extraordinary wasteful of computing time. Moreover, it is also the steepest descent neighborhood structure in all the neighborhood structures. Thus we will use this neighborhood structure as less frequently as possible.

Since a complete solution includes the frequency variable, we always use the above neighborhood structures and the neighborhood structure N_{FA} together to optimize the frequency allocation. So in the following section, N_{DM}, N_{AM}, N_{SM} and N_{CA} really are $N_{DM} + N_{FA}$, $N_{AM} + N_{FA}$, $N_{SM} + N_{FA}$ and $N_{CA} + N_{FA}$ respectively.

e) Termination criteria

In our optimization, the algorithm stops when one of the following termination conditions is satisfied:

—The number of iterations has reached the maximum number of iterations.

—The value of the returned cost function is equal to zero.

—The number of successive iterations without improvement of the cost function has reached a specified number.

f) Enhancements

To get better solution, we add some strategies to the global algorithm we present and we will evaluate the effect of these operators by a series of experiments presented in a later section.

- **Dynamic neighborhood selection strategy**

Usually, the neighborhood selection strategy follows a sequential strategy. Keeping this concept in mind, it is obvious that the application order of the neighborhood structures is crucial for the performance of VNS. The effect of this application is that the first neighborhood structures search more often than the ones at the end of the queue. Thus a significant question, which is important for the algorithm performance, is the order in which the neighborhoods shall be considered. Searching the neighborhoods in an appropriate order can increase solution quality and speed-up VNS. Here, we guide VNS by sorting the neighborhoods according to the estimation of the improvements potential, which is an improved dynamic neighborhood ordering strategy compared to our previous fixed neighborhood ordering strategy. This strategy is based on the reinforcement learning, which is a technique of machine learning and is used to reinforce the improvement ability of the neighborhood selection. If a structure gives improvements in a reasonable amount of time we prefer to still use it and give rewards to this structure to increase its improvement potential. The higher rewards give the structure with the higher solution improvements. The detail of the selection strategy is as shown below:

For each neighborhood structure k, there are two kinds of improvement potential according to the current selection state of structure k:

λ_{k0}: the improvement potential of non-selection of structure k.

λ_{k1}: the improvement potential of selection of structure k.

Those improvement potentials are positive during the entire search.

The rewards for the improvement potential are computed with respect to the output of the search in structure x:

$$reward = \begin{cases} \alpha + \beta \times nIt \times \left(x/x^* - 1\right) + \gamma \times \left(1 - t/t'\right) & \text{if objective improved} \\ -\alpha' - \beta' \times nIt & \text{else} \end{cases} \quad \textbf{(4.9)}$$

The positive reward for the objective improvement has three components. And α, β, γ are the weight for these components. The first component is a constant reward for the solution improvement state. The second component is a reward for the improvement in fitness (the current improved solution x to the previous improved solution x^*) with the number of iterations nIt. We add a fraction of the number of iterations because comparing the improvement of the objective is more difficult at the end. The third component is a reward for comparing the exploring time for this improvement t with the exploring time for previous improvement t'.

In case of non-improvement, the reward is a penalty, which is made up of two parts. Similarly, α' and β' are the weight for these parts. The first part is a constant penalty for the solution non-improvement state. The second part is a penalty for the solution non-improvement state with the number of iterations nIt.

For each structure k, two kinds of improvement potential are updated with the following rules:

In case of improvement, update λ_{k1}, the improvement potential of selection of structure k:

$$\lambda_{k1} = \lambda_{k1} + n \times \left(reward - \lambda_{k1}\right) \quad \textbf{(4.10)}$$

Where n is a strategy parameter controlling the influence of the reward.

In case of non-improvement, updateλ_{k0}, the improvement potential of non-selection of structure k:

$$\lambda_{k0} = \lambda_{k0} + n \times \left(-reward - \lambda_{k0}\right) \quad \textbf{(4.11)}$$

The intuition behind those update rules is that it can turn out that the selected structure k has more improvement potential on improvement and it may infer that the non-selected structure k has more improvement potential on non-improvement. As the parameter n is constant, those updates perform exponential smoothing on the rewards gathered and the influence of early rewards can be more or less reduced.

When combining λ_{k0} *and* λ_{k1}, E_k an estimation of the improvement potential of the structure k is defined by:

$$E_k = \frac{\lambda_{k1}}{\lambda_{k1} + \lambda_{k0}} \quad \textbf{(4.12)}$$

With this estimation, we can order the structures from high value to low value. However, in order to avoid a bias to that mechanism, the neighborhood structure ordering is not immediately sorted by improvements potential before processing several neighborhoods.

- **Double control of the degradation strategy**

During the optimization process, it is impossible to know in advance the geometric properties of the fitness then it is difficult to decide which region of the problem space to explore. A common landscape problem is that the objective function is fluctuating slightly in the process of descent. In this situation, we require to produce an appropriate new starting point which should not only be different from the local minimum (which is the current solution of our algorithm) but also should be closer to the best so far solution instead of a pure random restart.

To meet above requirements, the double control of the degradation acts as the acceptance criterion used in our optimization. This strategy is firstly proposed in (Mabed *et al.*, 2005). A double control of the degradation is carried out by two parts: one is to control the quantity of the degradation which is a probability of a worse solution acceptance; the other is to control the quality of the degradation that defines the amplitude of degradation. This amplitude is calculated relatively to the best solution and the current solution. A more detailed description of double control of the degradation is shown below:

Notation:

- x: the current solution
- x^*: the best solution so far
- x'' *:* the solution from the neighborhood of the current solution x
- *proba*: the probability of the current solution degradation
- *degrad1*: the coefficient of the degradation of the best solution so far
- *degrad2*: the coefficient of the degradation of the current solution

ALGORITHM 4: Double control of fitness degradation

1. **If** $f(x'') < f(x)$
2. Accept x'' as a current solution
3. **Else**
4. **If** $f(x'') < f(x^*) \times (1+degra1) + f(x) \times degra2$
5. Accept x'' as a current solution with the probability *proba*
6. **Endif**
7. **Endif**

- **Computation speed up with enhanced data structures**

As we have already stated, we can use the properties of the problem to reduce its computational complexity. Since such methods have the characteristics of strong specific aim, effect of computational complexity reduction is often particularly good. For our optimization, we propose filtering strategy which tries to reduce the computation of the fitness or to rule out parts of the search space that cannot contain the best solution.

The most obvious filtering strategy is to filter some RPs when calculating the positioning error. Unlike the QoS, the positioning error only depends on RSS vector at RP. Since in our propagation model, the signal strength from each AP is mutual independent, the positioning error only depends on the operators such as added AP, deleted AP, swapped AP or reallocated configuration at AP. Thus for each move in search process, we just need to recalculate the average positioning error of these RPs which are contained in the coverage of APs changed in this move. In fact, according to the neighbourhood structure definition, only two APs are changed at most in a move, and the most case is, one AP changed in a move. So it is entirely conceivable that the computation will be reduced drastically to RPs in one or two AP coverage instead of whole RPs in the calculation area.

Moreover, since the evaluation of solutions is computationally expensive, we maintain table for saving the value of known solutions. This strategy ensures that the fitness value of the same solution will not be calculated more than once within the whole procedure, even if we return to the same solution. However, such strategy is feasible and effective only if the size of the problem is not too large.

Recall that there are three kinds of indoor positioning error as plotted in Figure 4.5. One is called the aliasing error which describes the diversity of RSS vectors. One is called the GDOP which is a scalar dimension less quantity used for the positioning accuracy ratio. And one is the Average Positioning Error (APE) which describes the dynamic positioning error. And we also propose three positioning error indicators to evaluate the positioning errors. The indicator RSER is used to estimate the aliasing error. The indicator GDOP is used to establish the relationship between the accuracy and the geometric distribution of the APs and the indicator APE is used to estimate the average positioning error. The aliasing error is included in the APE, and this conclusion is possible to derive by definition of the aliasing error and the average positioning error. The GDOP partially reflects an overview about the accuracy degree of the average positioning error, this conclusion is shown in (Zirari, 2010). Moreover, at a given reception point the aliasing error and the GDOP are completely unrelated.

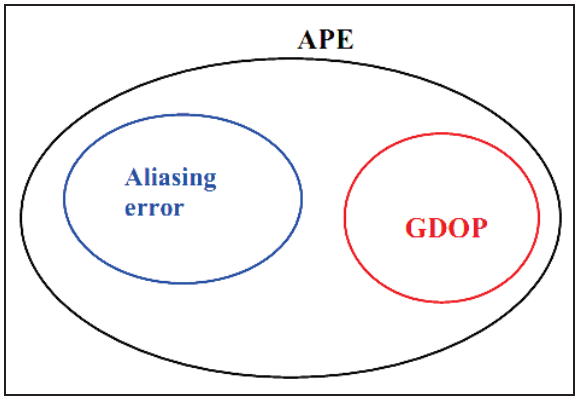

Figure 4.5 The inherent connections between aliasing error, GDOP error and average positioning error

As we known, each AP configuration at a site has a corresponding positioning error variation. Before we decide which APs will be chosen at each move, if we can estimate all the positioning error of the possible AP configuration at this site in advance, even if these pre-estimations are rough, they can help to filter some solutions and bring a beneficial choice. Since the computation of RSER is much lower than the computation of APE, thus we use the RSER of RPs in the coverage of the possible AP configuration to estimate the positioning error of this configuration on each site. Basically, if the average GDOP is between 1 and 3, we consider the position estimation with a good accuracy. Thus we will prefer to choose the solution having the lowest RSER among the candidate solutions whose average GDOP is between 1 and 3.

g) The algorithm description

The pseudo-code of Tabu Variable Neighbourhood Search is the following.

ALGORITHM 5: Tabu Variable Neighbourhood Search (TVNS)

Initialization:

1. Define the initial order of neighborhood structures for VNS: $N_1=N_{CA}$, $N_2=N_{SM}$, $N_3=N_{AM}$, $N_4=N_{DM}$. And N_{CFA} is considered as a supplement of above neighborhood structures for steepest descent search. For the neighborhood selection strategy, the improvements potentials λ_k of neighborhood structure k are initially identical: $\lambda_1=\lambda_2=\lambda_3=\lambda_4$.

2. Find an initial solution x by the algorithm described by ALGORITHM 1 and ALGORITHM 2. This initial solution is generated by two steps. In the first step, the coverage-based solution is found by a constructive heuristic GRASP. Then, in the second step, we choose ILS multi-start algorithm to obtain a good frequency allocation.

3. Let this initial solution x to be the present solution and the present optimum solution: x^*. Iteration number n=0.

1. $x^* \leftarrow x$

2. **While** the stop condition is not met **do**

3. $k \leftarrow 1$

4. **While** $k \leq 4$ **do**

5. A solution x' in the k^{th} neighborhood $N_k(x)$ is randomly selected

6. Local search: apply Tabu Search on x' as initial solution until a local minimum x'' is found
7. Update the reward for V_k
8. **If** x'' is better than x according to the double control of the degradation strategy
9. $x \leftarrow x''$
10. **If** x'' is better than x^*
11. $x^* \leftarrow x''$
12. **Endif**
13. Update the reward for the selected neighborhood structure
14. Update the improvement potential of the selected neighborhood structure λ_k
15. $k \leftarrow 1$
16. **Else**
17. Update the reward for all non-selected neighborhood structure
18. Update the improvement potential of all non-selected neighborhood structure $\lambda_{k'}$ *with* $k' \neq k$
19. $k \leftarrow k+1$
20. **Endif**
21. **Endwhile**
22. **If** n is larger than 300
23. Reorder the neighborhood structures based on their respective estimation
24. **Endif**
25. $n \leftarrow n+1$
26. **Endwhile**

In above algorithm, there is a Tabu Search in local search step. Before implementing Tabu Search, the three key elements must be discussed at first: they are neighborhood, Tabu list and stopping criteria.

—*Neighborhood*: In a narrow sense, a Tabu Search has only one neighborhood structure. However, we define four different neighborhood structures in our approach. To meet this requirement, we have two choices. One choice is to only use the current selected neighborhood structure N_k and to explore the neighborhood $N_k(x)$ by Tabu Search. The other choice is to combine all four moves into one neighborhood structure. In this case, the four moves N_{DM}, N_{AM}, N_{SM} and N_{CA} are all performed at each iteration of our TS, and the best move is selected. In this case, the cardinality of the neighborhood of a solution is $188+188\times N-2\times N^2$. Clearly, the number of neighbors for such neighborhood structure is very large. For example, when 30 APs are selected, 4028 candidate solutions in

neighborhood are generated. In a broad sense, a Tabu Search is a local search based on a memory metaheuristic. Thus we can select the four moves randomly or orderly at each iteration. Then the best solution in the neighborhood of the current solution is chosen as the new current solution if it is not tabooed. Otherwise, we select the best one from other neighborhoods. We have decided to exploit this case based on the use of the four neighborhood structures during Tabu Search.

—*Tabu list*: The Tabu list stores the last solutions that have been selected to prevent reverse moves. In our problem, the size of solution space is very large. That means the tabu tenure should be also large if we want a tabu list actually to work. Therefore, instead of the implementation of the solutions themselves, we put the solution attributes in the tabu list. Here, we define attribute as usually difference between two solutions, which is represented by the changed i^{th} component of solution as $\{(c_i, s_i), (c_i', s_i')\}$. (c_i, s_i) is the original value and (c_i', s_i') is the new value. Within this framework, we present the expression of the attribute by different move. For the solution from N_{DM} move, the attribute of this solution is $\{(c_i, s_i), (0, s_i)\}$; for the solution from N_{AM} move, the attribute of this solution is $\{(0, s_i), (c_i', s_i)\}$; for the solution from N_{SM} move, the attribute of this solution is $\{(c_i, s_i), (c_i', s_i')\}$; for the solution from N_{CA} move, the attribute of this solution is $\{(c_i, s_i), (c_i', s_i)\}$. The dynamic tabu tenure strategy is chosen in our algorithm, it is the best one. In this strategy, the tabu tenure has a length T that is chosen randomly at each iteration between two predefined parameters T_{min} and T_{max}. When T_{min} and T_{max} are equal, it is a fixed tabu tenure strategy. T_{min} and T_{max} have been chosen empirically after several tests. When tabu tenure is reduced, the oldest moves

—*Stopping criteria*: Our Tabu Search terminates when the given number of iterations for the local search is reached.

In addition, the algorithm of Tabu Search step is shown below:

Notation:

T : the tabu list

n: the tabu tenure

Selection probability: N_{CA}=0.3, N_{SM}=0.3, N_{AM} =0.2, N_{DM}=0.2

ALGORITHM 6: Tabu Search (TS) for local search

1. $T \leftarrow \Phi$
2. $n \leftarrow 0$
3. x″=x'
4. **While** the stop condition is not met = the given number of iteration is not reached **do**
5. Select one from four neighborhood structures k based on its selection potential
6. **For** all $x''' \in N_k(x') \backslash T$
7. $x'' \leftarrow MinE(x''')$ \\ Keep the best neighbor among the set of x''
8. **Endfor**

9. n=random[T_{min} , T_{max}]
10. Update T
11. **If** x'' is better than x'
12. $x' \leftarrow x''$
13. **Endif**
14. **Endwhile**
15. **Return** x''

4.2.2.3 The experimentation of mono-objective optimization

a) Test environment

To evaluate the model and the algorithm, we did some experiments. The experiments were held in the environment described by Figure 4.6. The test bed is composed of a two-floor building which is the building B in UTBM campus. Each floor size is 150m x 40m. We defined 94 candidate sites for AP installation. The green points show the location of these candidate sites. We assigned more candidate sites in the first floor since the topology of the first floor is more complex. According to the discrete requirements of our model, we distribute the MP every one meter, thus there are 6000 MPs in each floor. For the sake of convenience in illustrating, we use one black point to represent five MPs to show the distribution of these MPs in each floor.

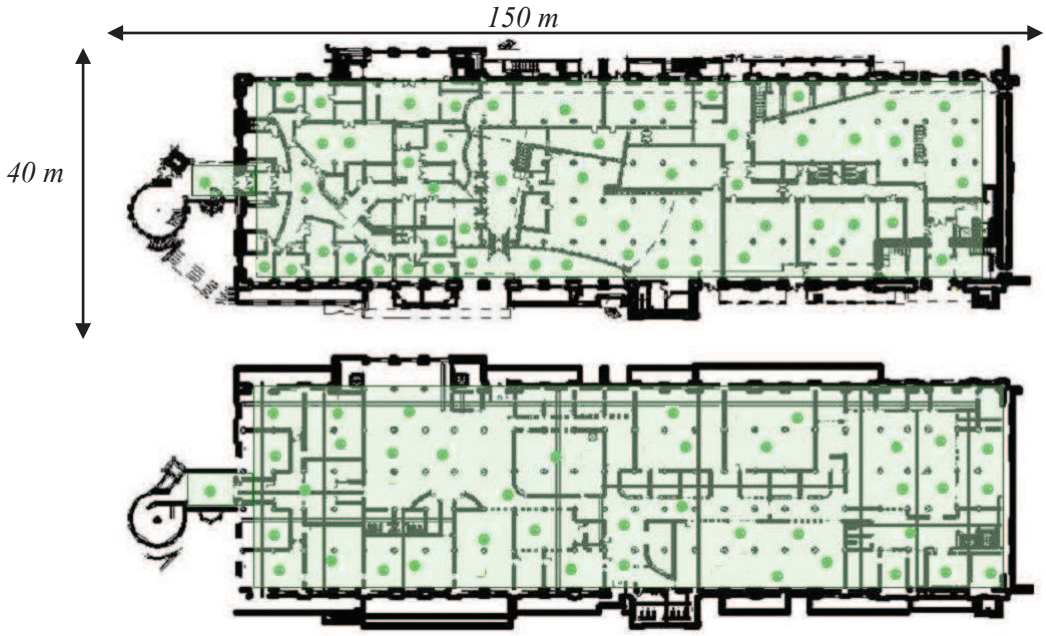

Figure 4.6 The topology of the test building

In order to define the traffic demand and positioning demand, we set one service zone and one positioning zone in each floor respectively. For easing the test analysis, service zone and positioning zone in each floor are the same. These zones are represented by the polygons covering the green areas of the building on Figure 4.6. Note that since we do not consider the building envelope, those

two kinds of zones only correspond to 7728 MPs on 12000 MP at all. In other words, 7728 TP are defined for SINR computation and 7728 RP are defined for RSER computation. We also set each zone with positive zone priority that is they must be satisfied for demand and positioning requirements. For the service zone, 300 users are uniformly distributed on each service zone (each floor) and each user demand is about 500 kbps real bit rate. Then, the global demand for the whole building is 300 Mbps. For the positioning zone, the required positioning accuracy at each RP is set as zero. In my model, the deviation between a_p (the positioning accuracy required at RP r in the positioning zone p) and APE_r (the positioning accuracy estimated at RP r in the positioning zone p): $\Delta_r = APE_r - a_p$. This a_p can be considered as a reference point. It can be zero or the value more than zero. When $a_p=0$, $\Delta_r = APE_r$

AP parameter settings are one type of AP with a unidirectional pattern and 2 possible values of power. Thus we have 2 possible configurations for each site, and then 188 candidate configurations for whole building. For the frequency allocation, each site must use one frequency among the 13 which are available in France for the standard 802.11b/g. Then, the WLAN AP network design consists in installing some AP configurations among 188 candidate configurations and in assigning frequency channels that is 188x13 combinations. To focus on the different strategies, optimization does not take into account the financial requirements. We limit at 30 the maximum selected AP for a solution.

Assuming there are N APs selected in this experiment, we can calculate the size of neighborhood for each move. For adding one AP in the current solution, $2\times(94 - N)$ candidate solutions are generated. For removing an AP from the current solution, N candidate solutions are generated. The size of neighborhood of swapping AP is $2\times N\times(94 - N)$. And the cardinality of the neighborhood of configuration allocation is N.

To better understand the relationship between QoS and positioning error, we ignore the economical cost objective and only focus on the positioning accuracy objective and QoS objective. Then we have the single objective function we want to minimize as shown below:

$$\beta \times \sum_{t \in T} \max(0; -u_c^T \times \Delta_t) + \gamma \times \sum_{r \in R} APE_r \qquad \textbf{(4.13)}$$

The set of total TPs in service zone is T and the set of total RPs in positioning zone is R. Where u_c^T is the number of user in the TP t and Δ_t is the deviation between the downlink bit rate provided by the network and the bit rate required at the TP t. APE_r is the average error at a RP r. The constant γ and β are chosen in order to obtain a linear combination of the two errors; several values will be checked later. For convenience, we use the value of the radio γ / β to replace the constant γ and β.

b) Computational results

The application of mono-objective optimization algorithm to our WLAN indoor positioning system described in the Chapter 3 were implemented in C++ and run on a Dell computer. We test a set of instance to study and evaluate the algorithm.

- **Algorithms comparison**

Since our model is completely new, we cannot use any existing benchmark to study and evaluate the performance of TVNS. Thus a practical solution is to compare TVNS with other two

typical VNS algorithms which are reported to lead to many successful applications.

One is called Random VNS (RVNS). In this algorithm, instead of predefining the order of neighborhood structures, each neighborhood structure is allocated to a fixed selection probability. At each iteration, the neighborhood structure is randomly selected in regards to the probability and a local optimal solution is selected from the neighbourhood. If an improvement is obtained, we accept this solution as an initial solution for the next iteration. Although this algorithm is very simple, it has been proved effective in WLAN planning reported by (Gondran 2008). Thus we choose this algorithm as a reference algorithm.

The other algorithm for comparison is a powerful VNS called the General VNS (GVNS). In this approach, the order of neighborhood structures is predefined and fixed. The local search is replaced by the Variable Neighborhood Descent (VND) where changes of neighborhood structure are made in a deterministic way, as described as follows.

ALGORITHM 7: Variable Neighborhood Descent (VND)

Initialization: a finite set of pre-selected neighborhood structures $\{N_1=N_{CA}, N_2=N_{SM}, N_3=N_{AM}, N_4=N_{DM}\}$ and an initial feasible solution x.

1. **Repeat**
2. k ← 1
3. **Repeat**
4. Find the best neighbor x' of x in $N_k(x)$
5. **If** x' is better than x
6. $x \leftarrow x'$
7. $k \leftarrow 1$
8. **Else**
9. $k \leftarrow k+1$
10. **Endif**
11. **Until** $k = 4$
12. **Until** no improvement is obtained

According to our previous analysis, the APs in the initial solution cannot provide coverage for communication, thus it is better to increase the number of AP at the beginning of the algorithm. In order to improve the algorithm efficiency, we put the neighborhood structure N_{AM} forward from the 3rd to the 1st until all TPs are covered for communication.

In this experiment, the value of the ratio γ/β is fixed to 0.1 in order to obtain a linear combination of the two errors, so that the two terms have approximately the same weight. The magnitude of the variation of the positioning error fitness is ten times bigger than the magnitude of the variation of the communication fitness. When we add this weight, the magnitude of their respective variation will be approximately equal. This value has been experimentally determined

based on the orders of magnitude of their respective variation.

The first significant result is the convergence speed of the algorithms and the absolute value of the objective function that they reach.

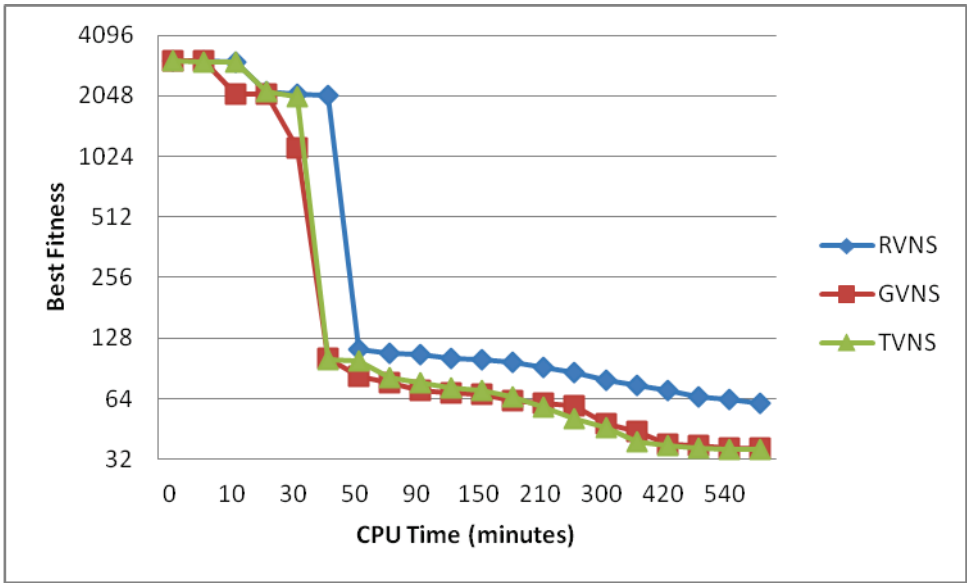

Figure 4.7 Typical traces for the three algorithms: best solution found against CPU time

Figure 4.7 shows a representative trace of the execution of each algorithm. CPU time is on the horizontal axis while the vertical axis reports the best value found up to that moment. In all cases, due to the way of defining objective function expressions, the minor is the objective function value, the better is the solution. We use the variable sample rate since a quite common behavior in local search techniques: improvements tend to concentrate at the beginning and to slow down after the most probable minima have been found. In the first hour of running we sample the best value after 5 minutes, 10 minutes then every 10 minutes. After the first hour, we define the sampling time interval as half an hour until the 4^{th} hour and then the sampling time interval is one hour. The running time is limited to 10 hours (600 minutes which is the last value on *x*-axis) because the algorithms have converged to a local optimum after 10 hours.

Initially, the performances of three algorithms were almost same in the first hour even if GVNS is more efficient than the other two algorithms because GVNS always selects the best neighbor. After the first hour, the search efficiency of every algorithm gradually reduces. RVNS performs the worst; this is because RVNS has less freedom and less useful information from previous iterations (neighborhood probability are fixed) so that the algorithm tends to remain for a longer time around a local minimum. In fact, in our tests, the performance of RVNS is not consistent. In ten times running, RVNS prematurely converges into a local minimum (within two hours) four times. TVNS tends to have a better performance than GVNS; on 10 runs, the best solution of TVNS is 8 times better than GVNS. This result may be attributed to the advantages of variable neighborhood and tabu memory, thus it gives us a good qualification of our algorithm performance and allows us to go on more details about the problem to optimize.

- **Positioning error objectives comparison**

Recall that, we proposed to speed-up the optimization processes by reducing the computational complexity of fitness. However, this proposal needs to be verified experimentally. Moreover, in

indoor positioning system, the random error is difficult to be minimized, while aliasing error may be relatively easier to handle since it is directly relative to AP configurations. This implies that the solution space of aliasing error is highly likely to be simpler than the solution space of the average positioning error. Thus we also suppose that maybe we can obtain a better solution through using aliasing error instead of average positioning error. To verify above hypothesis, we run TVNS under the two conditions which are: using aliasing error as positioning error objective (hereinafter referred to as Aliasing condition) and using average positioning error as positioning error objective (hereinafter referred to as Average condition). For this experiment, the value of the ratio γ/β=0.1 and we run each condition 5 times. For consistency in the comparison, we only save the AP configurations of all the improvements under two conditions. Then we recalculate positioning error fitness with the average positioning error for each improvement according to the AP configurations. Finally we re-rank these improvements and pick up the best fitness in each situation respectively. Table 1 reports different values: T_{Avg}, the average search time before convergence; T_{Better}, the average percentage of search time that the selected condition (APE or aliasing error) performs better during a given running time (we set this time as the search time before convergence under Average condition since Average condition is easy in premature convergence); P_{Better}, the times that the selected condition finally performs better for all 5 times running; F_{Avg}, the average fitness; F_{Best}, the best fitness obtained by one of the tested algorithms; F_{SD}, the standard deviation; F_{Fre}, the number of times the best known fitness is obtained. All these results were got with TVNS under the two conditions of aliasing error objective and average positioning error objective.

TABLE 1 THE PERFORMANCE OF ALIASING CONDITION AND AVERAGE CONDITION

Positioning error objective	T_{Avg} (mn)	T_{Better} (%)	P_{Better} (%)	F_{Avg}	F_{Best}	F_{SD}	F_{Fre}
Average positioning error	615.6	11.8	0	35.37	35.08	0.32	2
Aliasing error	862.2	88.2	100	28.76	28.41	0.57	1

The results shown in the above table indicate that the performance of Aliasing condition is significantly better than the performance of Average condition: always having better final fitness on 5 runs (P_{Better} =100%), having better average final fitness (F_{Avg}=28.76) and better best final fitness (F_{Best}=28.41). And such performance superiority is also quite stable as the standard deviation of final fitness (F_{SD} =0.57) is small relatively to F_{Best}. Meanwhile, the results also confirm that using aliasing error as a positioning fitness has speed-up effects since the Aliasing condition performs better for at least 88.2% of the specified period. Moreover, TVNS with aliasing error optimization has longer search time before convergence which is beneficial to obtaining better best solution.

In the subsequent experiments, we also run RVNS under these two conditions to verify if there is a bias linked to TVNS algorithm. What is even more exciting is that RVNS has the worst performance algorithm under Average condition but tends to have the similar performance as TVNS under Aliasing condition. It can be inferred from this result that our hypothesis about using aliasing criteria for optimizing the positioning error is really correct.

- **Varying objective weight**

In the non-Pareto optimization, the weights γ and β are preset to assign a numerical relative importance to the multiple objectives and then the optimization algorithm is used to find the minima

of this single function. In the above experiments, a relative trade-off between objectives was chosen. However, in real-world situation, the decision maker may want to check different optimal trade-off between the conflicting objectives, for example by preferring higher positioning accuracy.

In this experiment, we vary the ratio γ/β to obtain the different trade-off between the conflicting objectives and to study the relationship between QoS and the positioning accuracy. Three test scenarios have been defined to evaluate the γ to β ratio in mono-objective search:

$$\sum_{t\in T}\max(0;-u_c^T\times\Delta_t)+0.1\times\sum_{r\in R}APE_r \quad \textbf{(4.14)}$$

$$\sum_{t\in T}\max(0;-u_c^T\times\Delta_t)+0.01\times\sum_{r\in R}APE_r \quad \textbf{(4.15)}$$

$$\sum_{t\in T}\max(0;-u_c^T\times\Delta_t)+100\times\sum_{r\in R}APE_r \quad \textbf{(4.16)}$$

We run TVNS for these three test scenarios. We were expected that the scenario with the highest γ to β ratio (γ/β=100) should output the solution with best positioning accuracy but bad QoS coverage while the scenario with the lowest γ to β ratio (γ/β=0.01) should output the solution with best QoS coverage but bad positioning accuracy. This is because on one hand the objective associated with a high penalty coefficient is emphatically optimized while on the other hand a high penalty coefficient also prevents the improvement of other conflicting objectives. At first we run optimization with the average positioning error as the positioning error objective; the testing results indicate that the best QoS coverage is obtained with γ/β=0.1 instead of 0.01 and the positioning accuracy with 0.1 is close to 100 scenario. We thought that these results may have been caused by the too large and too complex search space and the algorithm should need much more time or run to find good solutions for each case. In order to confirm this idea, we replace average positioning error with aliasing error to reduce the size and complexity of search space. Figure 4.8 and Figure 4.9 shows the total lack of QoS and total aliasing error value of three test scenarios at each improvement respectively.

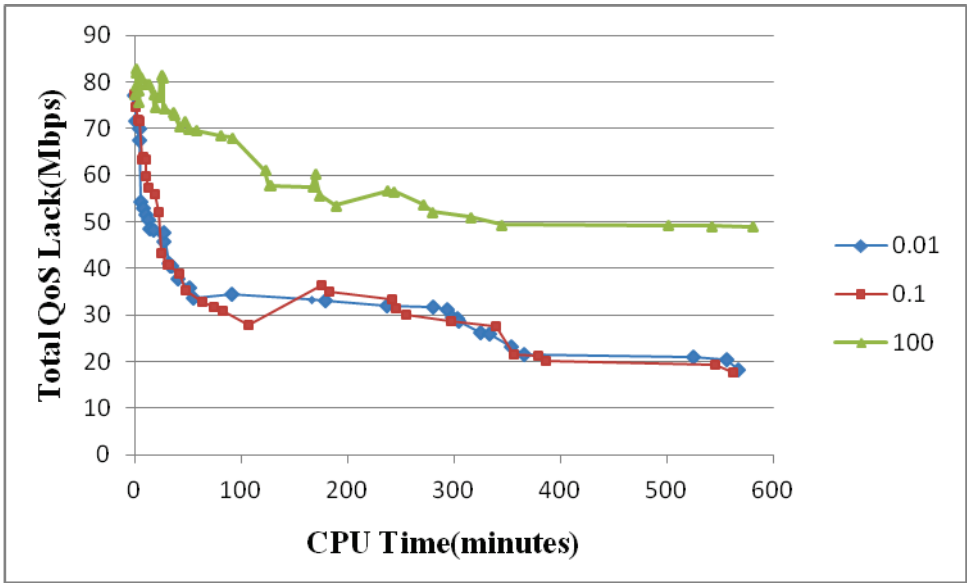

Figure 4.8 The variation of total QoS lack with different γ to β ratio in each improvement

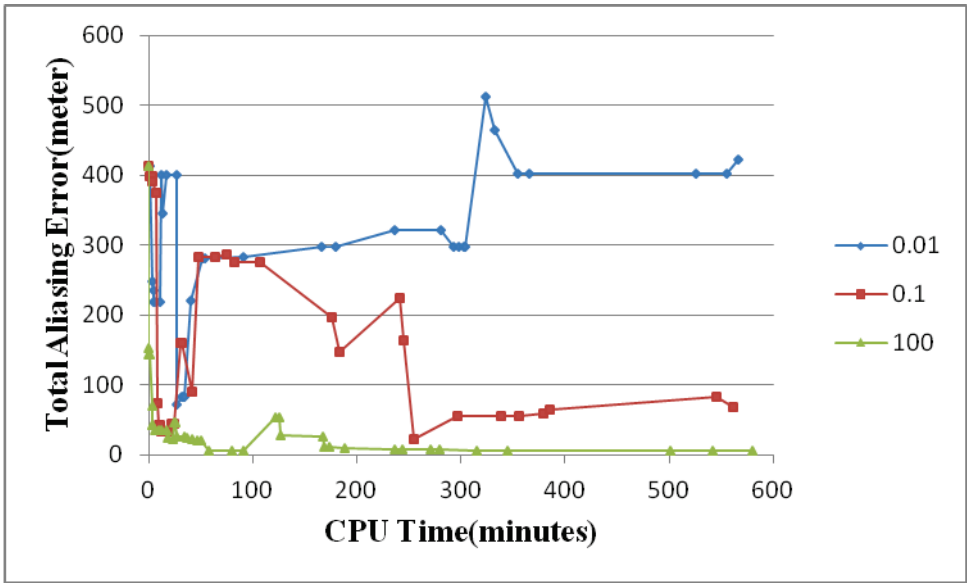

Figure 4.9 The variation of total Aliasing error with different γ to β ratio in each improvement

Table 2 describes the total average positioning error value of three test scenarios at final improvement respectively.

TABLE 2 THE TOTAL AVERAGE POSITIONING ERROR VALUE OF THREE TEST SCENARIOS

Scenarios γ/β	0.01	0.01	100
Total average positioning error (meter)	626.55	162.08	132.98

From Figure 4.8 and Figure 4.9, we easily conclude that a high γ to β ratio of 100 can guarantee a small total aliasing error while leading to a huge lack of total QoS (green curves: good positioning accuracy, bad QoS). In the same way, a low γ to β ratio of 0.01 only guarantees a low lack of total QoS but gives a high total positioning error (blue curves: bad positioning accuracy, good QoS). Figure 4.8 and Figure 4.9 also shows that treating these objectives equally is a good compromise; with an appropriate value of 0.1 for the γ to β ratio, our approach could find an AP configuration which might provide a good improvement not only on QoS demand but also on positioning accuracy (red curves: good positioning accuracy, good QoS). The results in Table 2 completely match our expectation since solution space becomes simpler the algorithm no longer traps in local minimal solution during 10 hours running. These results are very important and very new as they show that it is necessary to optimize the QoS and the positioning error in the same time for WLAN planning and it is difficult to optimally fix the compromise weights in advance for all instances.

- **Optimization models comparison**

As far as we know, our optimization model brings improvement in regards with the existing WLAN-based indoor positioning optimization models since we not only consider the positioning error but also consider the QoS requirement. The optimization model proposed in (Battiti *et al.*, 2003) is one of the most typical representative of existing WLAN-based indoor positioning optimization models. Thus we will compare our optimization model with this model. Since it is developed by Battiti and others, thus, in the following part, we call it as Battiti's model.

The positioning error estimation at each RP in Battiti's model is similar as the average

positioning error at each RP in our model, and the difference of positioning fitness are only the following three things:

—Firstly, in Battiti's model, they consider that the overall expected error is obtained by averaging the total error on the whole test area as the positioning fitness. However, in our model, we consider the total unsatisfied positioning requirement as the positioning fitness. Since the positioning accuracy requirement in this experiment is equal to zero, this fitness becomes the total error on the whole test area. Moreover, Battiti's model also considers a weighting factor that can be used whenever a higher precision is desired at certain locations at the expense of other less important places. The role of this parameter is just like the zone priority in our model, and the difference is that we consider a rough weighting factor with three levels and all the RPs in the same zone have the same weighting factor value. In fact, this weighting factor is obtained from a priori considerations. Since we cannot precisely determine such preliminary considerations by user, the zone priority method is a more practical way in this case.

—Secondly, the radio propagation model in Battiti's approach only considers the logarithmic loss model and the probability density of detecting signal strength is modeled as a Gaussian, where standard deviation is determined by empirical observations. In comparison with Battiti's model, our model is improved with respect to both the radio propagation model and the probability distribution of detecting signal strength. For example, we consider angle dependence of attenuation factors in the radio propagation model and we add heavy tail characteristics in the probability distribution of detecting signal strength.

—Thirdly, our model has two additional parameters. One parameter is to evaluate the total GDOP of each RP in all the positioning zones. GDOP represents a trend of the average positioning error, and it is roughly interpreted as ratio of position error to the signal strength variation range. Thus lower GDOP can bring stable positioning error estimation. The other parameter is the standard deviation of the average positioning error of each RP in all the positioning zones. This parameter can make the positioning accuracy homogeneous.

To sum up, basically, our positioning error model can be considered as an improvement version of Battiti's positioning error model. However, to adapt it for our experiment setting, in following comparison, we should make the following change in Battiti's positioning error model:

—Firstly, we assign the weighting factors in Battiti's model to the definition of zone priority. In our experimental setting, all the weighting factors are equal to one. In other words, these weighting factors are not considered.

—Secondly, we only use our radio propagation model and our probability distribution of detecting signal strength. The variation of RSS at RP from its serving AP is the same for both models.

Based on above modifications, we will give the mathematical expression of the positioning fitness in Battiti's model. Let say that at RP r, APE_r is the average error in our model and the set of total RPs is R. In Battiti's model, the positioning objective λ_P will be:

$$\lambda_P = \frac{1}{|R|}\sum_{r\in R} APE_r \qquad \textbf{(4.17)}$$

Unlike the positioning error estimation, our QoS estimation is much more complete than in Battiti's model. In fact, Battiti's model only supposes that QoS estimation is determined by the RSS of the serving AP and the coverage area. Thus they define the suitability of a solution on the QoS side by finding the lowest RSS from the serving AP in the area. The network card will usually associate to the strongest signal, so that the serving RSS at a TP is the maximum RSS at this TP. Moreover, a RSS threshold is defined for connective requirement. Then the coverage area is the set of all TPs in the networked area for which the serving RSS is greater than this threshold. In the Battiti's model, the QoS objective will be to maximize the coverage area with a given AP number by optimizing the placement and configuration of the access points.

From these considerations, we give the mathematical expression of the QoS fitness in Battiti's model. Let say that the set of total TPs is T and the maximum RSS in the RSS vector at TP t is rss_t^{max}. The signal strength threshold for connective requirement is τ. The QoS objective in Battiti's model λ_C is the size of the coverage area defined by the number of TPs and represented as:

$$\lambda_C = \left|\left\{t \in T \middle| rss_t^{\max} \geq \tau\right\}\right| \qquad \textbf{(4.18)}$$

Clearly, the great flaw of the QoS estimation in Battiti's model is that it only considers the Automatic Cell Planning (ACP) problem but ignores the Automatic Frequency Planning (AFP) problem. In (Xu *et al.*, 2010), the author considers the adjacent channel interference as a kind of additional signal attenuation on the serving RSS and propose a correcting parameter by adding an attenuation value. However, such method is imprecise and not efficient. In our model, we use the SINR to estimate QoS. SINR is a popular indicator to estimate QoS in radio planning. With SINR, we can deal with ACP and AFP simultaneously by a unique QoS fitness. Moreover, we also prefer a homogeneous required QoS distribution.

In conclusion, we can give the single fitness function of Battiti's model we want to minimize as shown below:

$$\beta \times \frac{1}{\lambda_c} + \gamma \times \lambda_P \qquad \textbf{(4.19)}$$

Where, λ_P and λ_C are the cost functions for positioning error and signal coverage. The constant γ to β ratio is chosen in order to obtain a linear combination of the two errors such that the two terms have approximately the same absolute values (the value of γ to β ratio is set to 0.005, which has been experimentally determined).

According to above fitness function, the goal of Battiti's model is to place the APs by minimizing the average error and by maximizing the size of the covered zone. However, these two objectives are not conflicting objectives for AP number. It means increasing the AP number may improve both objectives. Thus unlike in our model where there is limitation in the AP number due to

the adjacent channel interference consideration, the Battiti's model always accepts the maximum AP number. In other words, Battiti's model is only able to optimize the AP placement and the AP setting. Then to tackle this problem, we fix the AP number to 30 (it has been experimentally determined for providing good positioning accuracy and good QoS) and we only change the AP placement and the AP setting in the optimization process. So we only consider the AP swap and the frequency assignment moves.

To obtain the optimized solution, we run the TVNS algorithm for Battiti's model and our model for 8 hours for 3 times. Since the fitness of Battiti's model is different from our model, for consistency in the comparison, the fitness of Battiti's model will need to be converted and made compatible with our model definition according to its corresponding AP configuration. The results of the average value of 3 times running are summarized in Table 3. P_{error} is the average of the total average positioning error, Q_{lack} is the average of the total lack of QoS and $TP_{unsatisfied}$ is the average of the number of unsatisfied TP (SINR at these TP are less than SINR required for communication).

TABLE 3 THE PERFORMANCE OF BATTITI'S MODEL AND OUR MODEL

Model type	P_{error} (meter)	Q_{lack} (Mbit/s)	$TP_{unsatisfied}$
Battiti's model	157.73	73.28	6
Our model	191.12	35.86	0

As expected, the total QoS lack in the best solution of Battiti's model (73.28 Mbit/s) is much poorer than the total QoS lack in the best solution of our model (35.86 Mbit/s) since the frequency interference is not being considered in Battiti's model. And there are even six TPs which cannot provide enough bitrate for communication due to the frequency interference. On reducing only the positioning error side, the Battiti's model tends to have a better performance than our model since the positioning error definition in both models is similar but the coverage constraint in Battiti's model is much simpler and thus QoS requirements are not tackled.

4.3 Pareto optimization

4.3.1 Pareto-based techniques

In the non-Pareto optimization, the γ to β ratio is preset and the solution to this problem can be reached in an optimal manner. However, it is impossible to get the solution that has the best possible rating for each criterion since our optimization objectives have an opposed influence to each other on the variables. For instance, networks made up of a high number of APs have good coverage and positioning performance but suffer from high interference levels. Thus the optimum of non-Pareto optimization results in the identification of a single point on the trade-off optimum surface. Figure 4.10 illustrates this case. The position of point depends on the γ to β ratio which comes from the decision maker's preconceptions. We know that the decision maker will take a better decision if the trade-off surface between the conflicting objectives can be inspected before this choice is made. From Figure 4.10, we can see that to explore the trade-off surface further a large number of different optimization runs with different weightings must be run. It needs expensive time-consuming and

computation.

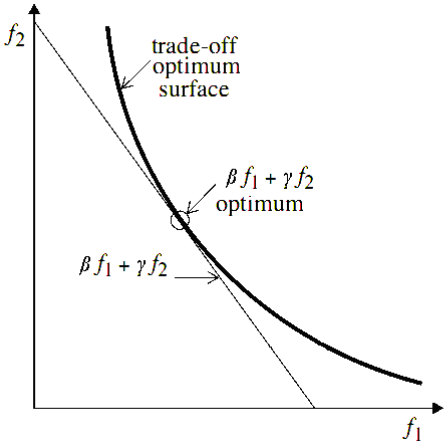

Figure 4.10 Non-Pareto optimization and Pareto optimization

To overcome the above drawbacks, we have developed the Pareto optimization which considers conflicting objectives in a fair way in a single run. According to the definition of the Pareto optimization in the introduction section, a Pareto optimization looks for a set of Pareto-optimal solutions defined as the set of non-dominated solutions. Each non-dominated solution represents a different optimal trade-off between the objectives. This set of non-dominated solutions is also called the theoretical Pareto front as shown in Figure 4.11.

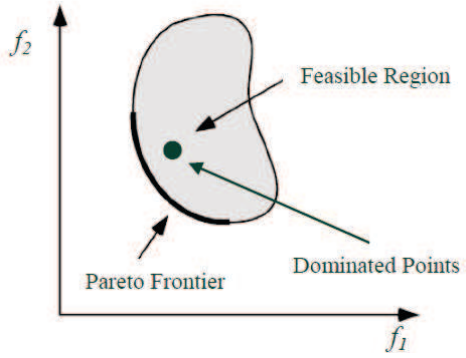

Figure 4.11 The theoretical Pareto front

From this front, a decision maker can finally choose the configurations that, in his opinion, suit best the theoretical Pareto front of the problem. However, such pure Pareto optimization can have undesirable consequences: the complete Pareto optimal set is often not the wanted result of an optimization algorithm. Usually, we are rather interested in some special areas of the Pareto front only. So in this case, we can add some predefined constraints to prevent searching all these non-dominated solutions which may need a lot of time.

For the solution comparison in mono-objective optimization, solutions are compared using the operators =, > and < acting on the objective function values for those solutions and the best solution has the best objective value. Similarly, solutions in a multi-objective problem can be compared in the same way by using the concepts of Pareto equivalence (=) and dominance (> and <) but for all objectives. Solutions are said to be Pareto equivalent (PE) when they are non-dominated by each other.

4.3.2 The Parallel Tabu Variable Neighbourhood Search Algorithm

To search directly for the entire Pareto-optimal set of solutions (PO), a Pareto-based algorithm is proposed in this section. This algorithm is derived from the previously hybridization of Tabu Search and Variable Neighbourhood Search algorithm. As the mono-objective algorithm, the Pareto-based algorithm looks for the AP number, the AP location, the power and the direction of emission of the APs, and the frequency of the APs too. Its aim is to minimize concurrently the three defined objectives: the economical cost objective, the positioning accuracy objective and the QoS objective.

4.3.2.1 Parallelization strategy

Currently, most Pareto-based algorithms are population-based algorithms. Population-based algorithms seem particularly suitable to solve multi-objectives (MO) problems, because they deal simultaneously with a set of possible solutions. This allows us to find several members of the Pareto optimal set in a single run of the algorithm, instead of having to perform a series of separate runs as in the case of the trajectory methods.

To take advantage of population-based algorithms, we introduce the parallelization strategy in the algorithm TVNS. Within the parallel processing, a number of solution evaluations at each iteration and a large potential speed up can be offered. Currently there are three ways in which algorithm may be parallelized.

The first one is a functional decomposition in which problem is decomposed into non-interacting components executed in parallel for each iteration of the search. The second one is a domain decomposition in which the search domain is decomposed and individually searched. The third one is a multi-threaded search in which several searches are executed in parallel and information is shared between the searches.

Since all three strategies have advantages and disadvantages, we have to do further analysis. First, we can reject domain decomposition immediately. The performance of domain decomposition strategy is poor since the search domain in our problem cannot be easily equally divided and highly constrained. Also the functional decomposition is not fit well since our problem cannot be easily decomposed and the necessary operation cannot be implemented separately in TVNS. Finally, we prefer to choose the multi-threaded search strategy. A multi-threaded search strategy is straightforward to implement and coupled parallel search algorithms may give a super-linear speed-up in certain conditions (Shirts & Pande, 2001).

4.3.2.2 Initialization

Since we implement the parallelization strategy, the solutions of the initial search front are generated instead of a single initial solution. To trade off the diversity and the intensity of the search, the solutions of the initial front are generated by adding various modifications on the initialization of non-Pareto optimization.

- Let n_i denote the AP number of initialization of non-Pareto optimization
- Let n_{max} denote the maximum AP number

- Let n_{site} denote the total site number

There are five modification modes shown as below:

- Adding a selected AP
- Adding n_{max}-n_i selected APs
- Adding *round*($(n_{max}$-$n_i)/2$) selected APs
- Changing *round*($min(n_i/2,(n_{site}$-$n_i)/2)$) selected AP to a different position
- Reallocating *round*($n_i/2$) AP configurations

The removing selected APs will not be considered since the initialization of non-Pareto optimization is the lower bound of optimization.

4.3.2.3 Metaheuristic: Parallel Tabu Variable Neighbourhood Search

In this section, we will present a Pareto-based algorithm for our optimization problem. This algorithm is based on the previously presented hybridization of Tabu Search and Variable Neighbourhood Search algorithms. Since we introduce the parallelization strategy, some properties of population-based algorithms are also introduced in the same time.

a) Pareto ranking

A key aspect of our algorithm is that we deal with a population of potential solutions to a problem instead of only one candidate, thus we cannot determine the candidate solution directly. Referring to the selection mechanism of MO evolutionary algorithms, the Pareto ranking can be used to determine which elements of the population are selected to be candidate solutions for the next iteration. It is necessary to establish some criteria to determine if one solution is better than another.

There are many ranking methods proposed (Mallor *et al.*, 2003). We have taken one most usual ranking method which is proved to be a simple and effective method in many reports (Dai *et al.*, 2011), (Goldberg, 1989), (Jaffrès-Runser *et al.*, 2008). In this method, a solution rank is defined by the number of solutions by which it is dominated in its solution set. The solutions of the theoretical Pareto front have a rank which is equal to zero. After ranking the solution set, we can calculate the acceptance probability. It is done according to how good or bad a solution is from its rank. The better it is, the higher is its probability to survive, and so, it has a higher probability of being selected for the next generation. In our algorithm, the acceptance probability of rank r is given by:

$$P_r = \begin{cases} 0.8 \times (1-0.8)^r & if\ r < |R| - 1\ \ and\ \ |R| \geq 1 \\ (1-0.8)^R & if\ r = |R| - 1\ and\ \ |R| \geq 1 \\ 0.8 & if\ r = |R| - 1 = 0 \end{cases} \quad \textbf{(4.20)}$$

Where, P_r is the acceptance probability of rank r. $|R|$ is the total number of rank in the solution set. We use a geometric progression as decision formula since the geometric progression is generally easy to satisfy our two expected conditions: the higher acceptance probability should be assigned to the solution with lower rank and the sum of the acceptance probabilities for all rank r must be equal to one. The parameter 0.8 is an empirical data.

b) Diversity preservation

At the end of the search, we will obtain numerous solutions. However, these solutions may have a tendency to convergence so that to reduce the efficiency of algorithm to search new different solution. For this reason, a method must be introduced to achieve the maintenance or expansion of solutions diversity. The solutions diversity is usually implemented in two aspects: the objective space and the search space.

In the *objective space*, we consider the dissimilarity of the objective trade-off. A current principle for one solution is that if the density of neighboring solutions is great it reduces the chance of this solution of being selected. This is because the greater density of neighbor brings the lower dissimilarity of the solutions. Fitness sharing is the most popular technique of neighbor density estimation (Mallor *et al.*, 2003). In this technique, the density around a solution i is estimated by a sharing weight σ_i which depends on the sum of the sharing function value of the number of neighborhoods within a ball of radius r. The sharing function $S_{i,j}$ is given by:

$$S_{i,j} = \begin{cases} 1 - (\frac{d_{i,j}}{r})^2 & if\ d_{i,j} < r \\ 0 & otherwise \end{cases} \quad \textbf{(4.21)}$$

In above equation, $d_{i,j}$ is the Euclidean distance between solution i and j in the normalized objective space as follows for 3 objectives:

$$d_{i,j} = \sqrt{\sum_{k=1}^{3} \left(\frac{f_i^k - f_j^k}{f_{\max}^k - f_{\min}^k} \right)^2} \quad \textbf{(4.22)}$$

Where, f_i^k and f_j^k are the value of the objective function of solution i and j respectively. f_{min}^k and f_{max}^k are the minimum and maximum value of the objective function observed so far during the search, respectively.

When the sphere of radius r has been determined, the sharing weight σ_i can be calculated and then the fitness of each solution is adjusted by adding the reciprocal value of its sharing weight to the raw fitness value.

In the *search space*, we consider the dissimilarity of the selected solutions without their fitness. As mentioned before, every solution of the problem can be expressed as $\{c_1, ..., c_n\}$. n is the total number of candidate site. c_i is the configuration in site i. With such style, we can use the concept of Hamming distance to evaluate the dissimilarity of the selected solutions. In information theory, the Hamming distance between two strings of equal length is the number of positions for which the corresponding symbols are different. In our problem, the distance d between two solutions i and j in the search space is achieved by calculating the following function:

$$d_{i,j} = \sum_{r=1}^{n} \rho_r,\ \rho_r = \begin{cases} 1 & c_r^i = c_r^j \\ 0 & c_r^i \neq c_r^j \end{cases} \quad \textbf{(4.23)}$$

Then for a solution i, its dissimilarity in the search space can be seen as an average distance of it

to its neighbors. In our case we do not take into account the frequency assignment to the configuration as it is only an additional parameter to the configuration to determine the SINR value.

The dissimilarity in the search space is a measure of structural differences between two solutions. However, two solutions might be very close in the objective function space while they have very different structural features. Therefore, fitness sharing based on the objective function space may reduce diversity in the search space. Currently, it is difficult to say which kind of dissimilarity performs better since it depends on the problem itself. In our algorithms, we use the solutions diversity based on the dissimilarity in the search space for the following reasons: firstly, we do not know how to fix the radius parameter *r* in fitness sharing and secondly, the calculation fitness sharing needs more computational effort so we need much more time in computation. Also the diversity in search space is the only one which guarantees to explore different zones where the local optima might be.

c) Solution selection strategy

Based on the concepts of the acceptance probability and the solution dissimilarity, a solution selection strategy has been proposed as the following description. In this selection strategy, the acceptance probability based on rank *r* is the foremost priority here, followed by the consideration on the solution dissimilarity. To be more specific, for a set of input solutions, firstly, a rank *r* is selected based on the acceptance probability of rank. If the solutions of this rank have been completely selected, we chose a lower rank which has not yet been fully explored (some solutions were not selected). If all the lower ranks are completely explored, we choose the closest higher rank. Then we select a solution which has the highest solution dissimilarity and has not been selected yet and mark it as selected. Finally, we assign the selected solution to the output solution of the current loop.

Notation:

$\boldsymbol{X}$: a set of candidate solutions: $X=\{x_1,...,x_n\}$ (input parameter of ALGORITHM 8)

$\boldsymbol{X_r}$: a set of solutions in X with rank r

$\boldsymbol{Y}$: a set of selected solutions: $Y=\{y_1,...,y_m\}$

ALGORITHM 8: Solution selection algorithm

1. Rank X and calculate the acceptance probability of each rank in X
2. Sort the solutions in each rank by their dissimilarity
3. **For** i = 1...m **do**
4. Randomly select a rank r based on the acceptance probability of ranks
5. a←r
6. t←0
7. **When all** $x \in X_r$ have been selected **do**

   // Finding a new X_r in which all solutions have not been selected yet
8. **If** r = 0 // If the current rank is zero, find a higher rank not yet fully explored

9. t←1
10. r←r+1
11. **Endif**
12. **If** t=0 // If the current rank is larger than zero, find a lower rank not yet fully explored
13. r ← r-1
14. **Endif**
15. **Endwhen**
16. Select $x \in X_r$ which has the highest solution dissimilarity and not selected yet
17. Mark x as selected
18. $y_i \leftarrow x$
19. **Endfor**
20. **Return** Y

d) Tabu lists

In our algorithm, we define two tabu lists. One is a global tabu list. This tabu list stores the solutions and acts on both the VNS stage and the Tabu Search stage. At each iteration this tabu list is updated with the solutions of the starting solutions of current iteration. We implement a dynamic strategy for this tabu list. If one starting solution at current iteration improves, we increase the tabu tenure of this solution by one. Otherwise, the tabu tenure of this solution will be decreased by one. We set minimal and maximal values of tabu tenure to 10 and 100, respectively. It allows the algorithm to avoid choosing too rapidly improving solutions for the next step.

The second tabu list is a local tabu list in Tabu Search. This tabu list is reinitialized with null subset before Tabu Search starts and is updated inside the Tabu Search. This tabu list stores the attribute of the solution. The tabu tenure has a length that is chosen randomly between two predefined minimal and maximal values as we explain in the mono-objective process.

e) The algorithm description

The pseudo-code of Parallel Tabu Variable Neighbourhood Search is as follows:

Notation:

$\boldsymbol{F_P}$: Pareto set of optimal solutions produced by the search

$\boldsymbol{F_C}$: the current search front in iteration

$\boldsymbol{F_R}$: the current search front in thread

$\boldsymbol{R}$: the Pareto rank of solution

$\boldsymbol{R_{max}}$: the acceptable maximum Pareto rank

$\boldsymbol{T_g}$: the global tabu list

n_g: the tabu tenure for the global tabu list

T_l : the local tabu list

n_l: the tabu tenure for the local tabu list

ALGORITHM 9: Parallel Tabu Variable Neighbourhood Search (PTVNS) algorithm

Generate the initial solution X:

1. Define the initial order of neighborhood structures for VNS part: $N_1=N_{CA}$, $N_2=N_{SM}$, $N_3=N_{AM}$, $N_4=N_{DM}$. And N_{CFA} is considered as a supplement of above neighborhood structures for steepest descent search.

2. Find an initial solution x by the algorithm described in 4.2.1. This initial solution is generated by two steps. In the first step, the well coverage solution is found by a constructive heuristic GRASP. Then, in the second step, we choose ILS multi-start algorithm to obtain a good frequency allocation.

3. Create j solutions in each modification mode, thus there are total 5*j solutions.

4. Let these initial solutions $X=\{x_1,...,x_{5*j}\}$ to be the present solutions and the present optimum solutions. Iteration number n=0.

1. $F_P \leftarrow \Phi$
2. $T_g \leftarrow \Phi$
3. $n_g \leftarrow \{0,\ldots,0\}$
4. **While** the stop condition is not met **do**
5. $F_C \leftarrow \Phi$
6. **For** all $x \in X$ **do** // For all starting solutions
7. $F_R \leftarrow \Phi$
8. **While** the stop condition is not met **do**
9. $k \leftarrow 1$
10. **While** $k \leq 4$ **do** // For all modification modes
11. A solution x' in the k^{th} neighborhood $N_k(x)$ is randomly selected
12. $T_l \leftarrow \Phi$
13. $n_l \leftarrow 0$
14. Apply Tabu Search in the neighborhood $N_k(x')$ until a local minimum x'' is found
15. **If** x'' is better than x under a double control of the degradation strategy
16. $x \leftarrow x''$
17. $F_R \leftarrow F_R \cup \{x\}$

18. $k \leftarrow 1$ // If the k^{th} neighborhood is improving we use it again
19. **Else**
20. $k \leftarrow k+1$ // If the k^{th} neighborhood is not improving we use the next one
21. **Endif**
22. Remove the solutions with rank $R > R_{max}$ from F_R
23. **Endwhile**
24. **Endwhile**
25. $F_C \leftarrow F_C \cup F_R$
26. Remove the solutions with rank $R > R_{max}$ from F_C
27. **Endfor**
28. $T_g \leftarrow T_g \cup X$ // The starting solutions become tabu
29. Update n_g
30. $F_P \leftarrow F_P \cup F_C$ // Store the old and the new Pareto fronts
31. **If** $|F_P| > 5*j$
32. $X \leftarrow$ solution selection strategy (F_P);
33. **Else**
34. Q is a set of ($5*j - |F_P|$) solutions which are randomly selected in F_P and apply a move randomly selected in all possible moves
35. $X \leftarrow F_P \cup Q$
36. $R_{max} \leftarrow R_{max}+1$ // We need to get solutions from higher rank
37. **Endif**
38. Remove the solutions with rank $R > 0$ from F_P
39. **Endwhile**

4.3.2.4 The experimentation of multi-objective optimization

To illustrate the effectiveness and performance of the proposed algorithm, an experimental setting for MO is implemented. The experimental setting is the same as for mono-objective. For objective selection, we also only focus on the positioning accuracy objective and QoS objective for the same reason as in mono-objective case. We create one solution in each modification mode for initialization, so there are five initial solutions at the beginning and also five threads at each following iteration.

Figure 4.12 represents the practical Pareto front composed of 6 solutions (red points) in the function space after 30 hours running and 36072 function evaluations. The blue points are the value of solutions at each iteration. Clearly, these points fall into two groups, the up group and the down

group, according to their QoS lack values. In the up group the QoS lack value of all the solutions is larger than 1000 while in the down group the QoS lack value of all the solutions is less than 63. We assign a very high penalty coefficient (1000) to the TPs which are unable to satisfy the communication requirement. Since if the QoS value is higher than 1000 we know that coverage requirements are not satisfied, thus it is easy to see that the solutions in the up group always contain unsatisfied TP which are unacceptable solutions.

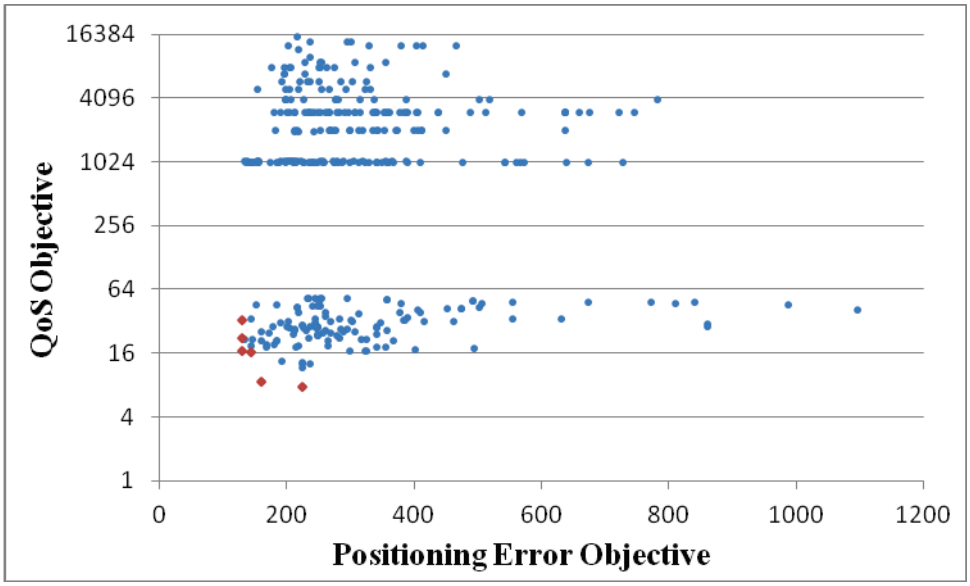

Figure 4.12 Estimated Pareto front for total lack of QoS and total positioning error

The results in Figure 4.12 show that Parallel Tabu Variable Neighbourhood Search can indeed tackle real world problems. The algorithm appears to be exploring a large fraction of the objective function space. The solutions in the Pareto front plotted in red present several trade-offs between the positioning objective and QoS objective. Among these available solutions, the user is able to choose a solution that either guarantees high throughput with an acceptable positioning accuracy or increase the positioning accuracy with a good QoS. We notice that the ratios between positioning objective and the QoS objective in all solutions are varying from 30 to 0.03 and such ratio in all solutions on the Pareto front are varying from 29 to 4. It means that the solution with the trade-offs out of the range from 30 to 0.03 are quite scarce.

We could also conclude that the estimated Pareto front is worse than the result of mono-objective optimization in the same running time due to the huge size of the search space with multi-objective optimization. The following reason causes this result: there is no prior choice of the weighting coefficients in multi-objective technique and the search process is more complex in the multi-objective technique algorithms which have to manage all the different trade-offs. However, in mono-objective optimization, the suitable values of weighting coefficients have been chosen empirically. But the estimated Pareto front is almost as good as the result of mono-objective optimization (see Figure 4.8 and Figure 4.9) after long time running (three times running time from 10 hours for mono-objective to 30 hours in multi-objective case) and this is good news. It means that doing multi-objective optimization in this problem of maximizing QoS and minimizing positioning

error, the user can get all the best compromise to take the right decision in network deployment.

4.4 Conclusion

The WLAN-based indoor positioning optimization problem can be clearly identified as a multi-objective problem where positioning accuracy and QoS need to be concurrently optimized. In this chapter, we have successfully developed two heuristics to provide a solution where WLAN planning for QoS and positioning error reduction are dealt simultaneously as an optimization problem.

The first heuristic is belonged to the weighting method, which is a kind of non-Pareto technique. In this heuristic, a global formulation based on a penalty function has been proposed in order to transform a multi-objective problem to a mono-objective problem. To build the initial solution, two simple algorithms GRASP and ILS are applied with a coverage constraint. Then TVNS algorithm is implemented to provide several alternative solutions in the optimization step. The originality of the basic VNS scheme consists of trying to escape from local optima by randomization and systematic change of neighborhoods structure during the search, while in TS the recency-based memories prevent cycling allowing the algorithm to overcome local optima. The TVNS proposed herein uses TS internally within VNS performing the local search for given neighborhood structures, while externally VNS performs systematical neighborhood changes and controls the shaking mechanism. In this case, Tabu Search tools are incorporated to local search to modulate the intensification and diversification of the search. Thus it is reasonable to expect a thorough and systematic exploration of the solution space by utilizing trajectory local search and neighborhood topologies.

Moreover, three enhanced strategies were introduced to improve the local search efficiency. The first enhanced strategy is the dynamic probabilistic strategy for neighborhood selection. In this strategy, the neighborhoods are sorted according to the estimation of the improvements potential. In this case, the more efficient the neighborhood is, the better the chances of it being chosen by the algorithm. The second enhanced strategy is the double control of the degradation strategy. In this strategy, to avoid falling into a local minimum, the algorithm can accept a worse solution according to the probability of a worse solution acceptance or the amplitude of degradation. The last enhanced strategy is a speed-up strategy. In this strategy, we can use the properties of the problem to reduce its computational complexity. For example, since the signal strength from each AP is mutual independent, thus for each move in search process, we just need to recalculate the average positioning error of these RPs which are contained in the coverage of APs changed in this move. We can estimate all the positioning error of the possible AP configuration at site in advance by calculate the GDOP and the RGER of the solutions.

Some experiments were done with the objective to study the model and the algorithm. The first test is the comparison between the proposed TVNS heuristic and other VNS heuristics (RVNS and GVNS) that are used in literature. TVNS yields substantially better result than RVNS and tends to have a little better performance than GVNS. In the next test, we replace the average positioning error with aliasing error which can simplify the search space and speed-up the search. The results prove that a better solution can be obtained through using aliasing error instead of average positioning error. In the weighting method, a hard decision is to choose the weighting coefficients of the aggregated evaluation function to get the desired trade-off between these objectives. The results in the third test

reveal a universal fact. The objective associated with a high penalty coefficient is emphatically optimized, while a high penalty coefficient also prevents the improvement of other conflicting objectives. Furthermore, we found that the trade-off between these objectives can influence the search since the size and complexity of the search space are associated with these trade-offs. Finally, the comparison between our optimization model and Battiti's optimization model (the best known model) indicates that with the consideration of QoS criterion our optimization model is able to produce consistently high quality solutions that are competitive to results of Battiti's optimization model. Especially, the performance of our model shows remarkable reduction on total QoS lack and the number of unsatisfied TP while ensuring a small positioning error.

The other heuristic relies on the Pareto-based techniques and looks for a set of Pareto-optimal solutions. In this way, each solution represents a different trade-off between the objectives that is involved. The algorithm we proposed for the Pareto-based technique, PTVNS, was originally inspired in TVNS and integrated with a multi-threaded parallelization strategy which can offer a large potential speed-up. To increase diversity and match the parallelization strategy, we use the initial search front instead of a single initial solution. The solutions of the initial search front are generated by adding various modifications on the initialization of non-Pareto optimization. With the same experiment setting, we run PTVNS to study the Pareto-based optimization. The estimated Pareto front obtained after 30 hours running is composed of 6 solutions. This result has highlighted the advantage of a Pareto-based approach which provides several alternative solutions in a single optimization step. However, in terms of computational time, the mono-objective search performs far better than the MO approach since the search process is more complex in MO optimization. But finally, MO optimization provides to the user a set of good solutions for both objectives and the user can choose the right network deployment with regards to his priority and the specific features of the instance to solve.

Conclusion and Perspectives

In this thesis manuscript, the main objective is to propose a new approach to define a WLAN-based Indoor Positioning System (IPS) as a combinatorial optimisation problem to solve. This approach is characterised by several difficult issues we tackled in three steps.

At first, we designed a WLAN-IPS and implemented it as a test framework. Using this framework, we looked at the system performance under various experimental constraints. Through these experiments, we went as far as possible in analysing the relationships between the positioning error and the external environmental factors. These relationships were considered as evaluation indicators of the positioning error. Secondly, we proposed a model that defines all major parameters met in the WLAN-IPS from the literature. As the original purpose of the WLAN infrastructures is to provide radio communication access, we introduced an additional purpose which is to reduce the location error within IPS context. Two main indicators were defined in order to evaluate the network Quality of Service and the positioning error for Location-Based Service (LBS). Thirdly, after defining the mathematical formulation of the optimisation problem and the key performance indicators, we proposed some algorithms based on metaheuristics to provide good solutions within a reasonable amount of time. The algorithm choice was driven by the complexity of the problem which contains some NP-hard sub-problems. Our contributions to the research field of IPS were done on these three steps and are detailed below.

To implement our WLAN-IPS, we faced some challenging problems. The first challenge was to create the radio map efficiently and accurately. In measurement-based methods, people move between different locations in the building, read both the physical coordinates and the signal strength from each Access Point (AP or radio transceiver) within range and record them. In model-based method, a indoor signal propagation model calculates the signal strength at each location from all neighbouring APs. Obviously, measurement-based method emphasizes the accuracy and reliability while model-based method emphasizes the efficiency and flexibility. A comprehensive analysis of the indoor propagation and related literatures on these two approaches revealed that it is too difficult to strictly decide to replace one method by the other. The best way to proceed is to choose the more suitable method to get the final user objective, delay and cost of IPS deployment. To our minds, the propagation modelling approach significantly reduces the effort and the cost of IPS with only one weakness: accuracy. According to studies and our experiments, in most situations the errors of the model-based method can be steadily controlled within several meters and this accuracy is acceptable for most indoor LBS.

In our work, the model-based method was the best for radio map generation because a series of large-scale radio maps with different network configurations were required during the optimization process. Thus, we chose the model-based method to generate radio map with the aim of finding one appropriate propagation model. Currently, two kinds of propagation models are widely used for indoor environment: the empirical models and the deterministic models. The empirical models are based on statistical information and the main drawback of

such models is that multiple paths are not properly considered. Deterministic models are calculation methods which physically simulate the propagation of radio waves. Therefore, the effect of the environment is taken more accurately than in empirical models. We investigated four empirical indoor models and two deterministic models. We finally chose a multi-wall model which requires a low computational load and is easy to achieve. However the Radio Signal Strength (RSS) values calculated by the propagation model are single values that do not reflect the RSS variation in the real world. Thus, we improved the propagation model to adapt it to the real environment and to reduce the error.

The first improvement was the concept of signal-distribution model. A common way is to use Gaussian distribution to simulate the signal distribution. However, we used a more realistic distribution proposed by IBM research. This distribution not only reflects the short-term signal strength distribution but also reflects the statistical properties of the long-term signal strength distribution. The second improvement was to add a calibration of the propagation model. The calibration works in both offline phase and online phase. The third improvement was to consider the device calibration since the measured RSS values from different mobile devices differ significantly.

In online phase, our IPS uses a probabilistic approach because of its ability to deal with interferences. Two practical and effective techniques were integrated into the system to enhance its performances. The first technique is called *Centre of Mass* which estimates the user location based on the list of candidate locations in the current estimation period. The second technique is called *Time Averaging* which estimates the user location using the history of consecutive estimations. One additional technique, *positioning filters*, was applied in order to combine the new measurements with the past measurements and the user mobility.

Computer simulations and real experiments have been done with the IPS we developed. The computer simulation took place on two artificial buildings with various AP configurations to emphasize the location error due to the AP numbers, the AP placement and the building architecture. The first building architecture was simple; in this building, we focused on the influence of the AP placement and the number of AP on location accuracy. The performances show that whatever the symmetry or asymmetry of the AP in the area, the average power of the signal is a major criterion to reduce location errors. For the second building, we focused on the influence of the obstacles on the location error. The stationary and tracking performances on the mobile device are entirely different. The obstacles have a positive effect on location of stationary device; they generate more diversity on RSS vectors. On the contrary, for tracking, location accuracy sometimes decreases. This is caused by the cumulated errors in the previous positions of the mobile device.

The real experiments took place in one building at UTBM with many classrooms and offices of different sizes. We split this floor into three scenarios (the whole floor, the left side with one corridor and the right side with one hall) with different AP configurations to emphasize the building topology and the network configuration effects. Based on the accuracy criterion, our system performs better within the left side with acceptable average error for most applications. We deleted the weakest AP to increase the average power. The results showed that the accuracy is improved by 12%. These results experimentally confirmed

our former conclusion in a simulation environment that increasing the average power can reduce the position error.

To enlarge the study on radio map importance, we did a comparison of our system (probabilistic algorithm) with RADAR (deterministic algorithm) and FRBHM (hybrid algorithm) within two real environments. One environment is the UTBM building where radio map is calculated using the propagation model; the building architecture is very irregular. The other environment is a medium sized building in University of Franche-Comté where radio map is measured; the building architecture is very regular. In the first experimental environment, the test for the right side floor returns bad results; its topology is more heterogeneous than the left side floor. Our positioning system always gets the best accuracy followed by RADAR and FRBHM. The signal probability distribution is well-performing. In the second environment, the positioning accuracy of all the systems is increasing when the number of AP is increasing. The performances of RADAR and our system are unstable when reducing grid density. On the opposite, the performance of FRBHM is quite stable. In both environments, all the systems show good performances to provide positioning support for context-aware applications. It means that a proper propagation model can meet positioning systems requirements in terms of accuracy. However, all the systems in the second environment have better good performances; it confirms that the positioning accuracy is affected by the building regularity and the radio map generation method.

We also focused on the comparison of our system to other major IPS from the literature by more realistic and fair criteria which include AP density and area size. Considering the median error as accuracy criteria, Battiti et al. (with Artificial Neural Network technique) shows the best performances while our system and ETF-ANN have the worse accuracy. But the experimental buildings are not of the same size for all papers and the AP density (number of AP relatively to the building size) is not the same too. However, relatively to the size of the experimentation area, Horus technique gets the most favourable result and our system performs correctly. While considering the AP density as additional factor of error estimation, our system is the best. Thus if we take into account both AP density and area size, the accuracy of our system is at the best level. During this work we emphasized that the WLAN configuration and the building configuration are the two major components of the location difficulty. If it is not possible to reconfiguration the building, it is possible to optimally configure the network to improve the IPS accuracy and this is what we did.

After these experimental works on IPS, we defined the indoor location as an optimisation problem with a mathematical formulation which allows to define algorithms to search for the best network configuration whatever the building. The purpose was to optimize the communication quality, which is the first purpose of the WLAN, and the location accuracy for LBS, which is the new deal for WLAN, as a unique process. In our formulation, we defined five decision variables: the site to locate the AP, the antenna pattern of AP, the azimuth, the emitted power and the frequency channel. And we defined a model for the AP description, the user requirement, the throughput calculation and the positioning requirement. The SINR (Signal to Interference plus Noise Ratio) was used as a quality of service indicator to estimate the throughput everywhere inside the building. Such estimation includes two steps. In the first step, we convert the SINR into the corresponding nominal bit rate according to the

received sensitivity of the Wi-Fi equipment. Then we can calculate the throughput according to the nominal bit rate, the different parameters of the MAC layer and the protocol CSMA/CA, the number of users communicating with the AP at different nominal bit rate allowed by the standard, etc. We proposed three positioning error indicators: the RSER (Refined Specific Error Ratio) which is used to estimate the aliasing positioning error, the GDOP (Geometric Dilution Of Precision) and the APE (Average Positioning Error). All problem components have been identified as objectives to optimize or constraints to solve, then we did some estimation of search space to emphasize the problem difficulty.

As some sub-problems are NP-hard (frequency assignment), it was not possible to tackle them optimally so we worked on approximate algorithms to find good solutions in a reasonable amount of time. Two heuristics were developed. The first heuristic belongs to the weighting method, which is a Non-Pareto technique using an aggregation of both criteria in one fitness. In this heuristic, a global formulation based on a penalty function has been proposed in order to transform a multi-objective problem to a mono-objective problem. To build the initial solution, two algorithms, GRASP and Iterative Local Search, were applied with a coverage constraint. Then a combination of Tabu Search and Variable Neighbourhood Search algorithms (TVNS) was implemented to provide several alternative solutions in the optimization step. Moreover, three enhanced strategies were introduced to improve the local search efficiency. The first strategy is the dynamic probabilistic strategy for neighbourhood selection. The second strategy is a control of the degradation strategy to escape from a local minimum. The third strategy is a speed-up strategy which uses the properties of the problem to reduce its computational complexity.

We have implemented and tested different variations of these algorithms. The first test was the comparison of TVNS with two others VNS heuristics (Random Variable Neighbourhood Search (RVNS) and General Variable Neighbourhood Search (GVNS)) from the literature. TVNS is significantly better than RVNS and has better performance than GVNS. Then we replaced the average positioning error by the aliasing error to reduce the search space and speed-up the search. The results proved that a better solution can be obtained using the aliasing error instead of the average positioning error. In the third test, we varied the weighting coefficients of the aggregated evaluation function to obtain different trade-off between the conflicting objectives and to study the relationship between the communication quality and the positioning accuracy. Finally, the comparison between our optimization model and Battiti's optimization model indicates that, for similar performance in location accuracy, we really improve QoS performance. This work shows that it is possible to design a WLAN for communication and location services simultaneously using a formal approach.

The second heuristic relies on the Pareto-based techniques and generates a set of solutions. Each solution represents a different trade-off between communication and location objectives. The algorithm we proposed for the Pareto-based technique, PTVNS, was originally inspired by TVNS and integrates a multi-threaded parallelization strategy which offers a large potential speed-up. For the solutions of the initial Pareto-front, we did the implementation to keep a trade-off between diversity and intensity of the search. With the same experimental setting as mono-objective optimisation, the Pareto-front composed of 6

solutions is obtained after 30 hours running and 36072 function evaluations instead of 10 hours and about 10000 evaluations with mono-objective approach. Due to the number of solutions and additional computation of this approach the computation time is longer to get the same quality of solutions than the other method. But the advantage is that at the end we have 6 different configurations of network and trade-offs between both objectives; it is so possible to deploy the network which corresponds to the adequate trade-off between communication QoS and device location.

The results and the conclusions of our research work open up several directions for future developments.

In the off-line phase, our system creates the radio map using the propagation modelling approach, and we use a multi-wall model which requires a low computational load and is easy to achieve. However, a significant drawback of this approach is that the computational load and the accuracy are conflicting. Thus, in the future we plan to choose an accurate deterministic propagation model in order to obtain a higher accuracy on radio map. A possible solution is to use the 3D indoor propagation prediction model MR-FDPF from the CITI lab (INSA Lyon). This propagation model has been proved to be an efficient tool for the complex indoor radio coverage prediction because all reflections and diffraction are taken into account. As our indoor positioning algorithm is very sensitive to the accuracy of radio map, we believe that the performance of our system can be improved after using a better propagation model.

We did experimentations on real building with real WLAN networks but it is not possible to generalise the performance of our approach today as the variations in building architecture are important. Our WLAN-IPS needs to be studied and qualified in different real world environment. The qualification must take into account the variation in the RSS due to the mobility inside the building and the density of people, and eventually the variation of the SINR due to other devices on uplink which were not taken into account in our model. We only focused on downlink estimation of radio signal. As well, we did not use any radio link information between the devices themselves; this is interesting to consider the surrounding devices to help the location of each of them by completing the radio links coming from the fixed AP.

In addition, improving the performance of optimization models and algorithms is a huge and very important task to do. For example, in the current model, we only consider the positioning error in the stationary mode for the device. The tracking mode can approximately be considered as a combination of the stationary mode but the main drawback of this consideration is that the impact of the previous position on the current position is neglected. In fact, according to the experiments in chapter 2, the positioning error at one reference point in the tracking mode is different from the positioning error at this reference point in the stationary mode. This is because the time average technique used in the tracking mode is based on prior knowledge and bad performance may come from errors accumulation at each previous position. Thus we may define an indicator to estimate the positioning error in the tracking mode in further. Concerning the algorithms we need to move through a population based method for the multi-criteria solving in order to allow the solutions to exchange information about the best and the worst zones of the search space. This method can be based on a genetic algorithm which will use the TVNS we developed as local search procedure.

Personal Publications

International conference with articles

(ICCSA'09) O. BAALA, Y. ZHENG, A. CAMINADA. *« Toward environment indicators to evaluate WLAN-based IPS »*. *In Proc. of* ACS/IEEE 7th International Conference on Computer Systems and Applications, Rabat (Maroc). May 2009.

(ICN'09) O. BAALA, Y. ZHENG, A. CAMINADA. *« The impact of AP placement in WLAN based Indoor Positioning System »*. *In Proc. of* IEEE 8th International Conference on Networks 2009, Cancun (Mexique). March 2009.

(IPIN'10) Y. ZHENG, O. BAALA, A. CAMINADA. *« Optimization Model for Indoor WLAN-based Positioning System »*. I*n Proc. of* IEEE International Conference on Indoor Positioning and Indoor Navigation 2010. Zurich (Suisse), September 2010.

(WD'10) Y. ZHENG, O. BAALA, A. CAMINADA. *« A new approach to design a WLAN-based positioning system »*. *In Proc. of* IEEE International Conference on Wireless Days 2010. Venice (Italy), Octorber, 2010.

(ICSPCS'10) Y. ZHENG, O. BAALA, A. CAMINADA. *« A new approach to design a WLAN-based positioning system »*. *In Proc. of* IEEE International Conference on Signal Processing and Communication Systems 2010. Gold Coast (Australia), December 2010.

(IPIN'11) F. LASSABE, Y. ZHENG, O. BAALA, A. CAMINADA. « Comparison of measurement-based and simulation-based indoor Wi-Fi positioning algorithms *»*. *In Proc. of* IEEE International Conference on Indoor Positioning and Indoor Navigation 2011. Guimarães (Portugal), September 2011.

National conference with articles

(JDIR'09) Y. ZHENG, O. BAALA, A. CAMINADA. *« Comparison of performance evaluation of several WLAN positioning systems ». In Proc. of* 10èmes Journées Doctorales en Informatique et Réseaux 2009. Belfort. February 2009.

(ROADEF'10) Y. ZHENG, O. BAALA, A. CAMINADA, A. GONDRAN. *« A New Model For Indoor WLAN Positioning System »*. *In Proc. of* 11ème Congrès de Recherche Opérationnelle et d'Aide à la Décision 2010. Toulouse. February 2010.

(ROADEF'11) Y. ZHENG, O. BAALA, A. CAMINADA. *« A Multi-Objective Approach To Design Wlan-Based Indoor Positioning System ». In Proc. of* 12ème Congrès de Recherche Opérationnelle et d'Aide à la Décision 2011. Saint-Étienne. March 2011.

National conference with oral without articles

(ResCom'08) Y. ZHENG, O. BAALA, A. CAMINADA. *« The impact of AP placement in WLAN-based indoor positioning system ».* Journées CNRS ASR (Architecture Système et Réseaux). Pôle Réseaux et Communications 2008. Strasbourg. October 2008.

Bibliography

(Aguado Agelet *et al.,* 2000) Aguado Agelet, F., A. Formella, et al. (2000). "Efficient ray-tracing acceleration techniques for radio propagation modeling." IEEE Transactions on Knowledge and Data Engineering, 49(6): 2089-2104.

(Ali-Loytty *et al.,* 2009) Ali-Loytty, S., T. Perala, et al. (2009). Fingerprint Kalman Filter in indoor positioning applications. 2009 IEEE Control Applications, (CCA) & Intelligent Control, (ISIC), : 1678-1683.

(Alliance, 2010) Alliance, Z. (2010). "ZigBee Standards ". from http://www.zigbee.org/.

(Altini *et al.,* 2010) Altini, M., D. Brunelli, et al. (2010). Bluetooth indoor localization with multiple neural networks. 5th IEEE International Symposium on Wireless Pervasive Computing, ISWPC 2010 295-300.

(Amaldi *et al.*, 2004) Amaldi, E., A. Capone, et al. (2004). WLAN coverage planning: optimization models and algorithms. 2004 IEEE 59th Vehicular Technology Conference, 2004. VTC 2004-Spring. **4:** 2219-2223.

(Amaldi *et al.*, 2005) Amaldi, E., A. Capone, et al. (2005). Algorithms for WLAN Coverage Planning Wireless Systems and Mobility in Next Generation Internet. G. Kotsis and O. Spaniol, Springer Berlin / Heidelberg. **3427:** 52-65.

(Anwar et al., 2008) Anwar, A. K., G. Ioannis, et al. (2008). Evaluation of indoor location based on combination of AGPS/ HSGPS. 3rd International Symposium on Wireless Pervasive Computing, 2008. ISWPC 2008.**:** 383-387.

(Arulampalam *et al.,* 2002) Arulampalam, M. S., S. Maskell, et al. (2002). "A tutorial on particle filters for online nonlinear/non-Gaussian Bayesian tracking." IEEE Transactions on signal processing 50(2): 174-188.

(Ascension, 2010) Ascension Technology,. (2010). "Motion Star." from http://www.ascension-tech.com/realtime/RTMotionSTARTethered.php.

(Baala & Caminada, 2006a) Baala, O. and A. Caminada (2006). WLAN-based Indoor Positioning System: experimental results for stationary and tracking MS. International Conference on Communication Technology, 2006. ICCT '06. : 1-4.

(Baala & Caminada 2006b) Baala, O. and A. Caminada (2006). Location Precision in Indoor Positioning System. Innovations in Information Technology, 2006: 1-5.

(Baala *et al.*, 2009) Baala, O., Y. Zheng, et al. (2009). The Impact of AP Placement in WLAN-Based Indoor Positioning System. Proceedings of the 2009 Eighth International Conference on Networks, IEEE Computer Society: 12-17.

(Bahl & Padmanabhan, 2000) Bahl, P. and V. N. Padmanabhan (2000). RADAR: an in-building RF-based user location and tracking system. Proceedings IEEE INFOCOM 2000. Nineteenth Annual Joint Conference of the IEEE Computer and Communications Societies. . **2:** 775-784.

(Battiti *et al.*, 2002) Battiti, R., T. L. Nhat, et al. (2002). Location-aware computing: a neural network model for determining location in wireless LANs, Universita degli Studi di Trento.

(Battiti *et al.*, 2003) Battiti, R., M. Brunato, et al. (2003). Optimal Wireless Access Point Placement for Location-Dependent Services, University of Trento.

(Battiti & Protasi, 1996) Battiti, R. and M. Protasi (1996). "Reactive search, a history-based heuristic for MAX-SAT." ACM Journal of Experimental Algorithmics.

(Battiti & Tecchiolli, 1994) Battiti, R. and G. Tecchiolli (1994). "The reactive tabu search." ORSA journal on computing **6**: 126-126.

(Bekkali *et al.*, 2007) Bekkali, A., H. Sanson, et al. (2007). RFID Indoor Positioning Based on Probabilistic RFID Map and Kalman Filtering. Third IEEE International Conference on Wireless and Mobile Computing, Networking and Communications, 2007. WiMOB 2007. **:** 21-21.

(Bernardos *et al.*, 2010) Bernardos, A. M., J. R. Casar, et al. (2010). Real time calibration for RSS indoor positioning systems. 2010 International Conference on Indoor Positioning and Indoor Navigation (IPIN), : 1-7.

(Besada *et al.*, 2007) Besada, J. A., A. M. Bernardos, et al. (2007). Analysis of tracking methods for wireless indoor localization. 2nd International Symposium on Wireless Pervasive Computing, 2007. ISWPC '07. .

(Bing, 2002) Bing, B. (2002). Wireless local area networks, Wiley Interscience.

(Blum & Roli, 2003) Blum, C. and A. Roli (2003). "Metaheuristics in combinatorial optimization: Overview and conceptual comparison." ACM Computing Surveys (CSUR) **35**(3): 268-308.

(Borenovic *et al.,* 2008) Borenovic, M., A. Neskovic, et al. (2008). Utilizing artificial neural networks for WLAN positioning. IEEE 19th International Symposium on Personal, Indoor and Mobile Radio Communications, 2008. PIMRC 2008. : 1-5.

(Bosio *et al.*, 2010) Bosio, S., A. Eisenblätter, et al. (2010). "Mathematical Optimization Models for WLAN Planning." Graphs and Algorithms in Communication Networks: 283-309.

(Brimberg *et al.*, 2000) Brimberg, J., P. Hansen, et al. (2000). "Improvements and comparison of heuristics for solving the uncapacitated multisource Weber problem." Operations Research: 444-460.

(Chang *et al.,* 2009) Chang, Y. K., C. L. Yang, et al. (2009). A RSSI-based Algorithm for Indoor Localization Using ZigBee in Wireless Sensor Network. IEEE International Conference on Distributed Multimedia Systems 2009, DMS2009**:** 1-5.

(Chen *et al.,* 2005) Chen, Y.-C., J.-R. Chiang, et al. (2005). Sensor-assisted wi-fi indoor location system for adapting to environmental dynamics. Proceedings of the 8th ACM international symposium on Modeling, analysis and simulation of wireless and mobile systems., Quebec, Canada, ACM: 118-125.

(Chen *et al.,* 2010) Chen, F., W. S. A. Au, et al. (2010). Compressive Sensing Based Positioning Using RSS of WLAN Access Points. 2010 Proceedings IEEE INFOCOM, : 1-9.

(Chih-Hao *et al.*, 2008) Chih-Hao, C., C. Chun-Yuan, et al. (2008). Location-Constrained Particle Filter human positioning and tracking system. IEEE Workshop on Signal Processing Systems, 2008. SiPS 2008.: 73-76.

(Chopard *et al.,* 1997) Chopard, B., P. O. Luthi, et al. (1997). Lattice Boltzmann method for wave propagation in urban microcells. IEEE Proceedings Microwaves, Antennas and Propagation,. 144: 251-255.

(Chun-cheng *et al.,* 2007) Chun-cheng, C., L. Haiyun, et al. (2007). Rate-Adaptive Framing for Interfered Wireless Networks. IEEE INFOCOM 2007. 26th IEEE International Conference on Computer Communications.**:** 1325-1333.

(Culler *et al.,* 2004) Culler, D., D. Estrin, et al. (2004). "Guest Editors' Introduction: Overview of Sensor Networks." IEEE Computer **37**(8): 41-49.

(Cypriani *et al.,* 2009) Cypriani, M., F. Lassabe, et al. (2009). Open Wireless Positioning System: A Wi-Fi-Based Indoor Positioning System. 2009 IEEE 70th Vehicular Technology Conference Fall, VTC 2009-Fall 1-5.

(Dai *et al.*, 2011) Dai, N., M. Shokouhi, et al. (2011). Multi-objective optimization in learning to rank. In Proceedings of the 34th Annual ACM SIGIR Conference on Research and Development in Information Retrieval. beijing, ACM**:** 1241-1242.

(Davison, 2003) Davison, A. C. (2003). Statistical Models, Cambridge University Press.

(Depenthal & Schwendemann, 2009) Depenthal, C. and J. Schwendemann (2009). iGPS–Ca New System for Static and Kinematic Measurements. Proceedings of Optical 3-D Measurement Techniques IX**:** 131-140.

(Devarenne *et al.*, 2006) Devarenne, I., H. Mabed, et al. (2006). Intelligent Neighborhood Exploration in Local Search Heuristics. Proceedings of the 18th IEEE International Conference on Tools with Artificial Intelligence, IEEE Computer Society**:** 144-150.

(DIB, 2010) Dib, M. (2010). Tabu-NG : hybridation de programmation par contraintes et recherche locale pour la résolution de CSP. Informatique, Université de Technologie Belfort-Montbéliard. **Doctor**.

(Dutt *et al.*, 2007) Dutt, V. B. S. S. I., G. S. B. Rao, et al. (2007). "Investigation of GDOP for Precise user Position Computation with all Satellites in view and Optimum four Satellite Configurations." Journal of Indian geophysics Union **13**(3): 139-148.

(Evennou, 2005) Evennou, F. (2005). Sensor Fusion for UWB and Wifi Indoor Positioning system, France Telecom.

(Feldmann *et al.*, 2003) Feldmann, S., K. Kyamakya, et al. (2003). An indoor Bluetooth-based positioning system: concept, implementation and experimental evaluation. International Conference on Wireless Networks. USA**:** 109-113.

(Feo & Resende, 1995) Feo, T. A. and M. G. C. Resende (1995). "Greedy Randomized Adaptive Search Procedures." Journal of Global Optimization **6**(2): 109-133.

(Finkenzeller, 2003) Finkenzeller, K. (2003). RFID Handbook: Fundamentals and Applications in Contactless Smart Cards and Identification, John Wiley.

(Frank *et al.*, 2009) Frank, K., B. Krach, et al. (2009). Development and Evaluation of a Combined WLAN & Inertial Indoor Pedestrian Positioning System, Institute of Communications and Navigation, Germany.

(Fukuju *et al.,* 2003) Fukuju, Y., M. Minami, et al. (2003). DOLPHIN: an autonomous indoor positioning system in ubiquitous computing environment. IEEE Workshop on Software Technologies for Future Embedded Systems, 2003. **:** 53-56.

(gatech, 2011) gatech (2011). Pareto Optimality, Georgia Institute of Technology.

(Gezici *et al.,* 2005) Gezici, S., T. Zhi, et al. (2005). "Localization via ultra-wideband radios: a look at positioning aspects for future sensor networks." Signal Processing Magazine, IEEE **22**(4): 70-84.

(Giaglis *et al.*, 2002) Giaglis, G. M., P. Kourouthanassis, et al. (2002). "Towards a classification framework for mobile location services." Mobile commerce: technology, theory, and applications: 67-85.

(Glover, 1986) Glover, F. (1986). "Future paths for integer programming and links to artificial intelligence." Computers & Operations Research **13**(5): 533-549.

(Glover & Laguna, 1998) Glover, F. and M. Laguna (1998). Tabu search, Kluwer Academic Pub.

(Glover & Taillard, 1993) Glover, F. and E. Taillard (1993). "A user's guide to tabu search." Annals of operations research **41**(1): 1-28.

(Godha & Lachapelle, 2008) Godha, S. and G. Lachapelle (2008). "Foot mounted inertial system for pedestrian navigation." Measurement Science and Technology **19**: 075202.

(Goldberg, 1989) Goldberg, D. E. (1989). Genetic algorithms in search, optimization, and machine learning, Addison-wesley.

(Goldsmith, 2005) Goldsmith, A. (2005). Wireless Communications, Cambridge University Press.

(Gondran, 2008) Gondran, A. (2008). Modélisation et optimisation de la planification des réseaux locaux sans fil. Informatique, Université de Technologie Belfort-Montbéliard. **Doctor**.

(Gondran *et al.,* 2007) Gondran, A., A. Caminada, et al. (2007). "Wireless LAN planning: a didactical model to optimise the cost and effective payback." International Journal of Mobile Network Design and Innovation **2**(1): 13-25.

(Gondran *et al.*, 2008a) Gondran, A., O. Baala, et al. (2008). Interference Management in IEEE 802.11 Frequency Assignment. VTC Spring 2008. IEEE Vehicular Technology Conference, 2008.**:** 2238-2242.

(Gondran *et al.*, 2008b) Gondran, A., O. Baala, et al. (2008). Hypergraph T-coloring for automatic frequency planning problem in wireless LAN. 2008. PIMRC 2008. IEEE 19th International Symposium on Personal, Indoor and Mobile Radio Communications. Cannes, IEEE**:** 1-5.

(Gorce *et al.,* 2003) Gorce, J. M., E. Jullo, et al. (2003). An adaptive multi-resolution algorithm for 2D simulations of indoor propagation. Twelfth International Conference on Antennas and Propagation, 2003. (ICAP 2003). .

(Guvenc *et al.,* 2003) Guvenc, I., C. T. Abdallah, et al. (2003). Enhancements to rss based indoor tracking systems using kalman filters. Global Signal Processing Expo and International Signal Processing Conference.

(Gwon & Jain, 2004) Gwon, Y. and R. Jain (2004). Error characteristics and calibration-free techniques for wireless LAN-based location estimation. Proceedings of the second international workshop on Mobility management and wireless access protocols. Philadelphia, PA, USA, ACM: 2-9.

(Hansen *et al.*, 2008) Hansen, P., N. Mladenovi , et al. (2008). "Variable neighbourhood search: methods and applications." 4OR: A Quarterly Journal of Operations Research **6**(4): 319-360.

(Hansen *et al.,* 2010) Hansen, R., R. Wind, et al. (2010). Algorithmic strategies for adapting to environmental changes in 802.11 location fingerprinting. 2010 International Conference on Indoor Positioning and Indoor Navigation (IPIN), : 1-10.

(Hansen & Mladenovic, 1999) Hansen, P. and N. Mladenovic (1999). An introduction to variable neighborhood search. MIC-97 : meta-heuristics international conference france**:** 433-458.

(Hansen & Mladenovic, 2001) Hansen, P. and N. Mladenovic (2001). "Variable neighborhood search: Principles and applications." European journal of operational research **130**(3): 449-467.

(Hattori *et al.,* 2009) Hattori, K., R. Kimura, et al. (2009). Hybrid Indoor Location Estimation System Using Image Processing and WiFi Strength. International Conference on Wireless Networks and Information Systems, 2009. WNIS '09.**:** 406-411.

(Hazas & Hopper, 2006) Hazas, M. and A. Hopper (2006). "Broadband ultrasonic location systems for improved indoor positioning." IEEE Transactions on Mobile Computing **5**(5): 536-547.

(He *et al.,* 2003) He, T., C. Huang, et al. (2003). Range-free localization schemes for large scale sensor networks. Proceedings of the 9th annual international conference on Mobile computing and networking. San Diego, CA, USA, ACM**:** 81-95.

(Hightower *et al.,* 2000) Hightower, J., R. Want, et al. (2000). SpotON: An indoor 3D location sensing technology based on RF signal strength, Department of Computer Science and Engineering, University of Washington.

(Hongpeng & Fei, 2007) Hongpeng, W. and J. Fei (2007). A Hybrid Modeling for WLAN Positioning System. International Conference on Wireless Communications, Networking and Mobile Computing, 2007. WiCom 2007.**:** 2152-2155.

(Hui *et al.,* 2007) Hui, L., H. Darabi, et al. (2007). "Survey of Wireless Indoor Positioning Techniques and Systems." IEEE Transactions on Systems, Man, and Cybernetics, Part C: Applications and Reviews, **37**(6): 1067-1080.

(Ito *et al.,* 2004) Ito, T., K. Oguri, et al. (2004). "A location information system based on real-time probabilistic position inference." Innovations in Applied Artificial Intelligence: 797-806.

(Jaegeol *et al.,* 2008) Jaegeol, Y., J. Seunghwan, et al. (2008). Utilizing Map Information for WLAN-Based Kalman Filter Indoor Tracking. Second International Conference on Future Generation Communication and Networking Symposia, 2008. FGCNS '08. . 5: 58-62.

(Jaffrès-Runser *et al.*, 2008) Jaffrès-Runser, K., J. M. Gorce, et al. (2008). "Mono-and multiobjective formulations for the indoor wireless LAN planning problem." Computers & Operations Research **35**(12): 3885-3901.

(JANET, 2010) JANET Network Access Programme team, (2010). A1. Overview of Location Technologies, Investigations in Location Awareness, Cardiff University.

(Jasmine *et al.*, 2008) Jasmine, P., L. Ara, et al. (2008). A WLAN planning proposal through computational intelligence and genetic algorithms hybrid approach. Proceedings of the International Conference on Mobile Technology, Applications, and Systems. Taiwan, ACM**:** 1-5.

(Jiansong *et al.*, 2008) Jiansong, Z., K. Tan, et al. (2008). A Practical SNR-Guided Rate Adaptation. IEEE INFOCOM 2008. The 27th Conference on Computer Communications.**:** 2083-2091.

(Jie *et al.,* 2005) Jie, Y., Y. Qiang, et al. (2005). Adaptive Temporal Radio Maps for Indoor Location Estimation. Pervasive Computing and Communications, 2005. PerCom 2005. Third IEEE International Conference on: 85-94.

(Johnson, 1967) Johnson, S. C. (1967). "Hierarchical clustering schemes." Psychometrika 32(3): 241-254.

(Jugl & Boche, 2000) Jugl, E. and H. Boche (2000). New techniques for the calculation of the average SIR and the outage probability of the uplink of CDMA systems. 2000 IEEE Wireless Communications and Networking Conference, 2000. WCNC. . **3:** 1477-1481

(Jun *et al.,* 2003) Jun, J., P. Peddabachagari, et al. (2003). Theoretical Maximum Throughput of IEEE 802.11 and its Applications. In Proceedings of the IEEE International Symposium on Network Computing and Applications Citeseer**:** 249-257.

(Kaemarungsi & Krishnamurthy, 2004a) Kaemarungsi, K. and P. Krishnamurthy (2004). Properties of indoor received signal strength for WLAN location fingerprinting. The First Annual International Conference on Mobile and Ubiquitous Systems: Networking and Services, 2004. MOBIQUITOUS 2004. : 14-23.

(Kaemarungsi & Krishnamurthy, 2004b) Kaemarungsi, K. and P. Krishnamurthy (2004). Modeling of indoor positioning systems based on location fingerprinting. Twenty-third AnnualJoint Conference of the IEEE Computer and Communications Societies,INFOCOM 2004. . **2:** 1012-1022.

(Kanaan *&* Pahlavan, 2004) Kanaan, M. and K. Pahlavan (2004). A comparison of wireless geolocation algorithms in the indoor environment. Wireless Communications and Networking Conference, 2004. WCNC. 2004 IEEE. **1:** 177-182.

(Kelly *et al.,* 2002) Kelly, D., S. Reinhardt, et al. (2002). PulsON second generation timing chip: enabling UWB through precise timing. IEEE Conference on Ultra Wideband Systems and Technologies, 2002. Digest of Papers. 2002 117-121.

(King *et al.,* 2006) King, T., S. Kopf, et al. (2006). COMPASS: A probabilistic indoor positioning system based on 802.11 and digital compasses. Proceedings of the 1st international workshop on Wireless network testbeds, experimental evaluation & characterization. Los Angeles, CA, USA, ACM**:** 34-40.

(King *et al.,* 2007) King, T., T. Haenselmann, et al. (2007). "Deployment, calibration, and measurement factors for position errors in 802.11-based indoor positioning systems." Location-and Context-Awareness: 17-34.

(Klingbeil & Wark, 2008) Klingbeil, L. and T. Wark (2008). A Wireless Sensor Network for Real-Time Indoor Localisation and Motion Monitoring. Proceedings of the 7th international conference on Information processing in sensor networks, IEEE Computer Society**:** 39-50.

(Kovaevi-Vuji, 1999) Kovaevi-Vuji, V. (1999). "Tabu search methodology in global optimization." Computers & Mathematics with Applications **37**(4-5): 125-133.

(Krumm *et al.,* 2003) Krumm, J., G. Cermak, et al. (2003). Rightspot: A novel sense of location for a smart personal object. Proceedings of UbiComp 2003, Springer**:** 36-43.

(Kushki *et al.,* 2006) Kushki, A., K. N. Plataniotis, et al. (2006). Location Tracking in Wireless Local Area Networks with Adaptive Radio MAPS. Proceedings 2006 IEEE International Conference on Acoustics, Speech and Signal Processing, 2006. ICASSP 2006. 5: 5-10.

(Kwok-Wai *et al.,* 1998) Kwok-Wai, C., J. H. M. Sau, et al. (1998). "A new empirical model for indoor propagation prediction." IEEE Transactions on Vehicular Technology, 47(3): 996-1001.

(Kwon *et al.,* 2004) Kwon, J., B. Dundar, et al. (2004). Hybrid algorithm for indoor positioning using wireless LAN. 2004 IEEE 60th Vehicular Technology Conference, 2004. VTC2004-Fall. . **7:** 4625-4629.

(L.A.N., 1999) Los Alamos National Laboratory (1999). Time-of-arrival location technique.

(Lachapelle, 2004) Lachapelle, G. (2004). "GNSS Indoor Location Technologies." Journal of Global Positioning Systems **3**(1-2): 2-11.

(Langley, 1999) Langley, R. B. (1999). "Dilution of precision." GPS world **10**(5): 52-59.

(Laoudias *et al.,* 2010) Laoudias, C., M. P. Michaelides, et al. (2010). Fault tolerant positioning using WLAN signal strength fingerprints. 2010 International Conference on Indoor Positioning and Indoor Navigation (IPIN), .

(Lassabe *et al.,* 2005) Lassabe, F., P. Canalda, et al. (2005). A Friis-based calibrated model for WiFi terminals positioning. Sixth IEEE International Symposium on a World of Wireless Mobile and Multimedia Networks, 2005. WoWMoM 2005. : 382-387.

(Lassabe *et al.,* 2010) Lassabe, F., Z. You, et al. (2010). Comparison of measurement-based and simulation-based indoor Wi-Fi positioning algorithms, UTBM.

(Li *et al.,* 2006) Li, B., J. Salter, et al. (2006). Indoor positioning techniques based on wireless LAN, School of Surveying and Spatial Information Systems**:** 13-16.

(Lim *et al.,* 2006) Lim, H., L. C. Kung, et al. (2006). Zero-Configuration, Robust Indoor Localization: Theory and Experimentation. Proceedings in 25th IEEE International Conference on Computer Communications. INFOCOM 2006.: 1-12.

(Ling *et al.,* 2010) Ling, P., C. Ruizhi, et al. (2010). Inquiry-Based Bluetooth Indoor Positioning via RSSI Probability Distributions. Advances in Satellite and Space Communications (SPACOMM), 2010 Second International Conference on**:** 151-156.

(Mabed *et al.*, 2005) Mabed, H., I. Devarenne, et al. (2005). ALGOPDF - Spécification détaillé d'algorithme d'optimisation de fréquences pour PR4G, Laboratoire SeT, UTBM.

(Madigan *et al.,* 2005) Madigan, D., E. Einahrawy, et al. (2005). Bayesian indoor positioning systems. Proceedings IEEE INFOCOM 2005. 24th Annual Joint Conference of the IEEE Computer and Communications Societies. . **2:** 1217-1227.

(Mahfouz *et al.,* 2008) Mahfouz, M. R., Z. Cemin, et al. (2008). "Investigation of High-Accuracy Indoor 3-D Positioning Using UWB Technology." IEEE Transactions on Microwave Theory and Techniques, **56**(6): 1316-1330.

(Mallor *et al.*, 2003) Mallor, F., P. M. Mateo Collazos, et al. (2003). Multiobjective evolutionary algorithms: Pareto rankings. VII Jornadas Zaragoza-Pau de Matemática Aplicada y estadística. Jaca Prensas Universitarias de Zaragoza**:** 27-36.

(Mautz, 2009b) mautz, r. (2009). Current positioning systems according to their accuracy and coverage, ETH Zurich

(Mautz, 2009a) Mautz, R. (2009). "Overview of current indoor positioning systems." Geodesy and Cartography **35**(1): 18-22.

(Mestre *et al.,* 2010) Mestre, P., H. Pinto, et al. (2010). Multiple Wireless Technologies Fusion for Indoor Location Estimation. Indoor Positioning and Indoor Navigation, IPIN 2010**:** 69-70.

(Michel *et al.,* 2006) Michel, J. C. F., C. Mark, et al. (2006). Multisensor Based Indoor Vehicle Localization System for Production and Logistic. IEEE International Conference on Multisensor Fusion and Integration for Intelligent Systems, 2006 553-558.

(Milan *et al.,* 2009) Milan, R., Ó. C. Ciarán, et al. (2009). A hybrid method for indoor user localisation. The 4th European Conference on Smart Sensing and Context, EuroSSC 2009. Guildford, UK**:** 16-18.

(Milner, 2011) Milner, M. (2011). "Network Stumbler." from http://www.stumbler.net/.

(Minami *et al.,* 2004) Minami, M., Y. Fukuju, et al. (2004). DOLPHIN: A Practical Approach for Implementing a Fully Distributed Indoor Ultrasonic Positioning System. UbiComp 2004: Ubiquitous Computing. N. Davies, E. Mynatt and I. Siio, Springer Berlin / Heidelberg. **3205:** 347-365.

(Moraes & Nunes, 2006) Moraes, L. F. M. d. and B. A. A. Nunes (2006). Calibration-free WLAN location system based on dynamic mapping of signal strength. Proceedings of the 4th ACM international workshop on Mobility management and wireless access. Terromolinos, Spain, ACM: 92-99.

(Ni *et al.,* 2004) Ni, L. M., Y. Liu, et al. (2004). "LANDMARC: indoor location sensing using active RFID." Wireless Networks **10**(6): 701-710.

(Otsason *et al.,* 2005) Otsason, V., A. Varshavsky, et al. (2005). Accurate gsm indoor localization. UbiComp 2005: Ubiquitous Computing**:** 141-158.

(Paperno *et al.,* 2001) Paperno, E., I. Sasada, et al. (2001). "A new method for magnetic position and orientation tracking." IEEE Transactions on Magnetics, **37**(4): 1938-1940.

(Papliatseyeu *et al.,* 2009) Papliatseyeu, A., N. Kotilainen, et al. (2009). "FINDR: Low-cost indoor positioning using FM radio." MobileWireless Middleware, Operating Systems, and Applications: 15-26.

(Pavon & Sunghyun, 2003) Pavon, J. P. and C. Sunghyun (2003). Link adaptation strategy for IEEE 802.11 WLAN via received signal strength measurement. IEEE International Conference on Communications, 2003. ICC '03. **2:** 1108-1113.

(Pearl, 1985) Pearl, J. (1985). "Heuristics. Intelligent search strategies for computer problem solving." The Addison-Wesley Series in Artificial Intelligence, Reading, Mass.: Addison-Wesley, 1985, Reprinted version **1**.

(Pechac & Klepal, 2001) Pechac, P. and M. Klepal (2001). Effective indoor propagation predictions. IEEE VTS 54th Vehicular Technology Conference, 2001. VTC 2001 Fall. 3: 1247-1250.

(Pisinger & Ropke, 2010) Pisinger, D. and S. Ropke (2010). Large Neighborhood Search Handbook of Metaheuristics. M. Gendreau and J.-Y. Potvin, Springer US. **146:** 399-419.

(Prasithsangaree *et al.,* 2002) Prasithsangaree, P., P. Krishnamurthy, et al. (2002). On indoor position location with wireless LANs. The 13th IEEE International Symposium on Personal, Indoor and Mobile Radio Communications, 2002. **2:** 720-724.

(Priyantha *et al.,* 2000) Priyantha, N. B., A. Chakraborty, et al. (2000). The Cricket location-support system. Proceedings of the 6th annual international conference on Mobile computing and networking. Boston, Massachusetts, United States, ACM**:** 32-43.

(Ran *et al.,* 2004) Ran, L., S. Helal, et al. (2004). Drishti: an integrated indoor/outdoor blind navigation system and service. Proceedings of the Second IEEE Annual Conference on Pervasive Computing and Communications, 2004. PerCom 2004. **:** 23-30.

(Rappaport, 1996) Rappaport, T. S. (1996). Wireless communications: principles and practice, Prentice Hall PTR New Jersey.

(Roos *et al.,* 2002) Roos, T., P. Myllym ki, et al. (2002). "A probabilistic approach to WLAN user location estimation." International Journal of Wireless Information Networks 9(3): 155-164.

(Saha *et al.,* 2003) Saha, S., K. Chaudhuri, et al. (2003). Location determination of a mobile device using IEEE 802.11b access point signals. 2003 IEEE Wireless Communications and Networking, 2003. WCNC 2003. **3:** 1987-1992.

(Seybold, 2005) Seybold, J. S. (2005). Introduction to RF Propagation, wiley.

(Seybold & NetLibrary, 2005) Seybold, J. S. and I. NetLibrary (2005). Introduction to RF propagation, Wiley Online Library.

(Sheng-Po & Yu-Chee 2008) Sheng-Po, K. and T. Yu-Chee (2008). "A Scrambling Method for Fingerprint Positioning Based on Temporal Diversity and Spatial Dependency." IEEE Transactions on Knowledge and Data Engineering, 20(5): 678-684.

(Shih-Hau *et al.,* 2008) Shih-Hau, F., L. Tsung-Nan, et al. (2008). "A Novel Algorithm for Multipath Fingerprinting in Indoor WLAN Environments." IEEE Transactions on Wireless Communications, 7(9): 3579-3588.

(Shiraishi *et al.,* 2008) Shiraishi, T., N. Komuro, et al. (2008). Indoor Location Estimation Technique using UHF band RFID. International Conference on Information Networking, 2008. ICOIN 2008. International Conference on**:** 1-5.

(Shirts & Pande, 2001) Shirts, M. R. and V. S. Pande (2001). "Mathematical analysis of coupled parallel simulations." Physical Review Letters **86**(22): 4983-4987.

(Standard, 1999) Standard, I. (1999). Part 11: Wireless LAN Medium Access Control (MAC) and Physical Layer (PHY) Specifications. Information technology Telecommunications and information exchange between systems Local and metropolitan area networks Specific requirements IEEE.

(Steggles & Gschwind, 2005) Steggles, P. and S. Gschwind (2005). The Ubisense smart space platform. Adjunct Proceedings of the Third International Conference on Pervasive Computing. **191:** 73-76.

(Sugano, 2006) Sugano, M. (2006). Indoor localization system using rssi measurement of wireless sensor network based on zigbee standard. International Conference on Wireless and Optical Communications, 2006, IASTED/ACTA Press**:** 1-6.

(Suzuki & Mohan, 2002) Suzuki, H. and A. S. Mohan (2002). "Measurement and prediction of high spatial resolution indoor radio channel characteristic map." IEEE Transactions on Vehicular Technology, 49(4): 1321-1333.

(Taillard, 1991) Taillard, E. (1991). "Robust taboo search for the quadratic assignment problem." Parallel computing **17**(4-5): 443-455.

(Talbi, 2009) Talbi, E. G. (2009). Metaheuristics: from design to implementation, Wiley.

(Tesoriero *et al.,* 2010) Tesoriero, R., R. Tebar, et al. (2010). "Improving location awareness in indoor spaces using RFID technology." Expert Systems with Applications **37**(1): 894-898.

(Tetsuro & Teruya, 2002) Tetsuro, I. and F. Teruya (2002). "Fast Algorithm for Indoor Microcell Area Prediction System Using Ray-Tracing Method." Electronics and Communications in Japan 85(6): 1167-1177.

(Tilch & Mautz, 2010) Tilch, S. and R. Mautz (2010). Current investigations at the ETH Zurich in optical indoor positioning. 2010 7th Workshop on Positioning Navigation and Communication (WPNC), **:** 174-178.

(Tsung-Nan & Po-Chiang, 2005) Tsung-Nan, L. and L. Po-Chiang (2005). Performance comparison of indoor positioning techniques based on location fingerprinting in wireless networks. 2005 International Conference on Wireless Networks, Communications and Mobile Computing, . **2:** 1569-1574.

(Unbehaun & Kamenetsky, 2003) Unbehaun, M. and M. Kamenetsky (2003). "On the deployment of picocellular wireless infrastructure." Wireless Communications, IEEE **10**(6): 70-80.

(Vanhatupa *et al.*, 2007) Vanhatupa, T., M. Hannikainen, et al. (2007). Genetic algorithm to optimize node placement and configuration for WLAN planning. 4th International Symposium on Wireless Communication Systems, ISWCS 2007, IEEE**:** 612-616.

(Vaupel *et al.*, 2010) Vaupel, T., J. Seitz, et al. (2010). Wi-Fi positioning: System considerations and device calibration. 2010 International Conference on Indoor Positioning and Indoor Navigation (IPIN), : 1-7.

(Wang *et al.*, 2003) Wang, Y., X. Jia, et al. (2003). An indoors wireless positioning system based on wireless local area network infrastructure. The 6th International Symposium on Satellite Navigation Technology Including Mobile Positioning & Location Services. Melbourne, Australia: 22-25.

(Wang *et al.*, 2007) Wang, H., H. Lenz, et al. (2007). "Enhancing the map usage for indoor location-aware systems." Human-Computer Interaction. Interaction Platforms and Techniques: 151-160.

(Wang & Tang, 2008) Wang, X. and L. Tang (2008). "A Hybrid VNS with TS for the Single Machine Scheduling Problem to Minimize the Sum of Weighted Tardiness of Jobs." Advanced Intelligent Computing Theories and Applications. With Aspects of Artificial Intelligence: 727-733.

(Want *et al.*, 1992) Want, R., A. Hopper, *et al.* (1992). "The active badge location system." ACM Transactions on Information systems **10**(1): 91-102.

(Weber *et al.*, 2010) Weber, M., U. Birkel, et al. (2010). Comparison of various methods for indoor RF fingerprinting using leaky feeder cable. 2010 7th Workshop on Positioning Navigation and Communication (WPNC), : 291-298.

(widyawan *et al.*, 2008) widyawan, M. Klepal, et al. (2008). A novel backtracking particle filter for pattern matching indoor localization. Proceedings of the first ACM international workshop on Mobile entity localization and tracking in GPS-less environments. San Francisco, California, USA, ACM: 79-84.

(wikipedia, 2010a) wikipedia (2010) "LORAN" from http://en.wikipedia.org/wiki/LORAN.

(wikipedia, 2010b) wikipedia (2010) "Omega" from http://en.wikipedia.org/wiki/Omega.

(Wikipedia, 2011a) Wikipedia (2011) "Heuristic"from http://en.wikipedia.org/wiki/Heuristic.

(Wikipedia, 2011b) Wikipedia (2011). "Metaheuristic." from http://en.wikipedia.org/wiki/Heuristic _(computer_science).

(Wlfle *et al.,* 2005) Wlfle, G., R. Wahl, et al. (2005). Dominant path prediction model for indoor scenarios. German Microwave Conference(GeMIC). Germany: 1-5.

(Xiang *et al.,* 2004) Xiang, Z., S. Song, et al. (2004). "A wireless LAN-based indoor positioning technology." IBM Journal of Research and Development 48(5.6): 617-626.

(Xu *et al.*, 2010) Xu, Y., M. Zhou, et al. (2010). Optimization of WLAN Indoor Location Network Based on Signal Coverage Requirement. 2010 First International Conference on Pervasive Computing Signal Processing and Applications (PCSPA). Harbin, IEEE**:** 162-166.

(Yamasaki *et al.,* 2005) Yamasaki, R., A. Ogino, et al. (2005). TDOA location system for IEEE 802.11b WLAN. 2005 IEEE Wireless Communications and Networking Conference, . **4:** 2338-2343 Vol. 2334.

(Youngjune *et al.,* 2004) Youngjune, G., R. Jain, et al. (2004). Robust indoor location estimation of stationary and mobile users. INFOCOM 2004. Twenty-third AnnualJoint Conference of the IEEE Computer and Communications Societies. **2:** 1032-1043.

(Youssef & Agrawala, 2004) Youssef, M. and A. Agrawala (2004). Continuous space estimation for WLAN location determination systems. Proceedings. 13th International Conference on Computer Communications and Networks, 2004. ICCCN 2004. : 161-166.

(Youssef *&* Agrawala, 2008) Youssef, M. and A. Agrawala (2008). "The Horus location determination system." Wireless Networks **14**(3): 357-374.

(Yubin *et al.*, 2010) Yubin, X., Z. Mu, et al. (2010). Optimization of WLAN Indoor Location Network Based on Signal Coverage Requirement. 2010 First International Conference on Pervasive Computing Signal Processing and Applications (PCSPA)**:** 162-166.

(Yueming & Hongyi, 2008) Yueming, S. and Y. Hongyi (2008). A RSS Based Indoor Tracking Algorithm via Particle Filter and Probability Distribution. 4th International Conference on Wireless Communications, Networking and Mobile Computing, 2008. WiCOM '08. : 1-4.

(Yun *et al.*, 2002) Yun, D. and C. Kee (2002). Centimeter accuracy stand-alone indoor navigation system by synchronized pseudolite constellation. 15th International Technical Meeting of the Satellite Division of The Institute of Navigation, ION GPS 2002. USA, The Institute of Navigation**:** 24-27

(Zhang *et al.*, 2008) Zhang, T., Z. Chen, et al. (2008). "An improved RFID-based locating algorithm by eliminating diversity of active tags for indoor environment." The Computer Journal **52** (8): 902-909.

(Zirari, 2010) Zirari, S. (2010). Contributions aux systemes depositionnement hybride et combine Wi-Fi/GNSS : criteres de dilution de la precision, positionnement et dimensionnement. Informatique, Universite de Franche-Comte. **doctor**.

(Zirari *et al.*, 2009a) Zirari, S., P. Canalda, et al. (2009). A Very First Geometric Dilution of Precision Proposal for Wireless Access Mobile Networks. Advances in Satellite and Space Communications, 2009. SPACOMM 2009. First International Conference on.

(Zirari *et al.*, 2009b) Zirari, S., P. Canalda, et al. (2009). "Geometric and Signal Strength Dilution of Precision(DoP) Wi-Fi." International Journal of Computer Science Issues(IJCSI) **3**: 35.

SPIM

■ École doctorale SPIM - Université de Technologie Belfort-Montbéliard
F - 90010 Belfort Cedex ■ tél. +33 (0)3 84 58 31 39
■ ed-spim@univ-fcomte.fr ■ www.ed-spim.univ-fcomte.fr

utbm
université de technologie
Belfort-Montbéliard